Quality and safety implications of efavirenz and pyrimethamine crystal modifications

Zak Perold

12320587

B.Pharm, M.Sc. (Pharmaceutics)

Thesis submitted for the degree *Doctor Philosophiae* in Pharmaceutics at the Potchefstroom Campus of the North-West University

Promotor: **Dr. M. Brits**

Assistant Promotor: **Dr. E. Swanepoel**

November 2014

Table of contents

Chapter 1: The impact of solid state chemistry on the quality and safety of pharmaceuticals

Part I - Efavirenz

Chapter 2: Anomalous dissolution behaviour of a novel amorphous form of Efavirenz

Chapter 3: Crystallisation behaviour of Efavirenz Form A: Introducing an alternative quantitation technique

Part II- Pyrimethamine

Chapter 4: The risk of recrystallization: Changes to the toxicity and morphology of pyrimethamine

Chapter 5: Characterisation of two novel solid-state forms of Pyrimethamine

Annexures

Annexure A – American Journal of PharmTech Research (AJPTR) Author guidelines

Annexure B – Supplementary information for Chapter 2

Annexure C – AAPS Pharm SciTech Author guidelines

Annexure D –Journal of Pharmacy & Pharmaceutical Sciences (J Pharm Pharm Sci) Author guidelines

Annexure E – Supplementary information for Chapters 4 & 5

Annexure F –European Journal of Pharmaceutical Sciences (Eur J Pharm Sci) Author guidelines

List of Figures

List of Tables

Abstract

This study focused on two active pharmaceutical ingredients (APIs) that are used to treat two of the most notorious diseases in Africa, i.e. human immunodeficiency virus/acquired immune deficiency syndrome (HIV/AIDS) and malaria. It is well known that many African countries lack effective regulatory control over medicines and patients are subsequently at risk of receiving sub-standard treatments. This study set out to investigate how the modification of the crystal packing (i.e. polymorphism) of these APIs may impact on their quality, safety and efficacy. Efavirenz (an antiretroviral) and Pyrimethamine (an antimalarial) were selected as the two model APIs for investigation during this study.

It was found that a novel amorphous form (Form A) of Efavirenz had been prepared during this study through quench cooling. Form A was extensively characterised and compared to the preferred crystalline Form I, with the aim of providing a means of distinguishing between these two Efavirenz forms. In contrast to popular belief (that amorphous form should have improved dissolution and solubility properties over the crystalline counterpart), the powder dissolution of Form A was significantly lower than that of Form I. Further investigation indicated that this was due to the occurrence of agglomeration and phase-mediated transformation. This observation had led to the belief that Form A had poor thermodynamic stability.

The glass transition temperature and the crystallisation activation energy, required for the recrystallisation of Form A, were subsequently determined in an attempt to elucidate its thermodynamic stability. The glass transition temperature of Form A was found to be unfeasibly low, hence confirming its tendency towards agglomeration. The crystallisation activation energy of Form A was determined by non-isothermal determinations, using differential scanning calorimetry (DSC), hot stage microscopy (HSM) and capillary melting point (CMP) analysis. These studies not only elucidated the required activation energy for the conversion of Form A into Form I, but it also found that the results from CMP were similar to those of the universally accepted DSC technique, allowing for the proposal of CMP as a cost-effective alternative to DSC for the quantitative measurement of the crystallisation of Efavirenz. Isothermal studies revealed that Form A had a short half-life, which, together with its poor dissolution performance, exemplified why this form was unsuitable for pharmaceutical use.

The Pyrimethamine study focused on recrystallisation as a means of modifying its crystal packing and on an evaluation of the effect that such crystal modification may have on its safety and manufacturability. Anhydrous Pyrimethamine was recrystallised, using methanol, acetone, n-propanol, ethanol, N,N-dimethylformamide and N,N-dimethylacetamide. Ethanol, acetone and n-propanol altered the crystal habit of Pyrimethamine, without any modification of its crystal lattice. The different habits exhibited clear differences in flowability and compressibility, which could in turn affect

manufacturing and therefore the quality of the finished pharmaceutical product (FPP). These habits were subsequently extensively characterised by means of *in-silico* molecular modelling predictions.

It was found that recrystallisation from methanol, N,N-dimethylformamide and N,N-dimethylacetamide had resulted in solvatomorphism. These solvatomorphs contained their respective solvents in concentrations exceeding the allowed residual solvent limits, as set by the International Conference on Harmonisation (ICH) guidelines. These undesirable solvatomorphs were also comprehensively characterised as a service to the pharmaceutical industry, in order to identify the distinct characteristics that distinguish these forms from the preferred non-toxic form, and to provide techniques for transforming the toxic forms into the non-toxic form.

Keywords: Efavirenz, amorph, glass, crystallization, dissolution, Pyrimethamine, solvatomorph, desolvation, morphology.

Uittreksel

Hierdie studie het op twee aktiewe farmaseutiese bestanddele (APIs), wat vir die behandeling van twee van die mees bekende siektetoestande in Afrika gebruik word, naamlik menslike immuniteitsgebreksvirus/verworwe immuniteitsgebrek sindroom (MIV/VIGS) en malaria, gefokus. Dit is welbekend dat baie Afrika-lande oor ‘n gebrek aan effektiewe regulatoriese beheer oor medisyne beskik en pasiënte dra gevolglik grootendeels die risiko om sub-standaard behandelings te ontvang. Die doel van hierdie studie was om ondersoek in te stel oor hoe modulerings aan die kristalpakking (polimorfisme) van hierdie APIs hulle effektiwiteit, veiligheid en kwaliteit, en gevolglik ook die behandeling van MIV/VIGS en malaria pasiënte, mag beïnvoed. Efavirenz (‘n anti-retrovirale middel) en Pirimetamien (‘n anti-malaria middel) is as die twee aktiewe bestandele vir ondersoek tydens hierdie studie gekies.

Daar is bevind dat ‘n nuwe amorfe vorm (Vorm A) van Efavirenz tydens hierdie studie deur die blusverkoelings tegniek (“quench cooling”) berei is. Vorm A is daarna volledig gekarakteriseer en met die verkose Vorm I vergelyk, ten einde ‘n basis te bied op grond waarvan tussen hierdie twee vorme onderskei kan word. Die dissolusie-gedrag van beide vorme is voorts ook vergelyk. Die swak dissolusie-gedrag van die amorfe Vorm A het die verwagte uitkomstes, naamlik verbeterde dissolusie en oplosbaarheidseienskappe in vergelyking met dié van die ooreenstemmende kristalvorme, weerspreek. In teenstelling, was die poeier dissolusie van Vorm A aansienlik laer as dié van Vorm I, weens die voorkoms van agglomerasie en fase-gemedieërde omskakeling vanaf Vorm A na Vorm I. Hierdie bevinding het daartoe aanleiding gegee tot die aanname dat die termodinamiese stabiliteit van Vorm A laag kon wees.

Ten einde die termodinamiese stabiliteit van Vorm A op te klaar, is die glasomskakelingstemperatuur en die kristallisasie-aktiveringsenergie, wat benodig word vir die rekristallisasie van Vorm A, bepaal. Dit is bevind dat die glasomskakelingstemperatuur van Vorm A ontoereikend laag was, wat die geneigdheid daarvan tot agglomerasie bevestig het. Die kristallisasie-aktiveringsenergie van Vorm A is met behulp van non-isotermiese differensiële skanderingskalorimetrie (DSC), termiese mikroskopie (HSM) en kappillêre smeltpunt (CMP) analiese bepaal. Hierdie studies het nie slegs die kristallisasie-aktiveringsenergie van Vorm A vasgestel nie, maar daar is ook gevind dat die CMP resultate met dié van die bekende DSC-tegniek vergelykbaar was. Laasgenoemde het dit moontlik gemaak om CMP as ‘n koste-effektiewe alternatiewe metode om die kristallisasie van Efavirenz te kwantifiseer, voor te stel. Isotermiese studies het daarop gewys dat Vorm A ‘n kort halfleeftyd gehad het, wat, tesame met die swak dissolusie-resultate, dit duidelik gemaak het dat Vorm A ongeskik vir farmaseutiese gebruik was.

Die studie op Pirimetamien het op rekristallisasie, as ‘n metode om sy kristalpakking te verander, sowel as op ‘n evaluering van die moontlike impak wat sodanige kristalmodulerings op die effektiwiteit, veiligheid en vervaardigbaarheid daarvan mag hê, gefokus. Anhidriese Pirimetamien is

uit metanol, asetoon, n-propanol, etanol, N,N-dimetielformamied en N,N-dimetielasetamied gerekristalliseer. Etanol, asetoon en n-propanol het die uitwendige kristalvoorkoms daarvan verander, sonder dat die interne kristalpakking daarvan verander is. Die verskillende uitwendige voorkomste se vloeibaarheid en saampersbaarheid het onderling wesentlik verskil, wat daarop gewys het dat hierdie tegnieke die vervaardigbaarheid daarvan, sowel as die kwaliteit van die finale farmaseutiese produk, mag benadeel. Hierdie voorkomste is gevolglik omvattend deur middel van *in-siliko* molekulêre moduleringsvoorspellings gekarakteriseer.

Daar is bevind dat rekristallisasie vanuit metanol, N,N-dimetielformamied en N,N-dimetielasetamied gesolveerde vorme tot gevolg gehad het. Die inhoud van die onderskeie oplosmiddels in elke gesolveerde vorm het die Internasionale Konferensie op Harmonisasie (ICH) se vasgestelde riglyne vir beperking van residuele oplosmiddels oorskrei. Hierdie ongewensde gesolveerde vorme is voorts deeglik gekarakteriseer, as ‘n diens aan die farmaseutiese industrie, ten einde die spesifieke eienskappe te identifiseer wat hierdie toksiese gesolveerde vorme van die nie-toksiese vorm onderskei, asook om tegnieke aan te bied waardeur die toksiese vorme na die nie-toksiese vorm omgeskakel kan word.

Sleutelwoorde: Efavirenz, amorf, glas, kristalisering, dissolusie, Pirimetamien, solvatomorf, desolvering, morfologie

Aims and Objectives

The treatment and prevention of human immunodeficiency virus/acquired immune deficiency syndrome (HIV/AIDS) and malaria remain high priorities globally, but even more so in Africa, where treatment success rates are especially hampered by the exposure to sub-standard medicines.

Efavirenz and Pyrimethamine, the two active pharmaceutical ingredients (APIs) being investigated in this study, are used in the treatment of HIV/AIDS and malaria, respectively. Both APIs exhibit polymorphism, a phenomenon known to influence their solid state properties. Efavirenz and Pyrimethamine are both poorly soluble, hence their absorption would be limited by their poor dissolution behaviour. Large differences in the apparent solubilities of the various polymorphic forms of poorly soluble APIs are therefore likely to affect their bioavailability/bioequivalence. In an attempt to evaluate the potential impact that novel modifications to the crystal packing (if possible) may have on the solid state chemistry, safety and efficacy of these APIs, the following study objectives were set and pursued:

- Undertake a comprehensive literature review of polymorphism, solvatomorphism, amorphous forms and crystal morphology;
- Undertake a comprehensive literature review of all known polymorphic forms of Efavirenz and Pyrimethamine;
- Characterise the commercially available Efavirenz and Pyrimethamine raw materials procured for this study;
- Investigate the possibility of modifying the crystal packing of Efavirenz raw material by subjecting it to quench cooling and to characterise the form obtained, with special consideration of its dissolution and thermodynamic stability;
- Investigate the possibility of modifying the crystal packing of Pyrimethamine raw material through recrystallisation, using organic solvents, such as methanol, ethanol, n-propanol, acetone, N,N-dimethylacetamide and N,N-dimethylformamide. Characterise the forms obtained, with special consideration to the influence of solvent inclusion in the crystal lattice of any solvatomorphs formed;
- Elaborate on any unexplored characteristics of known crystal modifications of Efavirenz and Pyrimethamine;
- Investigate and propose possible alternative techniques that may be used to characterise the recrystallisation behaviour of amorphous Efavirenz; and
- Claim novelty of any Efavirenz and Pyrimethamine form that has not yet been reported in the literature at the time of this study.

Foreword

This thesis is presented in manuscript format in accordance with the guidelines of the North-West University. The thesis consists of 2 main parts, the first part pertains to Efavirenz and the second part to Pyrimethamine. Each part consists of two manuscripts (as chapters). The manuscripts are in different formats, each in accordance with their respective author guidelines specific to the chosen journal. The different journal author guidelines' have been included as annexures, together with any supplementary information pertaining to each individual study. The complete study is unified with a summative introduction and conclusion; however each manuscript does have its own relevant introduction and conclusion pertaining to the specific field of study/research topic at hand. Two manuscripts, Chapters 2 and 4, have already been accepted for publication, whereas the other two are in process of submission.

A summative layout of the study is presented below. It serves as a quick means to familiarise the reader with the layout of the work.

<table>
<tr><td rowspan="8">Quality and safety implications of Efavirenz and Pyrimethamine crystal modifications</td><td rowspan="8">Chapter 1
Summative introduction</td><td colspan="2">Individual studies</td><td rowspan="8">Chapter 6
Summative conclusion</td><td>Annexure</td><td>Description</td></tr>
<tr><td rowspan="3">Part 1
Efavirenz</td><td rowspan="2">Chapter 2</td><td>A</td><td>Author guidelines</td></tr>
<tr><td>B</td><td>Supplementary information</td></tr>
<tr><td>Chapter 3</td><td>C</td><td>Author guidelines</td></tr>
<tr><td rowspan="3">Part 2
Pyrimethamine</td><td rowspan="2">Chapter 4</td><td>D</td><td>Author guidelines</td></tr>
<tr><td>E</td><td>Supplementary information</td></tr>
<tr><td>Chapter 5</td><td>F</td><td>Author guidelines</td></tr>
</table>

Chapter 1

The impact of solid state chemistry on the quality and safety of pharmaceuticals

Introduction

An estimated 25 – 60 % of the pharmaceutical market comprises of sub-standard medicines (WHO, 2003). The World Health Organization (WHO) defines sub-standard medicines as "*products whose composition and ingredients do not meet the correct scientific specifications and which are consequently ineffective and often dangerous to the patient*" (WHO, 2003). It is believed that inferior medicines are, amongst other factors, the result of negligence, human error and/or counterfeiting (WHO, 2003). Many active pharmaceutical ingredients (APIs) exhibit polymorphism (Byrn *et al.,* 1999:28), a phenomenon that may influence the safety and efficacy thereof and contribute towards medicines being ineffective, should the incorrect, or unsuitable polymorphic form be incorporated into the final solid dosage form (Byrn *et al.,* 1999:3; Carstensen, 2001:117; Hilfiker *et al.,* 2006:1-2).

The pharmaceutical industry is a dynamic environment, aiming at ever improving and remaining current with developments and advancements in the field of medicine (Coombes *et al.,* 2010:111). Regulatory authorities demonstrate their commitment by necessitating the revision of standard operating procedures (SOPs), by ensuring that relevant parties keep up-to-date with changing legislation and that pharmacists (and other medical professionals) undergo continuous professional development (South African Pharmacy Council, 2012). Most regulatory authorities require a discussion/confirmation with regards to polymorph identification in API drug master files in adherence to the International Conference on Harmonization (ICH) Q6A guidelines (ICH, 1999). This guideline provides simple, yet effective specifications and acceptance criteria, to ensure that the pharmaceutical industry stays abreast with all polymorphic forms of APIs that may affect commercial, final pharmaceutical products (Chemburkar *et al.,* 2000:413; ICH, 2009). An excerpt from the ICHQ6A guideline, describing the need for setting acceptance criteria for polymorphism in APIs, is summarised in Figure 1.1.

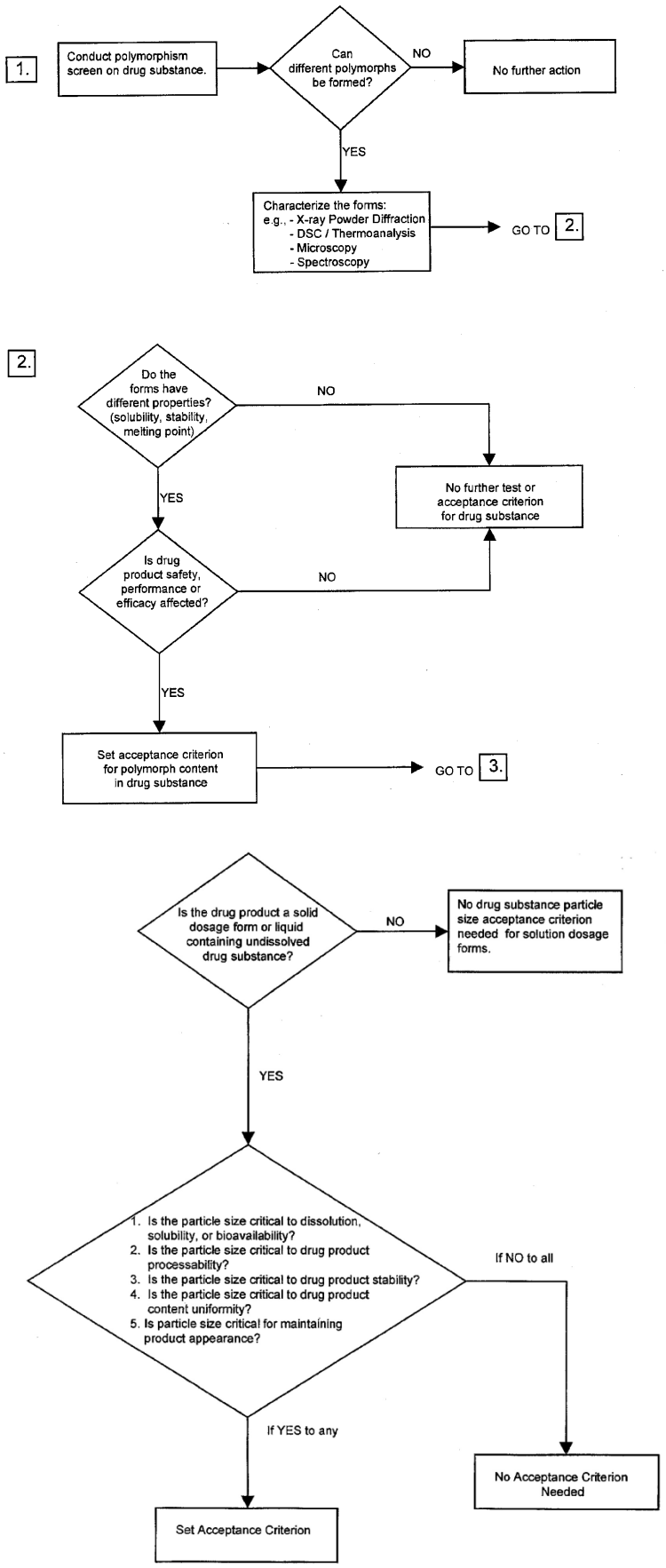

Figure 1.1 Decision tree: Investigation of the need for setting acceptance criteria for polymorphism in APIs and final pharmaceutical products (ICH, 1999).

According to the World Health Organization (WHO), half of the world's population is estimated to be at risk of contracting malaria (WHO, 2012a), while an estimated 33 million people are infected with Human Immunodeficiency Virus/Acquired Immune Deficiency Syndrome (HIV/AIDS) (United Nations News Centre, 2007). These two diseases rank amongst the top health priority concerns of the WHO (WHO, 2009; WHO, 2012b). Investigations into the quality, efficacy and safety of anti-retroviral (ARV) and anti-malarial medicines are necessitated by the staggering number of deaths and poor treatment efficacy statistics attributed to these diseases (WHO 2010a; WHO 2010b; WHO 2012c). Efavirenz is indicated for the treatment of HIV/AIDS (Raffanti & Haas, 2001:1153), whereas Pyrimethamine is used in the treatment of uncomplicated malaria (Tracy & Webster, 2001:1060). Both of these APIs are known to exhibit polymorphism (Sharma *et al.,* 2006; Tutughamiarso & Bolte, 2011:438) and surveillance studies have found final pharmaceutical products (FPPs) of these APIs to be susceptible to being sub-standard (Abdo-Rabbo *et al.,* 2005:28; Amin *et al.,* 2005:595; Chepkwony *et al.,* 2007:59; Ethiopian Pharmaceutical Association, 2009).

Both of these APIs are known to be poorly soluble in physiological media, hence differences in the solid state chemistry of these ingredients may influence their solubility or bioavailability. To evaluate the potential impact that the solid state chemistry of Efavirenz and Pyrimethamine may have on their safety and efficacy, the aims of this study were to:

i) Discover new crystal modifications of Efavirenz and Pyrimethamine (if possible);

ii) Comprehensively characterise and evaluate the physico-chemical properties of any newly identified crystal modifications of Efavirenz and Pyrimethamine; and

iii) Elaborate on any unexplored characteristics of known crystal modifications of Efavirenz and Pyrimethamine.

In light of the aims of this study, the purpose of this chapter was to present an overall introduction to the study by:

i) Describing the solid state chemistry of APIs (Section 1.1);

ii) Discussing the important roles of solid state chemistry in the pharmaceutical industry (Section 1.2); and

iii) Summarising available literature to date regarding the solid state chemistry of known forms of Efavirenz and Pyrimethamine (Section 1.3).

1.1 The solid state of active pharmaceutical ingredients

The solid state properties of an API are governed by the internal arrangement of its molecules (internal structure) and by the external shape/morphology thereof. It is the combination of these internal and external properties that defines the properties of the solid form (Byrn *et al.,* 1999:3). Sections 1.1.1-1.1.3 discuss the aspects relating to the internal structure of a solid, whereas Section

1.1.4 elaborates on the attributes pertaining to its external structure. Section 1.1.5 summarises the techniques and methodologies used to evaluate and study polymorphic differences.

1.1.1 Crystallisation, crystal classes and lattice types

Most APIs exist as solids at ambient conditions (Byrn *et al.,* 1999:3). These solids can be classified as either *crystalline*, or *amorphous* forms (Buckton, 2002:141). The process during which random molecules order themselves in a specific solid arrangement is referred to as crystallisation (Byrn *et al.,* 1999:15). Crystallisation usually occurs from a super-saturated solution, which requires the formation of a critical number of ordered molecules, or unit cells, into nuclei (i.e. nucleation) (Byrn *et al.*, 1999:16-17). The repetitive arrangement of unit cells within a three-dimensional matrix, called a lattice, gives rise to a specific solid form (Byrn *et al.,* 1999:5). A schematic representation of the formation of a solid is given in Figure 1.2.

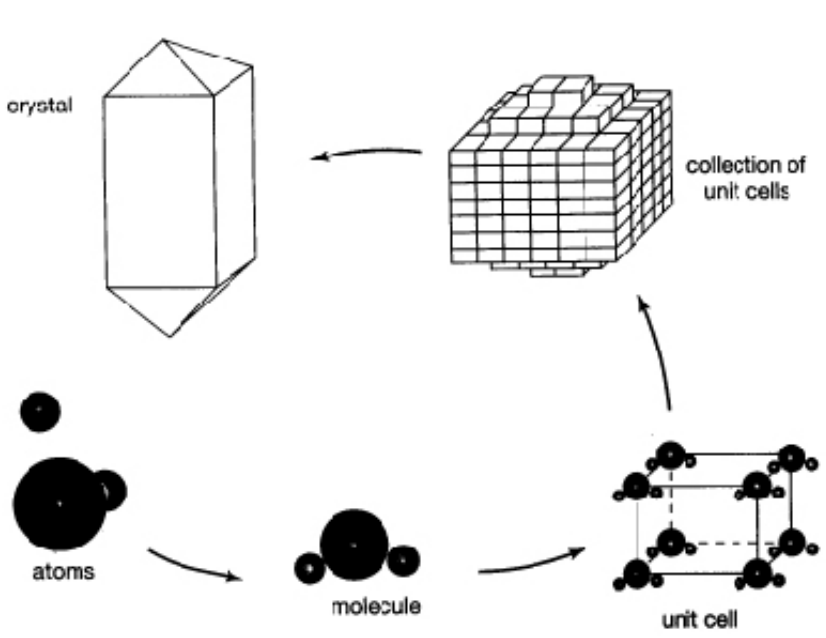

Figure 1.2 Schematic representation of the formation of a crystal (Anon, 2007).

The thermodynamic stability of the formed crystal is influenced by the binding forces holding the molecules together, as well as by the packing symmetry/density of the unit cells (Byrn *et al*., 1999:7).

1.1.1.1 Binding forces and packing symmetry

Different forces are responsible for holding crystals together. Ionic crystals are held together through ionic bonds, whereas organic crystals are maintained through non-covalent interactions (Byrn *et al*., 1999:7). Since the majority of APIs are organic crystals, only non-covalent interactions are discussed in this section. Non-covalent interactions are divided into hydrogen bonding and non-covalent

attractive forces. Hydrogen bonding (H-bonding) exists between donor and acceptor functional groups, whereas non-covalent attractive forces depend on dipole moments, polarity and the electron distribution of molecules. Hydrogen bonding is much stronger than non-covalent attractive forces. Duly, the type (strength) and intricacy of the bonds within a crystal contribute towards the thermodynamic (or physical) stability of the crystal lattice (Byrn *et al*., 1999:7).

The symmetry of the molecules (or lack thereof) determines the packing of a crystal. If the symmetry of the molecule allows for close packing through close fitting, stronger crystals are formed, compared to molecules that do not arrange easily (Byrn *et al.,* 1999:8). The close packing theory of Kitaigorodski (as cited in Byrn *et al*., 1999:8*)* suggests that the more efficient the packing density of a solid form, the less free energy it possesses. Similarly, the density rule of Burger and Ramberger (as cited in Byrn *et al.,* 1999:8) avers that with an increase in the packing density, comes an increase in crystal stability. A combination of these two rules have contributed towards the understanding that the solid form arrangement being the most stable, to possess the least amount of free energy, and to be the most densely packed out of the polymorph population. The energy differences amongst polymorphs therefore allow for a hierarchy of thermodynamic stability to exist within a polymorph group.

Now that it is known how crystals are formed, the discussion continues with crystal classes and lattice types.

1.1.1.2 Crystal classes and lattice types

The three-dimensional points of a crystal lattice (Figure 1.3) are defined by three fundamental translation vector axes (*a*, *b* and *c*) and the angles (α, β and γ) between two adjacent crystal axes (Brittain, 1999:75). The different possibilities that these crystal axes and their respective angles allow, are summarised in Table 1.1.

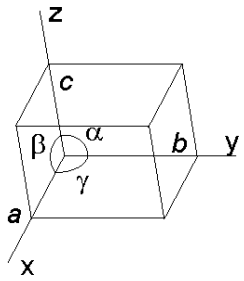

Figure 1.3 Schematic representation of the translation vectors and angles of a unit cell (Anon, 2007).

From the seven fundamental crystal classes (Table 1.1), Auguste Bravais (as cited in Brittain, 1999:78) concluded that fourteen types of lattices may exist in a three-dimensional space, with the assumption that the unit cell displays symmetry. The fourteen different types of lattices are summarised in Figure 1.4.

Table 1.1 The seven fundamental crystal classes defined according to their unit cells (Brittain, 1999:77)

Crystal class	Crystal axes	Angles
Cubic	a = b = c	$\alpha = \beta = \gamma = 90°$
Tetragonal	a = b ≠ c	$\alpha = \beta = \gamma = 90°$
Orthorombic	a ≠ b ≠ c	$\alpha = \beta = \gamma = 90°$
Monoclinic	a ≠ b ≠ c	$\alpha = \gamma = 90°; \beta \neq 90°$
Triclinic	a ≠ b ≠ c	$\alpha \neq \beta \neq \gamma \neq 90°$
Hexagonal	a = b ≠ c	$\alpha = \beta = 90°; \gamma = 120°$
Trigonal	a = b = c	$\alpha = \beta = 90°; \gamma \neq 90°$

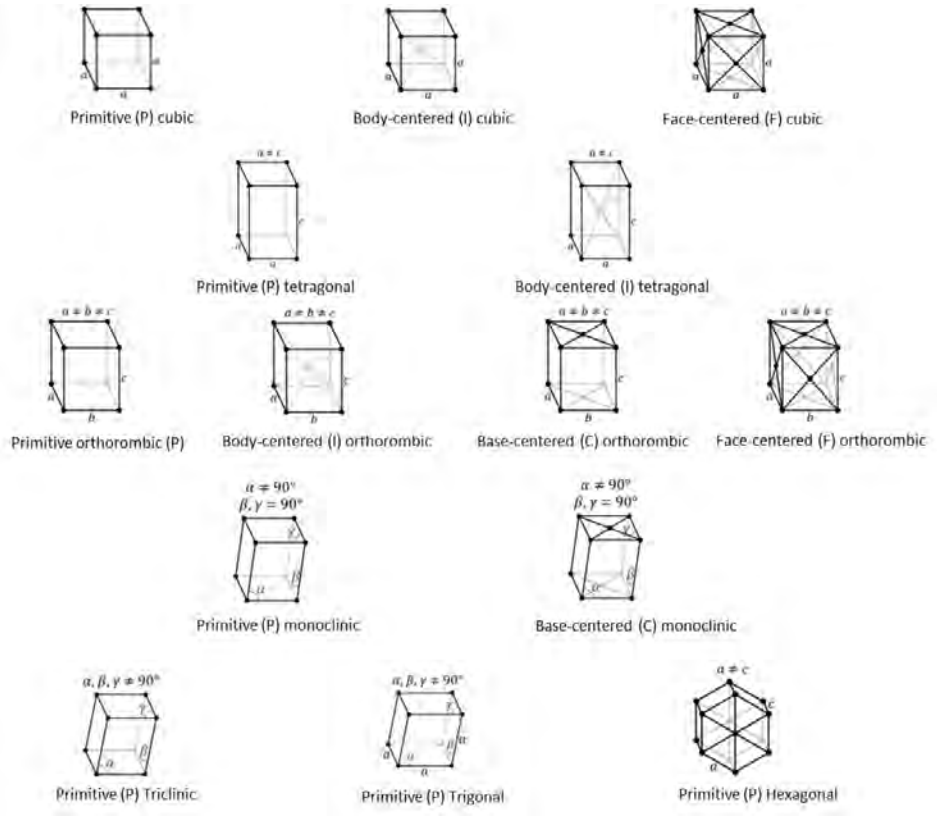

Figure 1.4 The fourteen Bravais lattice systems (as cited in Brittain, 1999:78).

The structure of a crystal is assigned to one of the seven crystal classes, to one of the fourteen Bravais lattices (Figure 1.4) and to one of the possible two hundred and thirty (230) space groups.

Space groups are representations of the ways in which the macroscopic and microscopic symmetry operations can be self-consistently arranged in space (Byrn *et al.,* 1999:54). The designation of a space group consists of the crystal system (Table 1.1), lattice centring designations (Figure 1.4 – P, I, C, F) and the description of the angle of rotation. 76% of organometallic and organic (including APIs) compounds occur in space groups $P2_1/c$ (monoclinic), $P2_12_12_1$ (orthorombic), $P1$ (triclinic), $P2_1$ (monoclinic) and C_2/c (monoclinic) (Byrn *et al.,* 1999:48; Sheth & Grant 2005:36).

1.1.2 Techniques used for crystal formation and modification

Crystals may be produced from a variety of techniques (Cains, 2009:76-138). A list of the most commonly used techniques include:

- Crystallisation from solution;
- Cooling crystallisation;
- Seeded crystallisation (seeding of a super-saturated solution with seeds of the specific crystal form of the same API);
- Evaporative crystallisation;
- Anti-solvent crystallisation;
- Reactive crystallisation;
- Crystallisation from melts;
- Mechano-chemical methods (such as liquid assisted grinding);
- Thermal methods;
- Slurrying;
- Crystallisation caused by additives (foreign seeding);
- Desolvation of solvatomorphs;
- Crystallisation by ultra-sound; and
- Crystallisation in capillaries.

The most commonly used technique for forming crystalline materials is through crystallisation from solutions (usually super-saturated solutions). Contrary, crystallisation from the melt is the technique least used (Cains, 2009:87). For the purpose of this study, both these techniques were utilised to evaluate their abilities in modifying the crystalline/amorphous states of Pyrimethamine and Efavirenz. These two methods are discussed next.

1.1.2.1 Crystallisation from solution

Crystallisation from solution was chosen to modify the crystal structure of Pyrimethamine. This technique is usually the first choice when it comes to research screening procedures and for manufacturing at large scale (Cains, 2009:87). Crystallisation usually produces thermodynamically stable forms and is considered the most reproducible technique for a given form under specified conditions (Cains, 2009:87-88). Since various solvents may be used to prepare different solid forms, an understanding of the solubility profile of the API is required.

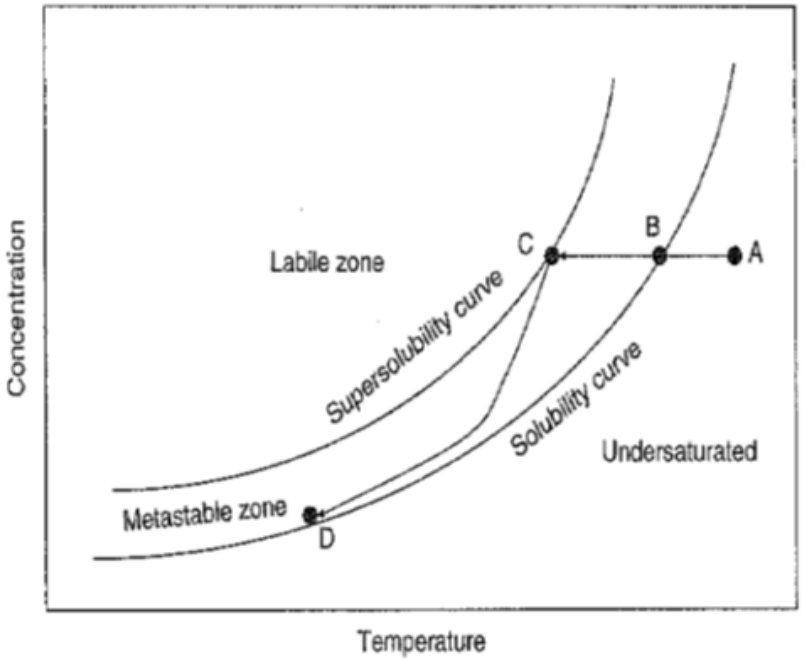

Figure 1.5 A solubility curve illustrating the formation of different stable forms of an API (Cains, 2009:91).

The above solubility curve (Figure 1.5) represents the Gibbs phase rule which states that, at a given temperature, a unique concentration of the solute would exist, corresponding to its equilibrium. Figure 1.5 demonstrates that, should an initially, under-saturated solution (point A) be cooled at a constant rate to pass the solubility line at point B, it would become super-saturated, which would initiate nucleation at point C to return the system back to equilibrium (point D). The temperature and rate of temperature change play a critical role in the formation of different crystal modifications when crystallisation occurs from a solution. The metastable zone (BC) is an indication of the kinetics of nucleation and represents the driving force that substantiates polymorph selectivity (Figure 1.6). Figures 1.5 and 1.6 represent a polymorphic system consisting of numerous possible solid forms, which may crystallise under varying kinetics of nucleation (Cains, 2009:90-91).

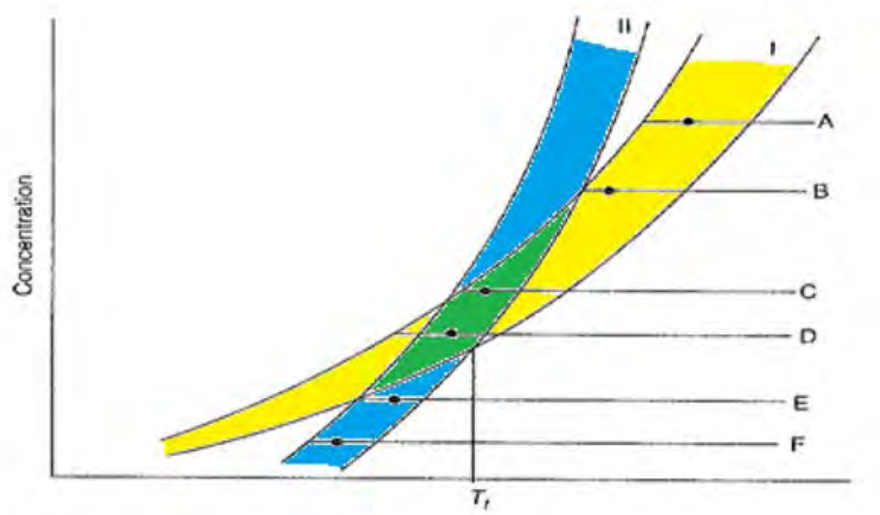

Figure 1.6 A solubility curve illustrating polymorph selectivity of crystal forms (adapted from Cains, 2009:93).

Figure 1.6 illustrates that Form II is stable below T_t, whilst Form I is stable above T_t. Cooling from point A would result in the crossing of the metastable zone of Form I, causing crystallisation, while the solution would remain unsaturated with respect to Form II. At point B, the nucleation of Form I would occur at the saturation point of Form II. At point C, the solution would become saturated with Form I, but in this case saturation of Form II would occur before the metastable zone of Form I is reached. Crystallisation of Form I would therefore occur from a solution that is also super-saturated with Form II, and are mixtures of the two forms therefore also possible as a result of cross-seeding. At point D, a mixture of forms is even more likely. Points E and F represent the conditions under which Form II may be prepared (Cains, 2009:92).

Figure 1.7 shows that an increase in the cooling rate causes the metastable zone to expand. This larger area of the concentration *versus* temperature function that is created would then ultimately favour the nucleation of thermodynamically unstable forms (Cains, 2009:93).

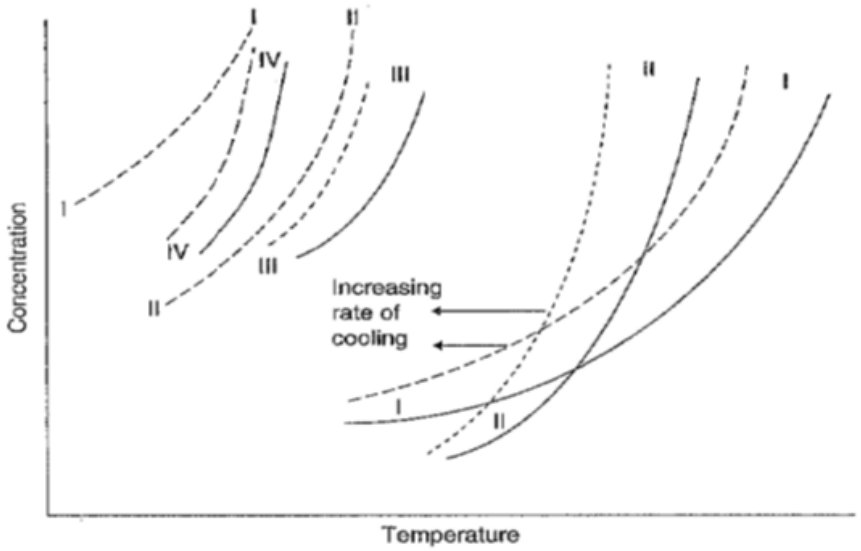

Figure 1.7 A solubility curve illustrating the broadening of the metastable zone and the possibility of unstable forms (Cains, 2009:93).

It can thus be concluded that crystallisation conditions are regulated by the solubility of the compound, which can either be controlled to produce a specific form, or deliberately manipulated to screen for or obtain potentially different polymorphic forms.

1.1.2.2 Crystallisation from the melt and quench cooling

Melt crystallisation is commonly used as a purification technique in the production of commodity crystal. It is not often used in pharmaceutical manufacturing, as most APIs decompose when approaching their melting points. Melt crystallisation could, however, produce forms that are inaccessible through solution based methods (e.g. recrystallisation) (Cains, 2009:107). Similarly to recrystallisation, crystallisation from the melt is governed by the same principles in terms of kinetics *versus* thermodynamics, but also by a cooling driving force (instead of super-saturation) (Figure 1.8).

Quench cooling is a forced solidification technique that often result in the formation of amorphous forms. It involves the rapid cooling of the melted substance to yield the solidification/"freezing" of the molecules in a disordered state (amorphous state). The quench cooling technique was selected for this study for the purpose of modifying the crystal characteristics of Efavirenz.

The phase diagram in Figure 1.8 illustrates the relationship between the crystalline and amorphous states at various temperatures as a function of density (volume) and energy. This graph shows that a molten solid (liquid) would return to the crystalline state with a gradual decrease in temperature, as it allows for the orderly (and dense) packing of unit molecules. An abrupt decrease in temperature would, however, force solidification of the melt (liquid form), resulting in a "frozen" state of motion of molecules in random order (glass) (Buckton, 2002:146).

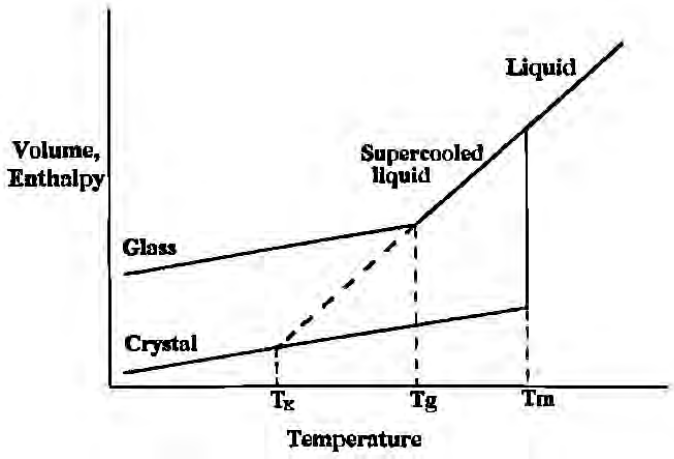

Figure 1.8 The difference in thermal behaviour between crystalline and amorphous solids (Hancock & Zografi, 1997:2), where T_K represents the crystallisation temperature, T_g the glass transition temperature and T_m the melting point of the crystal form.

Below the T_g (glass transition temperature) the amorphous form presents as a brittle, *glassy state* and above the T_g as a flexible, *rubber state* (Buckton, 2002:146; Yu, 2001:28). The molecules of an amorphous form in the rubbery state have substantially more configurational motion than those in the glassy state (Byrn *et al.,* 1999:249). Amorphous forms possess much more free energy and would therefore have an inherent tendency to convert into a more preferable resting (crystalline) state (Byrn *et al.,* 1999:249; Yu, 2001:30). For conversion to take place, the molecules of the amorphous form need to be in motion. Accordingly, keeping the glass at temperatures below the T_g, would cause it to remain in the amorphous state for longer periods, compared to when keeping it at temperatures exceeding T_g. The thermodynamic stability (ease of conversion) of an amorphous form is therefore largely dependent upon its T_g value, as well as the conditions it is exposed to.

Recrystallisation from solution (Section 1.1.2.1) may result in the formation of true polymorphs, solvatomorphs, amorphous forms and/or co-crystals, whereas quench cooling from a melt (Section 1.1.2.2) usually only results in the formation of amorphous forms. The classification and characteristics of these different types of solids are discussed in Section 1.1.3.

1.1.3 Classification of solid forms

Based upon their internal crystal structures, pharmaceutical solids can either be classified as *crystalline* (including polymorphs and solvates (solvatomorphs, and hydrates)), or as *amorphous solids* (Figure 1.9). The classification of solid forms is dependent upon certain criteria, as discussed in Sections 1.1.3.1 -1.1.3.4.

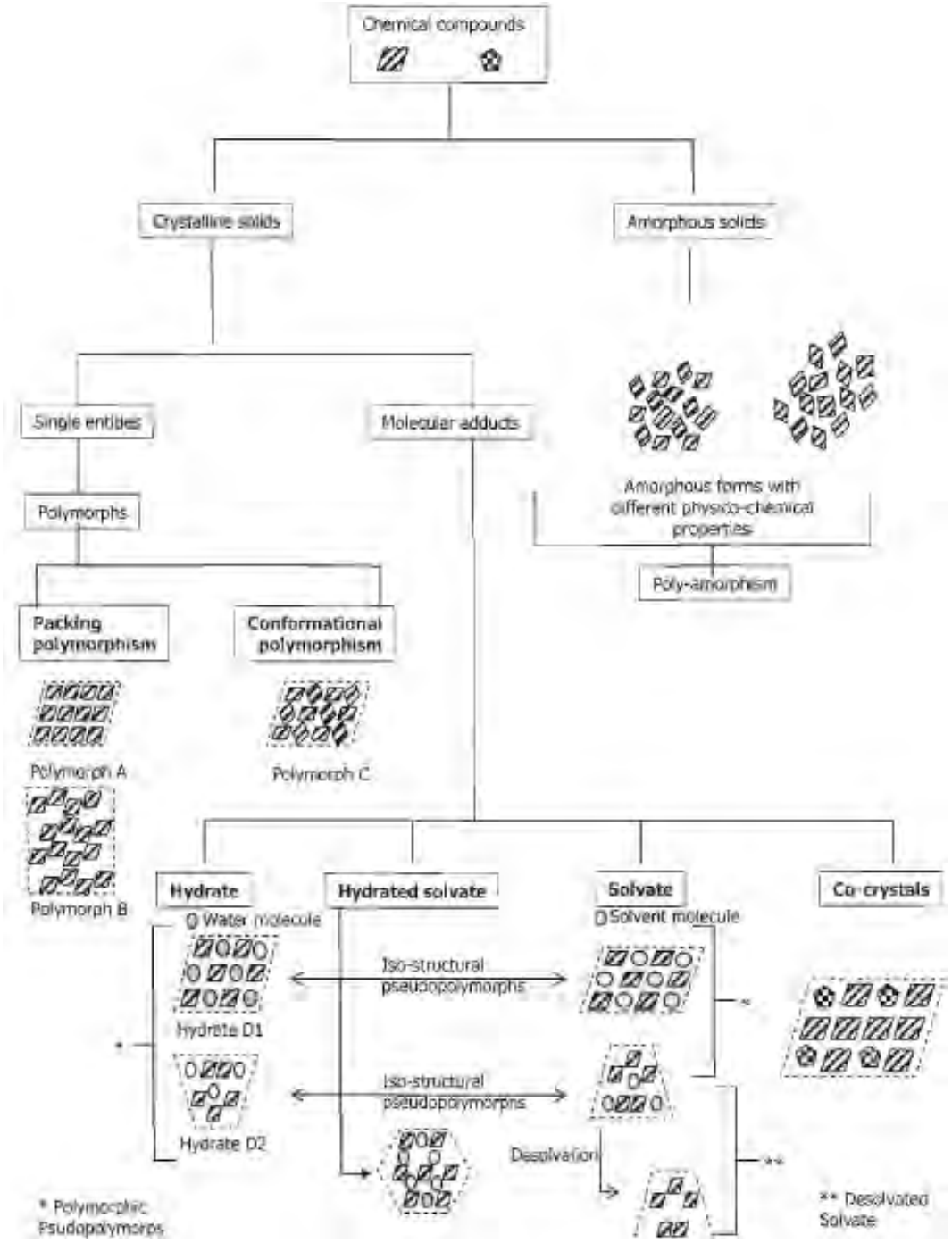

Figure 1.9 Classification of an API based upon its internal structure (Brits, 2008:5).

1.1.3.1 True polymorphs

True polymorphs (packing polymorphs) of a compound are solid forms that are chemically equivalent to each other (same elemental composition), while differing only in the specific order in which the unit cells occur (Carstensen, 2001:117). The various true polymorphs of an API usually exhibit different physical properties as a result of the different dimensions, shapes, symmetries and void volumes of

the unit cells of the various polymorphs (Grant, 1999:5-8). Different polymorphs of the same API may or may not have different crystal habits (see Section 1.1.4).

1.1.3.2 Pseudo-polymorphs

Different solvents (e.g. water, methanol, ethanol and acetone) are employed by the pharmaceutical industry during manufacturing processes, such as granulation, or as part of API synthesis (Byrn *et al.,* 1999:236; Grodowska & Parczewski, 2010:3). Solvents may be introduced into the crystal lattice through various methods, such as recrystallization from solvents, or moisture absorption (Brittain, 2009:505; Byrn *et al.,* 1999:239). Crystal products duly obtained are referred to as *hydrates*, or *solvates*, or *hydrated solvates* (Buckton, 2002:144). When the included solvent is water, it is referred to as a *hydrate.* When any other solvent molecule(s) is included in the crystal, it is referred to as a solvate. When both types of molecules (i.e. solvent and water) are included in the lattice, the form is referred to as a *hydrated solvate*. *Hydrates* and *solvates* of a compound are referred to as *pseudo-polymorphs*, or *solvatomorphs* (Yu *et al.,* 1998:118).

Pseudo-polymorphs cannot be considered as true polymorphs, due to the added solvent molecules within the lattice (not chemically equivalent to anhydrous forms, or true polymorphs) (Yu *et al.,* 1998:118). It is, however, possible for some pseudo-polymorphic forms to exhibit polymorphism, i.e. it is possible for a compound to present in two or more different pseudo-polymorphic forms, each containing the same solvent in the same quantities, within each respective lattice structure (Van Tonder *et al.,* 2004:417). The term *polymorphic pseudo-polymorphism* is commonly used for such instances, with the forms either being *polymorphic hydrates*, or *polymorphic solvates* (Yu *et al.,* 1998:118).

Solvent molecules can be incorporated in stoichiometric and non-stoichiometric quantities (in different ratios) within the crystal lattice of a solvate (Byrn *et al.,* 1999:234). The stoichiometry of solvent inclusion is normally depicted by the prefix of the pseudo-polymorph, for example, Estradiol *hemi*hydrate (Park *et al.,* 2005:407), Niclosamide *mono*hydrate (Van Tonder *et al.,* 2004:417), Pantoprazole *sesqui*hydrate (Zupancic *et al.,* 2005:59). As discussed in section 1.1.1.1, different forces are responsible in maintaining a crystal. Similarly, these forces are responsible for solvent inclusion within a pseudo-polymorphic form. It is thus understandable that certain forces would allow for stronger interactions between the solvent and host molecules (and *vice versa*). The thermal stability (ease of desolvation) of the pseudo-polymorph is therefore directly dependent upon the extent of intermolecular interaction that exists between the host and solvent molecule(s) and the way in which the solvent molecules are incorporated within the crystal lattice of the pseudo-polymorphic form (Byrn *et al*., 1999:7).

1.1.3.3 Desolvated (dehydrated) pseudo-polymorphs

Solvent molecules can be removed from the crystal lattice (i.e. desolvation) of a pseudo-polymorphic form through drying, for example. In most cases, removing the solvent from the lattice of a pseudo-polymorph would result in crystal collapse, as the solvent molecules contribute towards the integrity of the lattice arrangement thereof (Yu *et al.*, 1998:124). Crystal collapse would give rise to the formation of a different crystal, or *true polymorph* (Yu *et al.*, 1998:124). However, should the solvent not significantly impact on the stabilisation of the crystal lattice, it is likely that the lattice would not collapse during desolvation. In such case, the original lattice would remain approximately unchanged and display similar properties than those of its parent pseudo-polymorph (Yu *et al.*, 1998:124). The form resulting from this process is referred to as a *desolvated solvate*/*isomorphic desolvate*, or *isomorph* (Byrn, 1982:7; Yu *et al*., 1998:119).

1.1.3.4 Amorphous forms

When the unit cells of a solid form have no distinct packing arrangement within the lattice, it is called an *amorphous solid* (Buckton, 2002:145). Cholecalciferol, Sulfisoxazole, Stilbestrol, Phenobarbitol, Quinidine, Methyltestosterone, Phenylbutazone, Atropine and Ergocalciferol are some examples of APIs that may present in amorphous forms (Byrn *et al.,* 1999:251). *Amorphous solids* may be considered as super-cooled liquids in which the molecules are in a random order, equivalent to the liquid state (Sinko, 2006:37). Amorphous solids can be prepared through rapid cooling, grinding, lyophilisation, spray drying, desolvation of a solvate, granulation, and quench cooling of the melt (Byrn *et al.,* 1999:22; Hancock & Zografi, 1997:1; Yu, 2001:28). When a solid can present in different amorphous forms (i.e. amorphous forms with different thermodynamic stabilities), it is said to exhibit *poly-amorphism* (Hancock *et al.*, 2002:1152). *Poly-amorphism* is not an uncommon phenomenon, as it has been reported in relation to various compounds (Hancock *et al.*, 2002:1152; Kieffer, 2002:644).

Amorphous solids represent a broad (halo-shaped) X-ray powder diffraction (XRPD) pattern (discussed in Section 1.1.5; example shown in Figure 1.18) and have no definite melting points (Buckton, 2002:145). They do, however, have a specific temperature where major changes in their properties are exhibited, called the *glass transition temperature* (T_g) (see Section 1.1.2.2).

Amorphous solids possess properties, significantly different from their crystalline counterparts. They often have higher solubility, a higher dissolution rate and better compression properties than their corresponding crystalline form(s), and may be very useful in the pharmaceutical industry (Yu, 2001:28). Amorphous forms are, however, the least thermodynamically stable solid form among the solid form population, and often present with problems relating to thermodynamic stability and/or unpredictable behaviour (Yu, 2001:28).

As stated in Section 1.1.1, it is not only the internal arrangement of a crystal that may affect product quality, but a combination of internal and external characteristics that determine the feasibility of a solid form. The external shape (morphology) of crystals is discussed next in Section 1.1.4.

1.1.4 Crystal morphology

The external shape of a crystal is referred to as crystal morphology (or crystal habit) and may resemble many different forms, such as needles, rods and plates (Byrn *et al.*, 1999:12). Crystal shape is a consequence of the rate at which the different faces of a crystal grows (Figure 1.10).

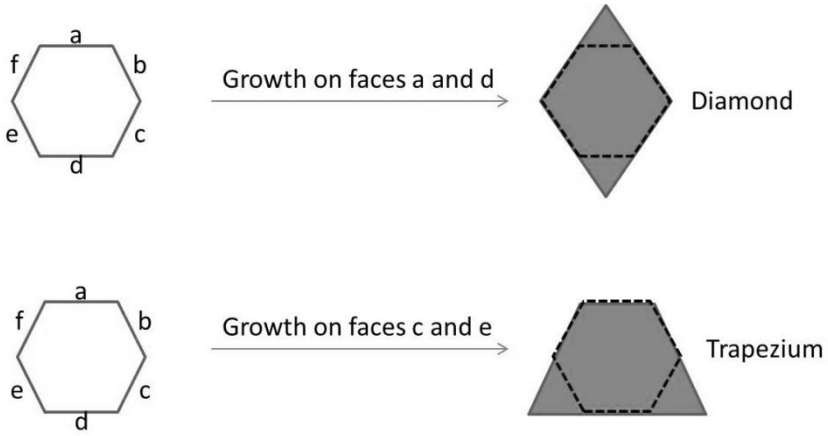

Figure 1.10 Varying growth rates of different crystal faces giving rise to different morphologies (adapted from Buckton, 2002:148).

The rate and extent of growth on a specific face is dependent upon the functional groups that are exposed on that specific surface (see Figure 1.11), and the affinity of the solute for the solvent and the faces of the crystal. The faces that are most likely to grow are those that have the highest affinity for the solvent (Buckton, 2002:148).

The Miller index, introduced by W.H. Miller (as cited in Byrn *et al.,* 1999:48), is used to describe the planes and directions of crystal lattices. This notation system allows for the labelling of crystal faces, based upon the three lattice vectors (known as *h*, *k* and *l*), which define a unit cell. Each index is assigned an integer value of 1 or 0 and denotes a plane orthogonal to a direction in the basis of the reciprocal lattice vectors. The most prominent faces of the crystal habits featured in Figures 1.11 and 1.13 are labelled with their respective Miller indices.

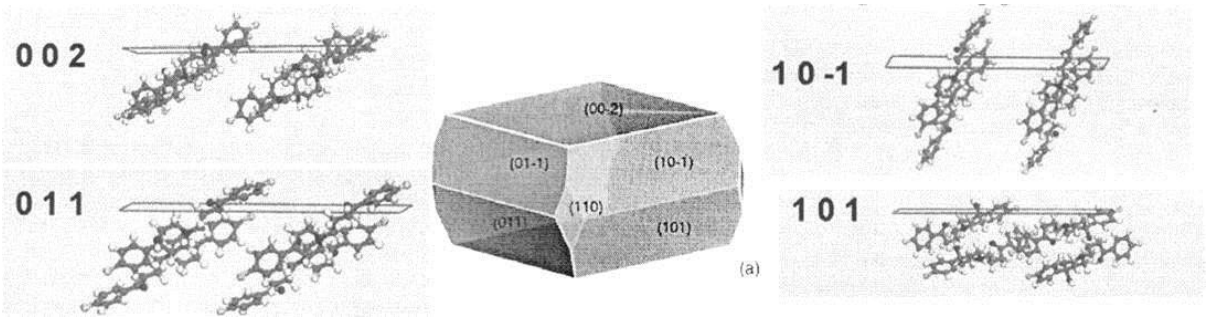

Figure 1.11 One possible crystal habit of Haloperidol (middle), along with stereoscopic views of its most prominent faces, showing the differences in orientation of haloperidol molecules and their functional groups on the different exposed surfaces (adapted from Destri *et al*., 2011:4902-4903).

Despite morphology and polymorphism being closely related, these properties are indeed independent from one another, meaning that a single form may present in different habits (Figure 1.12, top). However, a solid form should not be misconstrued as having the inability to change both of these properties (internal and external arrangement) during the same crystallisation process (Figure 1.12 bottom).

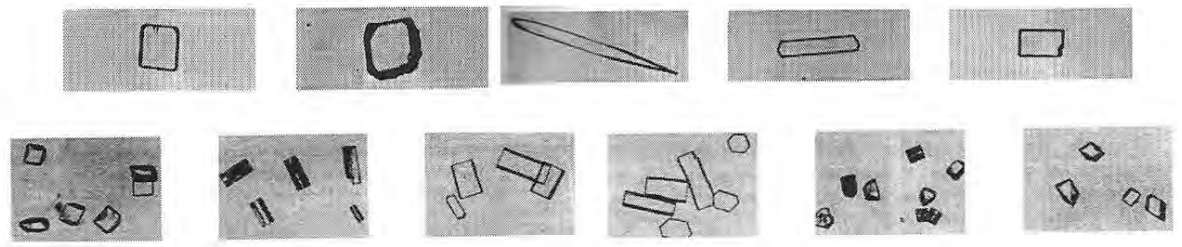

Figure 1.12 Different crystal habits of the same crystal lattice of Aspirin (top), and different crystal habits of different β-Estradiol solid forms (bottom) (adapted from Byrn *et al.,* 1999:13-14).

Computer assisted molecular modelling has improved significantly in recent years, owing to substantial advancements in computer processing and graphics performance. Several researchers in the pharmaceutical industry (Destri *et al*., 2011:4902-4903; Kiang *et al.,* 2009:80; Nowell *et al.,* 2005; Roberts *et al.,* 2000:277; Snyder & Doherty, 2007:1337) have proven that predicting and evaluating crystal morphology with computer technology could be very successful. Examples of predicted morphologies are illustrated in Figure 1.13.

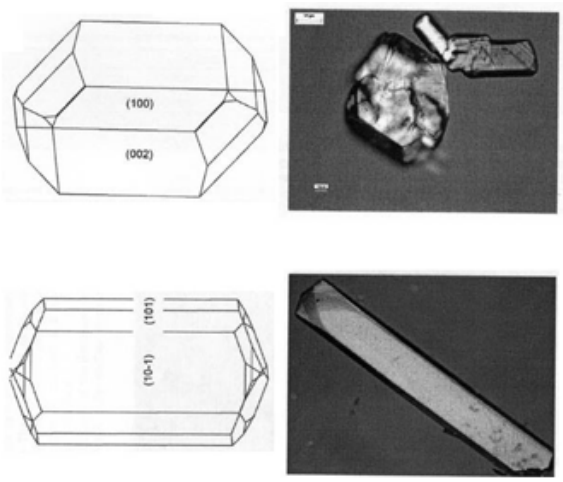

Figure 1.13 Computer predicted morphologies (left) of an investigated API, compared to their microscopic counterparts (right) (Kiang *et al.,* 2009:80).

Microscopy is the most commonly employed analytical tool for evaluating crystal morphology. It is discussed next in Section 1.1.5, together with a range of other techniques that are used in combination when studying polymorphism.

1.1.5 Analytical techniques and methodologies used in the characterisation of different solid forms

Table 1.2 summarises the methods and techniques that are employed to study the characteristics of solid forms. It should be noted that most of the techniques listed in Table 1.2, i.e. X-ray powder diffraction (XRPD), diffuse reflectance Fourier transform-infra red spectroscopy (DRIFT-IR), differential scanning calorimetry (DSC), Karl Fischer moisture analysis (KF) and thermo-gravimetric analysis (TGA), may either be used for quantitative determinations of crystallinity, or to describe polymorphic conversion, depending on the specific situation and on the extent to which the API allows for such determinations (bearing in mind that some techniques may be more suitable than others given the specific study conditions).

Table 1.2 Analytical techniques and methodologies used in polymorph research (adapted from Yu *et al.,* 1998:124)

Type	XRPD	DRIFT-IR	Thermal methods (such as DSC and TGA)	Microscopy	Dissolution / solubility	Water content
True polymorphs	Unique diffraction peaks.	Characteristic spectra. Sensitive to H-bonding.	Unique melting-, heat of fusion- and transition points.	Colour, crystal habit.	Due to differences in thermodynamic stabilities among different solid forms and the potential differences in particle sizes and morphologies, different solid forms present with different solubility and dissolution behaviours. Routine solubility measurements and powder dissolution studies are employed to study these differences.	N/A
Pseudo-polymorphs	Unique diffraction peaks.	Unique solvent bands. Shifted spectra bands. Sensitive to H-bonding.	Dehydration/desolvation peaks. Weight loss.	Colour, crystal habit. Desolvation or dehydration by hot-stage microscopy (in presence of silicon oil).		Together with TGA, KF may be used to determine the water content of hydrates.
Isomorphic forms	Slightly different pattern to that of parent pseudo-polymorph.	Solvent band absent compared to parent pseudo-polymorph. Spectra band shifted.	Disappearance of dehydration/desolvation peaks, same melting point as parent pseudo-polymorph.	Possibly visible cracks and fissures after parent desolvation.		N/A
Amorphous solids	No diffraction peaks/ broad/halo shaped.	Broadened spectra.	Glass transition, often followed by recrystallisation.	Irregularly shaped particles.		N/A
Mixture of crystal forms	Composite pattern of crystalline components.	Composite spectra of all components.	Mixture of composite components.	Composite of mixture.		Together with TGA, KF may be used to determine the water content of hydrates.

1.2 The influence of polymorphism on API synthesis, final product manufacture, final product integrity, treatment efficacy and patient safety

It is understood that various polymorphs of an API may exhibit different physical properties, due to differences in internal and external arrangements. Of the most common properties that may differ among polymorphs are crystal density, hardness, hygroscopicity, melting temperature, solubility, dissolution, stability (chemical and physical) and surface free energy (Grant, 1999:7). Differences in crystal habits (with or without polymorphic changes) may lead to differences in properties, such as flowability, syringeability, filterability, compressibility, bulk density and dissolution (Byrn *et al.,* 1999:4). The following sub-sections describe the ways through which the solid state chemistry of an API may influence different areas of pharmacy (from API synthesis to patient care) (Figure 1.14). As mentioned in the introduction to this chapter, human error and/or negligence during any of these steps may contribute to medicines becoming sub-standard or unsafe. This section reveals how even the smallest or seemingly insignificant influences may affect API polymorphism, and ultimately the quality and safety of a final pharmaceutical product (FPP).

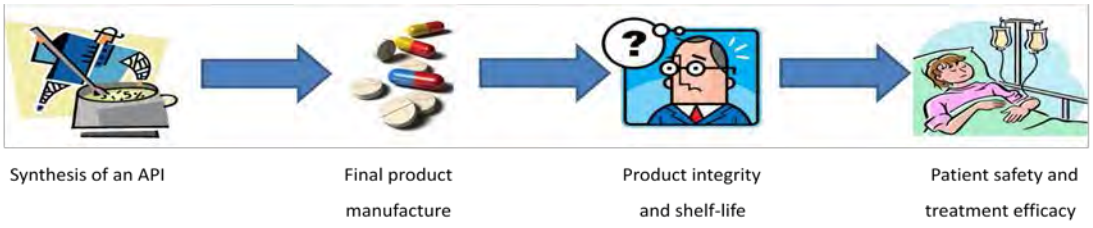

Figure 1.14 Aspects of pharmacy that may be influenced by the solid state chemistry of APIs.

1.2.1 Synthesis of an active pharmaceutical ingredient

As with any chemical compound, various potential pathways exist through which to synthesise an API (commonly referred to as route of synthesis). Most of the procedures associated with the synthesis of an API are patented, many of which solely describe the preparation of specific polymorphic, or pseudo-polymorphic, or amorphous forms of the API. The patents associated with the synthesis of Donepezil (its salts, polymorphic forms, intermediates, etc.) are summarised in Table 1.3 to serve as an example.

Table 1.3 Patents associated with the synthesis of Donepezil, its salts and different crystal forms

Patent title	Reference
Process for the preparation of Donepezil hydrochloride	Nagarimadugu *et al*., 2011
Process and intermediate for preparation of Donepezil	Pathi *et al.,* 2011
Crystalline forms of Donepezil hydrochloride	Parthasaradhi *et al.,* 2009
Procedure for the preparation of highly pure Donepezil	Aggarwal *et al.,* 2010
Synthesis and preparations of intermediates and new polymorphs thereof useful for the preparation of Donepezil hydrochloride	Soldevilla, 2009
Polymorphs of Donepezil salts, preparation methods and uses thereof	Zhang, 2010

It is possible for solid state inconsistencies to develop during routine API synthesis, if the recrystallisation process is not suitably controlled. Aptuit (2006), for example, faced such a challenge when an antibiotic product suddenly presented with poor flow properties after twenty years of routine manufacturing, using the same manufacturing techniques and principles. It was found that although there had been no change in polymorphic form among affected and unaffected batches, a slight difference in crystallisation temperature had allowed for smaller particles of the same polymorphic form to crystallise and to cause powder flow problems.

Sometimes, even controlled crystallisation conditions, and what had originally been regarded as reproducible practices, may not achieve the intended crystal form anymore. This phenomenon is referred to as *disappearing polymorphs* (or elusive polymorphs), which is characterised by the inability to obtain a known form, despite having produced it routinely over long periods of time (Bombicz *et al.,* 2003:1957; Dunitz & Bernstein, 1995:193). A typical example of a disappearing polymorph is Progesterone, having five known polymorphs (Figure 1.15), of which one form can no longer be prepared. It was found that the impurity profile of each polymorph plays an important role in obtaining a specific Progesterone crystal form. Each Progesterone polymorph has its own impurity profile that allows for the induction (“seeding”) of crystal growth of its different forms. Unfortunately, researchers have to date been unsuccessful in identifying the exact structures of all of the possible impurities for this compound that could enable them to recreate the crystal growth inducing conditions to prepare this “elusive polymorph” (Merrison, 2011).

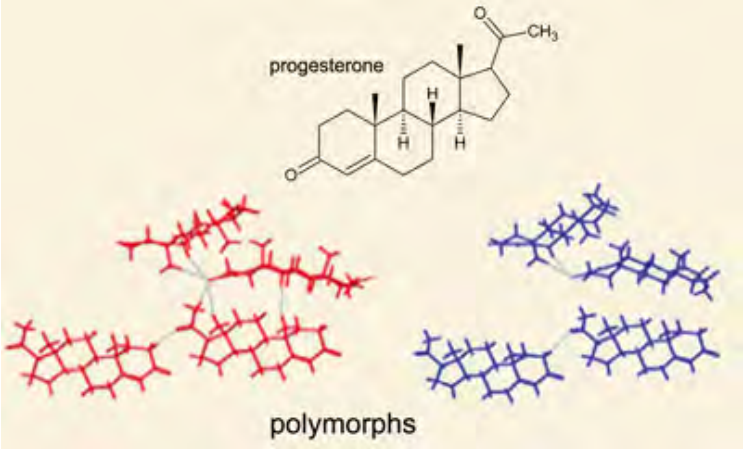

Figure 1.15 Diagrammatic representations of the two most common polymorphs of Progesterone (Merrison, 2011).

Recrystallisation is a technique that is commonly utilised as a final purification step during API synthesis. Some exemplary consequences of incorrect solvent usage are presented in Section 1.2.4.

Since an API is the main starting material in the manufacturing of a FPP, it is imperative to ensure that it is of high quality and that it possesses the desired properties for the required manufacturing procedure. The influence of polymorphism on final product manufacture is discussed in the section that follows.

1.2.2 The manufacturing of a final pharmaceutical product

Various pharmaceutical manufacturing techniques may influence the solid state characteristics of an API (Figure 1.16).

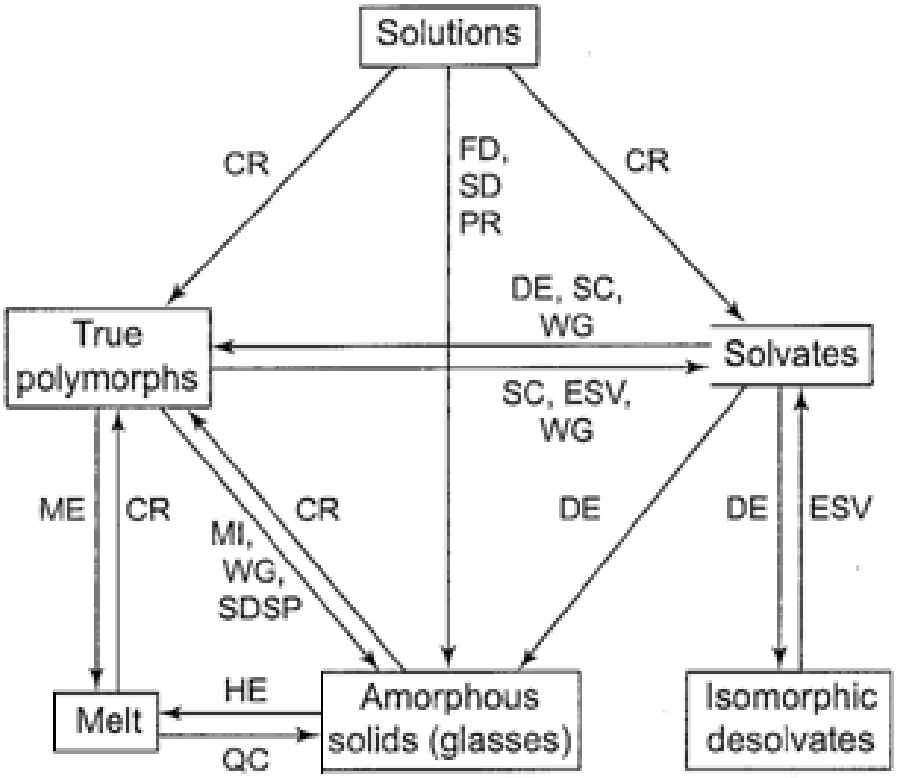

Figure 1.16 Pharmaceutical manufacturing techniques that may impact on polymorphism: Crystallisation (CR), desolvation (DE), exposure to vapour (ESV), freeze drying (FD), exposure to heat (HE), melting (ME), milling (MI), precipitation (PR), quench cooling (QC), slurry conversion (SC), spray drying (SD), solid dispersion (SDSP) and wet granulation (WG) (Yu *et al.,* 1998:119).

Figure 1.16 demonstrates how different types of solid forms of an API are intricately linked and how the possibility exists for each to interconvert, depending on the conditions being subjected to, hence emphasising the importance for the manufacturer to effectively control these techniques during manufacturing. Examples that illustrate how easily these manufacturing techniques may affect the solid state of an API are summarised in Table 1.4.

Table 1.4 Reported examples of commonly used manufacturing techniques having impacted on the solid state properties of certain APIs

Step	Effect/Example	Reference
CR	Recrystallisation, using different alcohols, resulted in different Rofecoxib solid forms, having different dissolution and solubility profiles.	Kumar *et al.*(2011:40)
WG	Incorrect mixtures of granulating solvent resulted in the transformation of anhydrous Carbamazepine into its sub-standard dihydrate.	Brittain (2009:527)
DE	Ineffective drying methods of Theophylline monohydrate resulted in mixtures of true polymorphs thereof.	Brittain (2009:533)
MI	Milling of crystalline Piroxicam resulted in its partial conversion into the amorphous form and in discolouration.	Brittain (2009:522)
HE/ME	Moricizine hydrochloride has two polymorphs, of which the one form is more prone to degradation than the other under the same conditions of increasing temperature. This may ultimately affect product quality, if using the one that is more prone to degradation.	Wu *et al.* (1994:1404)
FD	Slow freeze drying of 10% Mannitol resulted in a mixture of polymorphs (alpha and beta), whereas fast freeze drying of the same solution resulted in a different polymorph (delta).	Kim *et al.* (1998:931)
ESV	Exposing three different forms of Cephaloridine to the same humidity conditions showed differences in hygroscopicity. This revealed the potential for out-of-specification results during stability studies.	Byrn *et al.*(1995:951)
QC	Quench cooling of Glibenclamide resulted in an amorphous form thereof, while accompanied by chemical degradation.	Patterson *et al.* (2005:1998)
SD	Spray drying often produces materials of an unpredictable nature.	Brittain (2009:537)
SC	Rapid polymorphic conversion of Indomethacin occurred in an ethanol suspension (slurry).	Byrn *et al.* (1999:275)
PR	Different crystal forms of Sparfloxacin could be obtained from the same aqueous solution, if the precipitation kinetics are uncontrolled. The different forms exhibit differences in solubility, which may influence the bioavailability of this API.	Llinàs *et al.* (2008:114-118)
SDSP	Different ratios of Diflunisal and Polvinylpyrrolidone (PVP) during solid dispersion exhibited a preference for recrystallising as either polymorph I, or IV, depending on the ratio of the API:PVP.	Martinez-Ohárriz *et al.*(2002:717)

Theophylline serves as a typical example of how different conditions of granulation, drying and milling (pharmaceutical manufacturing techniques) may affect various characteristics of an API, and ultimately the dissolution profile of the final product (Debnath & Suryanarayanan,2004:1-11) (Figure 1.17).

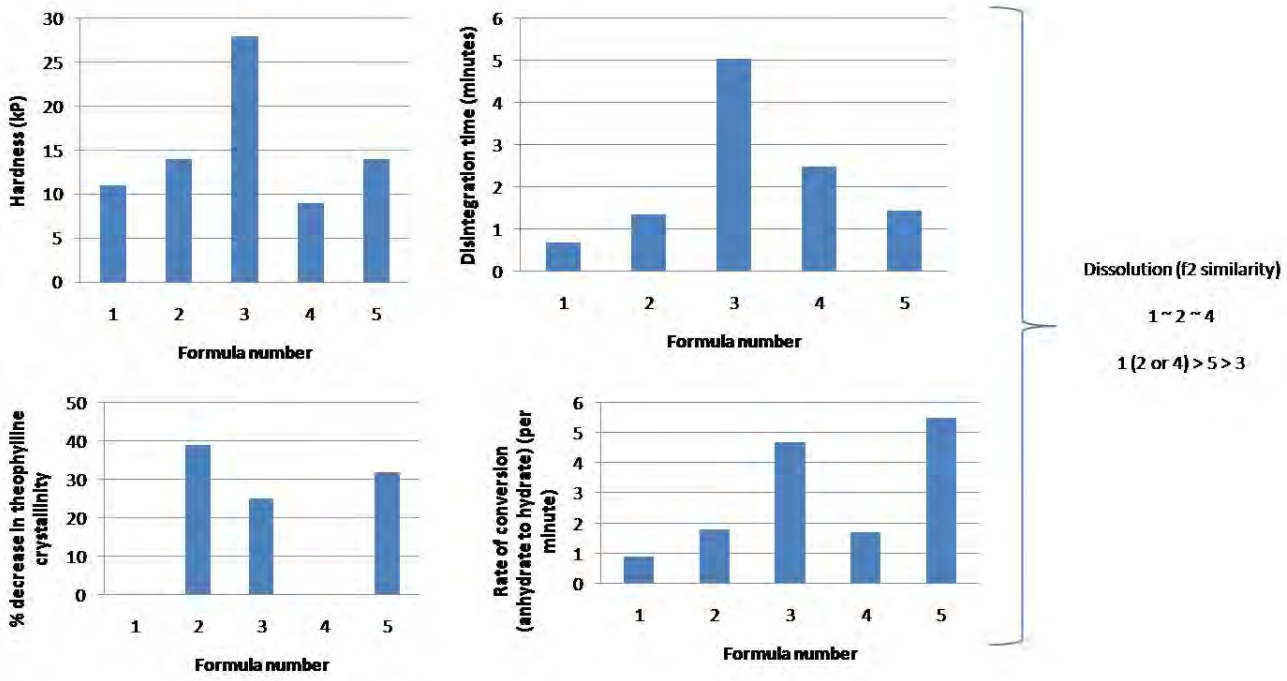

Figure 1.17 Graphs illustrating the impact of different manufacturing techniques on Theophylline tablet hardness (top left), disintegration (top right), percentage decrease in Theophylline crystallinity (bottom left), Theophylline conversion rate (bottom right), and ultimately the dissolution from different Theophylline formulae.

Where: 1 = unprocessed anhydrous Theophylline, 2 = anhydrous Theophylline ground for 30 minutes, 3 = wet granulation and drying of Theophylline at 50˚C, 4 = wet granulation and drying at 90˚C, 5 = anhydrous Theophylline ground for 10 minutes (adapted from Debnath & Suryanarayanan, 2004:1-11).

Besides manufacturing techniques (Table 1.4) that may induce polymorphic conversion during production (and subsequently affect the shelf life, or efficacy of a FPP), the suitability of the final product dosage form should also be considered. Two specific examples that link polymorphic form and the suitability of final dosage forms are Carbamazepine and Terazosin. It is well known that many APIs are formulated in suspensions for pediatric use (or powder for suspension). Carbamazepine may present in one of three possible polymorphs, each with a different morphology, of which all would convert into the dihydrate form upon exposure to water (following significantly different conversion kinetics), to ultimately render crystal forms unequal in their potential shelf lives (Tian *et al.,* 2006:271-280). Similarly to Carbamazepine, Terazosin is also susceptible towards polymorphic conversion upon exposure to water, to convert into a more stable, but less soluble hydrate. As a result, Terazosin cannot be encapsulated in soft gel capsules, as it is highly hygroscopic and would draw water from the capsules and ultimately convert into its hydrated form (Pharmaceutical Formulation Databases and Resources, 2003).

The examples in this section therefore demonstrate that it is imperative to study the suitability of a given crystal form in a specific dosage form, as well as to apply effective control procedures during manufacturing that would ensure that the correct polymorph is present in the final product. Apart from effectively controlling the API synthesis (Section 1.2.1) and manufacturing procedures (Section 1.2.2) with regards to a specific solid form, the remaining factor that requires careful consideration is the FPP shelf life, as discussed next.

1.2.3 Product integrity and shelf life

It was mentioned that different solid forms differ with respect to their density, free energy and subsequently their physical stability. It is therefore evident that a hierarchy in thermodynamic stability would exist among the different crystal forms of an API.

It would be the ideal if the most stable crystal form of a compound could present with the best possible properties, both with regards to manufacturing and efficacy. This is unfortunately not always the case. Numerous meta-stable and even amorphous forms (if proven suitably stable for the duration of the product shelf life) are incorporated in FPPs (Food and Drug Administration, 2002; Yu, 2001:39). Just as different manufacturing stresses (Section 1.2.2) may influence the thermodynamic stability of a given crystal form, so could environmental stresses, such as incorrect storage conditions (high humidity and/or temperatures) also result in polymorphic conversions. Fukuoka *et al.* (1989:1048), for example, had initially considered amorphous Indomethacin for use in one of its FPPs, but found that it had completely converted into the crystalline form within 67 days (Figure 1.18). Since amorphous Indomethacin is more soluble than its crystalline counterpart, it is understandable that it would be the preferred choice for use in a FPP, rather than the crystalline form. However, its thermodynamic stability is too poor and does not allow for an acceptable shelf life for use in a FPP. Scientists, however, keep researching the possibility of stabilising amorphous Indomethacin (Chokshi *et al.,* 2008:2286; Shibata *et al.,* 2009:205-206; Watanabe *et al.,* 2001:81; Wu *et al.,* 2007:5148).

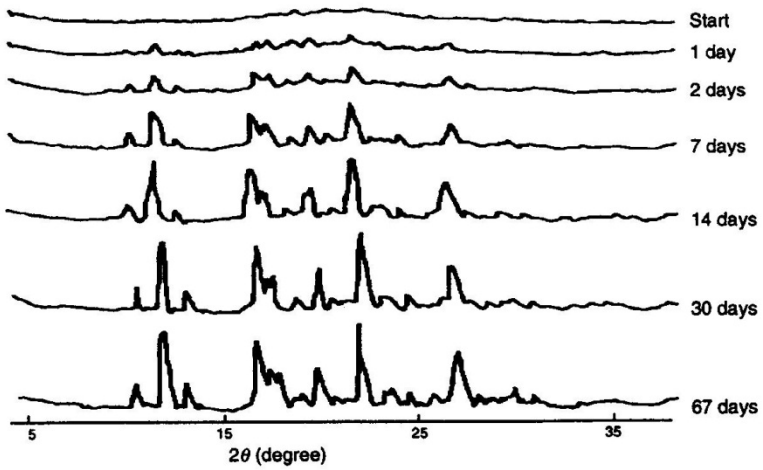

Figure 1.18 X-ray powder diffractograms illustrating the spontaneous and complete conversion of an amorphous form of Indomethacin in a FPP into its crystalline form over a period of 67 days (Fukuoka *et al.,*1989:1048).

Another possible consideration during pharmaceutical product preparation should be that preliminary screening studies may not have been successful in identifying all of the possible solid forms of a specific API. Norfloxacin and Ritonavir are good examples for illustrating the ever present possibility of discovering new solid forms of a given API, whether intentionally through focused research, or even by chance. Figure 1.19 represents the timeline of the discovery of different Norfloxacin solid forms, indicating that 21 years had elapsed since the discovery of the first form (the first hydrate) until the most recent discovery of Form C in 2007.

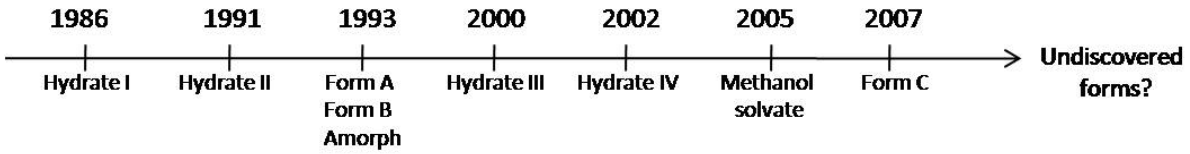

Figure 1.19 Timeline summarising the discovery of several Norfloxacin solid forms (adapted from Barbas *et al.,* 2007:687-692).

Ritonavir had been discovered by Abbott Laboratories in 1992, after which a new drug application (NDA) was filed in 1995. In 1996, Norvir semi-solid capsules (Abbott Laboratories) were launched, marketed and distributed. Two years later (1998), when quality control (QC) testing of Norvir capsules showed poor dissolution results, it was found to have been caused by polymorphic conversion into a more stable and less soluble form thereof (Chemburkar *et al.,* 2000:413).

Such examples demonstrate the potential effects that the discovery of new solid forms may have on pharmaceutical product integrity and re-iterate the need for extensive polymorph screening, starting

from the synthesis or acquisition of an API, right through to testing the final product, and/or to at least keep abreast of new discoveries.

The shelf life of a FPP directly relates to its physical (thermodynamic) and chemical stability. Since polymorphism may affect both the physical and chemical stability of the final product (Byrn *et al.,* 1999:15), it is imperative to study the possible impact of polymorphism on these aspects. Since shelf life is interrelated with other factors, the discussion on shelf life overlaps to some extent with the risks associated with polymorphic differences in general. The potential risk of polymorphism on the patient treatment efficacy and safety are discussed in section1.2.4.

1.2.4 Potential risks of polymorphism on patient treatment efficacy and safety

Although many possible factors, associated with solid state chemistry, may contribute to the quality and safety of medicines (Byrn *et al.,* 1999:15), only those of particular concern to this study are discussed herein, namely:

- Differences in solubility and dissolution behaviour;
- Thermodynamic stability (conversion);
- Toxicity; and
- Crystal habit.

Examples where these factors are known to pose risks to the patient are summarised in Table 1.5.

Table 1.5 Examples of APIs displaying differences in solubility/dissolution, toxicity and/or crystal habit, which may potentially affect the quality and safety of such medicines

Description	Reference
Mebendazole has three known solid forms (A, B and C). The preferred Form C is the only form providing a therapeutic effect. Form B is toxic, whilst Form A has no therapeutic effect and is it significantly less soluble than Form C.	Brits *et al.*(2010:1138)
A toxic Rifampicin solvatomorph was prepared as a result of using a contaminated, organic solvent during manufacturing.	De Villiers *et al.* (2011:877)
Toxic pseudo-polymorphs of Dapsone were identified and characterised.	Lemmer *et al.* (2012:1683)
Different Amoxicillin trihydrate crystal habits were prepared from different recrystallisation solvents, showing extremely poor powder flow and differences in dissolution behaviour. Differences in dissolution may result in differences in bioavailabilty, whereas problems with powder flow are expected to affect manufacturability (and subsequently product quality).	Shahnet *et al.* (2011:92)
A pharmaceutical compound (its name was kept confidential by the reference) was found to have converted from a monoclinic form (Form A) into a triclinic form (Form B) during dissolution. The phase mediated transformation also allowed for a change in crystal habit from an acicular to a tabular shape. The conversion caused a significant reduction in dissolution behaviour, which may lead to sub-therapeutic levels of the API being absorbed.	Garcia *et al.* (1999:1360)
Chloramphenicol palmitate has three known polymorphic forms. The thermodynamically stable Form A is pharmaceutically inactive and Form B is the active modification, whilst Form C is extremely unstable.	Gamberini *et al.* (2006:216)
Different crystal habits of the same Phenytoin polymorph showed differences in dissolution behaviour, which may result in differences in the systemic absorption thereof.	Nokhodchi *et al.* (2003:87)
DL-Ala-Met amorphous form is more prone to oxidation and ultraviolet (UV) degradation than its crystalline form, which would impair its shelf life if the amorphous form is to be used in the manufacturing of the FPP.	Byrn *et al.* (2001:120)
Tablets containing Form I or Form II of Acetazolamide resulted in poor quality tablets (split, broken or capped). Tablet defects may cause the patient to doubt the product and cause non-compliance when deciding against taking them, whereas if chipped or broken tablets are taken, sub-therapeutic levels of the active may be achieved in the blood stream.	Martino *et al.*(2001:219)

This concludes the introduction to polymorphism. Each of the chapters in this thesis further presents a relevant literature overview specifically pertaining to the topic at hand.

Following is a literature overview of the known crystal forms of Pyrimethamine and Efavirenz, the APIs of focus for this study.

1.3 Literature overview on known crystal forms of Efavirenz and Pyrimethamine

This study aimed at investigating the possible effects of polymorphism of Efavirenz and Pyrimethamine (Figure 1.20). The purpose of this section is to briefly describe the known solid forms of these two APIs, whilst the expected contributions of this study to existing pharmaceutical industrial knowledge regarding these APIs are discussed Chapter 6 (Conclusion).

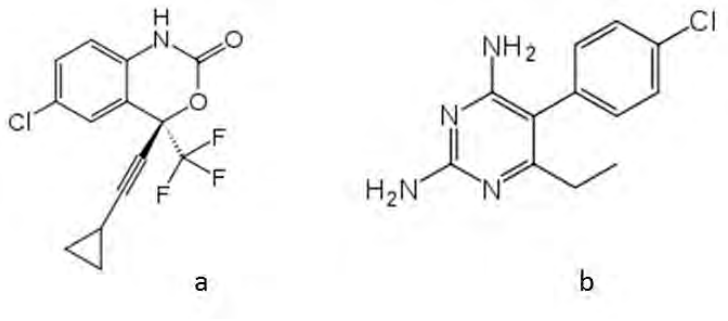

Figure 1.20 Chemical structures of (a) Efavirenz and (b) Pyrimethamine.

1.3.1 Efavirenz

Table 1.6 summarises existing information regarding the known forms of Efavirenz, to date. Accordingly, seventeen different solid forms of Efavirenz had been identified. Of specific interest to this study was that, among the known population, three different amorphous forms had been patented. It could thus be concluded that Efavirenz exhibits *poly-amorphism* (Section 1.1.3.4). Two of these patented amorphous forms (Doney, 2007; Reddy *et al.,* 2006) had been claimed to have improved bioavailability and/or dissolution properties, compared to the other crystalline forms (Figure 1.21).

It is claimed that Form I is the thermodynamically stable form (Clarke & Kukura, 1998; Radesca *et al.*,1998; Reddy *et al.,* 2006). Form I has the highest melting point (±137°C) and exposure to high temperatures convert all other known forms into Form I (Clarke & Kukura, 1998; Radesca *et al.*,1998; Reddy *et al.,* 2006). Although Form I may not have the best dissolution performance, compared to other known forms, it is claimed to be the preferred form in the pharmaceutical industry, due to its thermodynamic stability (Clarke & Kukura, 1998; Radesca *et al.*,1998).

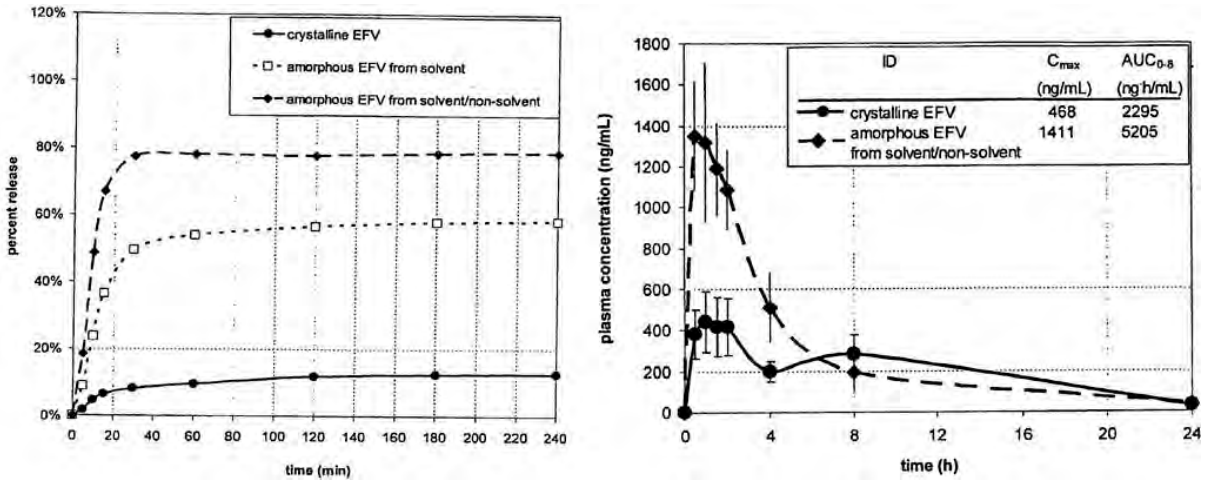

Figure 1.21 The dissolution and bioavailability of spray dried amorphous Efavirenz, compared to crystalline Efavirenz (EFV) (Doney, 2007).

Table 1.6 Summary of known solid forms of Efavirenz (compiled from Clarke & Kukura, 1998; Doney, 2007; Radesca *et al.*,1998; Reddy *et al.,* 2006)

Name/Form	Preparation	XRPD (Main diffraction peaks °2Θ)	DSC
Form I or 1*	Prepared through recrystallisation using heptanes/tetrahydrofuran (or a mixture thereof), or through heating/slurry conversion of Forms II, III, IV, V, or mixtures thereof.	10.3, 10.8, 14.1, 16.8, 20.0, 20.5, 21.1 and 24.8	Melting endotherm at ±138°C.
Form II or 2*	Prepared through rapid recrystalisation from an alkane solution.	6.8, 9.2, 12.3, 16.2, 21.4, 22.7, 24.1 and 28.0	Melting endotherm at ±118°C, followed by a recrystallisation exotherm at ±119°C and a final melting endotherm at ±137°C.
Form III or 3*	Slurry stirring of Form I, or II, or a mixture thereof in heptane.	7.1, 7.3, 11.0, 13.8, 20.9, 23.3 and 27.9	Broad endotherm at ±108°C, followed by a final melting endotherm at ±137°C.
Form IV or 4*	Recrystallisation from a mixed solvent system, together with anti-solvent addition.	3.6, 6.3, 9.7, 11.0, 12.7, 13.2, 16.1, 19.2, 19.5 and 20.6	Broad endotherm ranging between±74 -96°C, followed by a final melting endotherm at ±138°C.
Form V or 5*	Recrystallisation from a mixed solvent system.	10.2, 11.4, 11.6, 12.6, 19.1, 20.6, 21.3, 22.8, 24.8, 27.4, 28.2, 31.6	Melting endotherm at ±106°C, followed by a recrystallisation exotherm at ±108°C and a final melting endotherm at ±138°C.
Novel amorphous form	Prepared from a ketonic solution with water as anti-solvent (precipitating solvent).	Broad halo shaped XRPD pattern	Not available.
H1	Prepared from a mixture of an alcohol and ketonic solution, with subsequent drying at low temperatures.	11.6, 12.5, 15.3, 20.1, 20.8, 22.5, 23.1, 25.7, 27.9, 28.5, 29.5, 30.2 38.2	Not available.
Form I*	Recrystallisation with ethanol, or methanol, together with the addition of water as anti-solvent.	See Form I/1 above	See Form I/1 above.
Form II*	Recrystallisation, using 2-propanol.	See Form II/2 Above	See Form II/2 Above.
Amorphous Efavirenz	Spray drying a solvent blend, or solvent, or non-solvent blend, or a mixture of a solvent/polymer blend.	Not available	No distinct thermal behaviour.
A	Dissolving Efavirenz in a mixture of one or more halogenated hydrocarbons, and one or more hydrocarbon organic solvents.	3.4, 6.8, 11.2, 13.0, 13.6, 14.4, 15.1, 15.9, 16.5, 17.2, 18.1, 19.1, 19.6, 19.8, 20.3, 21.8, 22.2, 23.5, 24.0, 24.7, 25.2, 25.8, 26.5, 27.5, 28.9, 30.4, 31.4, 32.5	Melting endotherm at ±90°C, followed by a recrystallisation exotherm at ±95°C and a final melting endotherm at ±138°C.
Ω	Dissolving Efavirenz in one or more water miscible akanols, and then adding this solution to a mixture of one or more water miscible alkanols and water.	10.0, 11.3, 11.6, 14.9, 16.6, 17.5, 18.1, 19.0, 20.4, 22.7, 28.1, 29.8, 37.8	Broad endotherm ranging between±90 -100°C, followed by a recrystallisation exotherm at ±105°C and a final melting endotherm at ±138°C.
δ	Dissolving Efavirenz in a mixture of one or more halogenated hydrocarbons, and then adding this solution to an organic solvent, including C_{5-7} alkane, cycloalkane and petroleum ether.	7.8, 11.3, 13.4, 14.4, 15.4, 16.4, 17.0, 18.9, 20.1, 22.9, 23.9, 25.4, 26.0, 30.7, 31.7	Melting endotherm at ±95°C, followed by a recrystallisation exotherm at ±100°C and a final melting endotherm at ±138°C.

Table 1.6 (continued) Summary of known solid forms of Efavirenz (compiled from Clarke & Kukura, 1998; Doney, 2007; Radesca *et al.*,1998; Reddy *et al.,* 2006)

Name/Form	Preparation	XRPD (Main diffraction peaks °2Θ)	DSC
Amorphous Efavirenz	Dissolving Efavirenz in a mixture of one or more water miscible solvents, and then adding this solution to a solution of one or more inorganic salts.	Broad halo shaped	Not available.
O	Dissolving Efavirenz in a mixture of one or more water miscible solvents, then removing the solvent and subsequently grinding the product.	3.9, 7.9, 10.7, 13.2, 15.1, 17.3, 18.4, 19.6, 21.3, 22.1, 23.7, 25.4, 26.9, 27.6, 28.0, 29.0	Not available
N	Treating Form O with water, or mixing Form ω and seeding with Form N.	3.9, 7.8, 10.7, 12.0, 13.1, 15.7, 18.4, 19.5, 20.8, 23.7, 25.3, 26.9, 27.9, 28.9	Broad endotherm ranging between±90 -95°C, followed by a recrystallisation exotherm at ±100°C and a final melting endotherm at ±138°C.
y˙	Dissolving Efavirenz in one or more polar aprotic solvents, and then adding this solution to a salt solution.	6.1, 9.8, 11.0, 12.7, 13.1, 14.2, 15.7, 18.4, 19.2, 20.1, 21.9, 23.2, 24.7, 26.2, 28.0	Broad endotherm ranging between ±70 -85°C, followed by a recrystallisation exotherm at ±90°C and a final melting endotherm at ±138°C.
β	Dissolving Efavirenz in one or more water miscible organic solvents, and then adding this solution to a mixture of one or more water miscible organic solvents while stirring at ≤0°C.	11.2, 11.7, 12.3, 15.2, 16.4, 17.6, 18.6, 19.1, 20.9, 21.4, 22.9, 23.5, 24.5, 25.6, 26.1, 27.4	Melting endotherm at ±105°C, followed by a recrystallisation exotherm at ±110°C and a final melting endotherm at ±138°C.
y˙1 and y2	Dissolving Efavirenz in one or more lower alkanols, and then adding this solution to a mixture of one or more lower alkanols and a salt solution.	y˙1 6.1, 6.3, 11.0, 12.3, 13.1, 14.2, 15.3, 16.7, 17.9, 18.3, 21.2, 22.1, 23.2, 24.6, 26.4, 27.3 y2 12.4, 13.2, 15.6, 16.9, 17.2, 18.4, 19.3, 19.9, 21.2, 21.7, 22.0, 25.8, 26.4 31.6	y˙1 recrystallisation exotherm at ±90°C and a final melting endotherm at ±138°C. y2 recrystallisation exotherm at ±85°C and a final melting endotherm at ±138°C.

*Note that the use of roman numerals and integer values for Forms 1-5 (I-V) are interchangeably used throughout the literature.

1.3.2 Pyrimethamine

Very few true polymorphs and/or pseudo-polymorphs of Pyrimethamine are described in the literature. From the available literature it was concluded that the majority of the solid forms of Pyrimethamine are either complexes, or salts thereof (Table 1.7). The shaded cells in Table 1.7 depict the true polymorphs and pseudo-polymorphs of Pyrimethamine, whereas the unshaded cells depict salts/complexes and/or derivatives of Pyrimethamine. Despite it having been used in the treatment of uncomplicated malaria for at least thirty years (Tracy & Webster, 2001:1061), the crystal structure of its only known anhydrous form at the time, MUFMAB, was only published in 2002 (Sethuraman & Muthiah, 2002:817). In 2011, Tutughamiarso & Bolte (2011:428) described a new anhydrous form of Pyrimethamine (compound 1), a Pyrimethamine dimethylsulfoxide (DMSO) solvate (pseudo-polymorph Ia) and a Pyrimethamine NMP solvate (pseudo-polymorph Ib). Relevant studies (Sethuraman & Muthiah, 2002:817; Tutughamiarso & Bolte, 2011:428) had, however, not focused on the possible impacts that these forms (MUFMAB, compound 1, Ia and Ib) may have on the quality and safety of medicines, but rather on solving their crystal structures, on elaborating on their bonding geometries and on their crystal data.

Table 1.7 Available literature describing the known solid forms of Pyrimethamine

Description	Reference
A cyclodextrin inclusion complex of Pyrimethamine	De Araújo *et al.* (2007:5762)
Pyrimethamine nitrobenzoate complexes	Stanley *et al.* (2005:7201)
A cyclodextrin/Pyrimethamine inclusion complex	De Araújo *et al.* (2009:165)
Anhydrous Pyrimethamine [MUFMAB]	Sethuraman & Muthiah (2002:817)
Pyrimethamine dinitrate	Balasubramani *et al*. (2005:586)
Pyrimethamine 3,5-dinitrobenzoate	Subashini *et al*. (2007:3775)
Pyrimethamine formate	Stanley *et al*. (2002:631)
Pyrimethamine hydrogen glutarate	Stanley *et al*. (2002:631)
Pyrimethamine hydrogen maleate	Sethuraman *et al.* (2003:823)
Pyrimethamine hydrogen succinate	Sethuraman *et al.* (2003:823)
Pyrimethamine hydrogen phthalate	Sethuraman *et al.* (2003:823)
Pyrimethamine fumarate	Sethuraman *et al.* (2003:823)
Bis (Pyrimethamine hydrogen sulfate) monohydrate	Devi *et al.* (2006:857)
Pyrimethamine terephtalate methanol	Devi *et al.* (2011:1624)
Pyrimethamine terephtalate ethanol	Devi *et al.* (2011:1624)
Anhydrous Pyrimethamine (compound 1)	Tutughamiarso & Bolte (2011:428)
Pyrimethamine NMP (N-methylpyrrolidin-2-one)	Tutughamiarso & Bolte (2011:428)
Pyrimethamine DMSO solvate	Tutughamiarso & Bolte (2011:428)
Pyrimethamine methanol solvate	Delori *et al.* (2012:6835-6846)

Conclusion

It is well known that polymorphs (different solid forms of the same chemical compound) exhibit differences in physico-chemical characteristics (solubility, hardness, dissolution, thermodynamic stability, etc.). The quality and safety of medicines may therefore be influenced by the polymorphic profile of the API, and would most final pharmaceutical products (FPPs) as a result receive regulatory approval only for a particular crystal form. This study aimed at investigating the possible effects of polymorphism among Efavirenz and Pyrimethamine on the quality and safety of their final products.

Crystals are formed or modified by a range of preparation techniques. For this study, two techniques (one for each API) were chosen to evaluate whether they would modify and/or influence the quality and/or safety of these APIs. The technique chosen for Efavirenz was quench cooling (crystallisation from the melt), whereas crystallisation from solution was chosen for Pyrimethamine. Quench cooling comprises the forced solidification from solution (melt), due to rapid cooling, whereas crystallisation from solution brings forth different crystal forms, due to differences in solubility and concentration. Quench cooling most commonly results in amorphous forms, whilst recrystallisation from solution usually results in polymorphs and/or pseudo-polymorphs.

Several analytical techniques are used during polymorph research and screening, the most common being XRPD, DRIFT-IR, DSC, TGA, microscopy, dissolution/solubility testing and water determinations. All of these analytical techniques, amongst others, were used during this study.

API polymorphism should be considered, starting from pre-formulation, through the point where the API is synthesised, during the manufacturing of the final pharmaceutical product, and ultimately throughout the product shelf life (integrity), for the following reasons:

- Seemingly small differences and the inability to control synthesising steps may result in disappearing polymorphs, different polymorphic forms, inconsistencies and toxicity.
- FPP manufacturing techniques may induce phase transformations. Different APIs and different polymorphic forms differ in their susceptibility towards phase transformations during exposure to the various manufacturing techniques.
- A thermodynamic stability hierarchy exists among polymorphs. Differences in thermodynamic stability may in turn affect product quality and shelf life.
- Exposure of the patient to a FPP containing any crystal form, other than the intended/preferred form, may have serious health ramifications, due to treatment inefficacy and/or toxicity.

Seventeen different solid forms of Efavirenz have been reported to date, many of which are part of patented works, with little or no focus on the characteristics of these forms. From the available literature it became clear that Efavirenz Form I is considered the preferred form for FPP manufacturing. Contrary, very few pure polymorphs and/or pseudo-polymorphs of Pyrimethamine are

described in the literature. The most solid forms of Pyrimethamine are co-crystals, salts and other complexes.

The statistics that exist regarding the treatment successes and mortality rates of HIV/AIDS and malaria plead for more focused investigations into the quality and safety of the medicines that are being employed in the treatment of these diseases. The focus of this study was therefore to exploit the potential dangers associated with polymorphism among Efavirenz and Pyrimethamine, befitting of the collective title of this work: “Quality and safety implications of Efavirenz and Pyrimethamine crystal modifications”.

Bibliography

ABDO-RABBO, A., BASSILI, A. & ATTA, H. 2005. The quality of antimalarials available in Yemen. *Malaria Journal*, 4:28-34.

AGGARWAL, A.K., SRINIVASAN, C.V. & WADHA, L. 2010. Procedure for the preparation of highly pure donepezil. Patent: application number 2010/0113793.

AMIN, A.A., SNOW, R.W. &KOKWARO, G.O. 2005. The quality of sulphadoxine-pyrimethamine and amodiaquine products in the Kenyan retail sector. *Journal of Clinical Pharmacy and Therapeutics*, 30(6):559-565.

ANON. 2007. The University of Oklahoma crystallography laboratory: Crystallography. [Web:] http://xrayweb.chem.ou.edu/notes/crystallography.html [Date of access: 23 July 2012].

APTUIT. 2006. Case study:polymorph screening and control. [Web:] http://www.aptuit.com/~/media/Aptuit60/ResourceLibrary/Publications/CaseStudies/PDFs/CS2_Polymorph_Full.ashx [Date of access: 25 July 2012].

BALASUBRAMANI, K., MUTHIAH, P.T., RYCCHLEWSKA, U. & PLUTECKA, A. 2005. Hydrogen-binding patterns in pyrimethaminium dinitrate. *Acta Crystallographica C,* 61(10):o586-o588.

BARBAS, R., PROHENS, R. & PUIGJANER, C. 2007. A new polymorph of norfloxacin: complete characterization and relative stability of its trimorphic system. *Journal of Thermal Analysis and Calorimetry*, 89(3):687-692.

BOMBICZ, P., CZUGLER, M., TELLGREN, R. & KALMAN, A. 2003. A classic example of a disappearing polymorph and the shortest intermolecular H-H separation ever found in an organic crystal. *Angewadte Chemie International Edition,* 42:1957-1960.

BRITS, M., LIEBENBERG, W. & DE VILLIERS, M.M. 2010.Characterization of polymorph transitions that decrease the stability of tablets containing the WHO essential drug mebendazole. *Journal of Pharmaceutical Sciences,* 99(3):1138-1151.

BRITS, M. 2008. Solid-state properties of pharmaceuticals. Potchefstroom: North-West University. (Dissertation: PhD). 569p.

BRITTAIN, H.G. (ed). 1999. Polymorphism in pharmaceutical solids. 1st ed. Marcel Dekker, Inc. New York: Basel. 427p.

BRITTAIN, H.G. (ed). 2009. Polymorphism in pharmaceutical solids. 2nd ed. Informa Healthcare, Inc. New York: London. 640p.

BUCKTON, G. 2002. Solid-state properties. (*In* Aulton, M.E., *ed.* Pharmaceutics: the science of dosage form design. New York, NJ: Churchill Livingstone. p. 141-152.)

BYRN, S., PFEIFFER, R., GANEY, M., HOIBERG, C. & POOCHCIKIAN, G. 1995. Pharmaceutical solids: a strategic approach to regulatory considerations. *Pharmaceutical Research*, 12(7):945-954.

BYRN, S.R. 1982. Solid-state chemistry of drugs. New York: Academic press, Inc. 346p.

BYRN, S.R., PFEIFFER, R.R. & STOWELL, J.G. 1999. Solid-state chemistry of drugs. West Lafayette: Indiana, SSCI. 574p.

BYRN, S.R., XU, W. & NEWMAN, A.W. 2001. Chemical reactivity in solid-state pharmaceuticals: formulation implications. *Advanced Drug Delivery Reviews*, 48:115-136.

CAINS, P.W. 2009. Classical methods of preparation of polymorphs and alternative solid forms. (*In* Brittain, H.G. *ed.* Polymorphism in pharmaceutical solids. New York, NJ: Informa Healthcare U.S.A, Inc. p. 76-138.)

CARSTENSEN, J.T. 2001. Advanced pharmaceutical solids. New York, Marcel Dekker, Inc. 518p.

CHEMBURKAR, S.R., BAUER, J., DEMING, K., SPIWEK, H., PATEL, K., MORRIS, J., HENRY, R., SPANTON, S., DZIKI, W., PORTER, W., QUICK, J., BAUER, P., DONAUBAUER, J., NARAYANAN, B.A., SOLDANI, M., RILEY, D. & MCFARLAND, K. 2000. Dealing with the impact of ritonavir polymorphs on the late stages of bulk drug process development. *Organic Process Research and Development*, 4(5):413-417.

CHEPKWONY, H.K., MWAURA, N., GUANTAI, E., GATHONI, E., KAMAU, F.N., MBAE, E., WANG'ANG'A, G., MUTERU, S., BIRGEN, N. & WANDETO, M. 2007. Quality of antimalarial drugs analysed in the national quality control laboratory during the period 2002-2005. *East and Central African Journal of Pharmaceutical Sciences*, 10(3):59-62.

CHOKSHI, R.J., SHAH, N.H., SANDHU, H.K., MALICK, A.W. & ZIA, H. 2008. Stability of low glass transition temperature indomethacin formulations: impact of polymer-type and its concentration. *Journal of Pharmaceutical Sciences,* 97(6):2286-2298.

CLARKE, W. & KUKURA, J.L. 1998. Process for the crystallisation of a reverse transcriptase inhibitor using an anti-solvent. Patent: US 5,965,729.

COOMBES, I., AVENT, M., CARDIFF, L., BETTENAY, K., COOMBES, J., WHITFIELD, K., STOKES, J., DAVIES, G. & BATES, I. 2010. Improvements in pharmacist's performance facilitated by an adapted competency-based general level framework. *Journal of Pharmacy Practice and Research*, 40(2):111-112.

DEBNATH, S. & SURYANARAYANAN, R. 2004. Influence of process induced phase transformations on the dissolution of Theophylline tablets. *American Association of Pharmaceutical Scientists,* 5(1):1-11.

DE ARAúJO, M.V.G., MACEDO, O.F.L., NASCIMENTO, C.D.C., CONEGERO, L.S., BARRETO, L.S., ALMEIDA, L.E., DA COSTA, N.B. & GIMENEZ, I.F. 2009. Characterization, phase solubility and molecular modelling of α-cyclodextrin/pyrimethamine inclusion complex. *Spectrochimica Acta Part A*, 72:165-170.

DE ARAúJO, M.V.G., VIEIRA, E.K.B., LáZARO, G.S., CONEGERO, L.D.S., FERREIRA, O.P., ALMEIDA, L.E., BARRETO, L.S., DA COSTA, N.B. & GIMENEZ, I.F. 2007. Inclusion complexes of pyrimethamine in 2-hydroxypropyl-β-cyclodextrin: characterization, phase solubility and molecular modelling. *Bioorganic and Medicinal Chemistry*, 15:5752-5759.

DE VILLIERS, M.M., CAIRA, M.R., LI, J., STRYDOM, S.J., BOURNE, S.A. & LIEBENBERG, W. 2011. Crystallisation of toxic glycol solvates of rifampicin from glycerin and propylene glycol contaminated with ethylene glycol or diethylene glycol. *Molecular Pharmaceutics*, 8(3):877-888.

DELORI, A., GALEK, P.T.A., PIDCOCK, E. & DELORI, W. 2012. Quantifying homo-and heteromolecular hydrogen bonds as a guide for adduct formation. *European Journal of Chemistry*, 18:6835-6846.

DESTRI, G.L., MARRAZZO, A., RESCIFINA, A. & PUNZO, F. 2011. How molecular interactions affect crystal morphology: The case of haloperidol. *Journal of Pharmaceutical Sciences*, 100(11):4896-4906.

DEVI, P., MUTHIAH, P.T., BOCELLI, G. & CANTONI, A. 2006. Hydrogen bonding patterns in bis (pyrimethamine hydrogen sulfate) monohydrate. *Journal of Chemical Crystallography*, 36(12):857-861.

DEVI, P., NIRMALRAM, J.S. & MUTHIAH, P.T. 2011. Near supramolecular isomorphism involving homologous solvents: pyrimetaminium terephtalate methanol solvate and pyrimetaminium terephtalate ethanol solvate. *Journal of Chemical Crystallography,* 41:1624-1629.

DONEY, J.A. 2007. Amorphous efavirenz and the production thereof. Patent: US2007/0026073 A1.

DUNITZ, J.D. & BERNSTEIN, J. 1995. Disapearing polymorphs. *Accounts of Chemical Research,* 28:193-200.

ETHIOPIAN PHARMACEUTICAL ASSOCIATION. 2009. Comparative quality assessment of different brands of efavirenz found in Ethiopian market. [Web:] http://epaethiopia.org/book-of-abstract/item/51-comparative-quality-assessment-of-different-brands-of-Efavirenz-found-in-ethiopian-market [Date of access: 23 July 2012].

Food and Drug Administration (FDA). 2002. Scientific considerations of polymorphism in pharmaceutical solids: abbreviated new drug applications. [Web:] http://www.fda.gov/ohrms/dockets/ac/02/briefing/3900B1_04_Polymorphism.htm [Date of access: 25 July 2012].

FUKUOKA, E., MAKITA, M. & YAMAMURA, S. 1989. Glassy state of pharmaceuticals III:thermal properties and stability of glassy pharmaceuticals and their binary glass systems. *Chemical Pharmaceutical Bulletin*, 37(4):1047-1050.

GAMBERINI, M.C., BARALDI, C., TINTI, A., RUSTICHELLI, C., FERIOLI, V. &GAMBERINI, G. 2006. Solid state characterization of chloramphenicol palmitate: Raman spectroscopy applied to pharmaceutical polymorphs. *Journal of Molecular Structure,* 785:216-224.

GARCIA, E., VEESLER, S., BIOSTELLE, R. & HOFF, H. 1999. Crystallisation and dissolution of pharmaceutical compounds: an experimental approach. *Journal of Crystal Growth,* 198/199:1360-1364.

GRANT, D.J.W. 1999. Theory and origin of polymorphism. (*In* Brittain, H.G., *ed.* Polymorphism in pharmaceutical solids. New York, NJ: Marcel Dekker, Inc. p. 1-33.)

GRODOWSKA, K. & PARCZEWESKI, A. 2010. Organic solvents in the pharmaceutical industry. *Acta Poloniae Pharmaceutica Drug Research,* 67(1):3-12.

HALEBLIAN, J.K. 1975. Characterization of habits and crystalline modification of solids and their pharmaceutical applications. *Journal of Pharmaceutical Science*, 64(8):1269-1288.

HANCOCK, B.C. & ZOGRAFI, G. 1997. Characteristics and significance of the amorphous state in pharmaceutical solids. *Journal of Pharmaceutical Sciences*, 86(1):1-12.

HANCOCK, B.C., SHALAEV, E.Y. &SHAMBLIN, S.L. 2002. Polyamorphism: a pharmaceutical science perspective. *Journal of Pharmacy and Pharmacology*, 54:1152-1153.

HILFIKER, R., BLATTER, F. & VON RAUMER, M. 2006. Relevance of solid state properties for pharmaceutical products. (*In* Hilfiker R., *ed.* Polymorphism in the pharmaceutical industry. Verlag GmbH, Wiley-VCH.p.1-17.)

INTERNATIONAL CONFERENCE ON HARMONISATION) (ICH). 1999. ICH harmonised tripartite guideline:specifications: test procedures and acceptance criteria for new drug substances and new drug products: chemical substances, Q6A. [Web:] http://www.ich.org/fileadmin/Public_Web_Site/ICH_Products/Guidelines/Quality/Q6A/Step4/Q6Astep4.pdf [Date of access: 16 February 2014].

KIANG, Y.H., YANG, C.Y., STAPLES, R.J. & Jona, J. 2009. Crystal structure, crystal morphology, and surface properties of an investigational drug. *International Journal of Pharmaceutics,* 23;368(1-2):76-82.

KIEFFER, J. 2002. Structural transitions and poly-amorphism in glass-forming oxides. *Journal of Non-Crystalline Solids*, 307-310:644-653.

KIM, A.I., AKERS, M.J. & NAIL, S.L. 1998. The physical state of mannitol after freeze drying: effects of mannitol concentration, freeze rate, and a non-crystallizing cosolute. *Journal of Pharmaceutical Sciences,* 87(8):931-935.

KUMAR, S., RAMESH, Y. & KUMAR, C. 2011. Influence of solvents on the crystal habit and properties of rofecoxib. *Bulletin of Environment, Pharmacology and Life Sciences*, 1(1):40-49.

LEMMER, H., STIEGER, N., LIEBENBERG, W. & CAIRA, M.R. 2012. Solvatomorphism of the antibacterial dapsone: X-ray structures and thermal desolvation kinetics. *Crystal Growth and Design*, 12(3):1683-1692.

LLINAS, A., BURSLEY, J.C., PRIOR, T.J., GLEN, R.C. & GOODMAN, J.M. 2008. Concomitant hydrate polymorphism in the precipitation of sparfloxacin from aqueous solution. *Crystal growth and Design,* 8(1):114-118.

MARTINEZ-OHARRIZ, M.C., RODRIQUES-ESPINOSA, C., MARTIN, C., GONI, M.M., TROS-ILLARDUYA, M.C. & SANCHEZ, M.B. 2002.Solid dispersions of diflunisal-PVP: polymorphic and amorphous states of the drug. *Drug Development and Industrial Pharmacy,* 28(6):717-725.

MARTINO, P.D., SCOPPA, M., JOIRIS, E., PALMIERI, G.F., ANDRES, C., POURCELOT, Y. &MARTELLI, S. 2001. The spray drying of acetazolamide as method to modify crystal properties and to improve compression behaviour. *International Journal of Pharmaceutics*, 213:209- 221.

MERRISON, B. 2011.The mystery of the disappearing crystals. *Royal Society of Chemistry.* [Web:] http://www.rsc.org/chemistryworld/News/2011/February/03021101.asp [Date of access: 26 March 2014].

NAGARIMADUGU, M., GUPTA, A.K., DANDALA, R. & MEENAKSHIUNDERAM, S. 2011. Process for the preparation of donepezil hydrochloride. Patent: US 7,994,328 B2.

NOKHODCHI, A., BOLOURTCHIAN, N. & DINARVAND, R. 2003. Crystal modification of phenytoin using different solvents and crystallisation conditions. *International Journal of Pharmaceutics*, 250:87-97.

NOWELL, H., BUTCHART, B., COOMBES, D.S., PRICE, S.L., EMMERICH, W. & CATLOW, C.R.A. 2005. Increasing the scope for polymorph prediction using e-science. [Web:] http://discovery.ucl.ac.uk/702/1/9.9finalnowell.pdf [Date of access: 25 July 2012].

SOLDEVILLA, N. 2009. Synthesis and preparations of intermediates and new polymorphs thereof useful for the preparation of donepezil hydrochloride. Patent: US 2009/0253746 A1.

PARK, J., KANG, H.W., PARK, S.J. & KIM, C. 2005. Use of CP/MAS solid-state NMR for the characterisation of solvate molecules within estradiol crystal forms. *European Journal of Pharmaceutics and Biopharmaceutics*, 60:407-412.

PARTHASARADHI, R.B., RATHNAKAR, R.K., RAJI, R.R., MURALIDHARA, D. & CHANDER, R.K.S. 2009. Crystalline forms of donepezil hydrochloride. Patent: US 7,560,560 B2.

PATHI, S.L., ACHARYA, V., RAO, D.R. & KANKAN, R.N. 2011.Process and intermediate for preparation of donepezil. Patent: US 8,030,491 B2.

PATTERSON, J.E., JAMES, M.B., FORSTER, A.H., LANCASTER, R.W., BUTLER, J.M. & RADES, T. 2005. The influence of thermal and mechanical preparative techniques on the amorphous state of four poorly soluble compounds, *Journal of Pharmaceutical Sciences*, 94(9): 1998-2012.

PFORMULATE: PHARMACEUTICAL FORMULATION DATABASES AND RESOURCES. 2003.Pformulate a soft gel. [Web:] http://www.pformulate.com/labclass/pformsoftgel [Date of access: 26 March 2014].

RADESCA, L., RABEL, S. & MOORE, J. 1998. Crystalline efavirenz. Patent: WO 99/64405.

RAFFANTI, S.P. & HAAS, D.W. 2001. Chemotherapy of microbial diseases. (*In* Hardman, J.G., Limbird, L.E., Gilman, A.G., *eds*. Goodman and Gilman's: the pharmacological basis of therapeutics. New York: McGraw-Hill Medical Publishing Division. p. 1141-1380.)

REDDY, B.P., RATHNAKAR, K., REDDY, R.R., REDDY, D.M. & REDDY, K.S.C. 2006. Novel polymorphs of efavirenz. Patent: US 2006/0235008 A1.

ROBERTS, R.J., PAYNE, R.S. & ROWE, R.C. 2000. Mechanical property predictions for polymorphs of sulphathiazole and carbamazepine. *European Journal of Pharmaceutical Sciences,* 9(3):277-283.

SETHURAMAN, V. & MUTHIAH, P.T. 2002. Hydrogen bonded supramolecular ribbons in the antifolate drug pyrimethamine. *Acta Crystallographica E,* 58(8):o817-o818.

SETHURAMAN, V., STANLEY, N., MUTHIAH, P.T., SHELDRICK, W.S., WINTER, M., LUGER, P. & WEBER, M. 2003. Isomorphism and crystal engineering: organic ionic ladders formed by supramolecular motifs in pyrimethamine salts. *Crystal Growth and Design*, 3(5):823-828.

SHAHNET, L., AL-RAGHBAN, D. &CHEHNA, M.F. 2011. Improvement of the physicochemical properties of amoxicillin trihydrate powder by recrystallisation at different pH values. *International Journal of Pharmacy and Pharmaceutical Sciences*, 3(3):92-100.

SHARMA, R., BHUSHAN, K., ARYAN, R.C., SINGH, N., PANDYA, B. & KUMAR, Y. 2006. Polymorphic forms of efavirenz and processes for their preparation. Patent: WO 2006/040643 A2.

SHIBATA, Y., FUJITI, M., SUGAMURA, Y., NAKANISHI, S., YAMADAZ, M., OUCHIZ, K. & WATANABE, Y. 2009. Stability of amorphous indomethacin in a solid dispersion using crospovidone prepared by a twin-screw kneader or extruder and application of aqueous film coating to solid dispersion in tablets. *Journal of Drug Delivery Science and Technology,* 19(3): 205-210.

SHETH, A.R. & GRANT, D.J.W. 2005. Relationship between the structure and properties of pharmaceutical crystals. *KONA,* 23:36-48.

SINKO, P.J. 2006. Martin's physical pharmacy and pharmaceutical sciences. 5th ed. Lippincott Williams & Wilkins: Philadelphia. 795 p.

SNYDER, R.C. & DOHERTY, M.F. 2007. Faceted crystal shape evolution during dissolution or growth. *Materials, Interfaces and Electrochemical Phenomena*, 53(5)1337-1348.

SOUTH AFRICAN PHARMACY COUNCIL. 2012. Continuous professional development (CPD). [Web:] http:www.pharmcouncil.co.za/B_CPD_Overview.asp [Date of access: 23 July 2012].

STANLEY, N., MUTHIAH, P.T., GEIB, S.J., LUGER, P., WEBER, M. & MESSERCHMIDT, M. 2005. The novel hydrogen bonding motifs and supramolecular patterns in 2,4-diaminopyrimidine-nitrobenzoatecomplezes. *Tetrahedron,* 61:7201-7210.

STANLEY, N., SETHURAMAN, V., MUTHIAH, P.T., LUGER, P. & WEBER. 2002. Crystal engineering of organic salts: hydrogen-bonded supramolecular motifs in pyrimethamine hydrogen glutarate and pyrimethamine formate. *Crystal Growth and Design*, 2(6):631-635.

SUBASHINI, A., MUTHIAH, P.T., BOCELLI, G. & CANTONI, A. 2007. Hydrogen-bonding patterns in pyrimethaminium 3,5-dinitrobenzoate.*ActaCrystallographica E,* 63(9):o3775.

TIAN, F., SANDLER, N., AALTONEN, J., LANG, C., SAVILLE, D.J., GORDON, K.C., STRACHAN, C.J., RANTANEN, J. & RADES, T. 2007. Influence of polymorphic form, morphology, and excipient interactions on the dissolution of carbamazepine compacts. *Journal of Pharmaceutical Sciences*, 96(3):584-594.

TRACY, J.W. & WEBSTER, L.T. 2001. Chemotherapy of parasitic infections. (*In* Hardman, J.G., Limbird, L.E., Gilman, A.G., *eds*. Goodman and Gilman's: the pharmacological basis of therapeutics. New York: McGraw-Hill Medical Publishing Division. p. 1059-1140.)

TUTUGHAMIARSO, M. & BOLTE, M. 2011. A new polymorph and two pseudo-polymorphs of pyrimethamine. *Acta Crystallographica C*, (67):o428-0434.

UNITED NATIONS (UN) NEWS CENTRE. 2007. Revised UN estimates show over 33 million people worldwide living with HIV. [Web:] http://www.un.org/apps/news/story.asp?NewsID=24742 [Date of access: 23 July 2012].

VAN TONDER, E.C., MALEKA, T.S.P., LIEBENBERG, W., SONG, M., WURSTER, D.E. & DE VILLIERS, M.M. 2004. Preparation and physiochemical properties of niclosamide anhydrate and two monohydrates. *International Journal of Pharmaceutics*, 269:417- 432.

WATANABE, T., WAKIYAMA, N., IKEDA, M., ISOBE, T. & SENNA, M. 2001. Stability of amorphous indomethacin compounded with silica. *International Journal of Pharmaceutics, 226(1-2):81-91.*

WORLD HEALTH ORGANIZATION (WHO). 2003. Substandard and counterfeit medicines. [Web:] http://www.who.int/mediacentre/factsheets/2003/fs275/en/ [Date of access: 23 July 2012].

WORLD HEALTH ORGANIZATION (WHO). 2009. Priority Interventions: HIV/AIDS prevention, treatment and care in the health sector. [Web:] http://www.who.int/hiv/pub/priority_interventions_web.pdf [Date of access: 23 July 2012].

WORLD HEALTH ORGANIZATION (WHO). 2010a. World malaria report. [Web:] http://www.who.int/malaria/world_malaria_report_2010/en/ [Date of access: 23 July 2012].

WORLD HEALTH ORGANIZATION (WHO). 2010b. Global summary of the AIDS pandemic, 2010. [Web:] http://www.who.int/hiv/data/2011_epi_core_en.png [Date of access: 23 July 2012].

WORLD HEALTH ORGANIZATION (WHO). 2012a. 10 facts on malaria. [Web:] http://www.who.int/features/factfiles/malaria/en/index.html [Date of access: 23 July 2012].

WORLD HEALTH ORGANIZATION (WHO). 2012b. Global malaria programme. [Web:] http://www.who.int/malaria/ [Date of access: 23 July 2012].

WORLD HEALTH ORGANIZATION (WHO). 2012c. Sources, quality and prices of active pharmaceutical ingredients of antiretroviral drugs: results of a 2012 WHO survey. [Web:] http://www.who.int/hiv/pub/amds/api2012/en/index.html [Date of access: 23 July 2012].

WU, L.S., TOROSIAN, G., SIGVARDSON, K., GERARD, C. & HUSSAIN, M.A. 1994. Investigation of moricizine hydrochloride polymorphs. *Journal of Pharmaceutical Sciences,* 83(10):1404-1406.

WU, T., SUN, Y., LI, N., DE VILLIERS, M.M. & YU, L. 2007. Inhibiting surface crystallization of amorphous indomethacin by nanocoating. *Langmuir, 23(9):*5148-5153.

YU, L. 2001. Amorphous pharmaceutical solids: preparation, characterization and stabilization. *Advanced Drug Delivery Reviews,* 48:27-42.

YU, L., REUTZEL, S.M. & STEPHENSON, G.A. 1998. Physical characterisation of polymorphic drugs: an integrated characterization strategy. *PSTT*, 1(3):118-127.

ZHANG, H. 2010. Polymorphs of donepezil salts, preparation methods and uses thereof. Patent: US 2010/0311793 A1.

ZUPANCIC, V., OGRAJSEK, N., KOTAR-JORDAN, B. & VRECER, F. 2005. Physical characterization of pantoprazole sodium hydrates. *International Journal of Pharmaceutics*, 291:59-68.

Part I
Efavirenz

Chapter 2

Anomalous dissolution behaviour of a novel amorphous form of Efavirenz

Chapter 2 is presented in the form of a research article/manuscript and has already been published in the journal entitled: “American Journal of Pharmtech Research”. This journal is an open access, free source. Electronic access to this specific manuscript can be achieved via

http://www.ajptr.com/archive/volume-2/april-2012-issue-2/article-141.html

The guidelines for authors pertaining to this specific journal have been included as Annexure A.

Supplementary information to this manuscript has been included as Annexure B.

Please note that all requirements of the author guidelines were met at the time when the manuscript was submitted. The fact that the manuscript was accepted and published serves as proof to show adherence to the author guidelines. The manuscript presented in this Chapter is the work in its final printed format and not the separate documents as per the requirements at time of submission.

Also note that the page numbers in the bottom right corner applies to the thesis, whereas the page numbers in the bottom middle applied to the journal in which it was published.

Reproduction rights was obtained from the editor of the journal in November 2014.

AMERICAN JOURNAL OF PHARMTECH RESEARCH
Journal home page: http://www.ajptr.com/

Anomalous dissolution behaviour of a novel amorphous form of Efavirenz

Zak Perold[1], Erna Swanepoel[1], Marius Brits[2*]
1. Research Institute for Industrial Pharmacy, North-West University, South Africa
2. WHO Collaborating Centre for the Quality Assurance of Medicines, North-West University, South Africa

ABSTRACT

This study evaluated the dissolution behaviour of a novel amorphous form (Form A) and the commercially preferred crystalline form (Form I) of efavirenz. Generally, amorphous forms tend to achieve a greater extent and rate of dissolution compared to their crystalline counterparts. The results showed that the dissolution of Form A to be significantly lower than that of Form I due to agglomeration. Factors which contributed to the agglomeration behaviour of Form A include: high surface free energy, a lower degree of wetting, and the low glass transition temperature of Form A which caused the sample to convert to the rubber phase which is stickier. The agglomeration increased the relative particle size thereby reducing the exposed surface area of Form A; ultimately reducing the rate and extent of dissolution. The dissolution behaviour of Form A was found to be dependent on sample size and surfactant (SLS) concentration. Scanning Electron Microscopy (SEM) was employed to investigate surface area properties which provided information supporting the powder dissolution results. The solubility and intrinsic behaviour of the two forms were found to be comparable. Upon further investigation it was found that Form A undergoes phase mediated transformation into Form I during the solubility and dissolution experiments and that this too contributed to the apparent dissolution and solubility behaviour of Form A. It was found the nucleation rate of Form A was potentiated by higher SLS content in the dissolution medium.

Keywords: polymorph, amorph, dissolution, solubility, efavirenz.

*Corresponding Author Email: Marius.Brits@nwu.ac.za
Received 24 January 2012, Accepted 8 February 2012

Please cite this article in press as: Perold Z *et al.*, Anomalous Dissolution Behaviour of A Novel Amorphous Form of Efavirenz. American Journal of PharmTech Research 2012.

INTRODUCTION:

Efavirenz is a non-nucleoside reverse transcriptase inhibitor (NNRTI) which acts as an inhibitor of HIV-1 reverse transcriptase[1]. It is commonly administered in combination with nucleoside reverse transcriptase inhibitors (NRTI) due to the fact that resistance towards NNRTIs has been reported[1].The use of substandard medicines result in treatment failure and increases the risk of resistantance[2,3]. Substandard medicines are products whose composition and ingredients do not meet the final product specifications[3].

A total of 19 different solid forms of efavirenz are currently described in the literature: Forms I-V, H1, α, β, y, y1, y2, ω, δ, N, O and P as well as three amorphous forms[4-8]. The literature suggests Form I to be the most desired crystal form of efavirenz for pharmaceutical manufacturing[4,5]. Different solid forms of a compound may vary in solubility and rate of dissolution due to differences in thermodynamic properties of the crystal conformations[9,10]. The more stable the crystal form, the stronger the bonding forces between the molecules will be and vice versa[10]. For dissolution to take place, the intermolecular forces of a compound must be overcome[10], and therefore rate of dissolution is indirectly proportional to crystal stability. Efavirenz is a poorly water soluble compound[11] rendering its polymorphs susceptible to significant differences in bioavailability. Theoretically meta-stable forms will exhibit higher solubility compared to their crystalline counterparts[9,10]. Amorphous forms being the least stable form of a compound are therefore anticipated to exhibit the greatest dissolution rate and extent of dissolution compared to its crystalline forms[10].

Many other aspects (besides polymorphism) contribute to product quality, including the analytical methods and specifications which are used to assess performance indicators (like dissolution). A recent study proposed how changes to the current USP dissolution medium (0.1 N HCL with 1% (w/v) Sodium Laurel Sulfate-SLS) can aid with identification of the mebendazole polymorphic forms[12]. At the time of this study, we noticed that numerous manufacturer methods, guidelines and in-process monographs state the use of either 1% or 2% SLS as dissolution medium for Efavirenz final products[13-15].

In the light of the aforementioned, we set the following objectives for this study:

i) to prepare and characterize an amorphous form of efavirenz (Form A) prepared by a quench cooling technique;

ii) to evaluate the dissolution and solubility properties of efavirenz Form A and Form I, and

iii) evaluate the difference between the use of 1% w/v or 2% w/v SLS as dissolution medium on the dissolution behaviour of both forms

MATERIALS AND METHODS

Particle size analysis

Prior to any experimental procedure, both forms (Form A and Form I) were lightly ground with the use of a mortar and pestle. The resultant powder was sieved and subjected to particle size analysis to ensure a uniform particle size distribution. Particle size distribution measurements were done with a Malvern Mastersizer 2000 (Malvern Instruments Ltd., Malvern, UK) fitted with a Hydro 2000SM dispersion unit. Samples were dispersed in the sample suspension unit containing a dispersant (water). The average d(0.5) and d(0.9) values obtained for Form I were 44 µm and 122 µm respectively. The average d(0.5) and d(0.9) values obtained for Form A were 57 µm and 123 µm. The results obtained from particle size analysis rendered the particle size of the powder used for experimental procedures to be comparable.

Diffuse Reflectance Infra-red Fourier Transform (DRIFT) spectroscopy

The IR spectra were recorded on a Nicolet Nexus 470 spectrophotometer with the Avatar diffuse reflectance smart accessory (Nicolet Instrument Corp., Madison, WI) over a range of 4000 cm^{-1}-400 cm^{-1}. IR samples were prepared and analyzed in a potassium bromide (Merck®, Johannesburg, South Africa) matrix.

X-Ray Diffractometry (XRD)

A Bruker D8-Advanced diffractometer (Bruker, Frankfurt, Germany) was used to obtain X-Ray Powder Diffraction (XRPD) patterns. The following conditions were applicable: target, Cu; voltage, 40 kV; current, 30 mA; divergence slit, 2 mm; anti-scatter slit, 0.6 mm, detector slit, 0.2 mm; monochromator; scanning speed, 2/min with a step size of 0.025 and a step time of 1.0 sec.

Differential Scanning Calorimetry (DSC)

Approximately 2-5 mg of sample was weighed into a 40 µl aluminium sample pan, fitted with a pierced lid (Mettler Toledo, Greifensee, Switzerland) and crimped. Samples were analyzed using a Mettler Toledo DSC823^e (Mettler Toledo, Greifensee, Switzerland) at a heating rate of 10°C/minute with the nitrogen flow rate set to 80 ml/min. The thermal events were evaluated by means of the STAR^e software (version 9.0x) (Mettler Toledo, Greifensee, Switzerland).

Dissolution

Two different dissolution techniques were employed to study the dissolution properties of Form A and Form I, namely: powder dissolution and intrinsic dissolution. For both techniques an

Erweka D700 dissolution system (Erweka, Heustenstamm, Germany) fitted with paddles (50 rpm) was used. 1% and 2% (w/v) SLS solutions were used as dissolution media. The dissolution experiments were performed at 37.0±0.5°C.

The samples and standards were suitably diluted and filtered before analysis. Samples were analyzed by means of (High Pressure Liquid Chromatography) HPLC as described under the High Pressure Liquid Chromatography analysis section.

Powder dissolution

The technique described by Lötter and co-workers[16] was used for the powder dissolution testing. This technique has successfully been used to distinguish between different crystal forms of different active pharmaceutical ingredients[12,17]. Samples weighing approximately 50 mg, 200 mg and 600 mg were accurately transferred into test tubes containing glass beads with a diameter of 0.1 mm (Sigma Aldrich, Johannesburg, South Africa) corresponding to approximately 50% of the sample weight. 10 ml of dissolution medium was transferred into each test tube. The suspended samples were agitated using a Vortex Genie shaker (Scientific Industries Inc., Bohemia, New York) for 30 seconds, before being rinsed into the respective vessels. Samples were withdrawn after 7.5, 15, 30 and 45 minutes. The samples were filtered using Millipore 0.45 µm filters (supplied by Microsep, Sandton, South Africa) prior to HPLC analysis.

The dissolution profiles of Form A and Form I were compared using the similarity factor[18]. The equation for the similarity factor (f_2) is depicted by equation 1. Form I was used as the reference sample.

$$f_2 = 50 \cdot \log\left\{\left[1 + \frac{1}{n}\sum_{t=1}^{n}(R_t - T_t)^2\right]^{-0.5} \times 100\right\} \quad (1)$$

Where: n is the number of withdrawals; R_t is the % reference sample dissolved at time t and T_t is the % sample dissolved at time t.

Intrinsic dissolution

The intrinsic dissolution behaviour of Form A and Form I in 1% (w/v) SLS was evaluated using the guidelines described in the current United States Pharmacopeia[19] and British Pharmacopeia[20]. 300 mg samples were compressed (3 ton for 1 minute) using a Beckman 00-25 hydrolic press (Beckman, Glenrothes, Scotland) in tempered aluminum dies (diameter: 13 mm). Samples were withdrawn after 7.5, 15, 30, 60, 90, 120, 180 and 240 minutes. The samples were filtered using Millipore 0.45 µm filters (supplied by Microsep, Sandton, South Africa) and suitably diluted prior to HPLC analysis.

Solubility studies

The solubility of the two forms were determined in 0.1N HCl (pH 1.2), acetate buffer (pH 4.5), phosphate buffer (pH 6.8), 1% (w/v) SLS and 2% (w/v) SLS. Sieved fractions (approximately 200 mg) of the two forms were weighed and transferred into test tubes together with 5 ml of each medium respectively. The test tubes were sealed and affixed to sample holders in a temperature controlled water bath which was maintained at 37.0±0.2˚C. The samples were rotated at 50 rpm for 24 hours. The samples were filtered using Millipore 0.45 µm filters (supplied by Microsep, Sandton, South Africa) and suitably diluted prior to HPLC analysis.

Contact angle measurement (CAM)

Powder samples were transferred into suitable CAM sample holders. The surface of the powder bed was smoothened to ensure an even powder surface. A Krüss DSA 100S (Krüss, Hamburg, Germany) drop shape analyzer with Drop Shape Analysis for Windows, version 1.90.0.14 (Krüss, Hamburg, Germany) was used for contact angle measurements. The water drop size ranged from 7-13 µl. The sessile drop method was employed and the results were calculated using the tangent technique.

Hot stage microscopy (HSM)

A Nikon DS-Fi1 (Nikon, Tokyo, Japan) digital camera affixed to a Nikon ECLIPSE E400 light microscope (Nikon, Tokyo, Japan) was used for HSM. Samples were heated with the use of a Leitz hot stage (Leica Microsystems Inc., Bannockburn, IL). The captured images were analyzed using NIS-Elements F2.30 software (Nikon, Tokyo, Japan).

Scanning Electron Microscopy (SEM)

A small amount of sample was used to cover the carbon tape that was affixed to the pin. The sample was then covered with a gold-palladium film using an IB-2 Eiko engineering ion coater inside a vacuum (Eiko Engineering, Ibaraki, Japan). The coated sample was then affixed to the microscope sample holder and analyzed using a FEI Quanta 200 ESEM & Oxford INCA 400 EDS system (FEI, Hillsboro, OR).

High Pressure Liquid Chromatography (HPLC) analysis

The concentration of efavirenz from the dissolution and solubility samples was measured employing an isocratic HPLC method[21] on an Agilent 1200 HPLC system with Rev. B. 02.01-SR2 [260] ChemStation for LC 3D systems software (Agilent Technologies, Santa Clara, CA). A C18 (5 µm, 4.6 mm x 25 cm) column (Phenomenex, Torrance, CA) was used.

RESULT AND DISCUSSION

Preparation of the amorphous form of efavirenz

Efavirenz raw material (Matrix Laboratories Limited, Secunderabad, India), was obtained from a local pharmaceutical manufacturer. This raw material (Form I) was used as starting material for the preparation of the amorphous form by quench cooling the melt. A calibrated laboratory hot plate was covered with aluminum foil and set to 140°C. A desired amount of Form I raw material was placed onto the aluminum foil and allowed to melt. The aluminum foil was thereafter quickly removed from the hot plate and subjected to ambient conditions. The melt instantly solidified into a glassy solid. The obtained glass was dubbed efavirenz Form A. Form A was subjected to assay analysis using the method as described in the HPLC section to ensure that the employed preparation method did not result in any significant breakdown of the active. The recovery of efavirenz was found to be 99.6%.

Being an amorphous solid form, the stability of Form A was expected to be at risk. For this reason Form A was freshly prepared for each experimental procedure. The desired amount which was required for a given experimental procedure was prepared directly prior to use.

Characterization of the efavirenz crystal forms

Physico-chemical characterization by means of XRPD, DRIFT-IR and DSC was performed on the samples.

The x-ray powder diffractogram of the efavirenz raw material produced clearly defined diffraction peaks characteristic of a crystalline form (Figure 1). The presence of diffraction peaks at the following 2θ- angles: 6.0±0.2, 6.3±0.2, 10.3±0.2, 10.8±0.2, 14.1±0.2, 16.8±0.2, 20.0±0.2, 20.5±0.2, 21.10±0.2 and 24.8±0.2, confirmed the raw material to be Form I[4,5]. Form A revealed no distinct XRPD peaks (Figure 1), confirming absence of a definite crystal packing. The IR spectra of Form I and Form A differed significantly in the 2750-3500 cm^{-1} and 1600-1800 cm^{-1} regions (Figure 2). The IR spectrum of Form A did not reveal the secondary amine stretch at 3312 cm^{-1} which is prominent in the IR spectrum of Form I. Furthermore, the carbonyl stretch was observed at 1739 cm^{-1} and at 1750 cm^{-1} for Form A and Form I respectively.

The DSC thermogram of Form I revealed a melting endotherm (T_m) at 138.40˚C whilst that of Form A revealed a glass transition at 33.4˚C (T_g), a crystallization exotherm (T_c) at 83.26˚C and a melting endotherm (T_m) at 138.00˚C, when heated at a rate of 10˚C/min (Figure 3). The low T_g suggest that Form A will present in the rubber phase above this temperature and as a glass below this temperature[10].

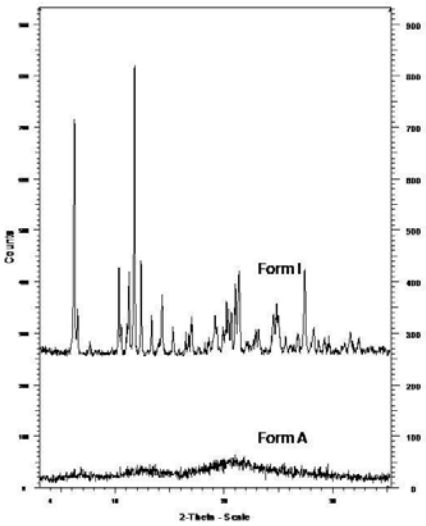

Figure 1: XRP diffractograms of efavirenz Form I and Form A.

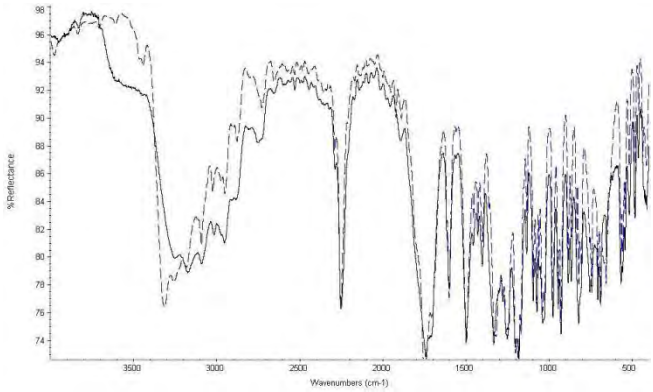

Figure 2: Overlay of the DRIFT-IR spectra of Form I (dotted) and Form A (solid).

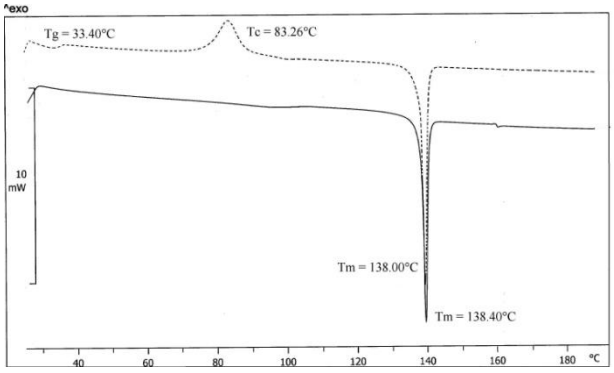

Figure 3: DSC thermograms of efavirenz Form I (solid line) and Form A (dotted line) when heated at a rate of 10˚C/min.

Hot stage microscopy (HSM) was used to elucidate and confirm the thermal events observed in the DSC thermograms of Form A and Form I. Form A revealed fine, superficial channels which formed during the preparation of the glass (Figure 4 - 1). No birefringence was detected when the sample was exposed to polarized light confirming the absence of crystalline phases in the

sample. Between 28-63°C the superficial channels disappeared and the sample displayed a smooth viscous-like surface, which could be attributed to the transition of the glass to the rubber phase. Small nuclei were detected at 76°C (Figure 4 - 3) which revealed a two dimensional growth when exposed to increased temperatures (Figure 4 - 4). Investigation of the sample at 84°C under polarized light confirmed the growth of the crystalline phase due to the presence of birefringence (Figure 4 - 6). The crystalline phase darkened at 132°C (Figure 4 - 7) and underwent complete melting at approximately 138°C (Figure 4 - 8). No remarkable HSM events were observed for Form I when exposed to increased temperatures. The melting of Form I initiated at 128°C and concluded at 135°C, confirming the single thermal event observed in the DSC thermogram thereof.

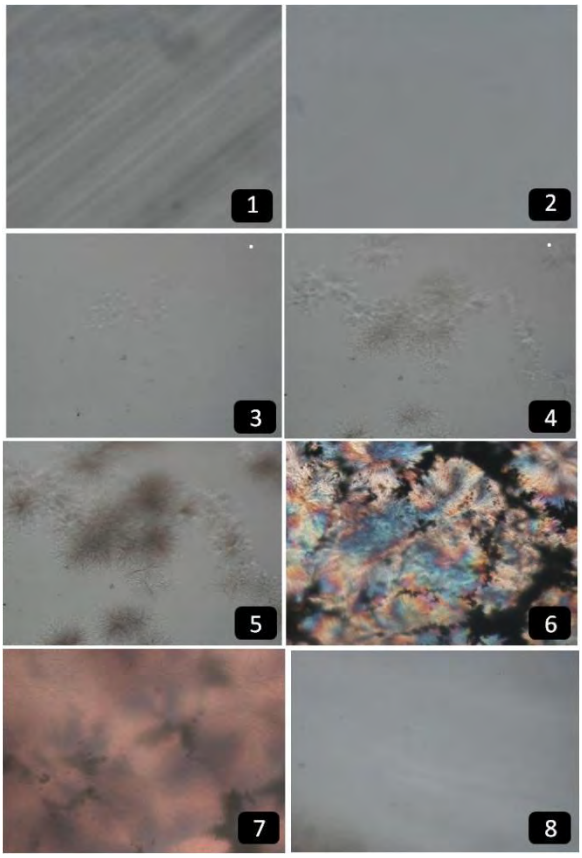

Figure 4: Hot stage photomicrographs of Form A at: (1) 15°C, (2) 55°C, (3) 76°C, (4) 79°C, (5) 80°C, (6) 84°C, (7) 132°C & (8) 138°C.

Based on the characterization techniques employed, it was clear that Form A and Form I were different solid forms of efavirenz. The study was furthered by examining the potential differences in dissolution behaviour of the two solid forms using powder and intrinsic dissolution techniques.

Powder dissolution

The objective of the powder dissolution studies was to determine potential differences in the dissolution behaviour of Form A and Form I. A two dimensional matrix approach was used for this study, evaluating the influence of variations in sample size and dissolution medium composition, on the discriminatory ability of the powder dissolution technique. The dissolution of Form A and Form I in sample sizes of 50 mg, 200 mg, and 600 mg were evaluated in 1% and 2% (w/v) SLS. The specific sample sizes were selected, as they represent the most common dosage strengths in the commercial pharmaceutical products[7]. The powder dissolution profiles are illustrated in Figure 5. The error bars included in the figures are based on ± 2 standard deviations.

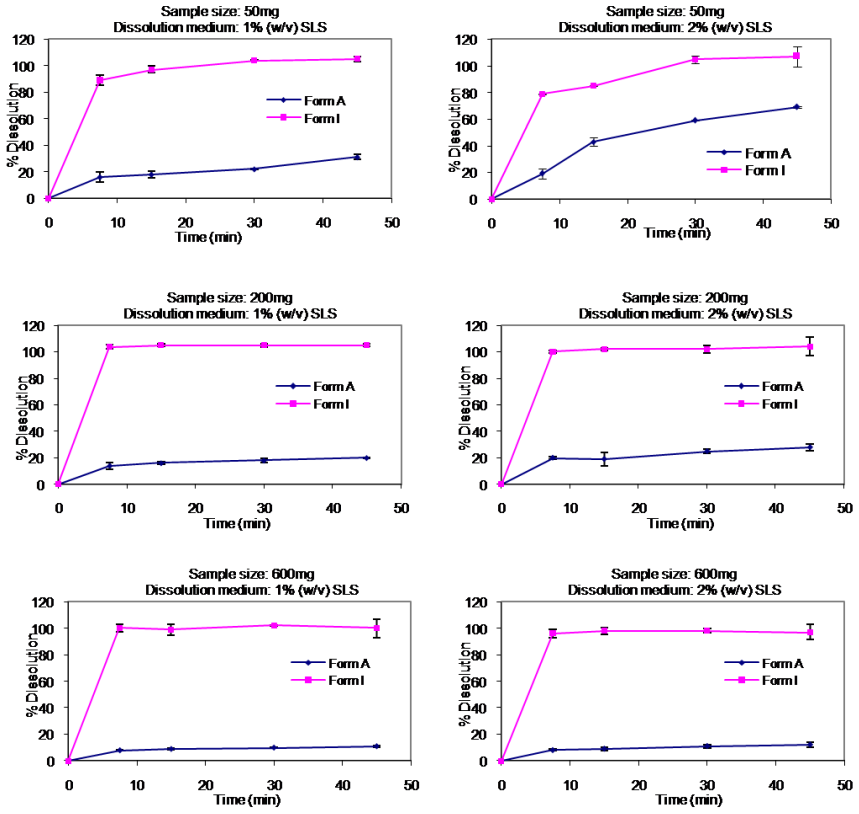

Figure 5: Dissolution profiles of Form I and Form A (sample sizes: 50 mg, 200 mg and 600 mg) in 1% and 2% (w/v) SLS respectively.

Differences in the rate and extent of dissolution of Form A and Form I were observed. Form I revealed 100% dissolution after 30 minutes regardless of the % SLS in the dissolution medium or the sample size used for the dissolution. The 50 mg dissolution profiles of Form A revealed that the extent of dissolution was approximately 2 times greater in 2% (w/v) SLS than in 1% (w/v) SLS at Q_{45min}. The difference between the Q_{45min} of Form A in 2% (w/v) and 1% (w/v)

SLS, was found to be 8% and ~0% for the 200 mg and 600 mg sample sizes respectively. The f_2-similarity factors calculated for all the profiles (Figure 6) revealed that the dissolution profiles of Form A and Form I in the various media and various sample sizes differed significantly (all $f_2 < 50$).

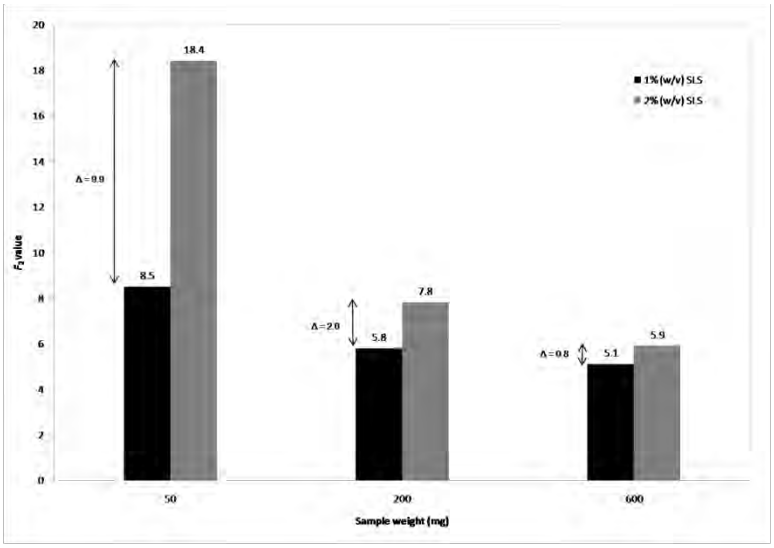

Figure 6: f_2-similarity factors calculated for the dissolution profiles of Form A and Form I using different sample sizes in 1% and 2% (w/v) SLS.

The discriminatory ability of the dissolution method was influenced by the variations in the sample size and the SLS concentration of the dissolution media (Figure 6). The effect of higher SLS concentration can predominantly be observed when comparing the 50 mg profiles in the different dissolution media. When using a sample size of 50 mg, the higher SLS content (2% SLS) resulted in a difference of 9.9 in the f_2 value when compared to the profiles in 1% SLS, however when using larger sample sizes, the higher SLS content did not significantly improve the dissolution of Form A in comparison with the dissolution behaviour thereof in 1% SLS.

Both Form A and Form I underwent agglomeration once introduced to the dissolution medium (in 1% and 2% SLS). The size of the Form A agglomerates increased with an increase in sample size, whereas the size of the Form I agglomerates remained fairly constant (Figure 7). The increased tendency towards agglomeration of Form A, increased the relative particle size of Form A, thereby reducing the exposed surface area of Form A; ultimately reducing the rate and extent of dissolution. The fact that Form I did not show an increased tendency towards agglomeration with an increase in sample size explains why much better dissolution of this form was possible. The increased tendency of Form A to form agglomerates once introduced into the medium may also be attributed to the temperature of the dissolution medium. The temperature at

which the dissolution experiments were performed (37.0±0.5°C), suggest Form A to present in the rubber phase at this temperature. The rubbery state is known to exhibit stickiness[10], which increased the tendency towards agglomeration.

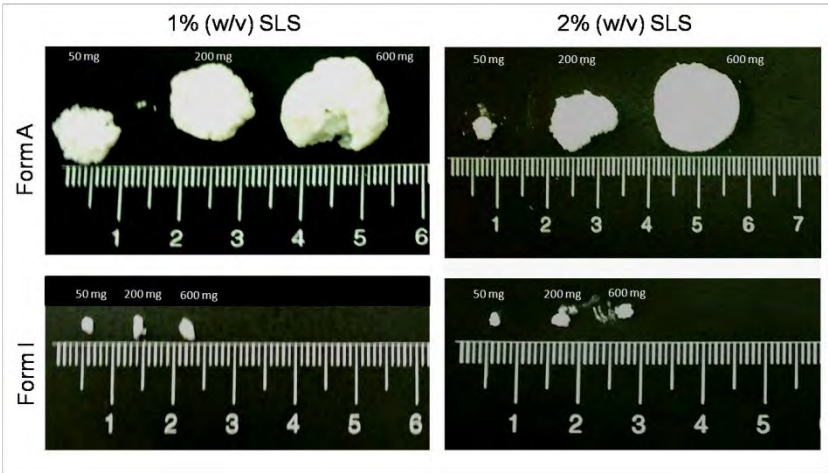

Figure 7: Typical agglomerates of Form A and Form I which formed once introduced into the dissolution media.

Although an increase in SLS content did not favour the dissolution of Form A in sample sizes of 200 mg and 600 mg in such a way as with the 50 mg sample size, the increase of SLS content did manage to potentiate the disintegration of Form A agglomerates. This observation was prominent in sample sizes of 50 and 200 mg, but less noticeable in the 600 mg sample size. Figure 8 (a) and (b) revealed that the amount of Form I dissolved after 45 minutes in both media ($C_{1\%}$ and $C_{2\%}$) was directly proportional to the sample size ($R^2 = 0.999$). The correlation between the sample size and $C_{1\%}$ or $C_{2\%}$ of Form A was diminished ($R^2 \leq 0.943$) due to the inconsistent formation and disintegration of agglomerates. The ratio of $C_{2\%}$:$C_{1\%}$ of Form A versus the sample size revealed that an increase in the SLS concentration of the medium potentiated the disintegration and dissolution of Form A. During the dissolution study it was observed that smaller agglomerates disintegrated faster compared to larger agglomerates (50 mg > 200 mg > 600 mg), elucidating the higher $C_{2\%}$ values at smaller sample sizes.

The results obtained in this study are inconsistent with anticipated behaviour of amorphous forms (i.e. improved dissolution)[10]. The dissolution behaviour of Form A can be elucidated utilizing the Noyes Whitney equation – equation 2[20].

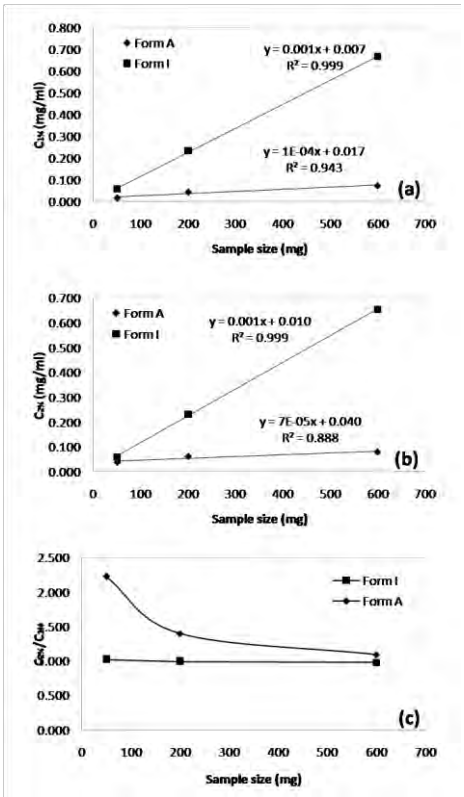

Figure 8: The amount of Form A and Form I dissolved in (a) 1% (w/v) SLS and (b) 2% (w/v) SLS after 45 minutes and (c) the ratio of the results obtained in 2% (w/v) SLS and 1% (w/v) SLS.

$$\frac{dm}{dt} = kA(C_s - C) \qquad (2)$$

Where $\frac{dm}{dt}$ is the dissolution rate, k the dissolution rate constant, A the surface area of the dissolving solid, C_s the concentration of the solid in the dissolution medium and C the concentration of the solid in the diffusion layer surrounding the solid.

The Noyes Whitney equation reveals that the dissolution rate is dependant on surface area (A) and solubility ($C_s - C$) of the solid. We investigated the solubility and surface area properties (by CAM and SEM) of the two forms in order to evaluate the potential influences these properties may have on the dissolution behaviour.

Solubility

Forms A and I were subjected to 24 hour solubility experiments in aqueous physiological- (0.1 N HCl pH 1.2, acetate buffer pH 4.5 and phosphate buffer pH 6.8) and non-physiological (1% (w/v) and 2% (w/v) SLS) media. The solubility results in the physiological media were extremely low, which corresponded well with the findings of Rowe *et al.*[23]. The solubility of efavirenz Form A and Form I in 1% and 2% (w/v) SLS are reported in Table 1. The increase in

the SLS concentration of the medium caused a two fold increase in the solubility of the two forms. The solubility ratios for Forms A and I in 1% and 2% (w/v) SLS ranged between 1.0 and 1.2, indicating that the solubility of Form A and Form I in the mentioned media did not differ significantly. Anomalous behaviour of amorphous forms has been reported in the literature where the amorphous forms revealed a lower/same solubility compared to their crystalline counterparts[17,24,25].

Table 1. The solubility (δ) of efavirenz Form I (I) and Form A (A) in 1% and 2% (w/v) SLS respectively at 37.0±0.2°C after 24 hours

	1 % (w/v) SLS	2% (w/v) SLS	$\delta^{2\%}/\delta^{1\%}$
Form A	$\delta_A^{1\%}$=11.02 ± 0.16 mg/ml	$\delta_A^{2\%}$=21.1 ± 0.27 mg/ml	$\delta_A^{2\%}/\delta_A^{1\%}$=2.1
Form I	$\delta_I^{1\%}$= 9.11 ± 0.83 mg/ml	$\delta_I^{2\%}$= 22.3 ± 1.29 mg/ml	$\delta_I^{2\%}/\delta_I^{1\%}$= 2.5
δ_A/δ_I	$\delta_A^{1\%}/\delta_I^{1\%}$=1.2	$\delta_A^{2\%}/\delta_I^{2\%}$=1.0	

Due to the fact that the equilibrium solubility was determined after 24 hours, the similarity in the solubilities of the two forms could have been attributed to the conversion of Form A to Form I in the aqueous media. The powder residue from the solubility experiments were subjected to further analysis (see phase mediated transformation section).

Wettability

Since wetting of a solid is the precursor to the dissolution process, it is understandable that differences in wettability will result in differences in dissolution rate. Contact angle measurements are commonly used to evaluate the extent of wettability and are often capable of elucidating differences in the crystal surface properties of polymorphic forms, making it possible to explain differences in dissolution behaviour[26,27].

The contact angles of Form A (θ=135.1±0.5°) and Form I (θ=113.2±0.2°) were calculated using the tangent method and the circle fill method – Figure 9. The results obtained from both methods were in agreement. The higher contact angle of Form A signifies a higher surface free energy of the solid and a lower degree of wetting compared to that of Form I. It has been reported that cohesive energy of a substance is directly proportional to the surface free energy of the solid[28]. CAM findings thus supports why the tendency of agglomeration was more prominent with Form A in comparison with Form I. Common techniques (such as interactive mixing, sonication and

vortexing with glass beads) that are employed to decrease the effect of agglomeration during powder dissolution are not always successful[28], as was the case with this study. The lower extent of wettability and high extent of agglomeration contributed to the lower dissolution of Form A when compared to Form I.

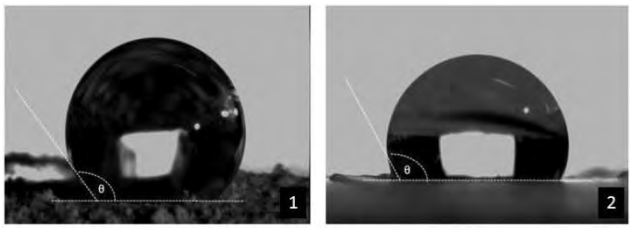

Figure 9: The contact angles of: 1) Form A (θ=135.1±0.5°) and 2) Form I (θ=113.2±0.2°).

Scanning electron microscopy (SEM)

SEM was used to compare the surface area properties of Form A and Form I. The SEM photomicrographs are depicted in Figure 10. The SEM photomicrograph of Form A revealed shapeless, plate-like particles with dense, smooth surfaces whereas Form I presented particles with varying morphology and prominent layering characteristics. The layered structure of Form I allowed for a greater surface area exposed to the dissolution medium, which benefitted its dissolution more than the morphology of Form A.

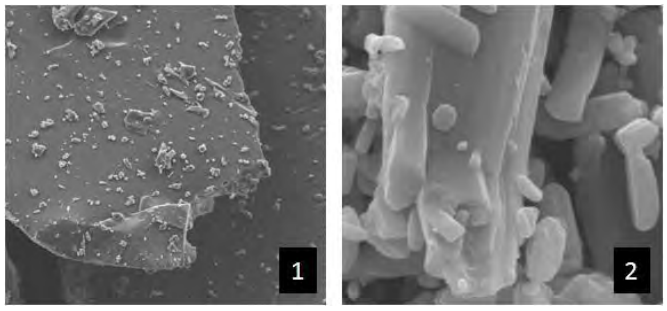

Figure 10: SEM photomicrographs of Form A (1) and Form I (2).

It can thus be concluded that the significant differences in the powder dissolution of Form A and Form I, could be attributed to the differences in the surface area properties of the two forms.

Intrinsic Dissolution

Intrinsic dissolution studies were performed on Form A and Form I in order to evaluate the dissolution behaviour with a constant surface area, thus minimizing the effect of surface properties and agglomeration. The intrinsic dissolution results of Form A and Form I are depicted in Figure 11.

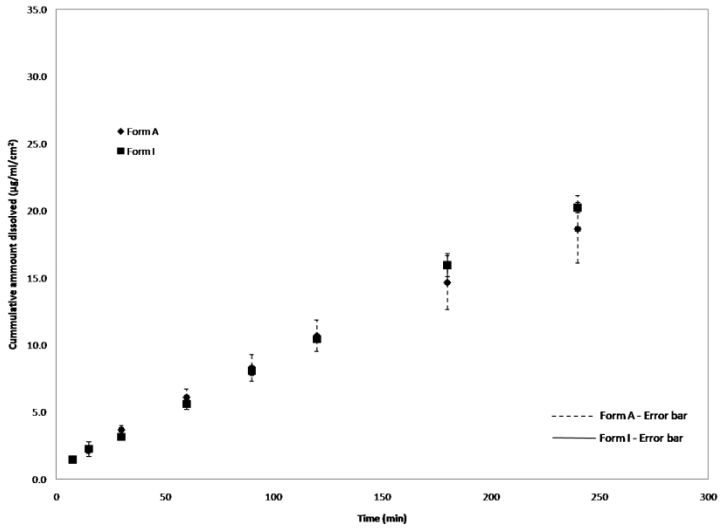

Figure 11. The intrinsic dissolution of Form A and Form I dissolved versus time in 1% (w/v) SLS at 37.0±0.5°C.

To ensure sink conditions during the intrinsic dissolution studies, the minimum dissolution medium volumes (V_{min}) were calculated for Form A and Form I using equation 3[29].

$V_{min} = (W \times 10)/ \delta$ (3)

Where V_{min} is the minimum dissolution medium volume required, W is the weight of the sample and δ the solubility of the form in the specific dissolution[29].

V_{min} was calculated for Form A and Form I, and found to be 272 ml and 329 ml respectively. Thus, the 900 ml dissolution medium volume that was used during this study was adequate to ensure sink conditions. The absence of a plato (Figure 11) confirmed the sink conditions.

Upon completion of the study it was observed that the surfaces of the Form A compacts revealed prominent, white encrustments (Figure 12). It has been reported that dissolution may induce a solvent mediated phase transformation of meta-stable crystal phases[30]. We investigated this possibility by performing DSC and XRPD analysis on these encrustments (refer to phase mediated transformation section).

Phase mediated transformation

Analysis of the powder remnants from the solubility and dissolution experiments by XRPD revealed that Form A had converted into Form I during these experiments. The XRPD no longer depicted a halo shape, but instead revealed the presence of the most prominent peaks characteristic of Form I (see section characterisation).

DSC is commonly employed to quantify amorphous content[31,32], and for this reason such a method was similarly developed to quantify Form A. Binary mixtures of Form A and I were

prepared and analysed by DSC. The difference in recrystallisation energy allowed for the linear calibration curve (Figure 13), which made it possible to calculate unknown concentrations of Form A from the dissolution and solubility samples.

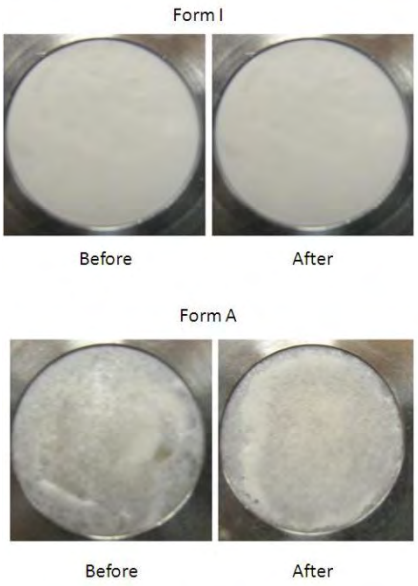

Figure 12: Appearance of the Form A & Form I compacts prior- and after the intrinsic dissolution studies revealed the prominent, white encrustments formed on the surface of the Form A compacts.

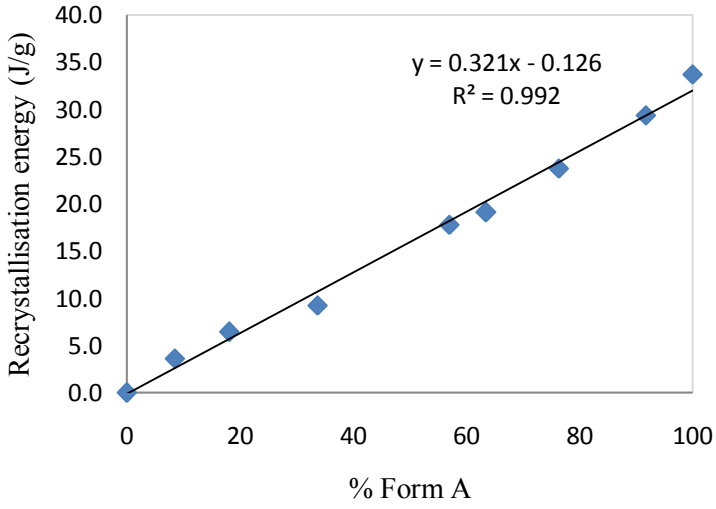

Figure 13: The relationship between recrystallization energy and theoretical % Form A.

The powder remnants from the solubility experiments after 24 hours revealed that Form A had completely transformed in Form I (% Form I ~ 100%) as the DSC thermogram did not present with a recrystallisation peak (recrystallisation energy = 0 J/g). The solubility of Form A, and its influence on the powder dissolution thereof, is therefore dependent on the rate and extent of the

conversion into Form I. The mediated phase transition of Form A during the solubility experiment elucidates the similarities in the solubility behaviour of Form A and Form I. The analysis of the white encrustments from the intrinsic dissolution experiments revealed that the exposed surface (encrustments) isolated from the compacts had completely transformed into Form I (% Form I ~ 100%) as the DSC thermogram did not present with a recrystallisation peak (recrystallisation energy = 0 J/g). The mediated phase transition of Form A elucidates the similarities in the intrinsic dissolution profiles of Form A and Form I. From Figure 11 and Table 2, it was clearly observed that the margin of error for the intrinsic dissolution of Form A increased over time. At the start of the dissolution, the margin of error is minuscule; however it intensified and reached a maximum of 2.5 µg/ml.cm^2 at the final withdrawal time. This error margin (error range) indicated that the phase transition of Form A was inconsistent amongst all the samples (vessels) and that the accuracy of the results was influenced by the varying rate and extent of phase transition.

Table 2.Intrinsic dissolution rates of Form A and Form I in 1% (w/v) SLS at 37.0±0.5°C

Form	Equation	r^2	Intrinsic dissolution rate (µg.min^{-1}.cm^{-2})	Error range (µg.ml^{-1}.cm^{-2})
A	y = 0.0735x + 1.393	0.997	0.074	0.1 – 2.5
I	y = 0.0817x + 0.815	0.999	0.082	0.1 – 0.9

The powder dissolution conditions were simulated in the same fashion as previously described, but instead of evaluating the % dissolved, we analysed the remaining powder from the vessels at the original withdrawal times, by DSC. These results (Figure 14) show that a linear relationship (R^2 > 0.990) was obtained for the phase transformation of Form A into Form I over time for the different sample sizes. These results not only made it possible to predict the extent of transformation at any given time, but also showed that the phase transformation was influenced by the agglomeration/sample size, as the phase transformation rate was found to be indirectly proportional to sample size (Figure 15). The DSC analyses of the powder samples of Form A from the powder dissolutions in 2% w/v SLS revealed that it had completely converted to Form I from 7.5 minutes regardless of the sample size.

The solubility and dissolution results obtained for Form A is not a true reflection of the behaviour of Form A, seeing that this form underwent a phase mediated transformation. It is known that surfactants (like SLS) may promote the nucleation process during the phase mediated transformation[33]. This study supports this hypothesis, seeing that the powder dissolution of Form A in 2% SLS revealed a faster transition (and dissolution) compared to that in 1% SLS.

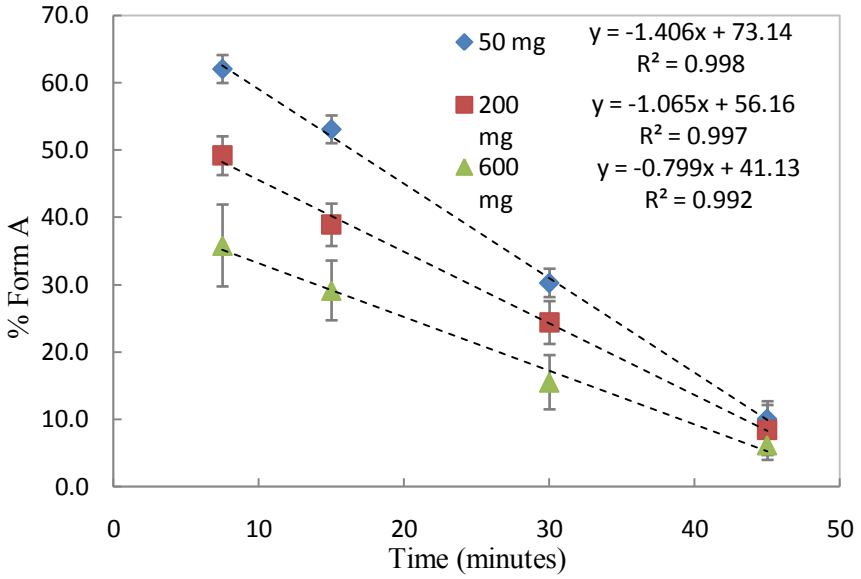

Figure 14: The % Form A at specific time intervals during powder dissolution experiments in 1% SLS for different sample sizes.

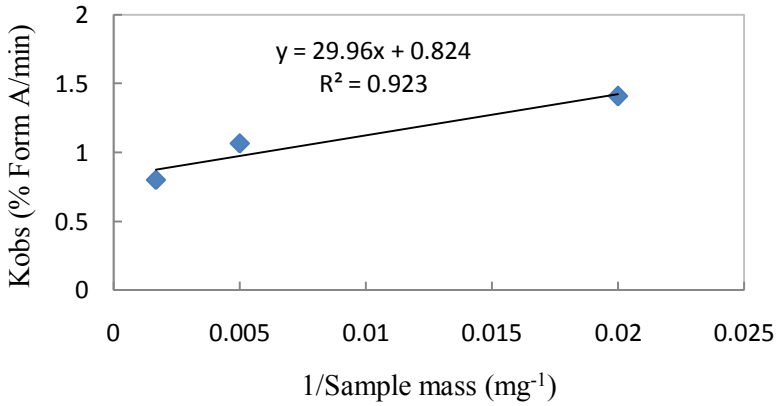

Figure 15. The relationship between the rate of phase transformation (K_{obs}) and sample size (mg^{-1}).

CONCLUSION:

An amorphous form of efavirenz (Form A) was successfully prepared by means of a quench cooling technique. Form A and the preferred polymorphic form of efavirenz (Form I), were characterized and thereafter subjected to powder dissolution, intrinsic dissolution, solubility testing, CAM and SEM analyses to evaluate the possible differences between these two forms.

Form A underwent agglomeration once introduced into the dissolution media, which limited the dissolution thereof, causing significant differences between the dissolution profiles of Form A and Form I (f_2 value < 50). The degree of the agglomeration was found to be proportional to an increase in sample size. Using higher levels of SLS potentiated the dissolution performance of

Form A in smaller sample sizes, as increased SLS content in the dissolution medium promoted the disintegration of the agglomerates at the smaller sample size. CAM and SEM supplemented the findings of the powder dissolution results.

Intrinsic dissolution and solubility studies were performed in an attempt to elucidate the findings of the powder dissolution studies. The results from the intrinsic dissolution and solubility studies showed no significant differences between Form A and Form I. Further study into the behaviour of Form A revealed it to be susceptible to phase mediated transformation in the dissolution media. It was found the transformation of Form A to be potentiated when using smaller sample sizes and higher SLS content.

Agglomeration and thermodynamic instability are unwanted characteristics during and after product manufacture which may influence the quality of a final product and ultimately the effectiveness of treatment. The use of Form A during manufacturing is discouraged.

REFERENCES:

1. Safrin S. Antiviral Agents. In, Katzung BG(ed). Basic & Clinical Pharmacology. 8th ed., New York, NY: McGraw-Hill Companies Inc; 2001; 823-44.
2. Werthemeier AI, Norris J. Safeguarding against substandard/counterfeit drugs: Mitigating a macroeconomic pandemic. Res Soc Adm Pharm 2009; 5:4-16.
3. Newton PN, Green MD, Fernandez M. Impact of poor-quality medicines in the 'developing' world. Trends Pharmacol Sci 2009; 31:99-101.
4. Clarke W, Crocker LS, Kukura JL. Process for the crystallization of reverse transcriptase inhibitor using an anti-solvent. Patent WO 98/33782 1998;29p.
5. Radesca LA, Maurin MB, Rabel SR, Moore, JR. Crystalline efavirenz. Patent WO 99/64405 1999;72p.
6. Reddy BP, Rathnakar K, Reddy RR, Reddy MD & Reddy, KS. Novel polymorphs of Efavirenz. Patent US 2006/0235008A1 2006;6p.
7. Doney JA. Amorphous efavirenz and the production thereof. Patent US 2007/0026073A1 2007;16p.
8. Sharma R, Bhusan KH, Aryan RC, Singh N, Pandya B, Kumar Y. Polymorphic forms of Efavirenz and processes for their preparation. Patent WO 2006/040643A2 2006;49p.
9. Bauer J, Spanton S, Henry R, Quick J, Dziki W, Porter W, Morris J. Ritonavir: An extraordinary example of conformational polymorphism. Pharm Res 2001; 18(6):859-66.

10. Buckton G. Solid-state properties. In Aulton ME(ed.) Pharmaceutics: The science of dosage form design. New York, NY: Churchill Livingstone; 2001; 141-52.
11. Gao JZH, Hussain MA, Motheram R, Gray, DAB, Benedek IH, Fiske WD, Doll WJ, Sandefer E, Page RC & Digenis GA. Investigation of human pharmaco scintigraphic behaviour of two tablets and a capsule formulation of a high dose poorly water soluble/highly permeable drug (Efavirenz). J Pharm Sci 2007; 96: 2970-77.
12. Swanepoel E, Liebenberg W, de Villiers MM. Quality evaluation of generic drugs by dissolution test: changing the USP dissolution medium to distinguish between active and non-active Mebendazole polymorphs. Eur J Pharm Biopharm 2003; 55: 345-49.
13. WHO.int [Internet]. World Health Organization online resources [updated 2010 Sep; cited 2012 Jan 12]. Available online at http://www.who.int/medicines/services/expertcommittees/pharmprep/EfavirenzTabs_QAS10-355Rev1_01102010.pdf
14. FDA.gov [Internet]. US Food and Drug Administration – Dissolution methods [cited 2012 Jan 12]. Available online at http://www.accessdata.fda.gov/scripts/cder/dissolution/dsp_SearchResults_Dissolutions.cfm?PrintAll=1
15. USP.org [Internet]. United States Pharmacopeial convention. Efavirenz capsules pending monograph version 1 [updated 2009; cited 2012 Jan 12]. Available online at http://www.usp.org/pdf/EN/pendingStandards/m4047.pdf
16. Lötter AP, Flanagan DR, Palepu NR, Guillory JK. A simple reproducible method for determining dissolution rates of hydrophobic powders. Pharm Tech 1983; April: 59-66.
17. Henwood SQ, Liebenberg W, Tiedt LR, Lötter AP, de Villiers MM. Characterization of the solubility and dissolution properties of several new rifampicin polymorphs, solvates and hydrates. Drug Dev Ind Pharm 2001; 27(10):1017-30.
18. Moore JW, Flanner HH. Mathematical comparison of dissolution profiles. Pharm Tech 1996; June: 64-68.
19. USPNF.com [Internet]. United States Pharmacopeia online. [Updated 2012; cited 2012 Jan 12]. Available online at http://www.uspnf.com
20. Pharmacopeia.co.uk [Internet]. British Pharmacopeia online [updated 2012; cited 2012 Jan 12]. Available online at http://www.pharmacopeia.co.uk

21. USP.org [Internet]. United States pharmacopeial convention. Authorize USP Salmous standards version 1. [Updated 2007; cited 2012 Jan 12]. Available online at http://www.usp.org/pdf/EN/international/efavirenz.pdf
22. Aulton ME. Dissolution and solubility. In Aulton ME (ed.) Pharmaceutics: The science of dosage form design. 2nd ed., New York, NY: Churchill Livingstone; 2002; 15-32.
23. Rowe S, Fontalbert L, Rabel S, Maurin M. Physical chemical properties of efavirenz. Aapsj.org [Internet]. American Association of Pharmaceutical Sciences Journal [updated 1999; cited 2012 Jan 12]. Available from http://www.aapsj.org/abstracts/AM_1999/1005.htm
24. Hancock BC, York P, Rowe RC. The use of solubility parameters in pharmaceutical dosage form design. Int J Pharm 1997; 148: 1-21.
25. Henwood SQ, Liebenberg W, Tiedt LR, Lötter AP & de Villiers MM. Characterization of the solubility and dissolution properties of several new rifampicin polymorphs, solvates and hydrates. Drug Dev Ind Pharm 2001; 27(10):1017-30.
26. Buckton G (1993) Assessment of the wet ability of pharmaceutical powders. J Adh Sci Technol 1993; 7(3): 205-19.
27. Kiesvaara J, Yliruusi J, Ahomäki E (1993) Contact angles and surface free energies of theophylline and salicylic acid powders determined by the Washburn method. Int J Pharm 1993; 97:101-09.
28. De Villiers MM. Influence of agglomeration of cohesive particles on the dissolution behavior of furosemide powder. Int J Pharm 1996; 136:175-79.
29. Fahmy R, Marnane B, Bensley & Hollenback RG. Dissolution test development for complex veterinary dosage forms: oral boluses. AAPS PharmSci 2001; 4:4 article 35.
30. Garcia E, Veesler S, Biostelle R. & Hoff H (1999) Crystallization and dissolution of pharmaceutical compounds: An experimental approach. J cryst growth 1999; 198/199: 1360-64.
31. Lappalainen M, Pitkänen I, Harjunen P. Quantification of low levels of amorphous content in sucrose by hyper DSC. Int J Pharm 2006; 307:150-55.
32. Lefort R, De Gusseme A, Willart JF, Danède F, Descamps M. Solid state NMR and DSC methods for quantifying the amorphous content in solid dosage forms: an application to ball-milling of trehalose. Int J Pharm 2004; 280:209-19.
33. Šehić S, Betz G, Hadžidedić S, El-Arini SK, Leuenberger H. Investigation of intrinsic dissolution behaviour of different carbamazepine samples. Int J Pharm 2010; 386: 77-90.

Chapter 3

Crystallisation behaviour of Efavirenz Form A: Introducing an alternative quantitation technique

Chapter 3 is presented in the form of a research article/manuscript and is aimed towards publication in the journal entitled: “AAPS PharmSciTech.

The guidelines for authors pertaining to this specific journal have been included as Annexure C.

The manuscript is presented in sufficient detail. No supplementary data has been included.

Please Note:

Although the text, figures, tables, etc. need to be submitted as separate files (in accordance with the author guidelines – Annexure C), the manuscript is presented here as a single file with text, figures and tables in a single document for ease of evaluation. For the purpose of submission, all files will be submitted as stipulated by the guidelines.

Secondly, even though the author guidelines stipulate that line numbering should be used, the manuscript presented here does not have line numbering. Line numbering will however be included before submitting the manuscript to the journal.

Crystallisation behaviour of Efavirenz Form A: Introducing an alternative quantitation technique

Zak Perold, Marius Brits*

Research Institute for Industrial Pharmacy® incorporating CENQAM® , North-West University, Potchefstroom 2520, South Africa;

*corresponding author: marius.brits@nwu.ac.za; tel: +27(18) 299 2268; fax: +27(18)299 2291; Research Institute for Industrial Pharmacy® incorporating CENQAM® , Pharmaceutics Building G2, North-West University, Potchefstroom 2520, South Africa

ABSTRACT

The thermodynamic properties and recrystallisation behaviour of an amorphous form of Efavirenz (Form A) was investigated. The glass transition temperature (T_g) and activation energy are useful parameters indicative of the thermodynamic stability of amorphous forms and were investigated for Form A. Differential Scanning Calorimetry (DSC), Hot Stage Microscopy (HSM) and Capillary Melting Point analysis (CMP) were used in conjunction with suitable kinetic models such as Kissinger-Akahura-Sunrose, Matusita and Johnson-Mehl-Avrami-Erofeyev-Kolomogorov to investigate the non-isothermal and isothermal crystallisation behaviour of Form A. The T_g of this amorphous form was determined as 28.5˚C. Microscopic and DSC studies indicated a two-dimensional growth of Form I. Non-isothermal DSC, HSM and CMP studies calculated the activation energy of Form A as 183, 210 and 186 kJ/mol respectively. The non-isothermal activation energy values calculated using DSC and CMP showed a good correlation, which shows great promise for the application of CMP in recrystallisation studies. The use of CMP for the quantification of crystallisation (and subsequent use in activation energy determinations) has never before been reported in literature and is herewith proposed as an alternative means to DSC to do so. Isothermal studies using DSC determined the recrystallisation activation energy to be 305.3 kJ/mol and half-life of Form A to be 69.2, 5.3 and 1.5 hours at 30, 35 and 40 ˚C respectively. The significant differences between isothermal and non-isothermal recrystallisation activation energies suggest that nucleation occurs though a site-saturated mechanism and the growth rates of the crystalline phase appears to be limited by surface incorporation rather than diffusion. The thermodynamic instability of this amorphous form has clearly been illustrated by the narrow thermal stability range, small reduced recrystallisation temperature and ineffectual short half-life thereof, rendering this crystal modification not suitable for pharmaceutical application.

Keywords: amorphous, glass transition, activation energy, recrystallisation, kinetics

INTRODUCTION

Amorphous forms often have higher solubilities, higher dissolution rates and/or better compression properties (amongst others) than their corresponding crystalline form(s) (1). For these reasons, the use of the amorphous form may be preferred by the pharmaceutical industry (1-3). On the other hand, the thermodynamic instability of these forms often presents problems relating to their shelf-life and/or unpredictable behaviour, which may influence the bioavailability of the Active Pharmaceutical Ingredient (API) (1-3).

Amorphous forms are thermodynamically defined as out of equilibrium states due to the fact that they contain an excess of Gibbs (G) energy (unlike their crystalline forms). The excess energy causes the amorphous form to be thermodynamically unstable. Release of the excess energy can occur either completely through crystallisation associated with $\Delta G < 0$ or partially by means of an irreversible relaxation process (4). Both aforementioned mechanisms have an influence on the physical and thermodynamical properties of the amorphous forms (4,5). The thermodynamical instability of amorphous forms may thus introduce a risk to the quality, safety, efficacy and/or the manufacturability of APIs (1-3, 6). For this reason, great interest is taken in the thermodynamic and kinetic behaviour of amorphous APIs (1-3, 4, 7).

The energetic features of an amorphous form (also referred to as a glass) are best described by an enthalpy (H) or volume (V) vs. temperature diagram (Fig. 1). The slope of each segment in the diagram represents the heat capacity of the corresponding state. From Fig. 1 it can be seen that when the liquid (molten substance) is cooled to the melting point (T_m) of the crystalline form (A-B) a first-order phase transition is observed. If crystallisation of the liquid is observed (B-C) a crystalline phase will be formed (C-D), otherwise, if crystallisation does not occur upon cooling below the melting point (T_m), a super-cooled liquid will be obtained (B-E). The equilibrium state of the super-cooled liquid is similar to that of the liquid phase, and is often referred to as the rubber state. When the super-cooled liquid is further cooled to the glass transition temperature (T_g), it will transform to a glass phase (E-F) with a decreased slope (i.e. decreased heat capacity, compared to the super-cooled liquid). At this equilibrium intersection (T_g), the slope of the function (H or V vs. temperature) changes, so that the material in the glass form presents as a solid having a higher level of H (and G) and V compared to the crystalline form. The high amount of free energy (G) serves as a driving force for the amorphous form to return to an equilibrium state, i.e. crystallise in an ordered state (devitrification) (7).

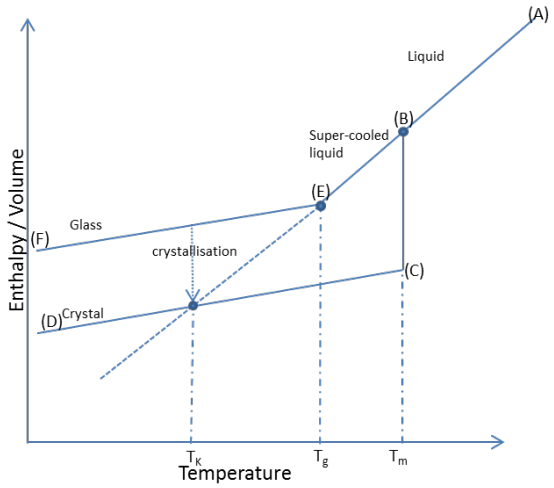

Fig. 1 Enthalpy (E) / Volume (V) vs. temperature diagram depicting the relationship between the crystal form, amorphous glass, super-cooled liquid and liquid state. Where T_g is the glass transition temperature, T_m is the fusion temperature (melting point), and T_K the Kauzmann temperature (adapted from 3).

The glass transition temperature (T_g) dictates the molecular mobility of the amorphous form. When stored at a temperature below T_g the amorphous form presents in a glass/brittle state with low molecular mobility, and at a temperature exceeding the T_g, the amorphous form presents in a rubber state with higher molecular mobility. The higher the molecular mobility, the more favourable the conditions for recrystallisation become (1,6). Thus the glass transition temperature of amorphous solids needs to be identified as a stability indicating factor.

From Fig. 1 it is clear that the heat capacity of the crystalline and amorphous phases do not differ significantly, however their physical and thermodynamical properties do differ. From the Kauzmann paradox, the Kauzmann temperature (T_K) is defined as the temperature at which the enthalpy of the super-cooled liquid and that of the crystalline phase is the same (i.e. there is no more configurational entropy in the system). T_K is considered a mathematical extrapolation (rather than a physical significant value), which serves as an indicator of the temperature of zero molecular mobility in the amorphous phase, where there is considered to be no risk of crystallisation (8).

The intrinsic instability of the amorphous form should induce an irreversible evolution towards a thermodynamically more stable crystalline state, by means of crystallisation. The crystallisation of an amorphous phase is a complex process involving simultaneous nucleation and growth of the crystalline phase (9). The crystallisation rate may be influenced by numerous, possibly interdependent parameters, where temperature (amongst others) plays a key role – Fig. 2. The nucleation rate in a super-cooled liquid increases exponentially when the temperature decreases from T_m towards T_g. However, the molecular mobility (which is required for the crystalline growth step) decreases exponentially with such a temperature decrease. From Fig. 2 it is clear that the enhanced tendency

for supercooling (caused by lowering the temperature and increased viscosity that accompanies this reduction in temperature) should give rise to a maximal crystallisation rate at some temperature between T_g and T_m (3). The rate of nucleation in the amorphous phase reaches its maximum at a temperature somewhat higher than the T_g and then decreases rapidly with increasing temperature. The crystal growth rate reaches its maximum at a temperature that is higher than the temperature of maximum nucleation rate (3).

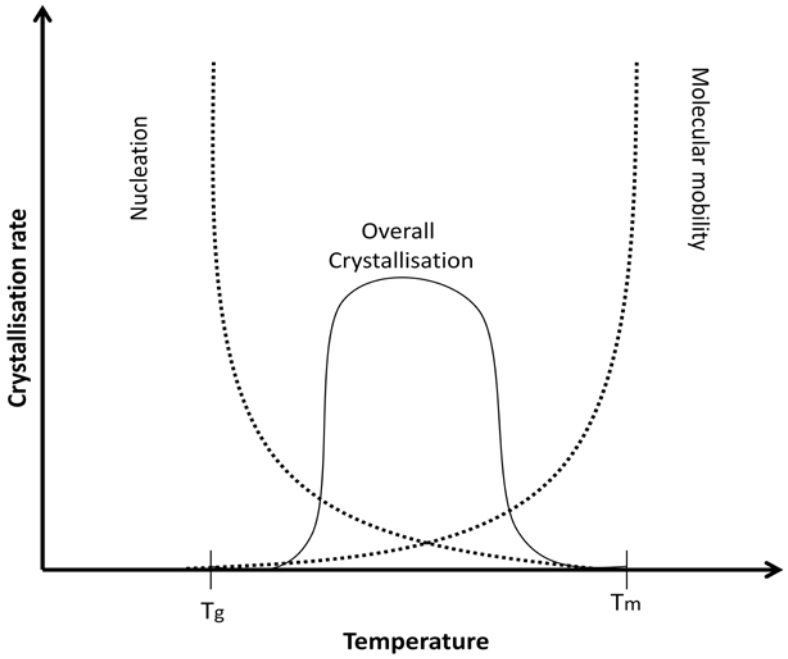

Fig. 2 Schematic presentation of the influence of temperature on the nucleation rate, magnitude of molecular mobility and crystallisation rate of super cooled liquids (adapted from 3).

Despite having a high amount of free energy, an amorphous form will not spontaneously recrystallise - an energy barrier, referred to as activation energy (E_a), needs to be overcome in order for this reaction to take place (10). Many factors (such as grinding, humidity, temperature, etc.) can aid the amorphous form to overcome the required activation energy to induce the recrystallisation process (10-15). Kinetic studies (based on thermal induction) are commonly employed to determine the activation energy for crystallisation (10-15).

Several analytical techniques, such as X-Ray Powder Diffraction (XRPD), Differential Scanning Calorimetry (DSC), Hot-Stage Microscopy (HSM) and Infra-Red Spectroscopy (IR) may be employed to quantify crystallisation behaviour, however not all APIs react in the same way and do not provide the same response under similar experimental conditions (10-15). It is therefore not uncommon for different techniques to provide varying results (16-17).

Crystallisation kinetics can be investigated either isothermally or non-isothermally using a variety of thermal techniques (10-23). During isothermal methods, the sample is heated at a constant temperature (above T_g) and the degree of conversion (from amorphous phase ➔ crystalline phase) is determined. On the other hand, in non-isothermal methods, the sample is heated at a fixed heating rate (β) and the degree of conversion (from amorphous phase ➔ crystalline phase) is determined. The calculations used for the quantification of the degree of conversion (by various techniques used in this study) are discussed in the **MATERIALS AND METHODS** section. The applicable models used for the crystallisation kinetic studies are described in the **RESULTS** section.

The stability of an amorphous form can be evaluated using semi-empirical relations based on the characteristic thermal events observed in the DSC thermogram thereof. Examples of such semi-empirical relations are: thermal stability range (24), Hruby's criterion (25) and T_m/T_g ratio (3). These relations were utilised in this study.

In a previous publication (26), a novel amorphous form (Form A) of Efavirenz (Fig. 3) was presented, which was found to be susceptible towards transformation into Form I. The work presented in this manuscript serves to compliment the work of Perold *et al*. (26) by elaborating on the thermodynamic stability and recrystallisation kinetics of Form A (using isothermal and non-isothermal methods). During this study two alternative detection methods (HSM and automated Capillary Melting Point analysis (CMP)) for the determination of the non-isothermal recrystallisation activation energy were investigated, of which one was found suitable for its intended purpose.

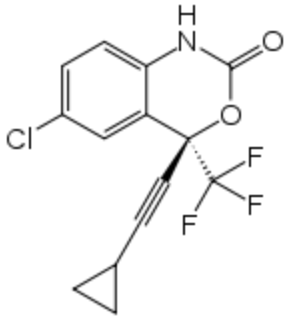

Fig. 3 The chemical structure of Efavirenz.

MATERIALS AND METHODS

Materials

Crystalline Efavirenz (Form I), batch number: EFE/0809011 (Matrix Laboratories Limited, India) was used as starting material to prepare Efavirenz Form A by means of a quench cooling technique as described in the literature (26).

Variable Temperature X-Ray Powder Diffractometry (VTXRPD)

A Bruker D8-Advanced diffractometer (Bruker, Germany) was used to obtain X-Ray Powder Diffraction (XRPD) patterns. The following conditions were applicable: target, Cu; voltage, 40 kV; current, 30 mA; divergence slit, 2 mm; anti-scatter slit, 0.6 mm, detector slit, 0.2 mm; monochromator; scanning speed, 2°/min with a step size of 0.025° and a step time of 1.0 sec. An Anton Paar TTK 450 low temperature camera (Anton Paar, Austria) with a heating rate of 0.1°C/sec was used for the collection of the diffraction patterns.

Differential Scanning Calorimetry (DSC)

For DSC analysis, approximately 2-5 mg of ground sample was weighed into a 40 µl aluminium sample pan, fitted with a pierced lid (Mettler Toledo, Switzerland) and crimped. Samples were analysed using a Mettler Toledo DSC823^e (Mettler Toledo, Switzerland) with the nitrogen flow rate set to 80 ml/min at 10˚C/minute heating rates (unless otherwise stated). The thermal events were recorded in the temperature range 25 - 170˚C and evaluated using the STAR^e software (version 9.0x) (Mettler Toledo, Switzerland). The instrument was calibrated using indium and zinc reference materials.

The volume fraction (α) of recrystallisation (Form A → Form I) was determined using equation 1, as described by Matusita *et al*. (23):

$$\alpha = \frac{S}{S_0} \qquad \text{Equation 1}$$

Where S_0 is the area under the DSC recrystallisation exotherm curve between T_1 (the onset temperature of recrystallisation) and T_2 (end temperature of recrystallisation) and S is the area between T_1 and T as illustrated in Fig. 4 (a).

Hot Stage Microscopy (HSM)

A Nikon DS-Fi1 (Nikon, Tokyo, Japan) digital camera affixed to a Nikon ECLIPSE E400 optical polarizing microscope (Nikon, Tokyo, Japan) was used for HSM experiments. Samples were heated with the use of a Leitz hot stage (Leica Microsystems Inc., Bannockburn, IL) at a heating rate of 10˚C/min (unless stated otherwise) from 25 – 170˚C. Images were captured and analysed using the NIS-Elements F2.30 software (Nikon, Tokyo, Japan).

HSM was used to elucidate the DSC thermal events of Form A and Form I in a previous work (26) and to verify the absence of nuclei in samples of Form A.

The volume fraction (α) of recrystallisation (Form A → Form I) was determined using equation 2, where a circle is drawn around the circumference of the crystal growth observed, similar to that described by other authors (27-29). This technique, Fig 4 (b), entails the measurement of the radius (R_t) from the center of the crystal growth (signaled by birefringence) in ratio to the final maximum radius (R_{max}) achieved at the completion of recrystallisation.

$$\propto = \frac{R_t}{R_{Max}} \qquad \text{Equation 2}$$

Where R_t is the radius of the spherical growth (two dimensional growth, n~2) at predetermined temperatures (*t*). R_{Max} is the point where radius is at a maximum (where crystal growth has stopped) – Fig. 4 (b).

Automated capillary melting point analyser (CMP)

From literature (26), it was observed that the transmission of Form A decreased during crystallisation. In this work an attempt is made to use this characteristic behaviour as a means to quantify the conversion from Form A → Form I by CMP.

Ground samples were transferred into thin-walled glass capillary tubes which were loaded into a Buchi M565 melting point monitor (Buchi, Switzerland) using Meltpoint Monitor version 1.0 software (Buchi, Switzerland). The analyser was programmed to detect the change in translucency of the samples when heated at different heating rates (as specified in the text) in the temperature range where recrystallisation of Form A was anticipated (i.e. 60 - 100˚C).

The volume fraction (α) of recrystallisation (Form A → Form I) was determined using equation 3 – Fig. 4 (c):

$$\alpha = \frac{T_{max} - T_t}{T_{max} - T_{min}} \qquad \text{Equation 3}$$

Where α is the volume fraction of Form A transformed, T_{max} is the maximum value of transmission (%), T_t is the transmission (%) at the specific temperature (*t*) and T_{min} is the minimum value of transmission (as %).

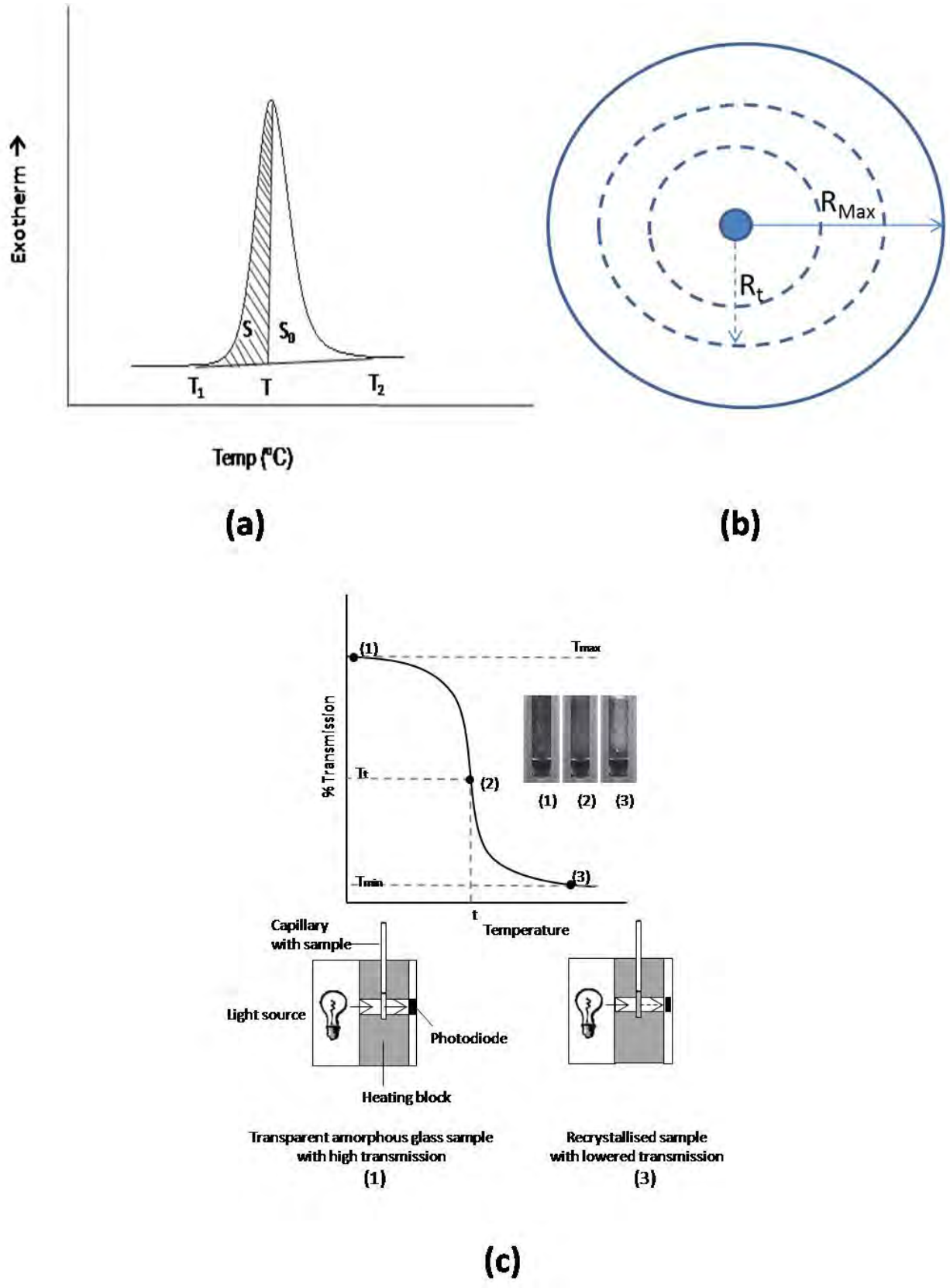

Fig. 4 Schematic presentation of how the fractions of recrystallisation (α) were calculated utilising: (a) the recrystallisation exotherm from DSC thermogram, (b) the two-dimensional growth from HSM and (c) the change in transmission recorded by CMP.

Isothermal reaction kinetic studies using DSC

A Binder®ED23 laboratory oven (Labotech, South Africa) was used to subject Efavirenz Form A to 30, 35 and 40˚C respectively. Samples were withdrawn at predetermined intervals and the recrystallisation energy (area under the recrystallisation exotherm) was calculated using DSC. The recrystallisation energies determined were used to calculate the volume fractions (α) of recrystallisation (Form A → Form I) using the method described in previous work (26).

Statistical evaluation of data

The accuracy and validity of the non-isothermal activation energy values obtained using the various thermal techniques (DSC, HSM and CMP) were evaluated using the following statistical parameters:

Accuracy

The average value for the non-isothermal activation energy determined using DSC (and the Kissinger Akahura Sunrose model - KAS) was used as reference for accuracy calculations – equation 4:

$$\%Accuracy = \frac{Avg_{X\ KAS}}{Avg_{DSC\ KAS}} \times 100 \qquad \text{Equation 4}$$

Where $Avg_{X\ KAS}$ is the average non-isothermal activation energy calculated using HSM or CMP (using the KAS model) and $Avg_{DSC\ KAS}$ is the average non-isothermal activation energy calculated using DSC (using the KAS model).

Analysis of variance (ANOVA)

The non-isothermal activation energy results obtained using HSM and CMP respectively, were compared to the reference non-isothermal activation energy value (calculated from DSC-KAS) by means of a double-sided ANOVA analysis using the Data Analysis toolpack® of MS Excel® (2010) at a 95% confidence interval. A p-value < 0.05 is indicative of a statistical significant difference between the data sets compared.

Precision

The variation within the replicate non-isothermal activation energy values (n=9) obtained using the various thermal techniques was evaluated by calculating the percentage relative standard deviation (%RSD).

RESULTS

The results are presented in three sections: i) Thermal properties of the amorphous and crystalline forms of Efavirenz, ii) Non-isothermal recrystallisation of Form A and iii) Isothermal recrystallisation kinetics of Form A.

Thermal properties of the amorphous and crystalline forms of Efavirenz

VTXRPD was utilised to assess the conversion of the amorphous form (Form A) into a crystalline form. The VTXRPD study (Fig. 5) clearly showed the amorphous broad/halo shaped XRPD pattern of Form A at ambient temperature (25˚C), which ultimately converted and stabilised into a crystalline form (Form I) (75˚C).

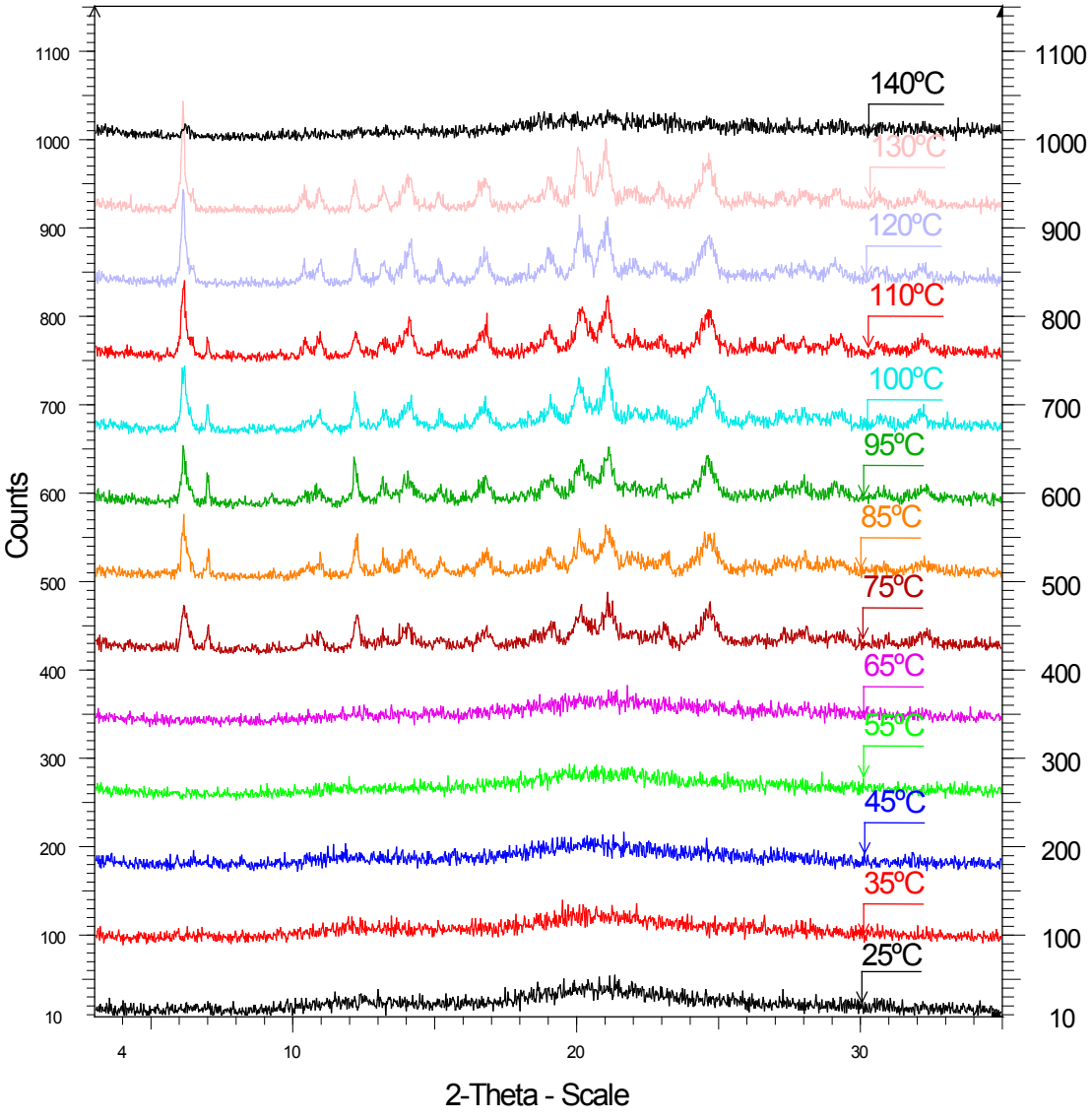

Fig. 5 VTXRPD of Form A from 25-140°C.

The DSC thermogram of Form I, Fig. 6 (a), revealed a melting endotherm at 138.40˚C (T_m) whilst that of Form A revealed a glass transition (T_g) at 31.89˚C, crystallisation exotherm (T_p) at 83.26˚C and a melting endotherm (T_m) at 137.88˚C, when heated at a rate of 10˚C/min. These thermal events were verified using HSM, and correlated with that reported (26). HSM verified the absence of nuclei in Form A at 25˚C.

The thermal behaviour of Form A at different heating rates (2, 5, 7, 10, 20 & 30˚C/min) was investigated – Fig. 6 (b). The glass transition of the sample heated at 2°C/min showed a weak, poorly detectable glass transition. The absence of lucid glass transitions in DSC thermograms of amorphous forms at low heating rates has been reported in the literature (30, 31). When the heating rate was increased, the glass transition shifted to a higher temperature and the DSC response increased due to an increase in the thermal resistance. The heating rate dependence of T_g is clearly illustrated in Fig. 6 (b).

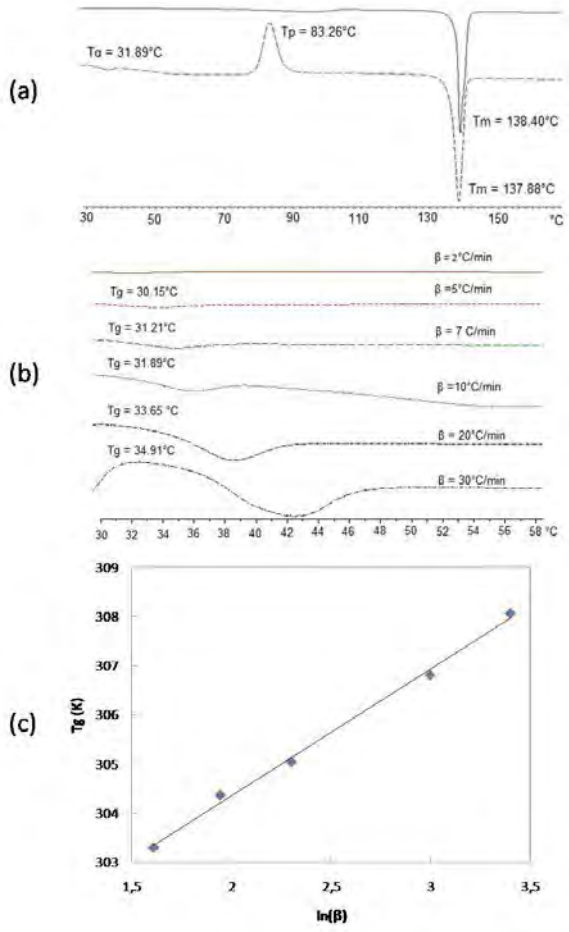

Fig. 6 Thermal properties of Efavirenz: (a) DSC thermograms of Form I (solid line) & Form A (dotted line) when heated at a rate of 10˚C/min. (b) Effect of an increase in the heating rate (β) on the intensity and position of the glass transition of Form A. (c) The Lasocka's relationship for Form A at 2°C/min ≤ β ≤ 30°C/min.

Numerous authors (32-34) observed the dependence of T_g on the heating rate (β) and found that it occasionally adhered to the Lasocka's relationship (35) – equation 5:

$$T_g = a + b \ln \beta \qquad \text{Equation 5}$$

Where *a* and *b* are constants for a specific glass composition or amorphous form.

T_g vs. ln β (Fig. 6 (c)) was plotted and it was evident that the T_g/(β) behavior was indeed described by the Lasocka relationship (r^2=0.996). In the range 2˚C/min ≤ β ≤ 30˚C/min, the values of the constants *a* and *b* were calculated as 299.1 K and 2.58 minutes respectively.

Non-isothermal crystallisation of Form A

The equation used to express the transformation rate of a solid-state reaction under isothermal conditions is generally described by equation 6 (36):

$$\frac{d\alpha}{dt} = k\ f(\alpha) \qquad \text{Equation 6}$$

Where (*dα/dt*) is the isothermal rate of the crystallisation, *k* the reaction rate constant and *f(α)* the reaction model for the fraction of the amorph that has been converted to the crystalline form.

It is known that the rate constant (*k*) has an Arrhenian temperature (*T*) dependence, which is delineated by the pre-exponential factor (*A*), the activation energy (*E*) and the universal gas constant (*R*) as defined in equation 7:

$$k = A^{\left(\frac{-E}{RT}\right)} \qquad \text{Equation 7}$$

Substitution of equation 7 into equation 6 produces equation 8:

$$\frac{d\alpha}{dt} = A^{\left(\frac{-E}{RT}\right)} f(\alpha) \qquad \text{Equation 8}$$

However, for non-isothermal conditions, equation 8 needs to be amended for the inclusion of the constant heating rate (*β*) parameter (*β = dT/dt*) (equation 9):

$$\frac{d\alpha}{dT} = \frac{d\alpha}{dt}\left(\frac{1}{\beta}\right) = \frac{A^{\left(\frac{-E}{RT}\right)}}{\beta} f(\alpha) \qquad \text{Equation 9}$$

The fractions of conversion of Form A (α) at different heating rates (β = 2, 5, 10˚C/min) were calculated by means of DSC, HSM and CMP, using equations 1, 2 and 3. A plot of the conversion fractions (α) vs. temperature (T) at the different heating rates produced sigmoidal curves (Fig. 7). The Kissinger-Akahira-Sunrose (KAS) model (37-39) and the Matusita model (23) have been successfully employed to calculate the activation energy from sigmoidal α vs. temperature curves (40, 41), therefore these two models were selected to establish the activation energy required for the recrystallisation of Form A.

DSC is a well-established thermal technique used for non-isothermal activation energy determinations (14, 15, 23, 42). For this reason it was decided to use the activation energy value obtained using DSC as the reference value for comparative purposes.

The fractions of conversion calculated using HSM and CMP were fitted to the KAS model, and the outcomes thereof were compared to that obtained from the DSC experiments.

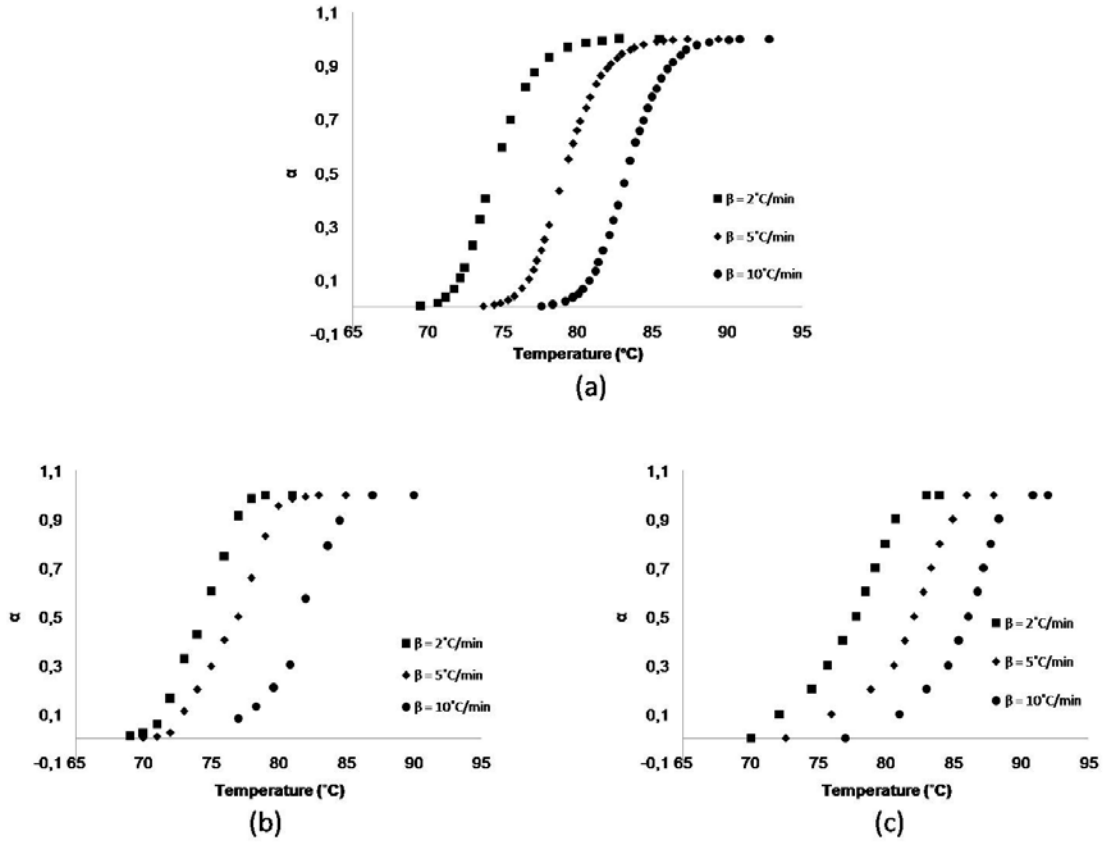

Fig. 7 Sigmoidal α vs. temperature curves obtained using (a) DSC, (b) HSM and (c) CMP.

Non-isothermal crystallisation of Form A using DSC

The non-isothermal activation energy for recrystallisation of Form A (using DSC) was calculated using the KAS model (39) and the Matusita model (23). The activation energy obtained from the Matusita model was used to verify that obtained from the KAS model.

The KAS model (equation 10) was obtained through the derivation and subsequent logarithm application of equation 9 at various heating rates (β_i):

$$ln\left(\frac{\beta_i}{T_{\alpha 1}^2}\right) = \ln\left[\left|\frac{df(\alpha)}{d\alpha}\right| \cdot \frac{AR}{E_\alpha}\right] - \frac{E_\alpha}{RT_{\alpha i}} \qquad \text{Equation 10}$$

The subscript, *i*, denotes the different heating rates. Joraid (36) suggested the simplification of equation 10 by the introduction of a thermal parameter ($C_{K(\alpha)}$):

$$C_{K(\alpha)} = \ln\left[\left|\frac{df(\alpha)}{d\alpha}\right| \cdot \frac{AR}{E_\alpha}\right] \qquad \text{Equation 11}$$

Where E_α denotes the activation energy for a specific α fraction. Thus equation 11 can be reduced to equation 12 by substituting $C_{K\alpha}$ into equation 10.

$$ln\left(\frac{\beta_i}{T_{\alpha i}^2}\right) = C_{K(\alpha)} - \frac{E_\alpha}{RT_{\alpha i}} \qquad \text{Equation 12}$$

To calculate the values of $E_{\alpha i}$ and $C_{K(\alpha)}$ the degree temperature ($T_{\alpha i}$) for a specific degree of conversion to Form I (α) at a specific heating rate (β_i) was determined and $ln\ (\beta_i/T^2_{\alpha i})$ versus $1/T_{\alpha 1}$ was plotted –Fig. 8.

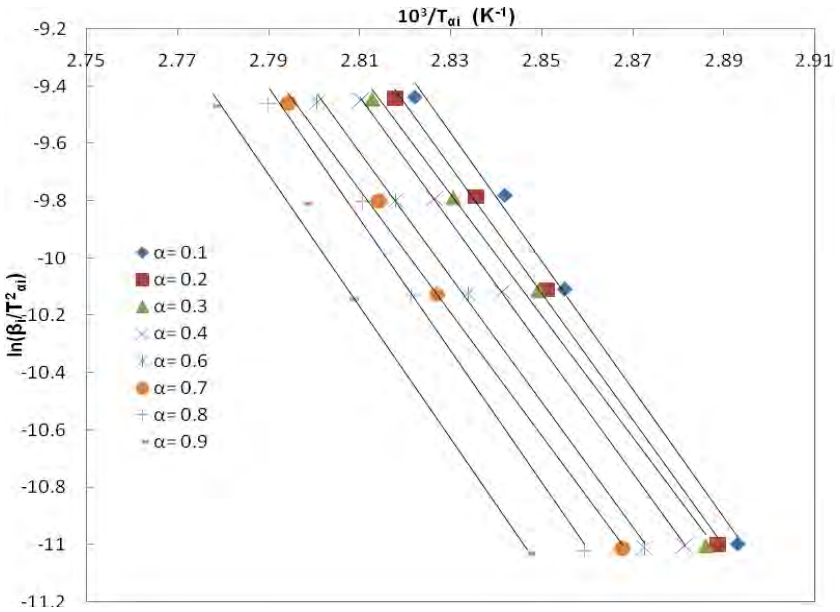

Fig. 8 Experimental plot of *ln* $(\beta_i/T^2_{\alpha i})$ vs. $1/T_{\alpha 1}$ using DSC KAS for Form A.

The value of the non-isothermal activation energy ($E_{\alpha i}$) was calculated from the slopes of the linear plots in Fig. 8 and found to be 183.63±7.4 kJ/mol. This result was verified using the Matusita model, described next.

The fractions of conversion calculated using DSC were fitted to the Matusita model (equation 13). Matusita *et al.* (23) proposed an equation (equation 13) to express the volume fraction (α) of a crystalline phase precipitating in an amorphous sample, when heated at a constant heating rate (β), when the crystalline phase grows *m*-dimensionally:

$$\ln\ [-\ln(1-\alpha)] = \ -n\ ln\beta - 1.052\ m\ \frac{E}{RT} + \ Constant \qquad \text{Equation 13}$$

Where *E* is the activation energy required for the crystal growth, *n* and *m* are numerical factors describing the nucleation (*n*) and growth process (*m*), *R* is the universal gas constant and *Constant* is a constant derivative (5).

Two parameters (*n* and E_a), were calculated using two separate plots from the Matusita model. The first plot, ln [-ln (1-α)] vs. ln *β* (Fig. 9 (a)) calculated the dimension of growth, *n*. For this plot, the fraction of conversion (α) was determined at 80, 83 and 85 ˚C (temperatures in the range of recrystallisation – Fig. 6 (a)) from DSC runs performed at heating rates of 2, 5, 7 and 10 ˚C/min. *n* was calculated to be ~2, which confirmed the two dimensional growth observed from HSM. The second plot, ln [-ln(1-α)] vs. the reciprocal temperature (Fig. 9 (b)), was used to determine E_a. The average non-isothermal activation energy required for the crystallisation of the crystalline phase (Form I) was calculated as 181.50 ± 6.9 kJ/mol from the slopes of the ln [-ln(1-α)] vs. the reciprocal temperature in the degree of conversion range: 0.2 ≤ α ≤ 0.9.

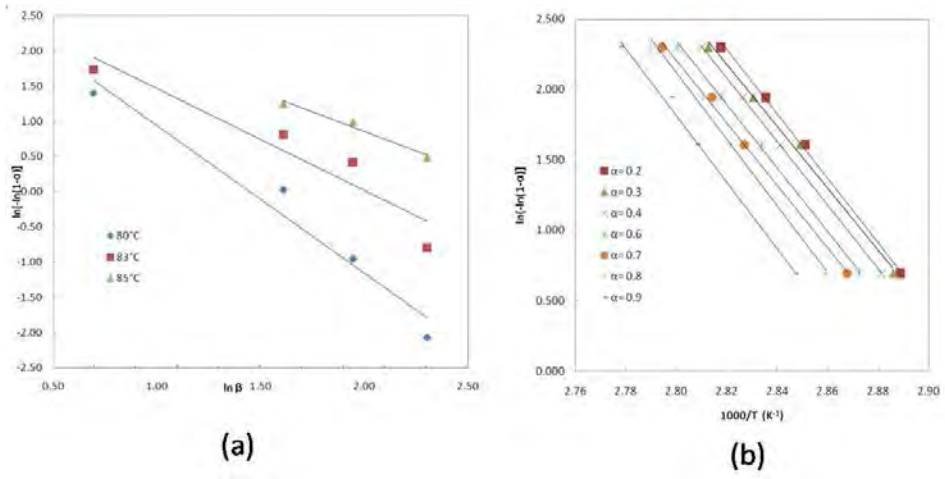

Fig. 9 (a) Variation of ln [-ln (1-α)] of Form A vs. the natural logarithm of the heating rate (*β*) at 80, 83 and 85°C respectively, (b) Plot of the ln[-ln(1-*α*)] vs. the reciprocal temperature, in the degree of conversion range: 0.2 ≤ α ≤ 0.9 of Form A.

Non-isothermal recrystallisation kinetics of Form A using HSM and CMP

HSM photomicrographs of Form A (26) showed that recrystallisation coincided with a decrease in translucency/transmittance, a visual observation well known to be resultant of phase transformations (33). Based on the aforementioned it was decided to investigate the potential application of an automated CMP equipped with a translucency detector to evaluate the recrystallisation of Form A - since automated CMPs rely on the change in optical properties (translucency) of the sample being analysed (43) as depicted in Fig. 4 (c).

A change in the translucency of the sample coincided with the exothermic recrystallisation events from DSC and the temperature range in which recrystallisation was observed by HSM (Fig. 10), which confirmed the change in translucency to be resultant of phase transformation. These observations fueled the belief that it might be possible to use translucency and HSM measurements to calculate the volume fraction of conversion, and ultimately serve as an alternative to the conventional DSC measurements for non-isothermal activation energy determinations.

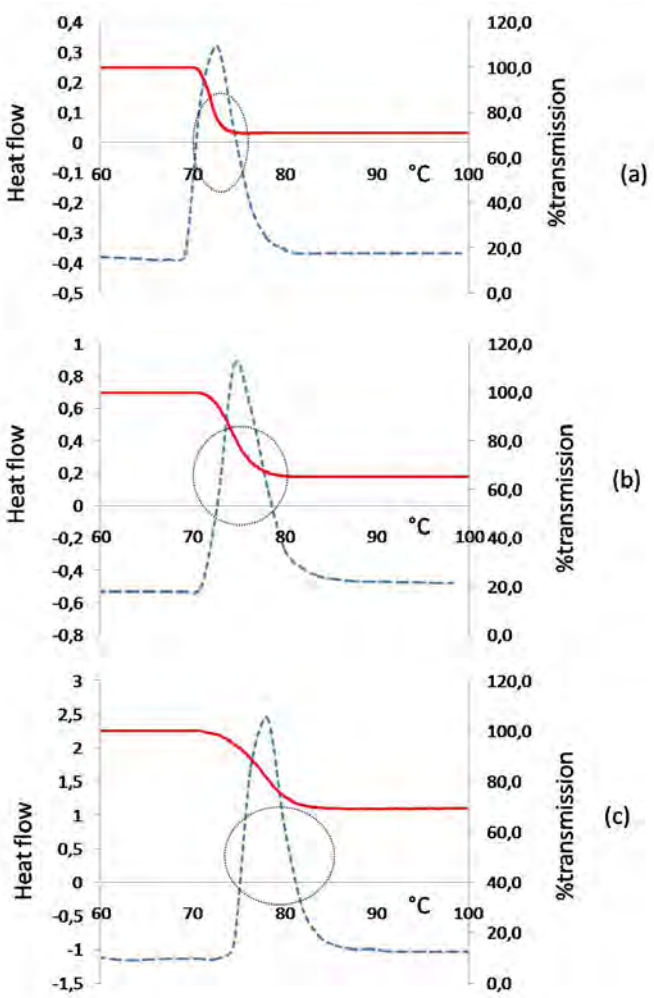

Fig. 10 The temperature range in which recrystallisation of Form A occurs as observed by DSC (dotted line), HSM (circles) and CMP (solid line) at heating rates: (a) 2°C/min, (b) 5°C/min and (c) 10°C/min.

The fractions of conversion (α) using HSM and CMP (at β = 2, 5 and 10˚C/min) were calculated using equations 2 and 3 respectively. A plot of the conversion fractions (α) vs. temperature (T) at the different heating rates produced sigmoidal curves (Fig. 7 (b) and (c)). The α-values from HSM and CMP were fitted to the KAS model (Fig. 11), which calculated the average $E_{\alpha i}$ value to be 210±10 kJ/mol from HSM and 185.5 ± 8.5 kJ/mol from CMP.

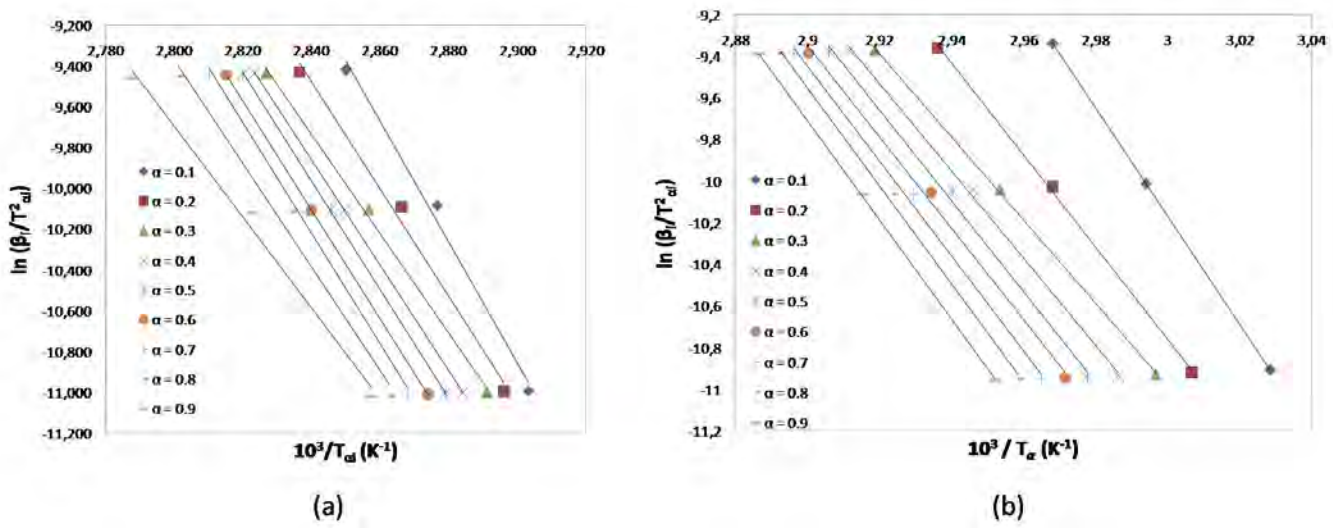

Fig. 11 Experimental plots of *ln* ($\beta_i/T^2_{\alpha i}$) vs. $1/T_{\alpha 1}$ for the (a) HSM and (b) CMP data.

Isothermal crystallisation kinetics of Form A

The isothermal crystallisation kinetics of Form A was investigated at 30, 35 and 40°C. Samples were withdrawn at predetermined intervals and the fractions of conversion (α) were calculated as described in the Materials and Methods section. The plots of α vs. time produced sigmoidal (S-shaped) curves – Fig. 12 (a).

The Johnson-Mehl-Avrami-Erofeyev-Kolmogorov (JMAEK) model (27) – equation 14, is a popular kinetic model applied to isothermal solid-state transformations of amorphous forms which is described by sigmoidal α vs. time curves (44):

$$\ln[-\ln(1-\alpha)] = \ln k + n\ln(t) \qquad \text{Equation 14}$$

The kinetics of transformation was evaluated by plotting [-ln(1-α)] at the various temperatures versus time on a double logarithmic plot (Fig. 12(b)).

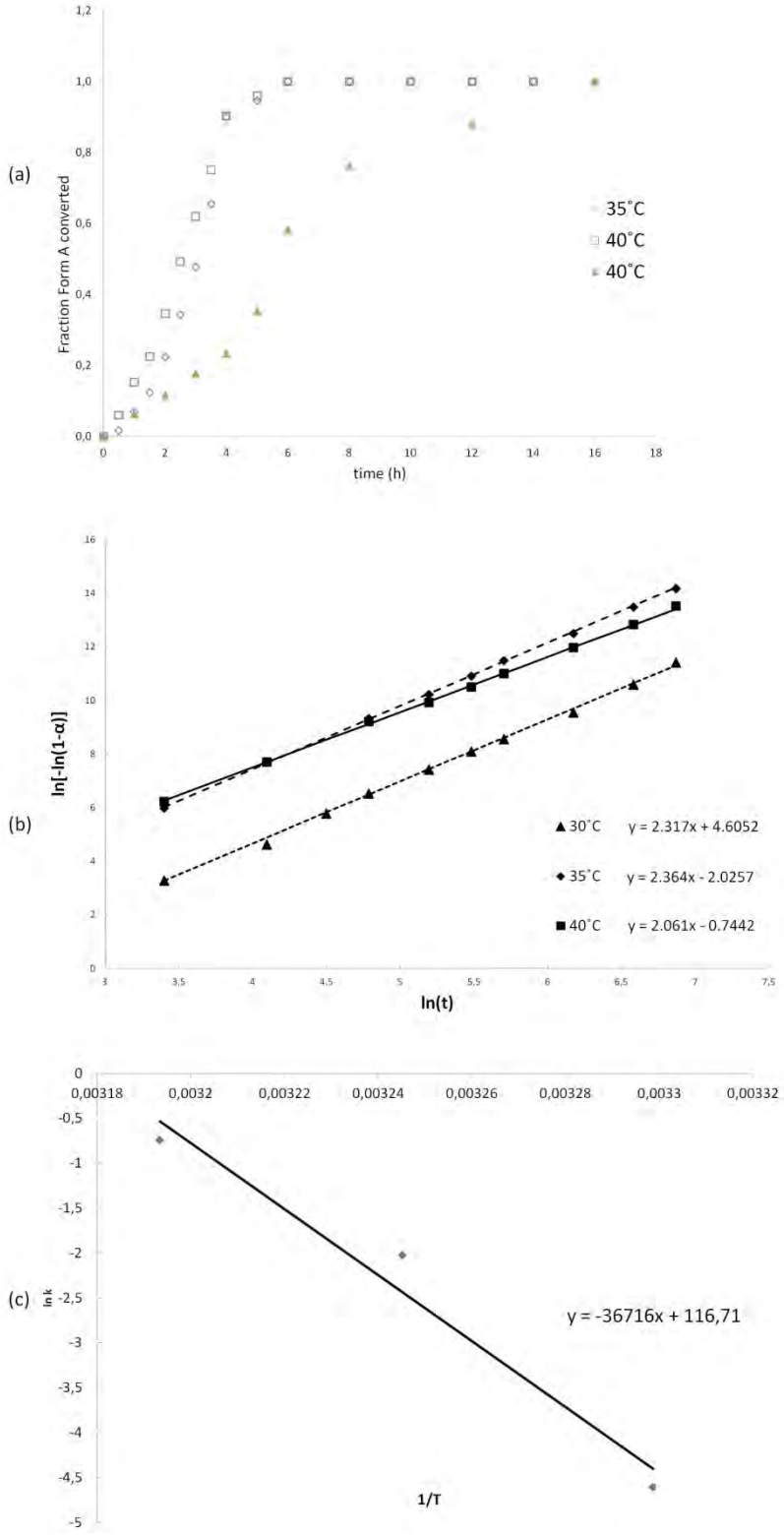

Fig. 12 Curves obtained from isothermal studies, where (a) sigmoidal α vs. Time curve, (b) ln [-ln(1-α)] vd. ln(t) and (c) ln(k) vs. 1/T.

The slopes of these calibration lines (linear fit using the JMAEK model: $r^2 > 0.98$) represented the dimensions of growth (*n*) and the y-intercepts the reaction rate constant (ln *k*). The half-life values for Form A were calculated at the different temperatures using equation (15).
The results obtained are presented in Table 1.

$$t_{0.5} = \frac{0.693}{k} \qquad \text{Equation 15}$$

Table 1 Calculated parameters for the isothermal crystallisation of Form A using the JMAEK model

Temperature (˚C)	r^2	*n*	*k* (x 10^{-2} h^{-1})	$t_{0.5}$(h)
30	0.991	2.3	1.00	69.18
35	0.989	2.4	13.19	5.25
40	0.986	2.1	47.51	1.46

Utilising the calculated reaction rate constants (*k*), a plot of ln *k* against 1/*T* (where T = 303.15K (30˚C), 308.15K (35˚C) and (313.15K (40˚C)) was made (r^2 = 0.97) – Fig. 12(c). The isothermal crystallisation experiments were conducted at temperatures exceeding the T_g, thus the assumption of Arrhenius dependence of nucleation and growth rates should be valid, thus the activation energy for isothermal crystallisation could be calculated using the Arrhenius-type equation (45):

$$\ln(k) = \ln k_0 - \frac{E_a}{RT} \qquad \text{Equation 16}$$

Where *k* is the reaction rate constant, k_0 is the frequency factor, E_a is the activation energy and *R* is the gas constant.
The activation energy for isothermal crystallisation was calculated to be 305.25 kJ/mol.

DISCUSSION

From the VTXRPD (Fig. 5) it can be seen that Form A remained unchanged between 25 - 65˚C, but at 75˚C the characteristic peaks of Form I (25) emerged. At 85˚C, the XRPD pattern showed that Form A had completely converted and stabilised into Form I, which is known to melt at approximately 138.40˚C, which explained the lack of XRPD peaks at 140˚C. The observed changes in the XRPD patterns correlated and elucidated the recrystallisation exotherm (T_p = 83.26˚C) and final melting endotherm (T_m = 137.88˚C) as observed in the DSC of Form A (Fig. 6(a)).

In a previous publication (26), HSM was used to elucidate and confirm the thermal events observed in the DSC thermograms of the samples. Small nuclei were first detected at 76°C which revealed a two dimensional growth when exposed to increased temperatures. Investigation of the sample at 84°C under polarised lightening confirmed the growth of the crystalline phase due to the presence of birefringence. Upon heating, the crystalline phase darkened at 132°C and underwent melting at

approximately 138°C. No remarkable events were observed for Form I when exposed to increased temperatures using thermal microscopy. It was observed that melting of Form I initiated at 128°C and concluded at 135°C (26).

The stability of Form A was evaluated using thermal stability range (**TSR**) and T_m/T_g ratio (semi empirical relations). The thermal stability range ($T_x - T_g$, where T_x = onset of crystallisation peak temperature = 77.21˚C) can be used to evaluate the stability of the amorphous form towards crystallisation. The larger the TSR (> 100˚C), the better the stability against crystallisation will be (46). The TSR of Form A was calculated to be 45.33˚C, which indicated that Form A has a low resistance (high tendency) towards crystallisation.

The T_m/T_g ratio is used to evaluate the ease of recrystallisation of an amorphous form (7). The T_m/T_g ratio of Form A (at β = 1˚C/min) was calculated to be 5.27. This relatively high ratio indicated that Form A underwent recrystallisation with greater ease compared to the more stable amorphous APIs such as Ritonavir (T_m/T_g =2.45) and ABT-229 (T_m/T_g =1.82) (7).

The reduced crystallisation temperature (**RCT**) (7) represents a normalised measure of how high above T_g the amorphous form must be heated before spontaneous crystallisation will occur and can be calculated using equation 17.

$$\mathrm{RCT} = \frac{T_c - T_g}{T_m - T_g} \qquad \text{Equation 17}$$

Where T_c is the peak temperature of the recrystallisation peak, T_g is the glass transition temperature and T_m is the melting temperature of the crystalline phase.

The RCT for Form A was determined as 0.75˚C, thus exposure of Form A to temperatures ≥ 32.64 ˚C (T_g + 0.75 ˚C) might result in spontaneous crystallisation. Due to this low value (of reduced recrystallisation temperature) it can be concluded that this amorphous form of Efavirenz is not suitable for pharmaceutical manufacturing as it may pose a risk of phase transformation during the shelf life of the API/final pharmaceutical product.

The adherence of Form A to the Lasocka relationship has been proven (Fig. 6 (c)). It has been suggested that the "correct glass transition temperature (T_{g0})" can be obtained for amorphous forms by extrapolation of the experimental results of the Lasocka relationship (Fig. 6 (c)) so that β = 0˚C/minute (35). However, T_{g0} cannot be estimated due to the fact that the $T_g(\ln\beta)$ function is non-linear. Utilising the equation obtained from the data in Fig. 6 (c) ($T_g = 2.579 \cdot \ln\beta + 299.1$), T_{g1} may be estimated by the extrapolation to β = 1. The T_{g1} was calculated as 28.53˚C, which is relatively low. It is known that materials with such low glass transitions (T_{g1}) are considered being sticky and exist in their rubbery phase at ambient or higher temperatures, which can cause erratic dissolution results (47). The anomalous dissolution behavior of Form A has indeed been described (26). Inadvertent crystallisation is likely to be avoided if the amorphous sample is maintained at 50K below T_g (1, 3).

Thus, to ensure the stability of Form A, it should theoretically be stored at or below -21.51˚C, which exemplifies why this crystal modification is not suitable for pharmaceutical use.

Non-isothermal studies were performed by means of DSC, HSM and CMP as described in the **MATERIALS & METHODS** and **RESULTS** sections. The activation energy calculated using DSC and the KAS model was verified by comparing the value obtained to that of DSC data fitted to the Matusita model (Table 2). The non-isothermal recrystallisation results obtained using HSM and CPM were statistically evaluated and are summarised in Table 2.

The non-isothermal activation energy calculated using DSC-Matusita and DSC-KAS models did not differ significantly ($p > 0.05$). The value obtained from the DSC-KAS model was thus deemed as a suitable reference. Seeing that the Matusita and KAS models provided comparable non-isothermal activation energy values, subsequent activation energies from other techniques (HSM and CMP) were only calculated by means of fitting to the KAS model.

The non-isothermal activation energy value calculated using HSM was found to differ significantly from that of the DSC-KAS results ($p < 0.05$). During the HSM analyses it was observed that the growth of the recrystallised regions from the nuclei continued until mutual impingement of the recrystallised regions occurred. The distribution of the recrystallised regions was found to be heterogeneous which complicated the measurement of R_t and R_{max}, which may have influenced the accuracy of the data generated. The use of HSM for the estimation of non-isothermal activation energy is thus not recommended.

The non-isothermal activation energy value calculated using CMP measurements were found to be comparable with that obtained by DSC-KAS ($p > 0.05$) with an acceptable accuracy (98.0% < 101.0% < 102.0%) and precision (4.6% < 5.0%). The use of CMP for the estimation of non-isothermal activation energy can thus be recommended.

Table 2 Calculated non-isothermal parameters from DSC, HSM and CMP

	DSC (M)	**DSC (KAS)**	**HSM (KAS)**	**CMP (KAS)**
E_a *(kJ/mol)* ± SD	181.5 ± 6.9	183.6 ± 7.4	210.0 ± 10.1	185.5 ± 8.5
Accuracy (DSC- KAS as reference)	98.9%	---	114.4 %	101.0%
ANOVA (p-value)	0.54	---	9.9×10^{-6}	0.62
Precision (as %RSD)	3.8%	4.0%	4.8%	4.6%
Dimension of growth (*n*)	n~2	N/A	2	N/A

M = Matusita model, KAS = Kissinger-Akahira-Sunrose model, ANOVA = Analysis of variance (95% confidence interval)

Isothermal crystallisation experiments were conducted at predetermined temperatures (30, 35 and 40˚C) which exceeded the T_g of Form A, as determined from the Lasocka relationship (T_{g1}= 28.5˚C).

From the isothermal studies, the half-life values of the amorphous phase at 30, 35 & 40˚C were determined (Table 1), which exemplified the thermodynamic instability of Form A: when stored at 30˚C, Form A will undergo complete conversion into Form I within 6 days, at 35˚C – within 11 hours and at 40˚C within 3 hours!

No visible nuclei were detected using HSM under polarised light, and it was illustrated that the crystalline phase formed after an induction period. Subsequent crystal growth occurred with no new nuclei appearing in the amorphous regions. Growth from a fixed number of pre-existing nuclei suggests that the activation energy from isothermal and non-isothermal recrystallisation should be equivalent (48). However, the activation energies calculated from the DSC isothermal (E_a = 305.3 kJ/mol) and non-isothermal (E_a = 183.6 kJ/mol) experiments differed significantly. This difference might be indicative of a site-saturated nucleation mechanism (48, 49), thus the crystal growth rate is limited by surface incorporation rather than diffusion.

With site-saturated nucleation and two-dimensional growth, the activation energy values obtained isothermally and non-isothermally are defined as: $\frac{(E_a^N + 2E_a^G)}{2}$ and E_a^G, respectively (48), where the superscripts N and G refer to nucleation and growth respectively. Using the experimental activation energy values, the activation energy for nucleation and growth can be calculated. The activation energies were calculated to be E_a^N = 242 kJ/mol and E_a^G= 184 kJ/mol. The fact that $E_a^N > E_a^G$ supported the site-saturated nucleation mechanism, and suggested that the activation energies determined from the induction periods may be related to the slow growth of initial nuclei (48), into growth nuclei rather than the actual nucleation step.

CONCLUSION

The amorphous form (Form A) of Efavirenz has been characterised with respects to its thermodynamic properties and recrystallisation behaviour. Estimation of the recrystallisation activation energy using isothermal and non-isothermal techniques allowed: i) investigation of both nucleation mechanism (two dimensional) and crystal growth, and ii) estimation of the activation energies for nucleation and growth. Nucleation appears to occur through a site-saturated mechanism and the growth rates of the crystalline phase appears to be limited by surface incorporation rather than diffusion. A new, cost- and time effective thermal detection method has been identified for the estimation of the non-isothermal recrystallisation energy of this amorphous form. The thermodynamic instability of this amorphous form has clearly been illustrated by the narrow thermal stability range, small reduced recrystallisation temperature and ineffectual short half-life thereof, rendering this crystal modification not suitable for pharmaceutical application.

ACKNOWLEDGEMENTS

The authors thank the Research Institute for Industrial Pharmacy incorporating the Centre for Quality Assurance of Medicines (CENQAM) of the North-West University (NWU) and PharmaCen of the NWU for financial assistance.

REFERENCES:

1. Yu L. Amorphous pharmaceutical solids: Preparation, characterization and stabilization. Adv.Drug Del. Rev., 2001;48:27-42.
2. Byrn R, Pfeiffer RR, Stowell JG. Amorphous solids. In: Solid-state chemistry of drugs. West Lafayette: Indiana, SSCI. 1999:249-258.
3. Hancock BC, Zografi G. Characteristics and significance of the amorphous state in pharmaceutical solids. J. Pharm. Sci., 1997;86(1):1-12.
4. Petit S, Coquerel G. The amorphous state. In: Hilfiker R. editor. Polymorphism in the pharmaceutical industry. Weinheim: Wiley-VCH Verlag GmbH & Co. KGaA; 2006. p. 259–285.
5. Stieger N, Liebenberg W. Recrystallization of Active Pharmaceutical Ingredients. In: Andreeta M editor. Crystallization – Science and Technology. InTech Online. 2012. http://cdn.intechopen.com/pdfs-wm/39135.pdf. Accessed 8 August 2014.
6. Buckton G. 2002. Solid-state properties. In: Aulton ME, editor. Pharmaceutics: the science of dosage form design. New York, NJ: Churchill Livingstone; 2002. p. 141-152.
7. Zhou D, Zhang GG, Law D, Grant DJ, Schmitt EA. Physical stability of amorphous pharmaceuticals: Importance of configurational thermodynamic quantities and molecular mobility. J Pharm Sci. 2002;91(8):1863-72.
8. Graeser KA, Patterson JE, Zeitler JA, Rades T. The role of configurational entropy in amorphous systems. Pharm. 2010:2(2), 224-244. Doi: 10.3390/pharmaceutics2020224.
9. Yinon H, Uhlmann, DR. Applications of thermoanalytical techniques to the study of crystallization kinetics on glass-forming liquids Part I: Theory. J Non-cryst solids, 1983;54:253-275.
10. Wigent RJ. Chemical kinetics. In: Troy DB, Beringer P editors. Remington: The science and practice of pharmacy 21st edition. Lippincott, Williams and Wilkins. 2006. p. 266-279.
11. Seefeldt K, Miller J, Alvarez-Nunez F, Rodriguez-Hornedo N. Crystallization pathways and kinetics of carbamazepine-nicotinamide cocrystals from the amorphous state by *In-situ* thermomicroscopy, spectroscopy and calorimetry studies. J Pharm Sci. 2007;5:1147-1158. Doi:10.1002/jps.20945.
12. Albers D, Galgoci M, King D, Miller D, Newman R, PeereyL, Tai E, Wolf R. Characterization of the polymorphic behaviour of an organic compound using a dynamic thermal and X-ray Powder Diffraction technique. Org Process Res Dev. 2007;11(5):846-860. Doi:10.1021/op700037w.
13. Ledinich RB, Aleman EC, Zuniga AE. *Conference proceeding.* Methodology to get the isothermal and non-isothermal bulk crystallization kinetics of iso-polypropylene by the use of a

hot stage and its comparison with data obtained by light polarized optical microscopy from film crystallization. *Eleventh Latin American and Caribbean Conference for engineering and technology*. 2013. Cancun, Mexico.

14. Chiu MH, Prenner. Differential Scanning Calorimetry: An invaluable tool for a detailed thermodynamic characterization of macromolecules and their interactions. J Pharm Bioallied Sci. 2011;3(1):39-59.
15. Yang J, Grey K, Doney J. An improved kinetics approach to describe the physical stability of amorphous solid dispersions. Int J Pharm. 2010;15(1-2):24-31. Doi: 10.1016/j.ipharm.2009.09.035.
16. Giron D. Investigations of polymorphism and pseudo-polymorphism in pharmaceuticals by combined thermoanalytical techniques. J Therm An Cal. 2001;64:37-60.
17. Fulias A, Vlase G, Vlase T, Soica C, Heghes A, Craina M, Heghes A, Ledeti I. Comparative kinetic analysis on thermal degradation of some cephalosporins using TG and DSC data. Chem Cent J. 2013;7(1):70. Doi: 10.1186/1752-153X-7-70.
18. Rodriguez-Hornedo N, Carstensen JT. Crystallization kinetics of oxalic acid dehydrate: nonisothermal desupersaturation of solutions. J Pharm Sci. 1986;75(6):552-558.
19. Alotaibi NM, Aouak T. Preparation and non isothermal crystallization kinetic of acetylsalicylic acid-poly(vinylalcohol-co-ethylene) blend. Application in drug domain. Macromol Res. 2013;21(7):747-756.
20. Brown ME, Glass BD. Pharmaceutical application of the Prout-Tompkins rate equation. Int J Pharm. 1999;190:129-137.
21. Ozawa T. Kinetics of non-isothermal crystallization. Polymer. 1971;12(3):150-158. Doi:10.1016/0032-3861(71)90041-3.
22. Kruger P. On the relation between non-isothermal and isothermal Kolmogorov-Johnson-Mehl-Avrami crystallization kinetics. J Phys Chem Sol. 1993;54(11):1549-1555. Doi: 10.1016/0022-3697(93)90349-V.
23. Matusita K, Komatsu T, Yokota R. Kinetics of non-isothermal crystallization process and activation energy for crystal growth in amorphous materials. J Pharm Sci. 1984;19: 291-296.
24. Bouchaour, ZC, Poulain M, Belhadji M, Hager I, Mallawany M. New oxyfluoroniobate glasses. Journal of non-crystalline solids, 2005;351:818-825.
25. Hruby A. Evaluation of glass-forming tendency by means of DTA. Czech J Phys B. 1972;22(11):1187-1193.
26. Perold Z, Swanepoel E, Brits M. Anomalous dissolution behavior of a novel amorphous form of Efavirenz. Am J PharmTech Res. 2012; 2(2):272-292.
27. Kissick DJ, Wanapun D, Simpson GJ. Second-order nonlinear optical imaging of chiral crystals. Annu Rev Anal Chem. 2011;4:419-437. Doi: 10.1146/annurev.anchem.
28. Jazaeri H, Humpreys FJ. Quantifying recrystallization by electon backscatter diffraction. J Micros. 2004;213:241-246.
29. Marentette JM, Brown GR. Polymer spherulites: II. Crystallization kinetics. J Chem Educ. 1993;70(7):539. Doi: 10.1021/ed070p539.

30. Watson ES, O'Neill MJ, Justin J, Brenner N. A Differential scanning calorimeter for quantitative differential thermal analysis. An Chem. 1964;36(7): 1233-1238.
31. Quinn RK. Compositioal dependence of structural and thermal properties of As---Te amorphous alloys. Mat Res Bull. 1974:9(6):803-813.
32. Abu-Sehly AA, Abu El-Oyoun M, Elabbar AA. Study of the glass transition in amorphous Se by differential scanning calorimetry. Thermochim Acta. 2008;472:25-30.
33. Abdel-Satar M, Abdel-Rahim MA, Korashy AE. A study of the crystallization kinetics of Ge-Se-Te glasses. Int J Pure App Phys. 2007;3(1):59-68.
34. Kumar P, Thangaraji R, Sathiaraj TS. Thermal analysis and annealing temperature dependence of electrical properties in $Sn_{10}Sb_{20}Se_{70}$ glassy semiconductor. J Mat Sci. 2008; 43:6099-6104.
35. Lasocka M. The effect of scanning rate on glass transition temperature of splat-cooled Te85Ge15. Mat Sci Eng. 1976; 23(2-3):173-177.
36. Joraid AA. Estimating the activation energy for the non-isothermal crystallization of an amorphous $Sb_{9.1}Te_{20.1}Se_{0.8}$ alloy. Thermochim Acta. 2007;456:1-6.
37. Kissinger HE. Variation of peak temperature with heating rate in differential thermal analysis. J Res Nat Bur Stand. 1956;57(4):217-221.
38. Vyazovkin S. Evaluation of activation energy of thermally stimulated solid-state reactions under arbitrary variation of temperature. J Comput Chem. 1997;18(3):393-402.
39. Kissinger HE. Reaction kinetics in differential thermal analysis. Anal Chem. 1957; 29(11):1702-1706.
40. Ye F, Lu K. Crystallization kinetics of Al-La-Ni amorphous alloy. J Non-Cryst Sol. 2000:228-235.
41. Ahmadi S, Shahverdi HR, Saremi SS. Nanocrystallisation of α-Fe crystals in $Fe_{52}CR_{18}Mo_7B_{16}C_4Nb_3$ bulk amorphous alloy. J Mat Sci Technol. 2011;27(6):497-502.
42. Rogers, RN, Morris ED. On estimating activation energies with a Differential Scanning Calorimeter. An Chem. 1966;38(3):412-414 DOI 10.1021/ac60235a009
43. Online document. Büchi Labortecnhnik AG. Melting point M-565. 2012. http://www.buchi.com/Melting-Point-M-565.12726.0.html. Accessed 10 August 2014.
44. Kruger P. On the relation between non-isothermal and isothermal Kolmogorov-Johnson-Mehl-Avrami crystallization kinetics. J Phys Chem Sol. 1993;54(11):1549-1555. Doi: 10.1016/0022-3697(93)90349-V.
45. Prasad S, Varma KBR. Crystallization kinetics of the $LiBO_2$-MeO_5 glass using differential thermal analysis. J Am Cer Soc. 2005;88:357-361.
46. Liao M, Li S, Sun H, Fang Y, Hu FI, Zhang J. Upconversion of properties of Tm^{31+}/Yb^{3+} codoped fluorophosphates glasses with low phonon density of states. Mat Lett. 2006;60:1783-1785.
47. Jadhav NR, Gaikwad VL, Nair KJ, Kadam HM. Glass transition temperature: Basics and application in pharmaceutical sector. Asian J Pharm. 2009:82-89.

48. Wolt E. The relationship between isothermal and nonisothermal description of Johnson-Mehl-Avrami-Kolmogorov kinetics. J Phys Chem Sol. 1992:521-527.
49. Schmitt EA, Law D, Zhang GGZ. Nucleation and crystallization kinetics of hydrated amorphous lactose above the glass transition temperature. J Pharm Sci. 1998;88(3):291-296.

Part II
Pyrimethamine

Chapter 4

The risk of recrystallization: Changes to the toxicity and morphology of pyrimethamine

Chapter 4 is presented in the form of a research article/manuscript and has already been published in the journal entitled: “Journal of Pharmacy and Pharmaceutical Sciences” (abbreviated as J Pharm Pharm Sci). This journal is an open access, free source, hosted and maintained by the University of Alberta. Electronic access to this specific manuscript can be achieved via

http://ejournals.library.ualberta.ca/index.php/JPPS/article/view/18912.

The guidelines for authors pertaining to this specific journal have been included as Annexure D.

Supplementary information to this manuscript has been included as Annexure E (combined with supplementary information for Chapter 5).

Please note that all requirements of the author guidelines were met at the time when the manuscript was submitted. The fact that the manuscript was accepted and published serves as proof to show adherence to the author guidelines. The manuscript presented in this Chapter is the work in its final printed format and not the separate documents as per the requirements at time of submission.

Also note that the page numbers in the bottom right corner applies to the thesis, whereas the page numbers in the bottom middle applied to the journal in which it was published.

Reproduction rights was obtained from the editor of the journal in November 2014.

The Risk of Recrystallization: Changes to the Toxicity and Morphology of Pyrimethamine

Zak Perold[1], Mino R Caira[2], Marius Brits[1]

[1] North-West University, Potchefstroom 2520, South Africa; [2] University of Cape Town, Cape Town, South Africa.

Received, March 9, 2014; Revised, April 16, 2014; Accepted, April 16, 2014; Published, April 21, 2014.

ABSTRACT - PURPOSE. Pyrimethamine, an anti-malarial agent known to exhibit solid state polymorphism, may be purified by means of recrystallization. Recrystallization may alter the solid state chemistry of pharmaceuticals, which may impact the toxicity and/or manufacturability thereof. We evaluated the risks associated with the recrystallization of pyrimethamine. **METHODS.** Pyrimethamine was recrystallized using several organic solvents. X-ray diffraction, thermal analysis, infra-red spectroscopy, microscopy, flowability -, solubility and dissolution testing as well as computational work were employed to evaluate the recrystallized products. **RESULTS.** A toxic solvatomorph of pyrimethamine (Pyr-MeOH) was found to be the product from methanol recrystallization. The elucidation of – and the elaboration on the unique characteristics of Pyr-MeOH provides the pharmaceutical industry with several means to identify Pyr-MeOH and to distinguish it from the pharmaceutically preferred anhydrous form (Pyr). Thermal methods of analysis found that the toxicity of Pyr-MeOH may be reversed by overcoming a desolvation activation energy of 148 kJ/mol. In addition it was found that recrystallization altered the morphology of Pyr. Angle of repose and tapped density determinations identified that the different morphologies of Pyr displayed differences in powder flow and compressibility behaviour and *In Silico* calculations were successful in rendering morphologies resembling that found experimentally. **CONCLUSION.** We present a solvatomorph of pyrimethamine and provide several characteristic means to identify this unwanted toxic form and quantified the energy required to overcome its toxicity. In addition we describe that Pyr may present in different morphologies and show how it may impact the manufacturability thereof.

INTRODUCTION

There will always remain a chance that not all the possible polymorphs and/or solvatomorphs of an active pharmaceutical ingredient (API) have been discovered (1) and it is therefore imperative for the pharmaceutical industry to stay abreast with newly discovered polymorphs and solvatomorphs to avoid problems associated with stability, treatment efficacy, safety and manufacturability (2). Pyrimethamine (Figure 1) has been used in the treatment of uncomplicated malaria for more than 30 years (3,4). Different solid forms of pyrimethamine have been described as early as 1976 (5), and yet the discovery of new solid forms in 2011 and 2012 (6,7) revealed that its solid state chemistry has still not yet been exhaustively elucidated.

Organic solvents are commonly employed in the pharmaceutical industry during processes such as purification (by means of recrystallization) and granulation (8, 9). The risk associated with the use of organic solvents should be governed by strict control procedures; however, the extent to which these regulations are enforced remains questionable. The WHO estimates that only 20% of countries have effective medicine regulatory authorities (10), and consequently sub-standard and/or unsafe medicines may inadvertently reach the market (11, 12).

Not so long ago, oral liquid preparations were contaminated with diethylene glycol (13) and serve as a tragic example of ineffective control over the use of organic solvents. More recently, de Villiers *et al.* described newly discovered toxic solvatomorphs of rifampicin which may have

Corresponding Author: Dr Marius Brits; North-West University, Potchefstroom 2520, South Africa; Email: Marius.Brits@nwu.ac.za

resulted as a consequence of contaminated organic solvents being used during manufacturing (14).

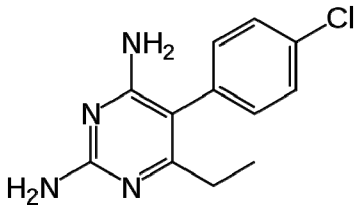

Figure 1. The chemical structure of pyrimethamine.

Pyrimethamine and some of its derivatives are purified by recrystallization with alcohol (15-18). Recrystallization is a technique employed universally to alter the solid state chemistry of an API (19,20). Organic solvents such as methanol, ethanol and acetone rank amongst the top 10 solvents which are most frequently used in pharmaceutical processes (9) and commonly result in solvatomorphism (20).

The purpose of this work was to evaluate the risks associated with the recrystallization of pyrimethamine using ICH Class II (methanol) and III (acetone, propanol and ethanol) organic solvents (21). In our work, we found it possible to prepare the methanol solvatomorph (hereinafter referred to as Pyr-MeOH) as first described by Delori *et al.* (7) from recrystallisation, as opposed to their technique of liquid assisted grinding. The focus of the work done by Delori *et al.* (7) was completely different to that which is presented herein. The work of Delori *et al.* (7) focused on the formation of co-crystals and salts of pyrimethamine, with the formation of Pyr-MeOH as a mere by-product of their study, being allocated, in passing, only two sentences in their manuscript (7). In particular, though they deposited the crystallographic data for this phase at the CSD (refcode XEGJEA), no description of the structure, morphology, thermodynamic properties or solubility profile were presented in their manuscript. The present account in part, serves to elaborate on the physicochemical properties of Pyr-MeOH, being distinctly unrelated to the study by Delori *et al*. (7). We found that recrystallization may not only risk the alteration of the toxicity of anhydrous pyrimethamine, but also its manufacturability. We present our work in an attempt to eliminate the potential health risks and manufacturing problems associated with the recrystallization of pyrimethamine using selected ICH Class II solvents.

MATERIALS AND METHODS

Recrystallization

Supersaturated solutions of anhydrous pyrimethamine (Bio-gen, India) were prepared by dissolving it in ethanol, methanol, acetone and propanol (Merck, South Africa), whilst the temperature was maintained at the boiling point of the solvent used. The supersaturated solutions were filtered and allowed to crystallize at ambient conditions until the crystal yield was sufficient for analysis (approximately 2 weeks). The anhydrous pyrimethamine raw material that was used in this work fit the description of the polymorph reported by Sethuraman and Muthiah (22) -CCDC number 193733, refcode MUFMAB.

X-Ray Powder Diffraction (XRPD) and Variable Temperature X-Ray Powder Diffraction (VTXRPD)

A Bruker D8 Advance diffractometer (Bruker, Frankfurt, Germany) was used to obtain XRPD patterns. The following conditions were applicable: target, Cu; voltage, 40 kV; current, 30 mA; divergence slit, 2 mm; anti-scatter slit, 0.6 mm, detector slit, 0.2 mm; monochromator; scanning speed, 2°/min with a step size of 0.025°, step time of 1.0 sec, radiation wavelength of 1.54Å and a scan range of 3-35° 2θ. For VTXRPD the same measuring conditions as above were used together with an Anton Paar TTK-450 low-temperature camera (Anton Paar, Austria) with a heating rate of 0.1K/sec.

Differential Scanning Calorimetry (DSC)

Approximately 2-5 mg of sample was weighed into a 40 µl aluminium sample pan, fitted with a pierced lid (Mettler Toledo, Greifensee, Switzerland) and crimped. The samples were analysed using a Mettler Toledo DSC823^e (Mettler Toledo, Greifensee, Switzerland) differential scanning calorimeter which was operated at a heating rate of 10K/min (unless stated otherwise) with a nitrogen flow rate of 80 ml/min. The thermal events were evaluated by means of the STAR^e software (version 9.0x) (Mettler Toledo, Greifensee, Switzerland). The instrument was calibrated using indium and zinc reference material.

Thermogravimetric Analysis (TGA)

Approximately 10-15 mg of sample was weighed into a 100 µl aluminium sample pan, fitted with a

pierced lid (Mettler Toledo, Greifensee, Switzerland) and crimped. The samples were analysed using a Mettler Toledo TGA/SDTA851^e (Mettler Toledo, Greifensee, Switzerland) thermogravimetric analyser which was operated at a heating rate 10K/min (unless stated otherwise) with a nitrogen flow rate of 80 ml/min. The thermal events were evaluated by means of the STAR^e software (version 9.0x) (Mettler Toledo, Greifensee, Switzerland). The instrument was calibrated using indium and aliminium reference material.

Karl-Fischer water determination

A Metro-ohm (Metro-Ω) KF Titrino (Metro-Ω, Switzerland) was used in the determination of water content in samples. The apparatus was calibrated using distilled water and sodium tartrate dihydrate (Merck®, Johannesburg, South Africa).

Hot Stage Microscopy (HSM)

A Nikon DS-Fi1 (Nikon, Tokyo, Japan) digital camera attached to a Nikon ECLIPSE E400 light microscope (Nikon, Tokyo, Japan) was used for HSM. Samples were heated with the use of a Leitz hot stage (Leica Microsystems Inc., Bannockburn, IL, USA) and the captured images were analysed using NIS-Elements F2.30 software (Nikon, Tokyo, Japan). Samples were suspended in silicone oil (Fluka, Switzerland) to visualize possible desolvation processes.

Diffuse Reflectance Infrared Fourier Transform (DRIFT-IR) Spectroscopy

The IR spectra were recorded using a Nicolet Nexus 470 spectrophotometer with the Avatar Smart diffuse reflectance accessory (Nicolet Instrument Corp., Madison, WI) over a range of 4000 cm^{-1}- 400 cm^{-1}. IR samples were prepared and analyzed in a potassium bromide (Merck®, Johannesburg, South Africa) matrix.

Gas Chromatography (GC)

An Agilent 6890 Gas Chromatograph with an Agilent 7697A Headspace sampler, together with a DB-624, 320.00µm X 30.0m column was used to perform residual solvent testing (where applicable) according to the USP general guidelines, Chapter <467> (23).

Single Crystal X-ray Diffraction

Colourless, prismatic single crystals of Pyr-MeOH showed poor cleavage and a tendency to produce fragments displaying multiple reflections. After several trials, a specimen was identified as suitable for full intensity data-collection. The latter was performed on a Bruker Kappa Apex Duo diffractometer with graphite-monochromated MoKα-radiation (λ = 0.71073 Å) and with the crystal cooled to 100(2) K to optimise diffraction quality. Comparison of the unit cell data at room temperature (294 K) and 100(2) K showed that no phase change had occurred on cooling the crystal. Intensity data-processing (SAINT, Version 7.60a, Bruker AXS Inc., Madison, WI, USA) included Lorentz-polarization corrections and multi-scan absorption corrections. For structure solution and refinement by full-matrix least-squares against F^2, programs in the SHELX-suite were employed (24).

The intensity data displayed only a centre of symmetry indicating the triclinic system; the centrosymmetric space group *P*(-1) was deduced from the parameter $|E^2-1| = 0.979$. Direct methods yielded all non-H atoms of the asymmetric unit (two molecules of the drug, designated A and B, and a single molecule of methanol). All non-H atoms refined anisotropically. All H atoms were located in difference Fourier maps and were generally included in a riding model with isotropic thermal parameters (U_{iso}) 1.2-1.5 times those of their parent atoms. Special attention was paid to the geometries of the amino groups, only one of which displayed trigonal planar geometry (that involving N14B) and was modelled as such. For the three remaining $–NH_2$ groups, some degree of pyramidisation at the nitrogen atom was noted and modelling of the H atoms in these cases involved free refinement with N-H distance restraints of 0.88(1) Å.

The crystallographic parameters for Pyr-MeOH following our X-ray analysis have been deposited at the Cambridge Crystallographic Data Centre (CCDC) (see Table 1).

Solubility Studies

The aqueous solubilities of Pyr and Pyr-MeOH were established in 0.1M HCl (pH 1.2 ± 0.05), acetate buffer (pH 4.5 ± 0.05) and phosphate buffer (pH 6.8 ± 0.05) at 303, 308 and 313 ± 1 K. A Heidolph RZR-2000 rotator (Heidolph, Germany) was used to rotate the sealed test tubes at 50 rpm in a thermally controlled water bath. Five ml of the medium was transferred to each test tube, each containing 50 mg of sample) and sealed. Each experiment was performed in triplicate. After 24 h the test tubes were removed from the instrument

and allowed to cool, then filtered and appropriately diluted. Sample aliquots were analyzed using a Cary 50 spectrophotometer (Varian, USA) running Varian WinUV version 3.00.

GC found the recrystallization product from methanol to contain 6.0% w/w methanol. To evaluate the influence of the methanol released from the lattice of Pyr-MeOH, the solubility of pyrimethamine was tested in the same manner as above, with the only exception that an equivalent amount of methanol (0.08% v/v, 6% with respect to the sample size) was added to the respective media.

A method was developed and validated specifically for the solubility studies. The validation parameters are described in the Supplementary Information section.

Particle Size

All samples (except for single crystal XRD, microscopy, powder flow and tapped density measurements) were slightly ground using a mortar and pestle and sieved to ensure a uniform particle size. The ground powder was sieved using a 106 µm sieve (Labotec, Midrand, South Africa) and subjected to particle size analysis. Particle size distribution measurements were performed using a Malvern Mastersizer 2000 (Malvern Instruments Ltd., Malvern, UK) fitted with a Hydro 2000SM dispersion unit using distilled water as dispersant. A cell stirrer prevented sedimentation of the dispersed particles and the latter were circulated through the sample cell by a sample pump. The acquired data were used to compute means, medians and standard deviations based on the particle population. The average $d_{(0.5)}$ values obtained were 22.6 µm (% RSD = 4.8%) and 24.3 µm (% RSD = 5.8%) for the Pyr and Pyr MeOH samples respectively.

Scanning Electron Microscopy (SEM)

A small amount of sample was used to cover the carbon tape that was affixed to the pin. The sample was then coated with a gold-palladium film using an IB-2 Eiko engineering ion coater inside a vacuum (Eiko Engineering, Ibaraki, Japan). The coated sample was then affixed to the microscope sample holder and analysed using a FEI Quanta 200 ESEM & Oxford INCA 400 EDS system (FEI, Hillsboro, OR).

***In silico* calculations**

Computational modulation studies were performed using Materials Studio™ 5.0 (Accelrys Software Inc., San Diego, CA, USA) software platform. The Bravais-Friedel-Donnay-Harker (BFDH) growth morphology (GM) and equilibrium morphology (EM) calculations within the Morphology™ module were used to predict the morphologies. BFDH, GM and EM calculations are based on mathematical theorems and assumptions, which have been extensively presented in related literature (25-27) and for this reason not presented in much detail here. In short, the BFDH method is a geometrical calculation that generates a habit taking into consideration the crystal lattice and symmetry operators in order to identify the growth faces and their growth rates. The GM method predicts a habit based on the assumption that the growth rate of a crystal face is proportional to its attachment energy, implying that faces with the lowest attachment energies are the slowest growing, and of the greatest importance to establish a habit. The EM method is similar to that of the GM method, as it also generates a habit using an energy parameter, the difference being that EM calculations use surface free energy.

The single crystal data file of anhydrous pyrimethamine (22), was retrieved from the Cambridge Crystallographic Data Centre (CCDC number 193733, refcode MUFMAB) and imported into the Material Studio platform and used for the predictions of Pyr morphologies. The single crystal data file of Pyr-MeOH (as elucidated in this manuscript), was imported into the Material Studio platform for the Pyr-MeOH morphology predictions. BFDH calculations were performed using the fine quality setting, the Forcite energy method, a minimum d(*hkl*) of 1Å (maximum $h = 5$, $k = 5$, $l = 5$) and the number of growing faces was limited to 300. GM and EM calculations were performed using the fine quality setting, Forcite energy method and the COMPASS forcefield. The summation method for GM and EM calculations was set to preset conditions (Electrostatic: Ewald and van der Waals: atom based). Faces for the GM calculations were controlled using preset conditions, which corresponded with those of the BFDH calculations. The habits considered to have been successfully predicted (i.e. comparable with those obtained experimentally) are presented and discussed in this manuscript.

Powder flow and powder density determinations

An Erweka GTL powder flow tester was used to characterize the powder flow of the different recrystallization products using different aperture sizes. In conjunction with the powder flow

determinations, a Erweka SVM121 tapped density meter was used to determine the Haussner ratios and Carrs Index of the recrystallized products. Powder samples were evaluated in untreated form (i.e., not ground or sieved) in order to maintain the integrity of the crystal habit.

RESULTS

Identification and classification of the recrystallization products

The XRPD, DSC and TGA results obtained from the recrystallization products from acetone, ethanol and propanol resembled those of anhydrous pyrimethamine (Pyr) (22); however, the morphology of these products differed, and is reported under **Morphology** together with that of Pyr-MeOH.

We have established that Pyr-MeOH may form by means of a simple process of recrystallization, a process far more familiar and common in the pharmaceutical industry than that which is presented in the work of Delori *et al.* (7). Interestingly, the latter authors in fact reported that their attempt to obtain a methanol solvate by recrystallization of the API from methanol was *not* successful, this phase, however, being obtained *via* grinding the API in a small amount of methanol. This indicates the vagaries of recrystallization experiments and the potential for conflicting outcomes, which are often due to subtle differences in experimental procedures. We emphasise that our findings resulted from the specific recrystallization technique described in this paper. Figure 2 depicts the XRPD pattern of Pyr-MeOH in comparison with one of the known anhydrous forms of pyrimethamine (Pyr) (6,22). Anhydrous pyrimethamine herein referred to as Pyr references to anhydrous pyrimethamine described by Sethuraman and Muthiah (22), whereas Pyr_2 refers to anhydrous pyrimethamine described by Tutughamiarso and Bolte (6).

The DSC trace of Pyr-MeOH (Figure 3) revealed a broad endotherm with peak maximum at 355.4 K and a melting endotherm at 514.3 K. The thermal events observed by DSC were visualized by means of HSM (Figure 3), which identified the first event as desolvation (crystal darkening and evolution of bubbles) and the second event as the melting process. In addition, HSM showed crystal growth to be concurrent with desolvation. Thermogravimetric analysis of Pyr MeOH (Figure 3) indicated a mass loss of 5.7 ± 0.2% in a single step in the region of 343-363 K that coincided with the temperature of desolvation as seen in the DSC of Pyr-MeOH. The thermal behaviour of Pyr-MeOH clearly differed from that of Pyr, which exhibited a single melting endotherm at 514K and no significant weight loss.

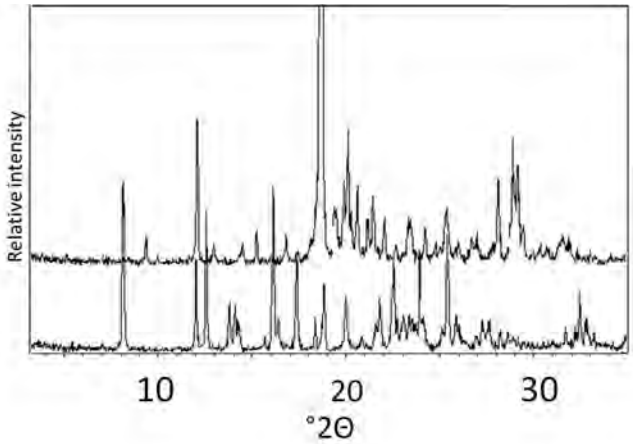

Figure 2. The XRPD patterns of Pyr (top) and Pyr-MeOH (bottom).

GC residual solvent testing identified that methanol was present in a concentration of 6.0% w/w (±0.9% w/w) in Pyr-MeOH. Karl-Fischer analysis did not detect the presence of water in Pyr-MeOH, which in conjunction with the GC and TGA results, proved Pyr-MeOH not to be a hydrated phase. A theoretical mass loss of 11.4% applies to a 1:1 stoichiometry of pyrimethamine and methanol, and therefore the TGA results for Pyr-MeOH (5.7%) indicated it to be a hemi-methanol solvated form of pyrimethamine (1:0.5 or 2:1).

The IR spectrum of Pyr-MeOH is depicted in Figure 4 together with that of Pyr. The IR spectrum of anhydrous pyrimethamine is reported to present characteristic bands between 3500 and 1400 cm^{-1} and at 3467, 3310, 3149, 1913 and 1793 cm^{-1} (28); these are present in the IR spectra of both forms. The **Discussion** section elaborates on the IR spectrum of Pyr-MeOH, in conjunction with findings from its single crystal XRD data.

Structural elucidation by single crystal XRD

Table 1 lists the crystal data and refinement parameters for Pyr-MeOH and Figure 5 shows the crystallographic asymmetric unit with non-H atoms drawn as thermal ellipsoids at the 50% probability level. The unit comprises two independent molecules of the drug (A and B) and a single molecule of solvent, giving the solvate a 2:1 stoichiometry, in accord with the TGA data.

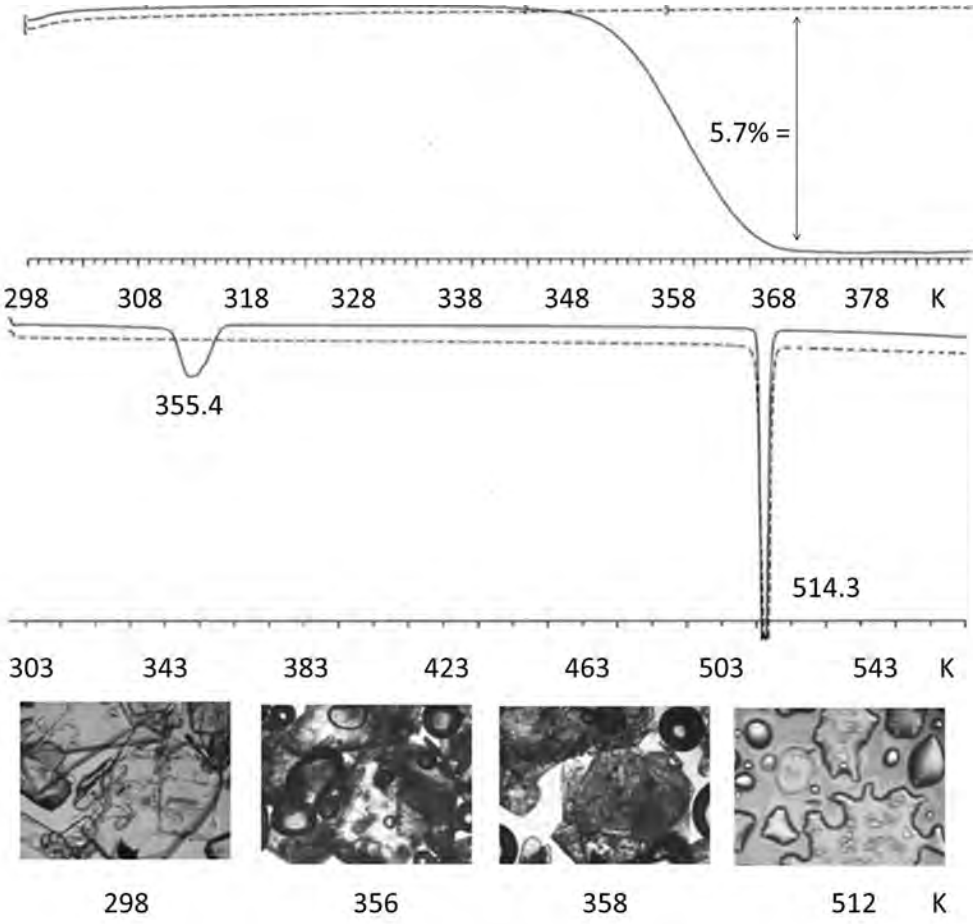

Figure 3. TGA (top) and DSC (middle) traces for Pyr (dotted lines) and Pyr-MeOH (solid lines). HSM photomicrographs of Pyr-MeOH (bottom) at 298, 356, 358 and 512K.

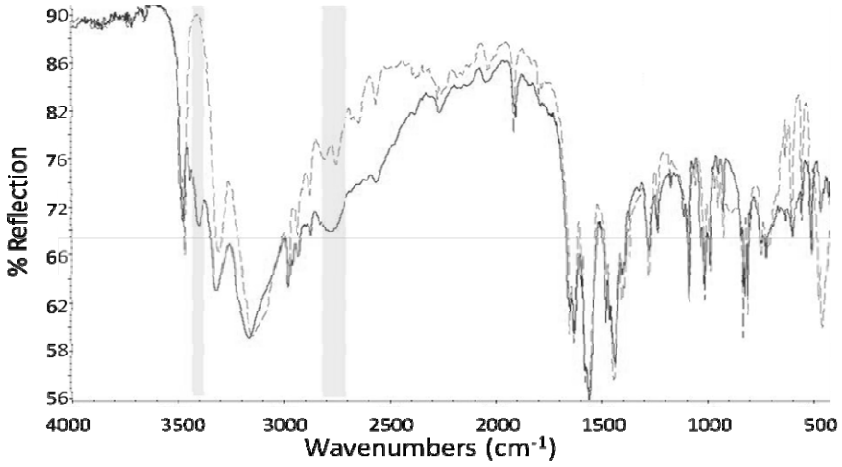

Figure 4. Superimposed IR spectra of Pyr (dotted line) and Pyr-MeOH (solid line).

Table 1. Crystal data and refinement parameters for Pyr-MeOH.

Parameter	Value
CCDC number	868963
Chemical formula	$C_9H_{10}O_3 \cdot C_6H_6N_2O$
Formula weight	529.47
D_{calc} (g cm^{-3})	1.316
Crystal system	Triclinic
Space group	*P* (-1)
a (Å)	8.450(2)
b (Å)	12.659(3)
c (Å)	14.008(3)
α (°)	64.441(4)
β (°)	89.908(4)
γ(°)	82.001(4)
V (Å^3)	1335.7(5)
Formula units, Z	2
F(000)	556
μ (MoK$_\alpha$) (mm^{-1})	0.277
Crystal size (mm^3)	0.19 x 0.26 x 0.39
T (K)	100(2)
θ-range (°)	1.8 - 30.5
Total reflections	31165
Unique reflections	8018
Data/restraints/ parameters	8018/6/353
R_1 (on F >4σ(F))	0.0369
wR_2 (on F^2, F >4σ(F))	0.0865
Goodness-of fit, S	1.012
Δρ max., min. (e Å^{-3})	0.42, -0.43

The inverted counterpart of molecule A is nearly superimposable on molecule B (weighted r.m.s.-fit = 0.59 Å) and the principal conformational parameter (C5-C4-C8-C9 in molecule A, corresponding geometrically to C3-C4-C8-C9 in molecule B) has the respective values -75.1(2)° and 104.7(2)°. In each case, the ethyl group is rotated out of the plane of the phenyl ring.

Molecular association in the solvate is mediated by extensive hydrogen bonding that generates a variety of supramolecular synthons. Self-association of type-A molecules is shown in the centrosymmetric array of Figure 6, which includes the methanol molecule and its hydrogen bonding to the API framework. In addition to the central cyclic hydrogen bonded motif with graph set descriptor $R_2^2(8)$ (29) generated by identical N-H···N bonds (N···N 3.040(2) Å), flanking cyclic motifs are formed with graph set $R_3^2(8)$ that include atom O19 of the solvent molecule as a hydrogen bond acceptor, engaging in bonds with donor groups N14A-H and N15A-H (N···O distances 2.883(2) Å and 2.949(2) Å respectively). Figure 6 also shows that the hydroxyl group of the solvent molecule acts as a donor in a hydrogen bond to N12B (O···N 2.729(2) Å) and is thus very tightly bound to the API framework.

An analogous, centrosymmetric tricyclic H-bonded motif occurs when type-B molecules associate, as shown in Figure 7. The central $R_2^2(8)$ motif again features identical N-H···N bonds (N···N 3.011(2) Å) but the flanking H-bonded $R_3^2(8)$ rings are now completed by nitrogen atom N12 of a type-A molecule (N···N distances 3.036(2) Å and 3.066(2) Å).

As stated earlier, the methanol solvate of pyrimethamine, herein designated as Pyr-MeOH, was found to be the same phase as that reported by Delori *et al*. (7), who, however, deposited their crystallographic data (T = 180 K, R = 0.0428) in the CSD without any discussion in their paper of the structural features presented here, since this phase was of peripheral interest only, their focus being on salts and co-crystals of pyrimethamine. Thus, all of the structural data presented above for Pyr-MeOH, as well as the further characterization studies reported in this paper represent previously unpublished results.

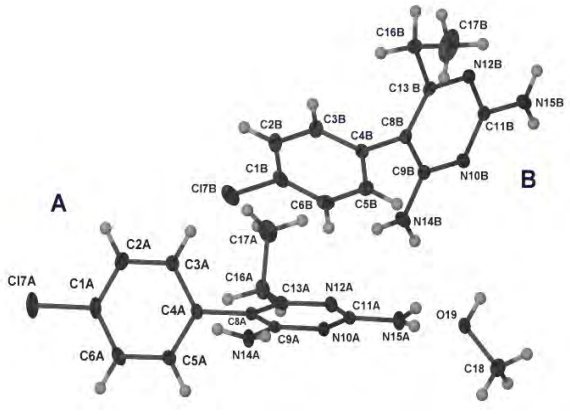

Figure 5. The crystallographic asymmetric unit in the solvate Pyr-MeOH. Non-hydrogen atoms are drawn as thermal ellipsoids at the 50% probability level and H atoms are drawn as spheres of arbitrary radius.

Thermodynamic stability of Pyr-MeOH

HSM, DSC and TGA indicated that Pyr-MeOH underwent desolvation at 343 – 373 K, which coincided with recrystallization (Figure 3). The melting point of the recrystallized product (post desolvation) corresponded with that of Pyr, which suggested that the desolvation of Pyr-MeOH led to crystal collapse and recrystallization into Pyr. In some cases, different polymorphic forms may have very similar melting points, and therefore it is advisable to confirm polymorphic identity by a combination of techniques. Since pyrimethamine has two known anhydrous forms, Pyr (22) and Pyr_2 (6), we employed VTXRPD analysis (Figure 8) to identify which anhydrous form will result upon the desolvation of Pyr-MeOH. The desolvation process was evident from VTXPRD, which showed changes in the XRPD pattern of Pyr-MeOH in the same temperature range as identified by DSC and TGA. The stabilized recrystallization product (at 473K) was identified as Pyr as it corresponded with the XRPD pattern of Pyr (22).

The desolvation of Pyr-MeOH was evaluated by TGA between 320 and 383 K at heating rates (β) of 2, 5 and 10 K/min. The fractions of desolvation (α) were calculated for each heating rate (Figure 9). The Ozawa-Flynn-Wall non-isothermal method (30-32) was used to determine the activation energy required for desolvation of Pyr-MeOH using the obtained results from the different TGA runs. The desolvation activation energy (E_a) of Pyr-MeOH was calculated to be 148.7 ± 9.3 kJ/mol (n=9).

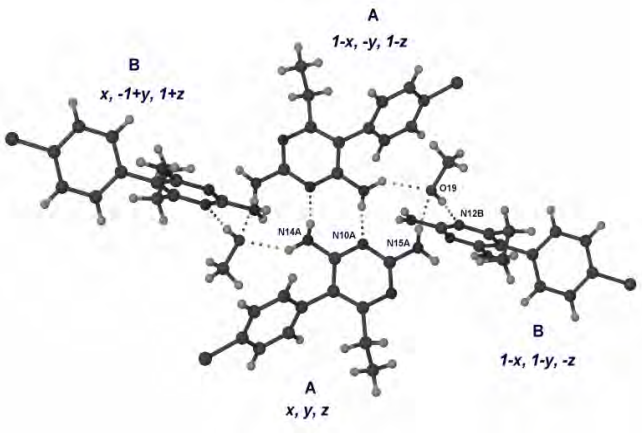

Figure 6. Self-association of type-A molecules in Pyr-MeOH and additional cyclic H-bond motifs involving the solvent molecules.

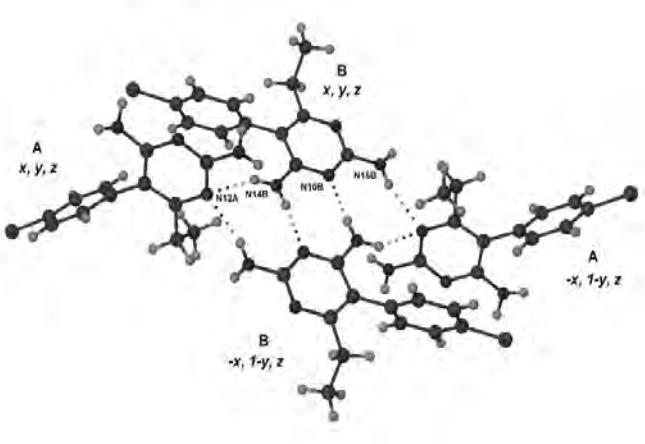

Figure 7. Self-association of type-B molecules in Pyr-MeOH and additional cyclic H-bond motifs completed by A···B hydrogen bonds

Solubility

Solubility studies were performed on Pyr-MeOH and Pyr for comparative purposes. The solubility results are summarized in Table 2. The data showed the solubility of pyrimethamine to be indirectly proportional to the pH of the medium (pyrimethamine being a weakly basic compound) and also showed the solubility of Pyr-MeOH to be superior to that of Pyr in the acidic media.

The influence brought forth by the release of methanol from Pyr-MeOH (6%) into the media was tested. The solubility of Pyr was tested in the same media containing an additional 0.08% v/v methanol, thereby recreating the altered media and simulating similar conditions as for Pyr-MeOH in the unchanged media. The test was conducted at a single temperature (308K), the results of which are shown in Table 2.

Morphology

As previously mentioned, the screening experiments (XRPD, DSC, TGA and IR spectroscopy) showed that the physicochemical properties of the recrystallization products from acetone and ethanol were not different from those of the starting material (Pyr). Interestingly, anhydrous pyrimethamine (Pyr) is described in literature as being needle/rod-shaped (33), whereas an investigation into the morphology of Pyr_A (from acetone) and Pyr_E (from ethanol) revealed that Pyr can present in morphologies other than needles.

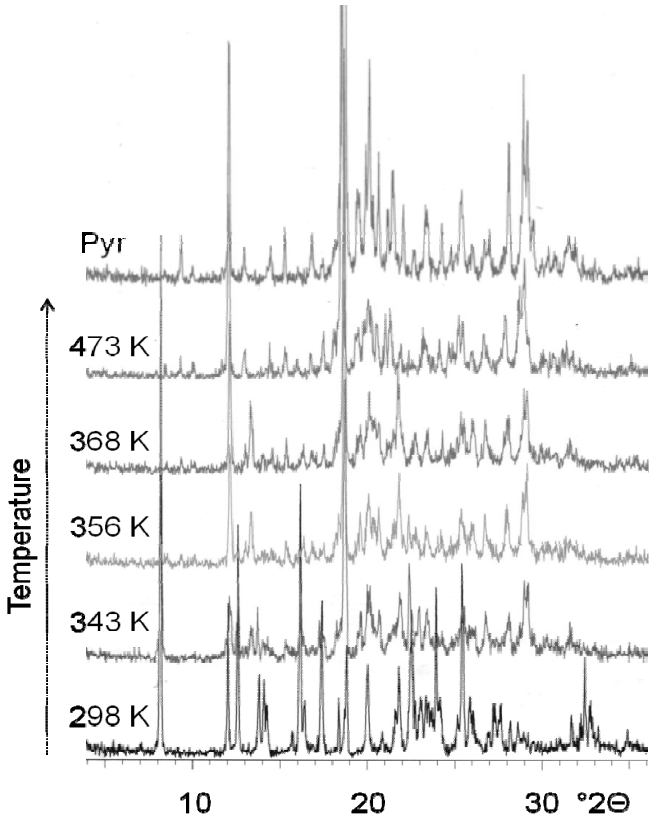

Figure 8. An overlay of the VTXRPD patterns of Pyr-MeOH at temperatures ranging between 298 and 473K together with a XRPD pattern of Pyr (at 298K).

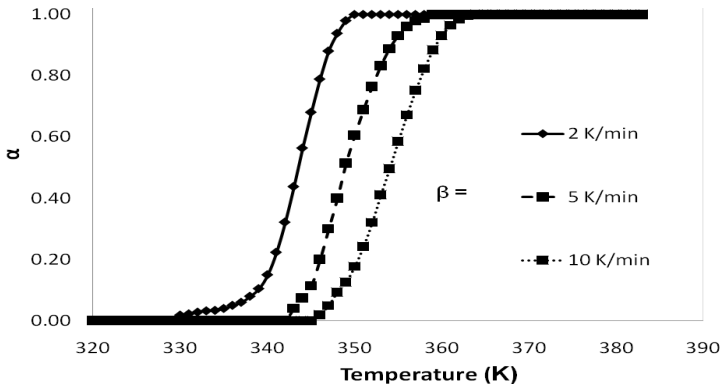

Figure 9. The desolvated fraction of Pyr-MeOH (α) as a function of temperature at different heating rates (β), β = 2, 5 and 10 K/min.

Table 2. The solubility of Pyr-MeOH in comparison with Pyr.

Medium	Solubility of Pyr-MeOH (mg/ml ± SD)			Solubility of Pyr (mg/ml ± SD)		
	303K	308K	313K	303K	308K	313K
HCl	3.3 ± 0.08	3.9 ± 0.10	4.3 ±0.10	2.9 ± 0.10	3.0 ± 0.13	3.2 ± 0.09
AB	1.4 ± 0.13	1.8 ± 0.07	2.3 ± 0.09	1.3 ± 0.06	1.4 ± 0.12	1.5 ± 0.10
PB	0.08 ± 0.02	0.07 ± 0.03	0.08 ± 0.02	0.07 ± 0.01	0.06 ± 0.04	0.07 ± 0.02
HCl^+	NA	NA	NA	NA	4.0 ± 0.06	NA
AB^+	NA	NA	NA	NA	2.0 ± 0.16	NA
PB^+	NA	NA	NA	NA	0.08 ± 0.04	NA

HCl is 0.1M (pH 1.2), AB is acetate buffer (pH 4.5), PB is phosphate buffer (pH 6.8), and $^+$ indicates the addition of MeOH to the specific medium.

The crystals that were obtained through recrystallization showed signs of fracture or imperfections (especially Pyr_E), and for this reason, computational predictions were used to elaborate on the different morphologies. The different morphologies are presented in Figure 10. Morphology calculations were successful in predicting the different crystal morphologies shown. Successful morphology renditions of Pyr_A and Pyr-MeOH were derived from BFDH calculations, whereas that of Pyr_E was obtained from GM calculation. The morphological characteristics of the predicted morphologies are presented in Tables 3-5.

From Figure 10 (and Tables 3-5) it can clearly be seen that the morphologies of anhydrous pyrimethamine differ from the known needle/rod-shaped habit (33). Powder flow/density determinations were performed in order to evaluate the potential differences brought forth by the three different morphologies of Pyr. Needle-shaped anhydrous pyrimethamine crystals were specifically prepared for this purpose by recrystallization from *n*-propanol (Pyr_P) - Figure 11.

The powder flow and compressibility properties of the different morphologies of Pyr are given in Table 6 and illustrated in Figure 12. It was found that Pyr_E was unable to pass through any aperture size, as the particles had a severe tendency towards agglomeration and clogging of the aperture (see Figure 12). Similarly Pyr_P could pass through the 25 mm aperture only. Pyr_A could not pass through the 6 mm aperture, but was able to pass through all subsequent larger apertures. Since Pyr_E and Pyr_P had difficulty passing through the various apertures, tapped density determinations were performed to provide some means to establish the powder flow characteristics of Pyr_E and Pyr_P.

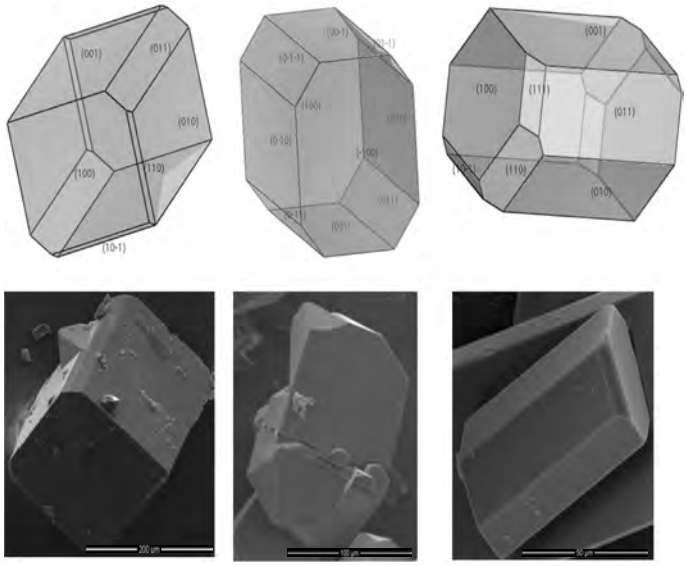

Figure 10. Calculated morphologies (top) and SEM photomicrographs (bottom) of Pyr_A (left), Pyr_E (middle), Pyr-MeOH (right).

Table 3. Predicted morphology data of Pyr_A.

h k l	**Multiplicity**	***d*$_{hkl}$ (Å)**	**% of total facet area**
1 0 0	2	9.50	26.20
0 1 0	2	10.52	24.66
0 0 1	2	12.26	34.10
0 1 1	2	8.86	8.44
1 1 0	2	7.57	4.80
1 0 -1	2	7.57	0.59
1 1 1	2	6.83	1.207

Table 4. Predicted morphology data of Pyr_E.

h k l	Multiplicity	E_{att} (kcal/mol)	% of total facet area
1 0 0	2	-36.99	37.55
0 1 0	2	-43.52	19.90
0 0 1	2	-46.82	20.64
0 1 1	2	-52.86	10.79
1 1 0	2	-57.60	1.67
0 1 -1	2	-48.94	8.72
1 1 1	2	-64.68	0.73

Table 5. Predicted morphology data of Pyr-MeOH.

h k l	Multiplicity	d_{hkl} (Å)	% of total facet area
1 0 0	2	8.35	20.19
0 1 0	2	11.28	20.92
0 0 1	2	12.61	29.52
0 1 0	2	11.28	20.92
0 1 1	2	11.17	20.82
1 1 0	2	7.27	4.66
1 0 -1	2	7.18	1.88
1 1 1	2	7.01	2.02

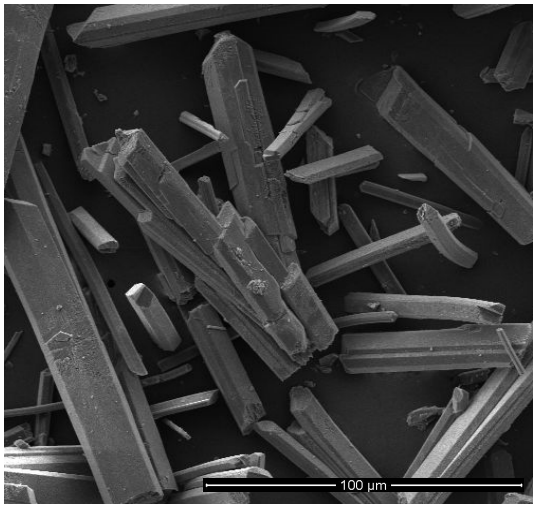

Figure 11. SEM photomicrograph of Pyr_P.

Table 6. The results from powder flow determinations (top) together with Hausnner ratios and Carrs indices (bottom) of Pyr_A, Pyr_E and Pyr_P.

Powder flow			
Aperture	**Pyr-$_A$**	**Pyr-$_E$**	**Pyr-$_P$**
6 mm	NA	NA	NA
10 mm	5.8 (±0.2) g/s	NA	NA
15 mm	15.1 (±3.6) g/s	NA	NA
25 mm	24.3 (±2.9) g/s	NA	3.6 (±1.2) g/s
Carrs Index (CI) and Hausner ratio (HR)			
Tapping time	**Pyr-$_A$**	**Pyr-$_E$**	**Pyr-$_P$**
2 minutes	CI = 11.8%	CI = 17.6%	CI = 25.1%
	HR = 0.89	HR = 0.85	HR = 0.80

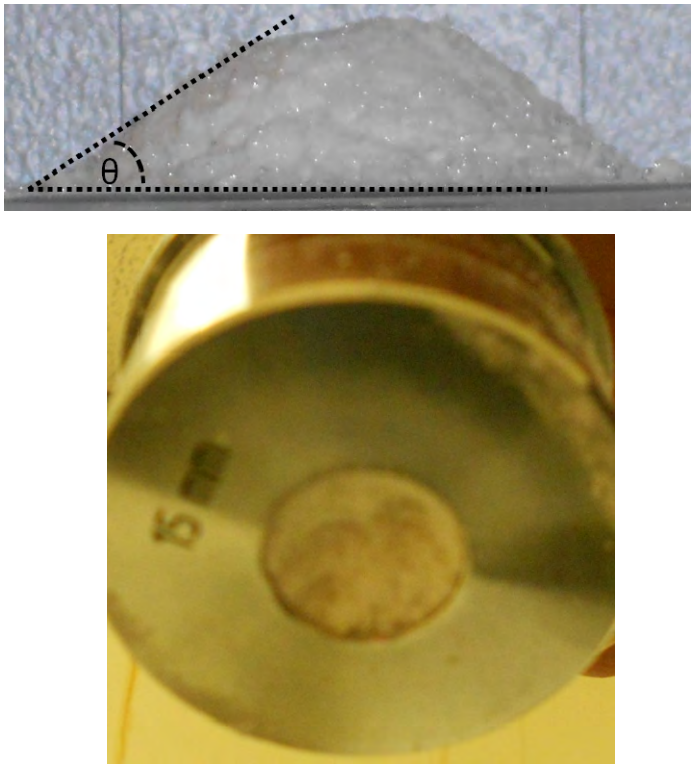

Figure 12. Angle of repose Pyr_A, where Θ=25° (±0.4°) using a 25 mm aperture (top), and a typical example of the clogging experienced during the powder flow determinations of Pyr_E and Pyr_P (bottom).

DISCUSSION

Polymorph screening, characterization and classification

The screening studies indicated that pyrimethamine may present in a toxic methanol solvatomorphic form (Pyr-MeOH) from recrystallization. Since it is known that pyrimethamine is recrystallized with alcohols for purification purposes, we felt obligated to elaborate on the characteristics of Pyr-MeOH (and distinguish it from the preferred form Pyr), given that a high potential exists for it to be formed during API manufacture/purification and subsequently inadvertently be used for final product manufacture.

The concentration of methanol incorporated into the lattice of Pyr-MeOH (±6% or 60000 ppm) greatly exceeds the maximum allowable/tolerable limit (3000 ppm) set by the ICH Q3C residual solvent guidelines (21). The inadvertent use of methanol as a recrystallization solvent, or its presence as an impurity in a non-solvating solvent used for the purification of pyrimethamine may therefore have serious health ramifications. With the public health interest at heart, we present our findings on the characterization of this form of the API and provide several unique characteristics that can be used to identify this unwanted form and distinguish it from the preferred anhydrous form (Pyr).

The XRD, DSC, TGA, DRIFT-IR properties of Pyr-MeOH clearly differed from those of Pyr. The differences between the two forms are summarized in Table 7 and serve as quick and easy analytical means to identify Pyr-MeOH and/or distinguish it from Pyr.

Structure elucidation

The main differences between the IR spectra of Pyr-MeOH and Pyr were at 3400 cm^{-1}, and in the region 2850-2650 cm^{-1}. These are characteristic bands of methanol (34,35) which confirmed the presence of methanol in the crystal of Pyr-MeOH, as they do not present in that of Pyr. Interestingly, a shift in the $-NH_2$ band position (broad band at 3200 cm^{-1}) was observed in the IR spectrum of Pyr-MeOH. A shift to a higher wavenumber (left) suggested participation in H-bonding. The shifting of the band was elucidated in the light of the findings from single crystal XRD.

Single crystal XRD is a sophisticated and fairly expensive technique, and for this reason not routinely used during polymorphic screening studies. Nevertheless, the results from single XRD provide unequivocal crystallographic information and a reliable means of identifying a specific crystal form. Single crystal XRD yielded the unit cell parameters of Pyr-MeOH (Table 1), which are uniquely different from those of Pyr (a = 9.585(2), b = 10.806(2), c = 12.484(2) Å, α =79.06(1), β = 89.44(2) and γ = 82.37(1)°, with 4 molecules per unit cell, assembled in the triclinic system, space group *P* (-1) resulting in a density of 1.313 g cm^{-3}). Furthermore, only one molecule of the API in the asymmetric unit of Pyr-MeOH has a principal torsion angle value (-104.7°(2)) equal to that of a molecule in the asymmetric unit of unsolvated Pyr; instead, for the other pair of molecules, the corresponding torsion angles are -75.1(2)° in Pyr-MeOH and -81.2(1)° in unsolvated Pyr (6).

Single crystal XRD showed that the methanol molecules of Pyr-MeOH occur as inversion-related pairs in isolated sites within the solvate crystal (Figure 13). In this arrangement the pyrimethamine molecules have a greater potential towards H-bonding, which is depicted by the -NH_2 band shift as observed in the IR spectra of Pyr-MeOH (Figure 4).

Thermodynamic stability

VTXRPD (Figure 8) confirmed that the desolvation of Pyr-MeOH led to crystal collapse and concurrent recrystallization into Pyr. The activation energy required for the desolvation of Pyr-MeOH (148.7 ± 9.3 kJ/mol) is high in comparison with other known methanol solvates (36, 37). The high activation energy required for desolvation is supported by the single crystal data of Pyr-MeOH which found the specific topology of solvent inclusion (Figure 13) to confer additional stability on the solvated crystal structure and indicated that the collapse of this phase would require considerable energy. Since the desolvation of Pyr-MeOH resulted in its transformation into Pyr, the activation energy may be considered as an indication of how much energy is required to convert from Pyr-MeOH to Pyr.

Table 7. The characteristic differences between Pyr-MeOH and Pyr.

Technique	Pyr-MeOH	Pyr
XRPD peaks (± 0.2 º2θ)	8.3, 12.7, 13.9, 14.4, 16.3, 19.0, 20.2, 22.0, 22.6, 23.3 and 28.8	9.9, 12.9, 18.6, 19.4, 19.9, 20.1, 20.6, 25.3, 28.9 and 29.2
DSC	Broad endotherm at 314K (desolvation) Sharp endotherm at 514K (melt)	None Sharp endotherm at 514K (melt)
TGA	±5.7% weight loss	None
GC	Identification and quantification of methanol	None
DRIFT-IR	Peaks at 3400 and 2850-2650 cm^{-1} (characteristic of MeOH) NH_2 band (3200 cm^{1}) shifting	None None

Solubility

The solubility of Pyr-MeOH was expected to differ from that of Pyr due to the influence of H-bonding and the presence of the methanol molecules within the crystal of Pyr-MeOH. We investigated the solubility behaviour of Pyr-MeOH at different temperatures and in different media. Significant differences in the solubility behaviour of Pyr-MeOH and Pyr provided yet another characteristic difference between the two forms (Table 2). Pyr-MeOH was more soluble than Pyr in the acidic media. Linear relationships of solubility vs. temperature were evident in acidic media (Figure 14), which indicated that the dissolution process of both forms is of an endothermic nature.

The solubility of the two forms was equally poor in the phosphate buffer and did not differ significantly (0.07 ± 0.02 mg/ml) regardless of the temperature. Single-sided ANOVA analysis of the solubility values of Pyr and Pyr-MeOH in 0.1M HCl indicated that the solubility of Pyr-MeOH was significantly higher ($p < 0.05$) compared to that of Pyr (Figure 15) in the range 303-313 K. In acetate buffer (pH 4.5) the difference in solubility of the two forms was not significantly different between 303 and 306 K ($p \geq 0.05$). Thus, 0.1M HCl was

deemed the most discriminatory medium to distinguish between Pyr and Pyr-MeOH by means of solubility.

From the solubility results it is believed that the release of methanol from the crystal of Pyr-MeOH changed the composition of the medium and by doing so created a more favourable environment for the dissolution of pyrimethamine. This theory was investigated by repeating the solubility testing of Pyr in the same media each containing 0.08% v/v methanol (equivalent to the release of 6% methanol from a 50 mg sample). The results (highlighted in Table 2) showed that adding methanol to the medium resulted in a significant increase in the solubility of Pyr, and that its measured solubility was similar to that of Pyr-MeOH at the same temperature (308 K). The additional methanol potentiated the solubility of Pyr by 30%, 29% and 17% in HCl, acetate buffer and phosphate buffer respectively.

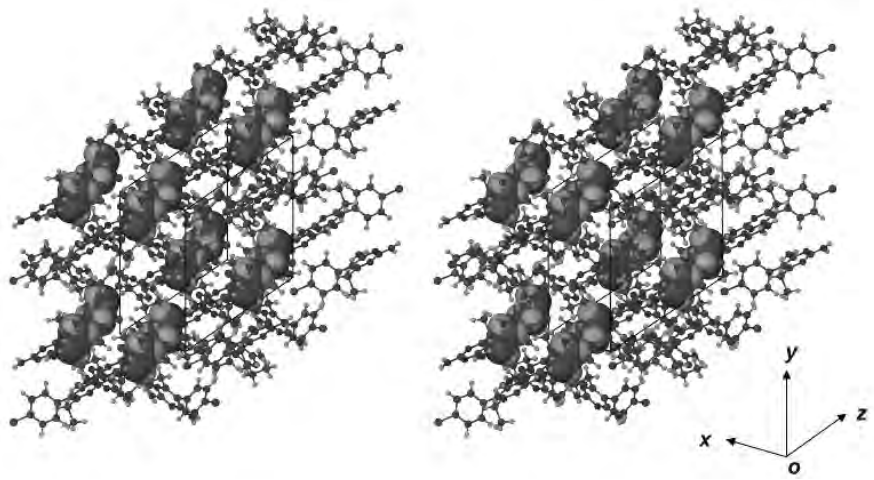

Figure 13. Stereoview of the crystal structure of Pyr-MeOH with the atoms of the API in ball-and-stick style and the solvent molecules in space-filling style.

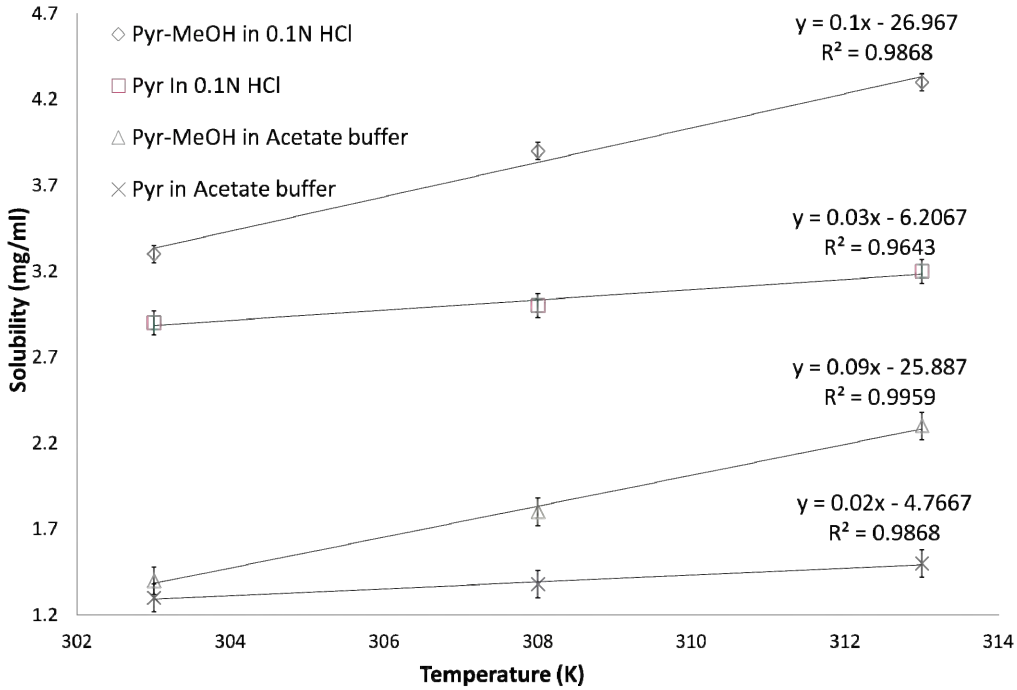

Figure 14. The solubility of Pyr-MeOH and Pyr in 0.1M HCl (pH 1.2) and acetate buffer (pH 4.5) as a function of temperature (error bars represent the standard deviation).

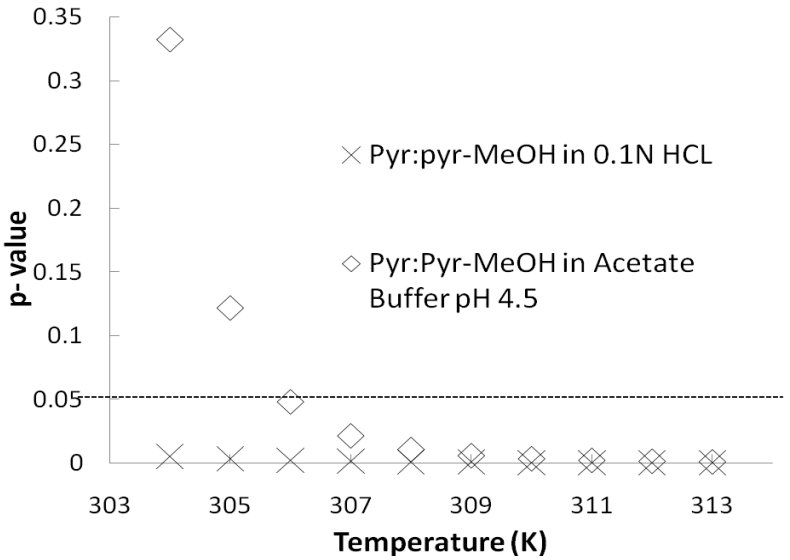

Figure 15. Calculated p-values showing the statistical significance of the differences in solubility between Pyr and Pyr-MeOH in 0.1M HCl and acetate buffer (pH 4.5).

Morphology

Recrystallization using other solvents (ethanol, acetone and propanol) did not result in any internal crystal or toxicological modification of Pyr, but did show that the triclinic form of Pyr [space group *P*(-1)] may crystallize in habits other than needles/rods (33). SEM photomicrographs showed that the different morphologies of Pyr and Pyr-MeOH exhibit imperfections and/or signs of fracture. The experimental findings from SEM were duly complemented using crystal morphology predictions. The characteristic details of these different morphologies are listed in Tables 3-5. The predicted morphology from BFDH calculation resembled that of Pyr_A. The derived lattice parameters were a = 9.58 Å, b = 10.81 Å, c = 12.48 Å and α = 79.1°, β = 89.4°, γ = 82.4°. The predicted morphology derived from the GM calculations resembled that of Pyr_E. The derived lattice parameters were a = 9.31 Å, b = 10.74 Å, c = 12.04 Å, α = 79.1°, β = 91.5° and γ = 88.7°. The derived lattice parameters of the predicted morphology of Pyr-MeOH (from BFDH calculation) were a = 8.45 Å, b = 12.659 Å, c = 14.008 Å, α = 64.44°, β = 89.91° and γ = 82.00°**.** The lattice parameters were in good agreement with the experimental findings from the single crystal XRD work (Table 1).

It is well known that coarse spherical particles will have the best powder flow (38). The powder flow and density results (Table 6) yielded the order of improving powder flow as Pyr_P < Pyr_E < Pyr_A. Understandably so, the powder flow of Pyr_A was the best since the particles were coarse (>100 µm) and of all the habits, the closest to being spherical, which allowed for relatively free-flowing powder. The particles of Pyr_P and Pyr_E were smaller and had greater surface-to-volume/mass ratios, which caused higher cohesive and adhesive forces, impairing their powder flow.

CONCLUSION

Pyrimethamine was recrystallized using acetone, *n*-propanol, ethanol and methanol to evaluate whether recrystallization with these solvents might affect the toxicity and manufacturability of the API. We presented a simple and reproducible recrystallization method to prepare a methanol solvate of pyrimethamine as an alternative to that described by Delori *et al.* (7).

The methanol content entrapped in the crystal of Pyr-MeOH (approximately 6% by mass) greatly exceeds the allowable limits provided by the ICH Q3C guidelines for residual solvent content, and therefore is deemed a health risk, should this form, even in relatively small quantity, inadvertently be included in final pharmaceutical products. Pyr-MeOH was comprehensively characterized, and the characteristics unique to this form were highlighted to serve as means to identify it and to distinguish it from the preferred anhydrous form (Pyr) in an attempt to minimize the risk of this toxic form inadvertently being incorporated into a final pharmaceutical product. It has now been established that there are at least two ways in which the methanol solvate of pyrimethamine can arise,

namely *via* recrystallization from MeOH or during grinding of the API in the presence of MEOH (7). Furthermore, seeing that an estimated 80% of countries have poor (or even no) regulatory control over medicines and their manufacture (10), the possibility exists that incorrect solvents may be used, as illustrated by the Haiti tragedy involving toxic diethylene glycol that had contaminated oral liquid preparations (13).

VTXRPD indicated that the desolvation of Pyr-MeOH resulted in its transformation into Pyr. The H-bonding patterns and the topology of methanol molecule inclusion (from single crystal XRD) led to the prediction that considerable energy would be required to eliminate the toxic solvent from the crystal. Non-isothermal reaction kinetics by TGA vindicated the single crystal XRD findings, as the desolvation activation energy was quantified as 148.7±9.3 kJ/mol, which is considerably higher than values reported previously for other methanol solvates (36,37).

Recrystallization with other solvents did not modify the internal crystal structure of Pyr; however, it was established that Pyr may present in different crystal habits. Computational work was successful in predicting morphology renditions comparable with those observed experimentally by SEM, and show that *in-silico* morphology predictions may be useful to complement experimental work. From powder flow experiments it was illustrated that these different morphologies have significantly different powder flow and compressibility behaviors, which may cause manufacturing difficulties.

SUPPLEMENTARY INFORMATION

UV spectrophotometry method development and crystallographic files include the CCDC Data Deposition confirmation, the CIF file and the CHECKcif report.

ACKNOWLEDGEMENTS

Z.P and M.B thank the Drug Research and Development unit and the Research Institute for Industrial Pharmacy of the North-West University (NWU) for financial assistance. Z.P further thanks the Laboratory for Applied Molecular Modelling (NWU), Accelrys Inc. (San Diego, USA) and the Centre for High Performance Computing (CHPC) for the help, use and licensing of Materials Studio. M.R.C. thanks the University of Cape Town and the NRF (Pretoria) for research support.

REFERENCES

1. Price SL. The computational prediction of pharmaceutical crystal structures and polymorphism. Adv Drug Deliver Rev, 2004; 56:301-319.
2. Bauer J, Spanton S, Henry R, Quick J, Dziki W, Porter W, Morris J. Ritonavir: An extraordinary example of conformational polymorphism. Pharm. Res, 2001; 18:859-866.
3. Pyrimethamine monograph, in Wade A (ed), Martindale The Extra Pharmacopeia. 27th ed., Jarold and Sons ltd, Great Britain, pp 354-357, 1979.
4. Tracy, JW.; Webster, L.T., Chemotherapy of parasitic infections - Drugs used in the chemotherapy of protozoal infections: Malaria, in Hardman JG: Limbird LE: Gilman AG (eds), The Pharmacological Basis of Therapeutics. 10th ed., McGraw-Hill Medical Publishing Division, New York, pp 1059-1068, 2001.
5. Rees, RWA, Chai, SY, Winkley, MW, Russell, PB. Antimalarial activity of some novel derivatives of 2,4-diamino-5-(p-chlorophenyl)-6-ethylpyrimidine (pyrimethamine). J. Med. Chem. 1976; 19:723-725.
6. Tutughamiarso M, Bolte M. A new polymorph and two pseudopolymorphs of pyrimethamine. Acta Cryst, 2011; C67:o428-o434.
7. Delori A, Galek PTA, Pidcock E, Jones W. Qauntifying Homo- and Heteromolecular Hydrogen Bonds as a guide for adduct formation. Chem. Eur. J, 2012; 18:6835-6846.
8. Grodowska K, Parczewski A. Organic solvents in the pharmaceutical industry. Acta Pol Pharm, 2010; 67:3-12.
9. Constable DJC., Jimenez-Gonzalez C, Henderson RK. Perspective on solvent use in the pharmaceutical industry. Org Process Res Dev, 2007; 11:133-137.
10. World Health Organization. [Internet]. EHO policy perspectives on Medicines – Effective medicine regulation: ensuring safety, efficacy and quality. [updated 2003, cited March 2012]. Available online at http://whqlibdoc.who.int/hq/2003/WHO_EDM_2003.2.pdf
11. Gaudiano MC, Di Maggio A, Cocchieri E, Antoniella E, Bertocchi P, Alimonti S, Valvo L. Medicines informal market in Congo, Burundi and Angola: counterfeit and sub-standard antimalarials. Malar J, 2007; 6:22.
12. Odeniyi MA, Adegoke OA, Adereti RB, Odeku OA, Itiola OA. Comparitive analysis of eight brands of sulfadoxine-pyrimethamine tablets. Trop J Pharm Res, 2003; 2(1):161-167.

13. Woolf A. The Haitian diethylene glycol poisoning tragedy: A dark wood revisited. J Am Med Assoc, 1998; 279(15):1215-1216.
14. De Villiers MM, Caira MR, Li J, Strydom SJ, Bourne SA, Liebenberg W. Crystallization of toxic glycol solvates of rifampicin from glycerine and propylene glycol contaminated with ethylene glycol or diethylene glycol. Mol Pharm, 2011; 8(3):877-888.
15. Jacob RM. Production of 2:4-diamino-5-(4'-chlorophenyl)-6-ethylpyrimidine. United States patent office, 1954; patent number 2,680,740.
16. Hitchings GH, Russell PB, Falco EA. 2,4-diamino-5-phenyl-6-akyl-pyrimidines. Unites States patent office, 1951; patent number 2,576,939.
17. Rosowksy A, Dey AS, Battaglia J, Modest EJ. Synthesis of 2,4-diamino-9H-indeno[2,1-*d*] pyrimidines. J Heterocycl Chem, 1969; 6(5):613-622.
18. Russell PB, Hitchings GH. 2,4-diaminopyrimidines as antimalarials. III. 5-Aryl derivatives. J Am Chem Soc, 1951; 3763-3770.
19. Buckton, G., Solid-state properties, in Aulton ME: editor, Pharmaceutics: The science of dosage form design. 2nd ed., Churchill Livingstone, New York, NY, pp. 141-152, 2002.
20. Byrn, S.R.; Pfeiffer, R.R.; Stowell, J.G., Solid-state chemistry of drugs. SSCI, West Lafayette, IND, USA, 1999.
21. European Medicines Agency. [Internet]. ICH Q3C (R4) CPMP/ICH/283/95. Impurities: Guidelines for residual solvents. [updated 2009, cited March 2012]. Available online at http://www.ema.europa.eu/docs/en_GB/document_library/Scientific_guideline/2009/09/WC500002674.pdf
22. Sethuraman V, Muthiah T. Hydrogen-bonded supramolecular ribbons in the antifolate drug pyrimethamine. Acta. Crystallogr, 2002; 58:817-818.
23. United States Pharmacopeia National Formulary [Internet]. General Chapter <467> Residual solvents. [updated 2014, cited 2014]. Available online at http://www.uspnf.com
24. Sheldrick GM. A short history of SHELX. Acta Crystallogr, 2008; A64:112-122.
25. Beyer T, Day GM, Price SL. The prediction, morphology and mechanical properties of the polymorphs of paracetamol. J. Am. Chem. Soc, 2001; 123:5086-5094.
26. Rohl AL. Computer prediction of crystal morphology. Curr. Opin. Solid. St. M, 2003; 7:21-26.
27. Coombes, DS, Catlow RA, Gale JD, Hardy MJ, Saunders MR. Theoretical and experimental investigations on the morphology of pharmaceutical crystals. J. Pharm. Sci, 2002; 7:1652-1658.
28. De Araújo MVG, Vieira EKB, Lázaro GS, Conegro LDS, Ferreira OP, Almeida, LE, Barreto LS, da Costa NB, Gimenez IF. Inclusion complexes of pyrimethamine in 2-hydroxypropyl-β-cyclodextrin and molecular modelling. Bioorg. Med. Chem, 2007;15:5752-5759.
29. Etter MC, MacDonald JC. Graph-set analysis of hydrogen-bond patterns in organic crystals. Acta. Crystallogr, 1990; B46:256-262.
30. Ozawa TA. new method of analysing thermogravimetric data. Bull. Chem. Soc. Jpn, 1965; 11:1881-1886.
31. Flynn JH. Early papers by Takeo Ozawa and their continuing relevance. Thermochim. Acta, 1996; 283:35-42.
32. Flynn JH, Wall LA. A quick, direct method for the determination of activation energy from thermogravimetric data. Pol. Lett, 1966; 4:323-328.
33. Hitchings GH, Russell PB, Falco EA. Process for preparation of 4-amino-5-aryl-pyrimidines. United States patent office, 1952; patent number 2,602,794.
34. Coates J. Interpretation of infrared spectra, a practical approach, in Meyers RA (ed), Encyclopaedia of analytical chemistry. John Wiley & Sons Ltd, Chichester, pp 10815-10837, 2000.
35. Boehm G, Dwyer M. Infrared spectrum of methanol. J Chem Educ, 1981; 58(10):809-811.
36. van Tonder EC, Mahlatji MD, Malan SF, Liebenberg W, Caira MR, de Villiers MM. Preparation and physicochemical characterization of 5 Niclosamide solvates and 1 hemisolvate. AAPS Pharm Sci, 2004; 5:86-95.
37. Hakanen A, Laine E. Characterization of two terfenadine polymorphs and a methanol solvate: kinetic study of the thermal rearrangement of terfenadine from the methanol solvate to the lower melting polymorph. Thermochim. Acta, 1995; 248:217-227.
38. Staniforth J., Powder flow, In Aulton ME (ed): Pharmaceutics. The science of dosage form design. 2nd ed., Harcourt Publishers Limited, London, UK pp 197-212, 2002.

Chapter 5

Characterisation of two novel solid-state forms of Pyrimethamine

Chapter 5 is presented in the form of a research article/manuscript and is aimed towards publication in the journal entitled: “European Journal of Pharmaceutical Sciences” (abbreviated as Eur J Pharm Sci)

The guidelines for authors pertaining to this specific journal have been included as Annexure F.

Supplementary information to this manuscript has been included as Annexure E (combined supplementary information for Chapters 4 & 5).

Please Note: Although the text, figures, tables, etc. need to be submitted as separate files (in accordance with the author guidelines – Annexure F), the manuscript is presented here as a single file with text, figures and tables in a single document for ease of evaluation. For the purpose of submission, all files will be submitted as stipulated by the guidelines.

Characterisation of two novel solid-state forms of Pyrimethamine

Zak Perold[1a], Mino R Caira[2b], Erna Swanepoel[1c], Marius Brits[1d]

[1] Research Institute for Industrial Pharmacy® incorporating CENQAM® , North-West University, Potchefstroom 2520, South Africa;

[2]Department of Chemistry, University of Cape Town, Rondebosch 7701, Cape Town, South Africa.

[a]zak.perold@diconsultants.co.za

[b]mino.caira@uct.ac.za

[c]erna.swanepoel@nwu.ac.za

[d]marius.brits@nwu.ac.za; tel: +27(18) 299 2268; corresponding author

Abstract

This study presents the characterisation of two new solvatomorphs of pyrimethamine, a dihydrofolate reductase inhibitor that is commonly used in synergistic combination with sulfadoxine in the treatment of uncomplicated malaria. Pyrimethamine was recrystallised from N,N-dimethylformamide (DMF) and N,N-dimethylacetamide (DMA). The recrystallisation yielded two novel solvates, both displaying 1:1 pyrimethamine:solvent ratios. The solvatomorphs were characterised by Differential Scanning Calorimetry (DSC), Thermogravimetric Analysis (TGA), several X-Ray Diffraction techniques, Scanning Electron Microscopy and Hot-Stage Microscopy (SEM and HSM), Infrared spectroscopy (IR) as well as solubility studies. Non-isothermal kinetic desolvation studies were also employed to evaluate the respective desolvation activation energies.

Keywords: pyrimethamine, solvatomorph, characterisation, thermal analysis, X-ray diffraction, solubility

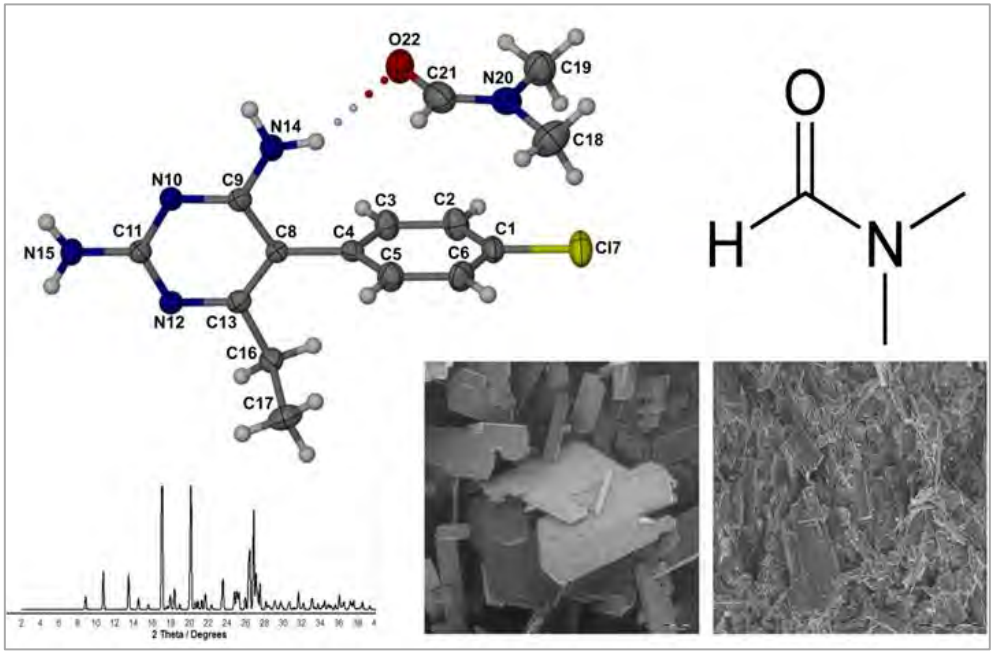

1.Introduction

Pyrimethamine, 5-(4-chlorophenyl)-6-ethyl-2,4-pyrimidinediamine (Fig. 1), is a dihydrofolate reductase inhibitor effective against the erythrocytic stage of *Plasmodium falciparum* (Nguyen-Dinh & Payne, 1980). It is listed by the World Health Organization (WHO) as an essential medicine when in synergistic combination with sulfadoxine and is therefore considered to play a crucial role in the treatment and prevention (prophylaxis) of malaria (WHO, 2010).

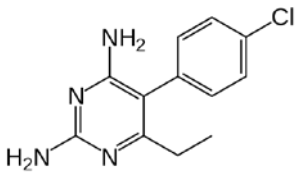

Fig. 1. Pyrimethamine.

Pyrimethamine has the ability to present in different polymorphs or solvatomorphs as well as different crystal morphologies (Delori *et al.*, 2012; Perold *et al.,* 2014; Sethuraman & Muthiah, 2002; Tutughamiarso & Bolte, 2011). The thermodynamically most stable anhydrous form, hereafter referred to as Pyr, has been described by Sethuraman and Muthiah (2002). It is well known that different morphologies and/or polymorphs may affect the manufacturability and quality of Active Pharmaceutical Ingredients (APIs) (Byrn *et al.*, 1999) and final pharmaceutical products (FPPs) (Carstensen, 2001; Hilfiker *et al.,* 2006). For this reason, thorough polymorphic screening needs to be conducted in order to identify all possible forms of an API and evaluate how the forms differ. Nowadays a lot of research is invested in polymorph screening of new chemical entities (Anderson, 2012; Conway, 2013; SSCI-INC, 2014). However, recent discoveries of previously undiscovered forms of older APIs (such as pyrimethamine), indicate that further research may reveal even more forms.

Taking into consideration the immense number of research manuscripts, patents, books and chapters on the subject, solvatomorphism seems to be a high priority in pharmaceutical polymorph research (Brittain, 1997, 2007, 2008; Chadha *et al.,* 2009*;* Mezei *et al.,* 2004; Murthy *et al.,* 2010). Although solvatomorphs cannot be incorporated into FPPs (due to their inherent toxicity) (de Villiers *et al.,* 2011; ICH, 2011; Perold *et al.,* 2014), one cannot ignore the fact that they are frequently formed as intermediate products during API synthesis, especially at the final recrystallisation (purification) step (Gradowska & Parczewski, 2010; ICH, 2011). In this case, the final purified material (solvatomorph) must be dried until the solvent content is at least below the allowed ICH Q3C limits (ICH, 2011). Only thereafter can it be used for incorporation into a FPP. Understandably, different solvents will have different potential for binding with the host molecule (Chadha *et al.,* 2009; Giron *et al.,* 2002; Saha *et. al.,* 2005). The differences in intermolecular forces (such as hydrogen bonding) may result in different solvatomorphs of the same host molecule displaying vastly different desolvation behaviour: some

stable solvatomorphs will require extreme conditions for desolvation, while others will lose the solvent quite readily (Chadha *et al.,* 2009). Therefore, the choice of recrystallisation solvent and the subsequent conditions (such as time and temperature) required for drying will influence the manufacturing of an API. For this reason, the characterisation of solvatomorphs and the study of their desolvation behaviour form an integral part of polymorph screening (Brittain, 2008).

In this study, two novel solvatomorphs of pyrimethamine were prepared by means of recrystallisation from DMA and DMF. These forms were comprehensively characterised by thermal, crystallographic, microscopic and spectroscopic analytical techniques, similar to those employed by Chawla *et al*. (2003) for the characterisation of their novel DMF and DMA solvates of celecoxib. In addition, XRD techniques were employed to attempt structural elucidation of the solvates while differences in their desolvation mechanisms were investigated using non-isothermal kinetics.

2. Materials and methods

2.1 Preparation of solvatomorphs

Supersaturated solutions of anhydrous pyrimethamine (Bio-gen, India) were prepared by dissolving the API in N,N-dimethylformamide (DMF) or N,N-dimethylacetamide (DMA) (Merck, South Africa), whilst the temperature was maintained at the boiling point of the solvent used. The supersaturated solutions were filtered and allowed to crystallise at ambient conditions until the crystal yield was sufficient for analysis (approximately 2 weeks). The crystals were thereafter removed from the solvent and allowed to dry at ambient conditions prior to analysis. The anhydrous pyrimethamine raw material that was used in this work fits the description of the crystal form reported by Sethuraman and Muthiah (2002) (CSD refcode MUFMAB).

2.2 Characterisation

2.2.1 X-Ray Powder Diffraction (XRPD) and Variable Temperature X-Ray Powder Diffraction (VTXRPD)

A Bruker D8 Advance diffractometer (Bruker, Frankfurt, Germany) was used to obtain XRPD patterns. The following conditions were applicable: target, Cu; voltage, 40 kV; current, 30 mA; divergence slit, 2 mm; anti-scatter slit, 0.6 mm, detector slit, 0.2 mm; monochromator; scanning speed, 2°/min with a step size of 0.025°, step time of 1.0 sec, radiation wavelength of 1.5418 Å and a scan range of 3-35 °2θ. For VTXRPD the same measuring conditions as above were used together with an Anton Paar TTK-450 low-temperature camera (Anton Paar, Austria) with a heating rate of 0.1 K/sec.

In an attempt to overcome/minimise the effect of preferred orientation, all samples were lightly ground using a mortar and pestle before analysis. Additionally, all samples subjected to conventional XRPD analysis were rotated using the rotating sample holder. VTXRPD samples could not be rotated as the heat stage was stationary. However these steps could not completely overcome the effects of preferred orientation as it clearly influenced the XRPD patterns. Further discussion on preferred orientation is presented under section 3.1.

2.2.2 Single Crystal X-Ray Diffraction

Intensity data for the DMF solvate were collected on a Nonius Kappa CCD four-circle diffractometer with graphite-monochromated MoKα-radiation (λ = 0.71073 Å) using ϕ- and ω-scans of 1.00°, with the crystal cooled in a stream of nitrogen vapour maintained at 173(2) K (Oxford Cryostream, UK). Data were corrected for Lorentz-polarisation and absorption effects. The intensity data displayed Laue symmetry 2/*m*, indicating the monoclinic crystal system. From systematic absences, the possible space groups were *Cc* and *C*2/*c*, the latter being used for structure solution as the intensity statistics displayed a centric distribution ($|E^2 - 1|$ = 0.914). The structure was solved by direct methods and refined by full-matrix least-squares techniques against F^2 using programs in the SHELX-suite (Sheldrick, 2008). Following refinement of the non-hydrogen atoms, all H atoms were located in difference Fourier maps and were generally placed in idealised positions in a riding model. However, both amino groups displayed pyramidal stereochemistry and the positions of the four H atoms involved were therefore not idealised but were instead individually refined with a common N-H distance restraint of 0.88 (1) Å. All non-hydrogen atoms refined anisotropically while H atoms were assigned isotropic thermal displacement parameters (U_{iso}) in the range 1.2-1.5 times those of their parent atoms. Table 2 lists crystal data, data-collection parameters and refinement details.

2.2.3 Differential Scanning Calorimetry (DSC)

Approximately 2-5 mg of sample was weighed into a 40 µl aluminium sample pan, fitted with a pierced lid (Mettler Toledo, Greifensee, Switzerland) and crimped. The samples were analysed using a Mettler Toledo DSC823^e (Mettler Toledo, Greifensee, Switzerland) Differential Scanning Calorimeter (DSC) which was operated at a heating rate of 10 K/min (unless stated otherwise) with a nitrogen flow rate of 80 ml/min. The thermal events were evaluated using STAR^e software (version 9.0x) (Mettler Toledo, Greifensee, Switzerland). The instrument was calibrated prior to use using indium and zinc reference materials.

2.2.4 Thermogravimetric analysis (TGA)

Approximately 10-15 mg of sample was weighed into a 100 µl aluminium sample pan, fitted with a pierced lid (Mettler Toledo, Greifensee, Switzerland) and crimped. The samples were analysed using a Mettler Toledo TGA/SDTA851^e (Mettler Toledo, Greifensee, Switzerland) thermogravimetric analyser which was operated at a heating rate of 10 K/min (unless stated otherwise) with a nitrogen flow rate of 80 ml/min. The thermal events were evaluated using STAR^e software (version 9.0x) (Mettler Toledo, Greifensee, Switzerland). The instrument was calibrated prior to use using indium and aluminium reference materials.

TGA was also used for non-isothermal desolvation activation energy determinations using heating rates (β) of 5, 10 and 15 K/min. The degree of conversion (α) (for desolvation) was determined using equation 1:

$\alpha = (m_0 - m_t) / (m_0 - m_f)$ (equation 1)

Where: m_0 is the initial mass of the sample, m_t the mass of the sample at time t, and m_f is the final mass.

The degree of conversion (α) calculated for each run (5, 10 and 15 K/min) was then fitted to the Ozawa-Flynn-Wall model (Flynn, 1996; Flynn & Wall, 1966; Ozawa, 1965), where the quantity log β was plotted against 1/T in the range $0.1 < \alpha < 0.9$. The activation energy was derived from the resulting linear plots.

2.2.5 Karl-Fischer water determination

A KF-Titrino (Metro-Ohm, Switzerland) was used to determine the water content in samples. Instrument verification was done using distilled water and sodium tartrate dihydrate (Merck®, Johannesburg, South Africa).

2.2.6 Hot Stage Microscopy (HSM)

A Nikon DS-Fi1 (Nikon, Tokyo, Japan) digital camera attached to a Nikon ECLIPSE E400 light microscope (Nikon, Tokyo, Japan) was used for HSM. Samples were heated with the use of a Leitz hot stage (Leica Microsystems Inc., Bannockburn, IL, USA) and the captured images were analysed using NIS-Elements F2.30 software (Nikon, Tokyo, Japan). Samples were suspended in silicone oil (Fluka, Switzerland) to visualise possible desolvation processes.

2.2.7 Scanning Electron Microscopy (SEM)

A small amount of sample was used to cover the carbon tape that was affixed to the pin. The sample was then coated with a gold-palladium film using an IB-2 Eiko engineering ion coater inside a vacuum (Eiko Engineering, Ibaraki, Japan). The coated sample was then affixed to the microscope sample holder and analysed using a FEI Quanta 200 ESEM & Oxford INCA 400 EDS system (FEI, Hillsboro, OR).

2.2.8 Solubility Studies

The aqueous solubilities of Pyr-DMA and Pyr-DMF (the respective recrystallised products from DMA and DMF) were established in 0.1 M HCl (pH 1.2 ± 0.05), acetate buffer (pH 4.5 ± 0.05) and phosphate buffer (pH 6.8 ± 0.05) at 30, 35 and 40 ˚C ± 1 ˚C. A Heidolph RZR-2000 rotator (Heidolph, Germany) was used to rotate the sealed test tubes at 50 rpm in a thermally controlled water bath. Five mL of the medium was transferred to each test tube, (each containing 50 mg of sample) and sealed. Each experiment was performed in triplicate. After 24 hours the test tubes were removed from the instrument and allowed to cool to ambient temperature; their contents were then filtered and appropriately diluted. Sample aliquots were analysed using a Cary 50 spectrophotometer (Varian, USA) running Varian WinUV version 3.00 software. A method was developed and validated for the solubility studies. The validation parameters are described in the Supplementary Information section.

2.2.9 Gas Chromatography (GC)

An Agilent 6890 GC with an Agilent 7697A headspace sampler, together with a DB-624, 320.00 mm X 30.0 m column (1.8 µm) was used for residual solvent testing according to the USP general chapter <467>.

2.2.10 Calculation of theoretical XRPD patterns

Calculated XRPD patterns were obtained using Lazy Pulverix software in accordance with that described by Yvon et al. (1977:73-74).

2.2.11 Diffuse Reflectance Infrared Fourier Transform (DRIFT-IR) Spectroscopy

The IR spectra were recorded using a Nicolet Nexus 470 spectrophotometer with the Avatar Smart diffuse reflectance accessory (Nicolet Instrument Corp., Madison, WI) over a range of 4000 cm-1- 400 cm-1. IR samples were prepared and analyzed in a potassium bromide (Merck®, Johannesburg, South Africa) matrix.

3. Results and discussion

3.1 XRPD and VTXRPD

X-ray diffraction remains one of the most suitable tools in identifying crystallographic differences between different solid forms (Brittain, 2001; Chao & Vail, 1987; Randall *et al.,* 2010). Pyr-DMA and Pyr-DMF were first subjected to XRPD analysis. As can be seen in Fig. 2, both diffractograms displayed distinct, sharp diffraction peaks, resulting in unique patterns that differed from each other and from those of previously described forms of pyrimethamine (Balasubramani *et al.,* 2005; De Araujo *et al.,* 2007, 2009; Delori *et al.,* 2012; Devi *et al.,* 2006*,* 2011; Sethuraman & Muthiah, 2002; Sethuraman *et al.,* 2003; Stanley *et al.,* 2002, 2005; Subashini *et al.,* 2007; Tutughamiarso & Bolte, 2011).

The experimental XRPD pattern in Fig. 2a labelled as Pyr serves as a point of reference for the anhydrous crystal form Pyr, which was used to crystallise the two solvatomorphs. The experimental XRPD trace of Pyr (obtained under the conditions stated in 2.2.1), was affected by preferred orientation, with the intensity of the peak at approximately 18.5 ˚2θ being much more intense in relation to the others when compared to the calculated XRPD pattern (Fig 2b), obtained using the refined single crystal data of MUFMAB as input (Sethuraman & Muthiah, 2002). The calculated XRPD trace of Pyr (Fig. 2b) is considered to be the more accurate representation of the XRD pattern of Pyr.

The differences between the diffractograms of Pyr-DMA and Pyr-DMF can be attributed to differences in the arrangements of molecules within their respective lattices. The unique diffraction peaks of Pyr-DMA and Pyr-DMF allow unambiguous identification of these forms and distinguish these forms from others. The characteristic peaks of Pyr-DMA were observed at 7.2, 14.5, 16.8 and 21.8 ± 0.2˚2θ, whereas the characteristic peaks of Pyr-DMF were observed at 8.2, 10.7, 13.4, 17.0, 17.9, 19.9, 20.1, 21.1, 21.5, 23.5, 24.4, 24.9, 26.6 and 26.8 ± 0.2˚2θ.

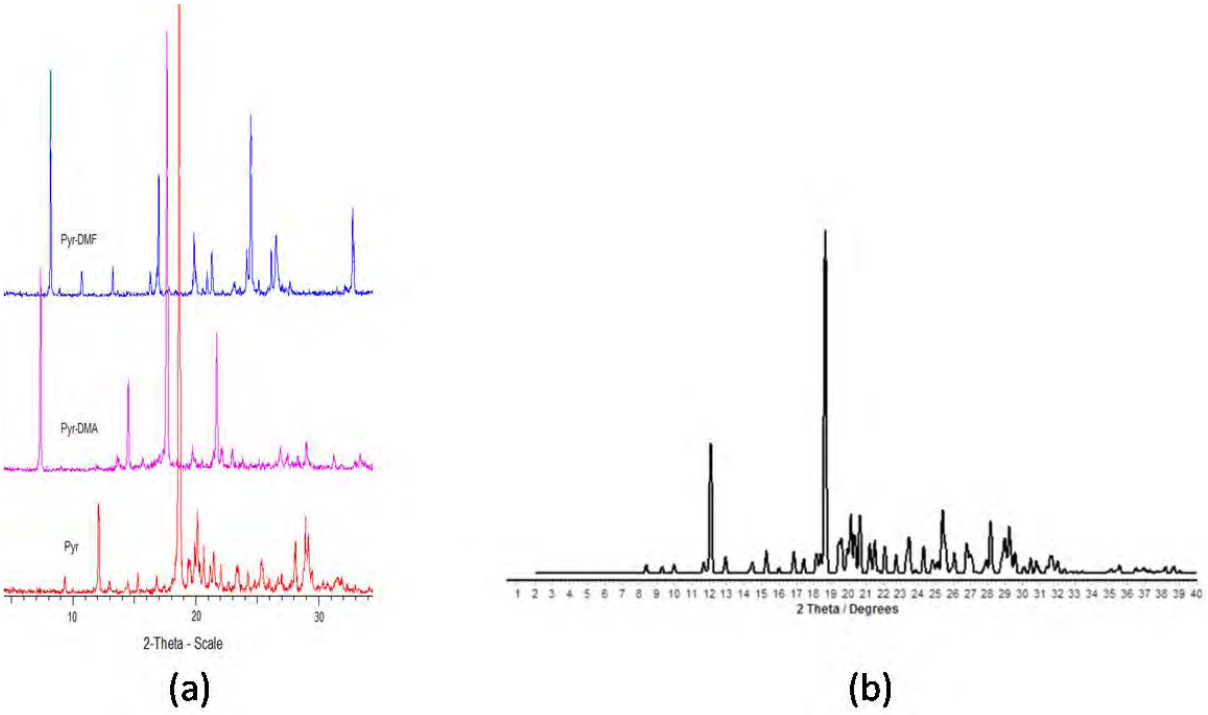

Fig. 2. An overlay of experimentally obtained XRPD diffractograms of (a) Pyr, Pyr-DMA and Pyr-DMF and (b) the calculated XRPD of Pyr.

VTXRPD of Pyr-DMA and Pyr-DMF (Fig.3) showed that both solvated forms underwent transformation upon heating. The XRPD trace of the stabilised form (after desolvation had occurred) corresponded with that of Pyr in both cases. The transformation of these forms into Pyr is discussed in conjunction with the characterisation by DSC and TGA in section 3.2.

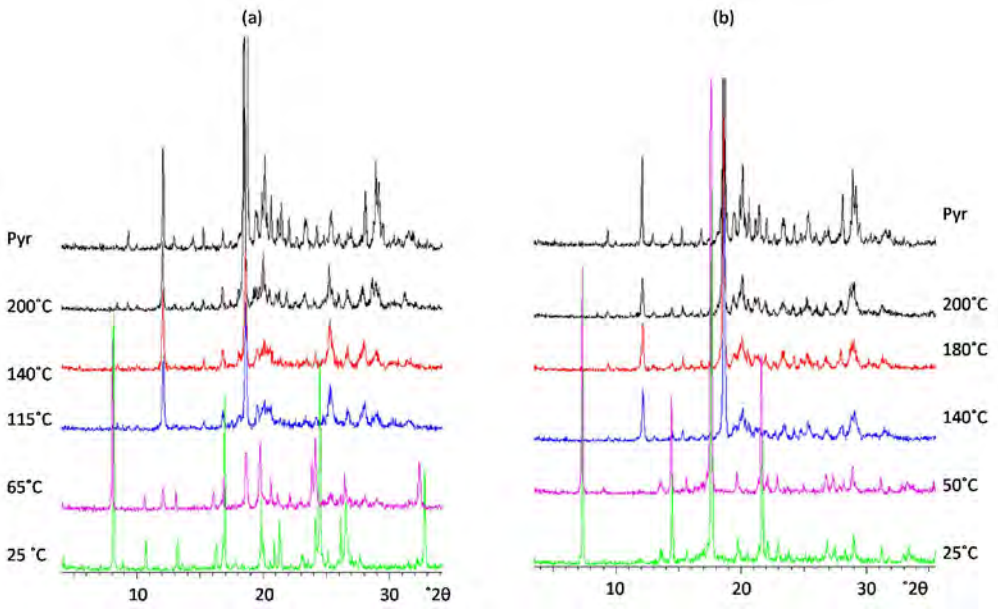

Fig 3. VTXRPD of (a) Pyr-DMF and (b) Pyr-DMA.

3.2 DSC, TGA, GC and KF

The thermal behaviours of Pyr-DMF and Pyr-DMA were evaluated by means of DSC (Fig. 4). The DSC traces of Pyr-DMF showed a broad endotherm in the temperature range 100 – 127 ˚C followed by a single sharp endotherm at 241.3 ˚C. The TGA curve of Pyr-DMF (Fig. 4) showed a total weight loss of 21.6% in the same temperature region as the broad endotherm in the DSC trace, which confirmed the weight loss to be indicative of desolvation. Karl-Fischer analysis and GC showed that Pyr-DMF was not a hydrated solvatomorph (Table 1). The % weight loss (from TGA) was in close agreement with a theoretical value of 22.7% applicable to a 1:1 stoichiometric DMF solvate.

The DSC and TGA traces of Pyr-DMA (Fig. 4) showed Pyr-DMA to have similar thermal behaviour compared to Pyr-DMF. The DSC trace showed a broad endotherm in the region of 110 – 136 ˚C, followed by a final sharp endotherm at 241.3˚C. The TGA trace of Pyr-DMA showed a weight loss of 28.8% that coincided with the broad desolvation endotherm of its DSC trace. As for Pyr-DMF, the GC and KF analysis of Pyr-DMA showed that the weight loss that occurred from this form was solely from DMA and that it too was a 1:1 stoichiometric solvatomorph (Table 1).

Table 1. Confirmation of stoichiometry of Pyr-DMA and Pyr-DMF

	% w/w (±SD)			Theoretical % weight loss for 1:1 solvate
	TGA	**KF**	**GC**	
Pyr-DMF	21.6 (±0.2) %	0.3 ~ 0 (±0.2) %	20.4 (±0.3) % DMF	22.7%
Pyr-DMA	28.8 (±0.7) %	0.4 ~ 0 (±0.1) %	24.2 (±0.5) % DMA	25.9%

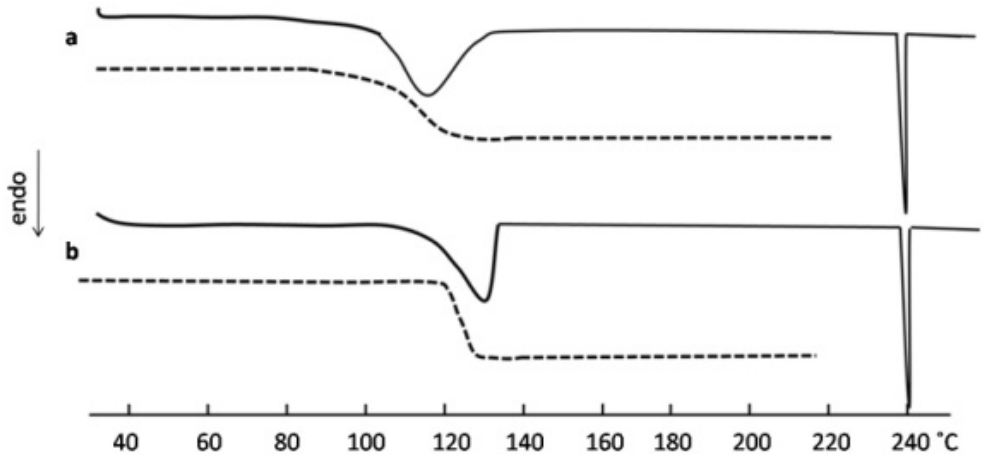

Fig. 4. DSC (solid line) and TGA (dashed line) traces for (a) Pyr-DMF and (b) Pyr-DMA.

Interestingly, the desolvation maxima (peak maxima of desolvation endotherms) of Pyr-DMA and Pyr-DMF occurred at temperatures 34˚C and 35˚C below the boiling points of DMA and DMF (165 and 153˚C) respectively, which is inconsistent with other pyrimethamine solvates, such as Pyr-MeOH (Perold *et al.,* 2014), a hemi-methanol solvate of pyrimethamine having a desolvation maximum that exceeded the boiling point of the solvent by 17 ˚C. Therefore, it was decided to determine the desolvation activation energy (E_a) of Pyr-DMA and Pyr-DMF by means of a non-isothermal TGA technique based on the Ozawa-Flynn-Wall method (Fig. 5). The E_a value for Pyr-DMF was calculated to be 52.2 ± 9.0 kJ/mol while that of Pyr-DMA was found to be 49.3 ± 7.2 kJ/mol; these estimates are not significantly different, but they are, however, lower than the activation energy for desolvation of Pyr-MeOH (148.7 ± 9.3 kJ/mol) (Perold *et al.,* 2014). From this result, it could be inferred that Pyr-DMA and Pyr-DMF might lose their respective solvents more readily than Pyr-MeOH, due to differences in host-guest interaction strengths as well as possible differences in the topologies of guest molecule inclusion within the solvate crystals.

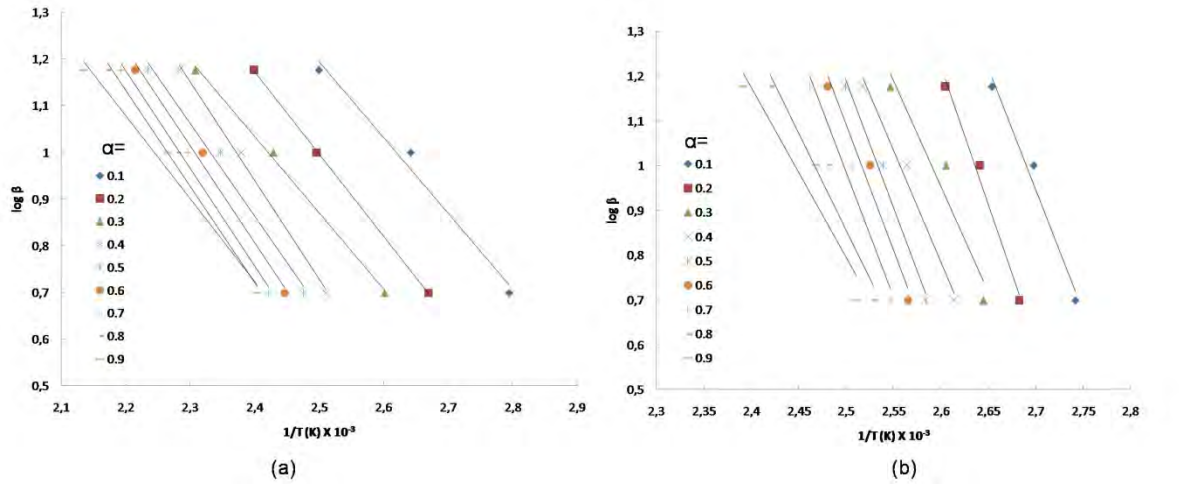

Fig. 5. Ozawa-Flynn-Wall non-isothermal plots obtained for (a) Pyr-DMF and (b) Pyr-DMA.

3.3 Single crystal XRD

Once it had been established that Pyr-DMA and Pyr-DMF were 1:1 stoichiometric solvates, it was desirable to attempt their X-ray crystal structure solution to establish the respective modes of guest inclusion and compare these with that observed in the crystal of Pyr-MeOH (Perold *et al.,* 2014). Unfortunately, the crystals of Pyr-DMA diffracted X-rays very weakly and structure determination was not possible for this phase. However, the quality of the Pyr-DMF crystals permitted full structure determination and a detailed description of the molecular and crystal structure follows. Table 2 lists crystal data, data-collection parameters and refinement details for Pyr-DMF.

The asymmetric unit comprises one molecule of pyrimethamine and one molecule of DMF (Fig.6). The least-squares planes of the aromatic rings of the pyrimethamine molecule intersect at an acute angle of 83.3(1)°. An alternative measure of this major conformational feature is the dihedral angle

C5-C4-C8-C9 with a value of 82.2(3)°. In Pyr-MeOH (Perold *et al.,* 2014), there are two crystallographically independent molecules of the API, the corresponding dihedral angles having statistically equal values of 75.3(2)° and 75.1(2)°. The terminal atom of the ethyl group is rotated out of the plane of the pyrimidine ring (dihedral angle C8-C13-C16-C17 = 86.3(3)°).

Table 2. Crystal data and refinement parameters for Pyr-DMF

Parameter	**Pyr-DMF**
Chemical formula	$C_{12}H_{13}N_4Cl \cdot C_3H_7NO$
Formula weight ($g.mol^{-1}$)	321.81
D_{calc} ($g.cm^{-3}$)	1.308
Crystal system	Monoclinic
Space group	*C*2/*c*
a (Å)	20.399(2)
b (Å)	7.5492(6)
c (Å)	21.753(1)
α (°)	90
β (°)	102.682(4)
γ (°)	90
V ($Å^3$)	3268.2(4)
Formula units, Z	8
μ (Mo Kα) (mm^{-1})	0.243
T (K)	173(2)
Crystal size (mm)	0.11 x 0.12 x 0.14
Reflections	4052
Parameters	218
Completeness (%)	99.4
R_1 (on $F>4\sigma(F)$)	0.0577
wR_2 (on F^2, $F>4\sigma(F)$)	0.1188
Goodness of fit (*S*)	1.006
Final Δ/σ	< 0.001
Δ*ρ* min.; max. (e $Å^{-3}$)	-0.26; 0.53
CCDC number	1025028

A detailed examination of the supramolecular structure of Pyr-DMF revealed that the crystal is composed of infinite ribbons of extensively hydrogen-bonded assemblies of pyrimethamine and DMF molecules, a representative portion of the ribbon being illustrated in Fig.7. The unique hydrogen bonds responsible for the resulting arrangement (Table 3) are of type N-H···N (linking pyrimethamine molecules) and N-H···O (linking pyrimethamine and DMF molecules).

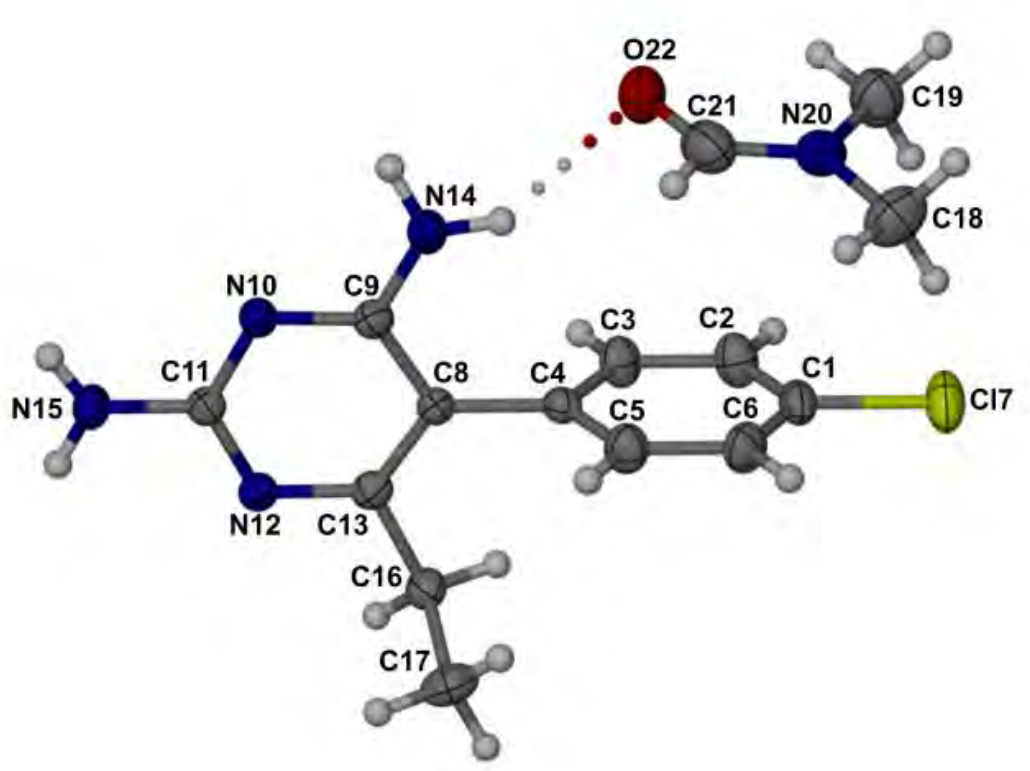

Fig.6. The asymmetric unit in the crystal of Pyr-DMF, showing one of the hydrogen bonds that links the host and guest molecules. Non-H atoms are drawn as thermal ellipsoids at the 50% probability level.

The unsymmetrical hydrogen-bonded ring labelled **1** (Fig. 7), in which the oxygen atom of the DMF molecule is the acceptor of two N-H···O hydrogen bonds, has the descriptor $R_3^2(8)$ in graph-set notation, while the ring motifs **2** and **3** (Fig. 7) are centrosymmetric and are of type $R_2^2(8)$ (Etter *et al.,* 1990). Similar motifs occur in other crystal structures containing pyrimethamine molecules (Cambridge Structural Database and Cambridge Structural Database Systems, 2014).

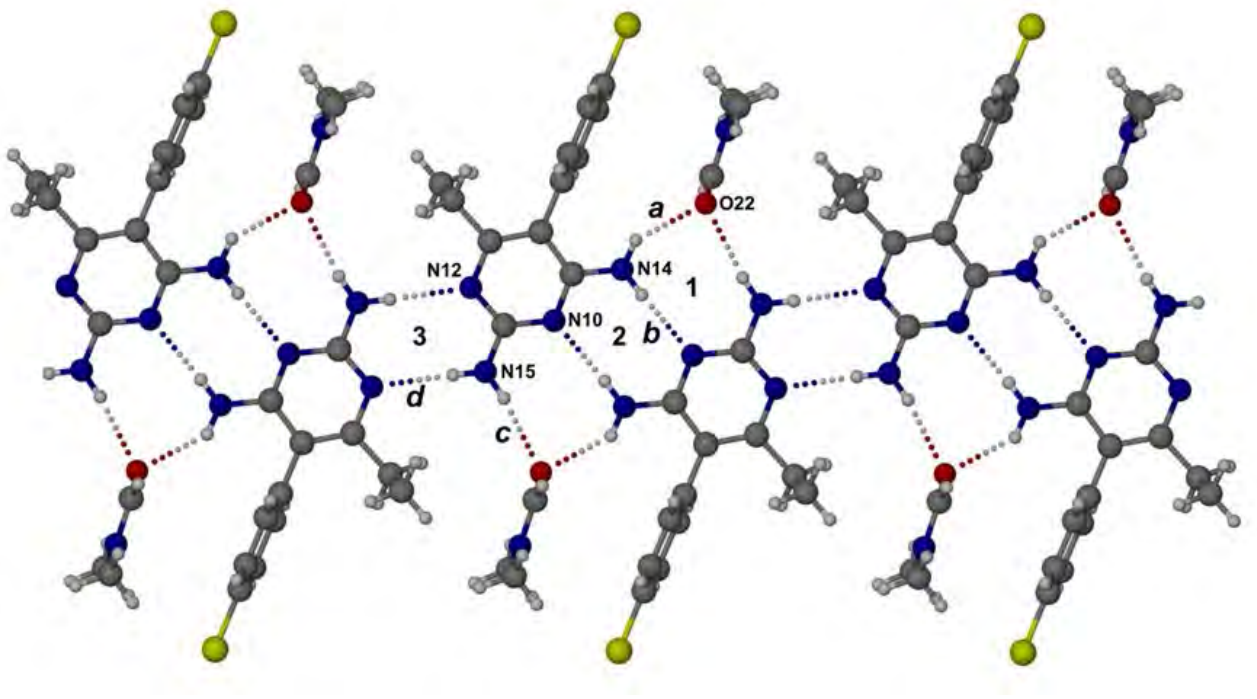

Fig.7. A representative portion of an infinite ribbon comprising hydrogen-bonded API and solvent molecules. Letters ***a*** – ***d*** identify the unique H-bonds contributing to the arrangement while the numbers **1** – **3** label the unique hydrogen-bonded ring motifs.

Table 3. Hydrogen bond data for Pyr-DMF (distances in Å, angles in degrees)

D-H···A	D-H	H···A	D···A	D-H···A(°)
a: N14-H14A···O22	0.88(2)	2.20(2)	2.953(3)	144(2)
b: N14-H14B···N10^{i}	0.88(2)	2.15(2)	3.033(3)	178(3)
c: N15-H15A···O22^{i}	0.88(2)	2.23(2)	3.096(3)	170(3)
d: N15-H15B···N12^{ii}	0.88(2)	2.20(2)	3.079(3)	178(2)

Symmetry codes: (i) *1/2-x, 3/2-y, 1-z*; (ii) *-x, 2-y, 1-z*

Analysis of the topology of inclusion of the solvent in the crystal indicates that successive DMF molecules are in close contact, forming an infinite zigzag ribbon arrangement around the two-fold screw axis parallel to the crystal *b*-axis. A packing diagram of the host molecules represented in space-filling mode with solvent molecules excluded shows that there are continuous channels in this direction (Fig.8). Thus, if sufficient energy is provided to sever the strong hydrogen bonds between the DMF molecules and the pyrimethamine crystal matrix, solvent migration along the crystal *y*-direction should be facilitated.

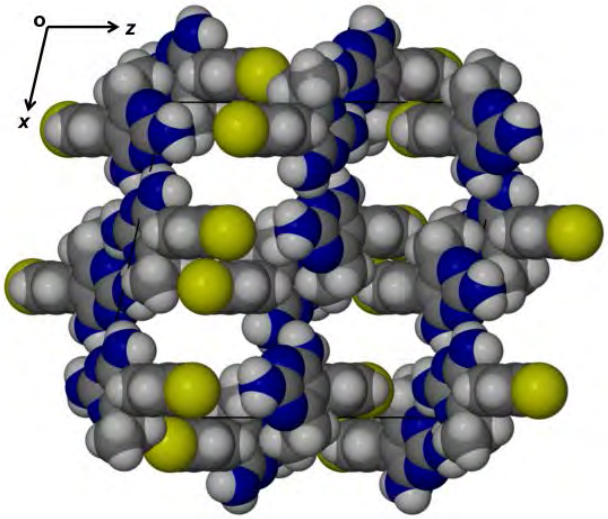

Fig. 8. Projection along [010] of the crystal assembly of the pyrimethamine molecules only in the crystal of Pyr-DMF. Solvent molecules have been omitted to reveal the channels they occupy.

A detailed analysis of the crystal structure of Pyr-MeOH (Perold *et al.,* 2014) also revealed strong host-solvent hydrogen bonding interactions [specifically, two (Pyr) N-H···O(methanol) and one methanol (OH)···N(Pyr)] which would require disruption as a first step in the desolvation mechanism. However, in strong contrast to the channel-occupation by the DMF molecules in the Pyr-DMF crystal described above, the methanol molecules in Pyr-MeOH occur as inversion-related pairs which are located in *isolated sites*, i.e. each such pair of methanol molecules is completely encapsulated by neighbouring host molecules. In this case, desolvation requires further significant rearrangement of the host structural framework to enable the eventual escape of methanol molecules. Thus, it is concluded that it is primarily the difference in the topologies of inclusion of DMF and methanol that is responsible for the very significantly higher activation energy for desolvation of Pyr-MeOH compared with that for Pyr-DMF. Given that the E_a values for desolvation of the Pyr-DMF and Pyr-DMA solvates were found to be essentially the same in the present study, it is reasonable to infer that the DMA molecules in the Pyr-DMA crystal are probably also located in channels. It is, however, prudent to note that there are limits to the interpretation of activation energy magnitudes when the crystals involved do not have a common (isostructural) host framework (Caira, 2004), as is the case for the three solvates discussed here.

The simulated XRPD pattern (CuKα radiation, λ = 1.5418 Å) for the Pyr-DMF solvate (Fig. 9) was calculated using the refined single crystal X-ray data as input. The level of agreement between the experimental XRPD (Fig. 2) and the simulated XRPD of Pyr-DMF (Fig. 9) was acceptable. It is clear, however, from differences in the intensities of corresponding peaks that the experimental sample displays preferred orientation.

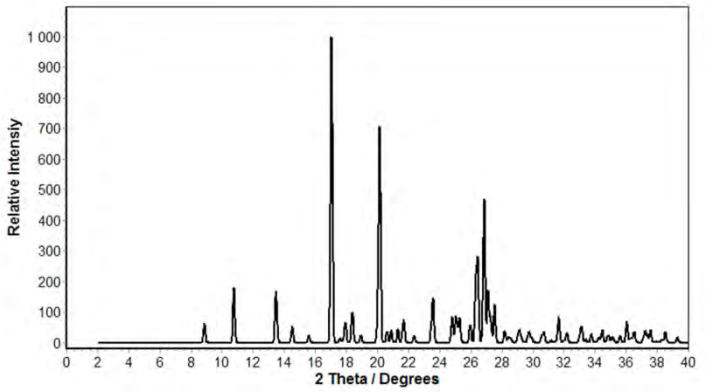

Fig.9. Calculated XRPD pattern for the Pyr-DMF solvate.

3.4 Microscopy

3.4.1 HSM

The thermal events of Pyr-DMA and Pyr-DMF evaluated visually by means of HSM (Fig. 10) were in close agreement with those deduced from DSC and TGA data (Fig 4). When examined in the presence of silicone oil, loss of solvent was observed as i) bubbles emerging from the solvatomorphs (Fig. 10 (a) at 112˚C and Fig. 10 (b) at 115˚C); and ii) by crystal darkening (Fig.10 (b) at 100 ˚C). Desolvation upon heating evidently involved loosening of the solvent and the rupture of the crystals to provide a pathway of escape for the solvent molecules. The rupturing of the crystals caused instantaneous crystal collapse and subsequent recrystallisation (Fig. 10 (a) between 112-123 ˚C and Fig10 (b) between 100-123 ˚C). Final melting of the stabilised form (post desolvation and crystallisation) occurred at approximately 240 ˚C, which is in agreement with that known for Pyr and with the results from DSC (Fig. 4) and VTXRPD (Fig. 3) presented earlier.

From the single desolvation endotherms observed in the DSC traces (Fig. 4) it can be deduced that it represented the summative energy required for desolvation and recrystallisation. Since crystal collapse, desolvation and recrystallisation occured rapidly and simultaneously, it was not possible to record photomicrographs that showed all thermal events in a single micrograph, which correlated with the broad desolvation endotherms observed in the respective DSC thermograms (Fig. 4).

HSM photomicrographs also indicated that both forms were polycrystalline material having multi-coloured grains when evaluated under polarised light (Fig. 10 at 25 ˚C). Pyr-DMA showed irregularly arranged grains of different colour, whereas Pyr-DMF displayed grains in parallel fashion along the long edge of the rod. The recrystallised product post desolvation (Fig. 10 (a) at 115 ˚C and Fig. 10 (b) at 123 ˚C) also showed parallel grains.

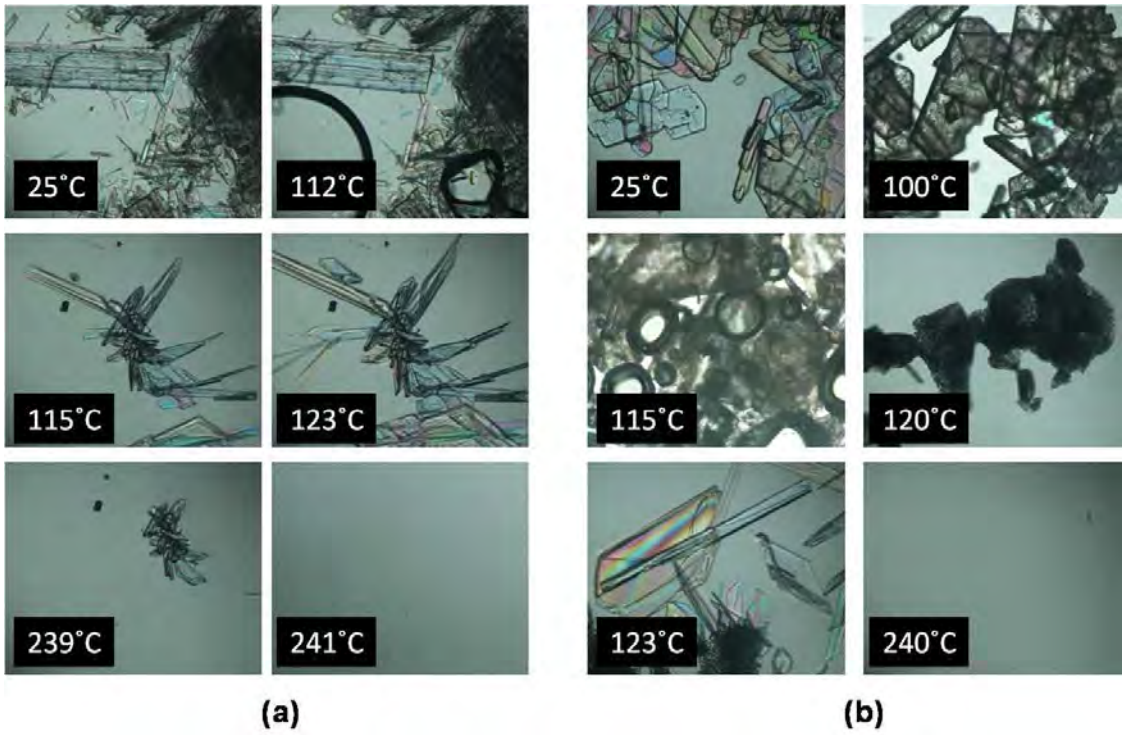

Fig. 10. HSM photomicrographs of (a) Pyr-DMF and (b) Pyr-DMA.

3.4.2 SEM

Crystal morphology plays a critical role during pharmaceutical manufacturing and product development as differences in this property may influence particle size and flowability (Byrn *et al.,* 1999). Crystal morphology is modified as a result of differences in the potential of solid-liquid interface interactions which affect crystal growth kinetics that either enhance or inhibit crystal growth on certain crystal faces (Buckton, 2002; Byrn *et al.,* 1999). The morphological differences between Pyr-DMA and Pyr-DMF were investigated by means of SEM (Fig 11).

Pyr-DMA presented in a thin, yet sturdy, sharp-edged, six-sided, plate-like habit with a smooth surface. Pyr-DMF presented as an aggregate mass of striated, bladed crystals, which were brittle and disintegrated into smaller, slender, columnar rods. As for HSM, the SEM samples that were analysed were also polycrystalline, showing a clear difference in particle size between crystals within the same population; however, the particle size range for the Pyr-DMA crystals was much larger than that of the Pyr-DMF sample. The morphologies of Pyr-DMA and Pyr-DMF crystals were not only significantly different from each other, but also differed from other known morphologies of anhydrous pyrimethamine (needles, cubes and octagonal plates) and of the Pyr-MEOH solvate (tabular shaped) (Perold *et al.,* 2014). Ideally, the particles comprising pharmaceutical powders should be smooth and spherical (Maghsoodi, 2012; Shotton & Harb, 1966). Bearing the above in mind, SEM findings showed that free flow would be impeded for both forms.

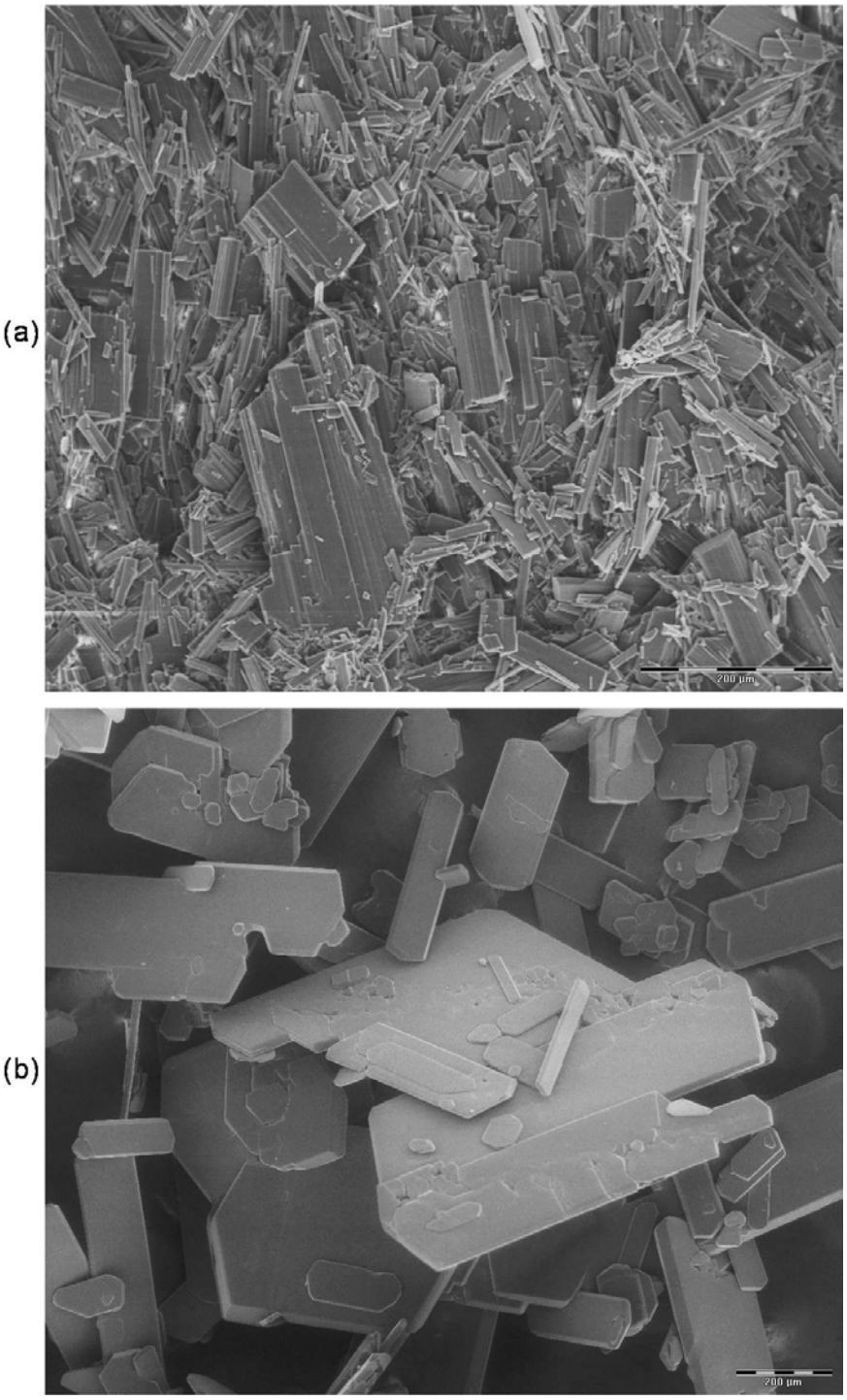

Fig. 11. SEM photomicrographs of (a) Pyr-DMF and (b) Pyr-DMA.

3.5 FTIR

Differences in molecular conformations, crystal packing and hydrogen bonding arrangements may result in FTIR spectral variations presenting as frequency shifts, splitting of absorption peaks or the emergence/fading of peaks (Brittain, 1997; Coates, 2000). The IR spectra of Pyr-DMF and Pyr-DMA share resemblances with Pyr at 3310, 3149, 1913 cm^{-1}, which are characteristic peaks of anhydrous pyrimethamine (Fig. 12) (De Araujo *et al.,* 2007). However, both presented with significant differences

in the regions of 3300-3600 cm^{-1} (OH), 3150 cm^{-1} (NH_2) and 1600-1700 cm^{-1} (C=O), all of which are related to the solvents. The characteristic bands of pure DMF are situated at 3291, 3139 and 1651 ± 20 cm^{-1}, while that of pure DMA are situated at 3436 and 1635 ± 20 cm^{-1} (Chawla *et al.,* 2003). All these characteristic bands were observed in the FTIR spectra of Pyr-DMF and Pyr-DMA respectively, which unequivocally prove the presence of these solvents in the respective solvatomorphs (as the anhydrous form does not display these bands). The shifting of the NH_2 band position at ~3150 cm^{-1} can be attributed to the varied H-bonding (Coates, 2000) between the host molecule and the solvents, as discussed under section 3.3, which is similar to that described for other pyrimethamine solvatomorphs (Perold *et al.,* 2014).

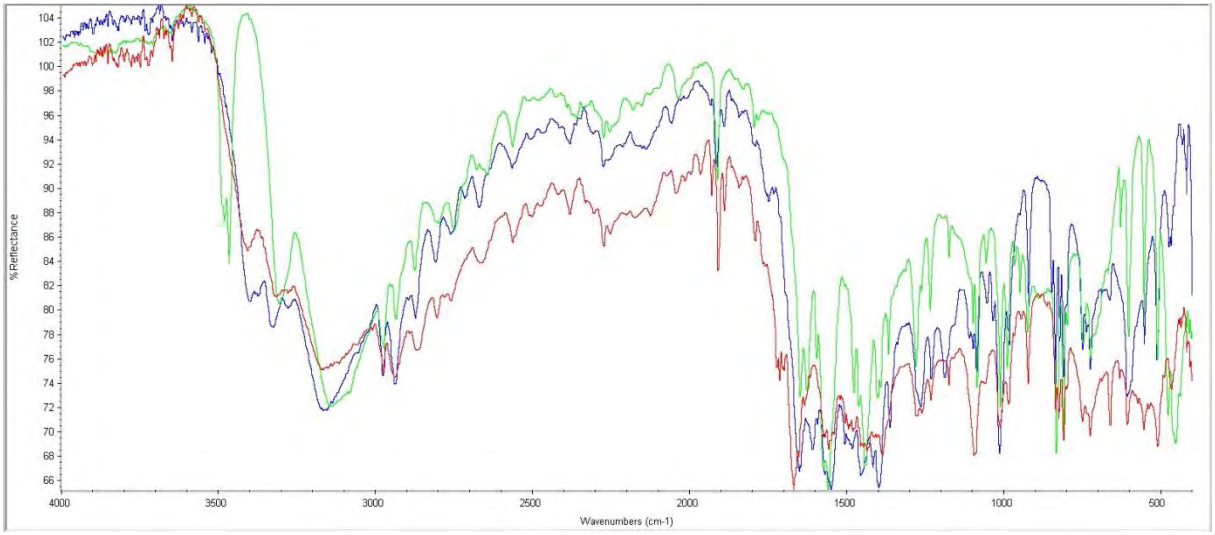

Fig. 12. Superimposed IR spectra of Pyr-DMA (red), Pyr-DMF (blue) and Pyr (green).

3.6 Solubility

Solubility experiments were performed in three different media and at three different temperatures (Table 4), in order to compare the solubilities of Pyr-DMA and Pyr-DMF. Each result reported in Table 4 represents the average and standard deviation of three determinations.

The results displayed in Table 4 yield linear relationships for the solubility versus temperature in the acidic media, which showed that the dissolution process was endothermic in nature. On the other hand solubility was poor in phosphate buffer (pH 6.8) as it remained fairly constant and was unaffected by an increase in temperature.

Table 4. The solubility of Pyr-DMA and Pyr-DMF in 0.1 M HCl (pH 1.2), acetate buffer (pH 4.5) and phosphate buffer (pH 6.8) at 30, 35 and 40 ± 0.5 ˚C

	Solubility (mg/ml) ± SD					
	Pyr-DMA			**Pyr-DMF**		
Medium	**30˚C**	**35˚C**	**40˚C**	**30˚C**	**35˚C**	**40˚C**
0.1 M HCl	3.40 ± 0.09	4.06 ± 0.06	4.47 ± 0.09	3.32 ± 0.07	3.83 ± 0.09	4.38 ± 0.13
Acetate buffer (pH 4.5)	1.91 ± 0.06	2.10 ± 0.09	2.36 ± 0.10	1.62 ± 0.10	1.89 ± 0.10	2.26 ± 0.04
Phosphate buffer (pH 6.8)	0.08 ± 0.01	0.08 ± 0.01	0.08 ± 0.01	0.07 ± 0.03	0.07 ± 0.04	0.07 ± 0.02

Despite the fact that the individual solubility values differed, double-sided ANOVA analysis found the solubility of Pyr-DMA and Pyr-DMF not to be statistically significantly different in all the media ($p > 0.05$, calculated at a 95% confidence interval). For this reason, solubility studies were not effective in differentiating between the two solvatmorphs.

4. CONCLUSION

Pyrimethamine was found to form two novel 1:1 stoichiometric solvatomorphs (Pyr-DMA and Pyr-DMF) upon recrystallisation from DMA and DMF. The XRPD patterns of the two forms differ significantly and from that of any prior art form. The solvatomorphs showed comparable thermal behaviour, namely desolvation coinciding with crystal collapse and recrystallisation into Pyr, which was observed using DSC, TGA and VTXRPD techniques. HSM visually confirmed these thermal events. Non-isothermal activation energy determinations yielded E_a values that are significantly less than that for Pyr-MeOH (the hemi-methanol solvate), suggesting that these new forms might more readily desolvate than Pyr-MeOH. The lower value for the activation energy for desolvation of Pyr-DMF relative to that for Pyr-MeOH was rationalised on the basis of the significantly different topologies of solvent molecule inclusion revealed by single crystal XRD, namely their respective locations in channels (DMF) and isolated sites (MeOH). Finally, solubility studies indicated that the Pyr-DMA and Pyr-DMF forms do not differ significantly in their solubility profiles.

SUPPLEMENTARY INFORMATION

UV spectrophotometry method development and crystallographic files include the CCDC Data Deposition confirmation, the CIF file and the CHECKcif report.

ACKNOWLEDGEMENTS

Z.P, E.S and M.B thank PharmaCen and the Research Institute for Industrial Pharmacy® incorporating CENQAM® for financial assistance and the use of its facilities. M.R.C. thanks the University of Cape Town and the NRF (Pretoria) for research support.

REFERENCES

Anderson, N.G. 2012. Final product form and impurities, in: Practical Process Research and Development – a guide for organic chemists. Academic Press, pp. 365-396.

Balasubramani, K., Muthiah, P.T., Rychlewska, U., Plutecka, A. 2005. Hydrogen-bonding patterns in pyrimethaminium dinitrate. Acta Cryst. C. 62(10), o586-o588.

Brittain H.G. 1997. Spectral methods for the characterization of polymorphs and solvates. J. Pharm. Sci. 86, 405-412.

Brittain, H.G. 2001. X-ray Diffraction III: Pharmaceutical Applications of X-ray diffraction. Spectros. 16(7), 1-18.

Brittain, H.G. 2007. Polymorphism and solvatomorphism. J. Pharm. Sci. 98, 1617-1642.

Brittain, H.G. 2008. Profiling the drug substance. Preparation and identification of polymorphs and solvatomorphs, in: Adeyeye, M.C., Brittain, H.G. (eds), Preformulation in solid dosage form Development. Taylor & Francis Group, Boca Rotan FL, pp. 185-228.

Buckton, G. 2002. Solid-state properties, in: Aulton, M.E. (ed), Pharmaceutics: The Science of Dosage Form Design. New York, Churchill Livingstone, pp.141-152.

Byrn, S., Pfeiffer, R.R., Stowell, J.G. 1999. Solid-state chemistry of drugs. New-York: Academic press, INC., 346p.

Caira, M.R. 2004. Isostructurality of Inclusion Compounds, in: Atwood, J.L., Steed, J.W. (eds), Encyclopedia of Supramolecular Chemistry. Marcel Dekker Inc., pp. 767-775.

Cambridge Structural Database and Cambridge Structural Database systems. [Web:] http://www.ccdc.cam.ac.uk/Solutions/CSDSystem/Pages/CSD.aspx [Date of access: 3 October 2014].

Carstensen, J.T. 2001. Advanced pharmaceutical solids. Marcel Dekker, Inc., New York.1-518p.

Chadha R., Arora P., Kaur, R., Saini, A., Singla, M.L., Jain, D.S. 2009. Characterization of solvatomorphs of methotrexate using thermoanalytical and other techniques. Acta Pharm. 59(3), 245-257.

Chao, R.S., Vail, K.C. 1987. Polymorphism of 1,2-dihydro-6-neopentyl-2-oxonicotinic acid: characterisation, interconversion, and quantification. Pharm. Res. 4, 429-432.

Chawla, G., Gupta, P., Thilagavathi, R., Chakraborti, A.K., Bansal, A.K. 2003. Characterisation of solid-state forms of celecoxib. Eur. J. Pharm. Sci. 20, 305-317.

Coates, J. 2000. Interpretation of Infrared Spectra, A Practical Approach, in: Meyers, R.A. (ed), Encyclopedia of Analytical Chemistry. John Wiley & Sons Ltd., Chichester, pp. 10815-10837.

Conway, B. 2013. Solids, in: Denton, P., Rostron, C. (eds), Pharmaceutics: The science of medicine design. Oxford University Press, pp. 14-34.

De Araujo, M.V.G., Vieira, E.K.B., Lazaro, G.S., de Souza Conegero, L., Ferreira, O.P., Almeida, L.E., Bareto, L.S., Da Costa, N.B., Giminez, I.F. 2007. Inclusion complexes of pyrimethamine in 2-hydroxypropyl-β-cyclodextrin: Characterization, phase solubility and molecular modelling. Bioorg.Med. Chem. 15, 5752-5759.

De Araujo, M.V.G., Macedo, O.F.L., Nascimento, C.D.C., de Souza Conegero L., Bareto, L.S., Almeida, L.E., Da Costa, N.B. Giminez, I.F. 2009. Characterisation, phase solubility and molecular modelling of α-cyclodextrin/pyrimethamine inclusion complex. Spectrochim. Acta Part A. 72,165-170.

Delori, A., Galek, P.T.A., Pidcock, E., Delori, W. 2012. Quantifying homo-and heteromolecular hydrogen bonds as a guide for adduct formation. Eur. J. Chem. 18, 6835-6846.

De Villiers, M.M., Caira, M.R., Li, J., Strydom, S.J. Bourne, S.A., Liebenberg, W. 2011. Crystallization of toxic glycol solvates contaminated with ethylene glycol or diethylene glycol. Mol. Pharm. 8(3), 877-888.

Devi, P., Muthiah, P.T., Bocelli, G., Cantoni, A. 2006. Hydrogen bonding patterns in bis (pyrimethamine hydrogen sulphate) monohydrate. J. Chem. Cryst. 36(12), 857-861.

Devi, P., Nirmalram, J.S., Muthiah, P.T. 2011. Near supramolecular isomorphism involving homogolous solvents: Pyrimethaminiumterephthalate methanol solvate and Pyrimethaminiumterephthalate ethanol solvate. J. Chem. Cryst. 41, 1624-1629.

Etter, M.C. Macdonald, J.C., Bernstein, J. 1990. Graph-set analysis of hydrogen-bond patterns in organic crystals. Acta Cryst. B46, 256-262.

Flynn, J.H. 1996. Early papers by Takeo Ozawa and their continuing relevance. Thermochim. Acta. 283, 35-42.

Flynn, J.H., Wall, L.A. 1966. A quick direct method for the determination of activation energy from thermogravimetric data. Pol. Lett. 4, 323-328.

Giron, D., Goldbronn, C., Mutz, M., Pfeffer,S., Piechon, P., Schwab, P. 2002. Solid state characterizations of pharmaceutical hydrates. J. Therm. Anal. & Col. 68, 453-465.

Gradowska, K., Parczewski, A. 2010. Organic solvents in the pharmaceutical industry. Act. Polon. Pharm. Drug. Res. 67, 3-12.

Hilfiker, R., Blatter, F., Von Raumer, M. 2006. Relevance of solid state properties for pharmaceutical products, in: Hilfiker, R. (ed) Polymorphism in the pharmaceutical industry. Verlag GmbH, Wiley-VCH, pp. 1-17.

ICH - International Conference on Harmonisation of technical requirements for registration of pharmaceuticals for human use. 2011. [Web:] http://www.ich.org/fileadmin/Public_Web_Site/ICH_Products/Guidelines/Quality/Q3C/Step4/Q3C_R5_Step4.pdf [Date of access: 3 October 2014].

Maghsoodi, M. 2012. How spherical crystallisation improves direct tableting properties: a review. Adv. Pharm. Bull. 2(2), 253-257.

Mezei, T., Simig, G., Lukacs, G., Porcs-Makkay, M., Volk, B., Molnar, E., Hofmanne, F.V., Kirallyi, S. 2004. New pseudopolymorph of desloratadine formed with carbon dioxide. Patent WO 2006003479 A.

Murthy, K.S., Zhao, Y., Rey, A., Che, D., Stradiotto, D.A., Kotipalli, U. 2010. Atorvastatin calcium propylene glycol solvates. Patent US 20110065931 A1.

Nguyen-Dinh, P., Payne, D. 1980. Pyrimethamine sensitivity in Plasmodium falciparum: determination in vitro by a modified 48-hour test. Bull. WHO. 58(6), 909-912.

Ozawa, T.A. 1965. New method of analysing thermogravimetric data. Bull. Chem. Soc. Jpn. 11, 1881-1886.

Perold, Z., Caira, M.R., Brits, M. 2014. The Risk of Recrystallization: Changes to the Toxicity and Morphology of Pyrimethamine. J. Pharm. Pharm. Sci. 17(2), 190-206.

Randall, C.S., Rocco, W.L., Ricou, P. 2010. XRD in Pharmaceutical Analysis: A Versatile Tool for Problem-Solving. [Web:] http://www.americanpharmaceuticalreview.com/Featured-Articles/115052-XRD-in-Pharmaceutical-Analysis-A-Versatile-Tool-for-Problem-Solving/ [Date of access: 3 October 2014].

Saha, B.K., Nangia, A., Jaskolskim M. 2005. Crystal engineering with hydrogen bonds and halogen bonds. Cryst. Eng. Comm. 7, 355-358.

Sethuraman, V., Muthiah, P.T. 2002. Hydrogen bonded supramolecular ribbons in the antifolate drug Pyrimethamine. Acta Cryst. E. 58(8), 817-818.

Sethuraman, V., Stanley, N., Muthiah, P.T., Sheldrick, W.S., Winter, M., Luger, P., Weber, M. 2003. Isomorphism and crystal engineering: Organic ionic ladders formed by supramolecular motifs in pyrimethamine salts. Cryst. Growth Des. 3(5), 823-828.

Sheldrick, G.M. 2008. A short history of SHELX. Acta Cryst. A64, 112-122.

Shotton, E., Harb, N. 1966. The effect of humidity and temperature on the cohesion of powders. J. Pharm. Pharmacol. 18(3), 175-178.

SSCI-INC. 2014. Screening and selection (Polymorphs, salts, cocrystals, Solid Dispersions). [Web:] http://ssci-inc.com/DrugSubstance/ScreeningPolymorphsSaltsCocrystals/tabid/76/Default.aspx . [Date of access: 3 October 2014].

Stanley, N., Sethuraman, V., Muthiah, P.T., Luger, P., Weber, M. 2002. Crystal engineering of organic salts: Hydrogen-bonded supramolecular patterns in pyrimethamine hydrogen glutarate and pyrimethamineformate. Cryst. Growth Des. 2(6), 631-635.

Stanley, N., Muthiah, P.T., Geib, S.J., Luger, P., Weber, M., Messerschmidt, M. 2005. The novel hydrogen bonding motifs and supramolecular patterns in 2,4-diaminopyrimidine-nitrobenzoate complexes. Tetrahedron. 61, 7201-7210.

Subashini, A., Muthiah, P.T., Bocelli, G., Cantoni, A. 2007. Hydrogen-bonding patterns in pyrimethaminium 3,5-dinitrobenoziate. Acta Cryst. E. 63(9), o3775.

Tutughamiarso, M., Bolte, M. 2011. A new polymorph and two pseudo-polymorphs of Pyrimethamine. ActaCryst. C. 67, 428-434.

WHO. 2010. WHO model list of essential medicines. [Web:] 16thlist.http://www.who.int/medicines/publications/essentialmedicines/en/index.html. [Date of access: 3 October 2014].

Yvon, K., Jeitschko, W., Parthé, E. 1977. *Lazy Pulverix*, a computer program for calculating X-ray and neutron diffraction powder patterns. J. Appl. Cryst. 10, 73-74.

Chapter 6

Summary and Conclusion

This study comprises of four individual manuscripts (Chapters 2 - 5) which address the quality and safety of different crystal modifications of Efavirenz and Pyrimethamine. Each of these manuscripts has its own Introduction and Conclusion, however an overall Introduction and Conclusion, as presented in Chapters 1 and 6 respectively, serve to unify all the studies.

An extensive literature study offered the content for an overview of the solid state properties of APIs, as discussed in Chapter 1, and for the overview on how crystal modifications may result in the formation of different solid forms (i.e. polymorphism) of the same chemical compound. A synopsis was also provided on how different polymorphic forms of APIs may exhibit different physico-chemical behaviour/characteristics, which may ultimately affect their manufacturability, safety and efficacy.

The unfavourable statistics pertaining to current treatment successes and high mortality rates of HIV/AIDS and malaria infected patients appeal for the conduct of more focused investigations regarding the quality and safety of medicines being employed in the treatment of these diseases. The focus of this study therefore was to exploit the potential dangers associated with possible polymorphism of Efavirenz and Pyrimethamine, befitting of the collective title of this study, “Quality and safety implications of Efavirenz and Pyrimethamine crystal modifications”. In Chapter 1, the known solid state forms of Efavirenz and Pyrimethamine were summarised, with the aim of identifying new research opportunities for this study.

The aims and objectives of this study were to:

i) Discover new crystal modifications of Efavirenz and Pyrimethamine (if possible);

ii) Comprehensively characterise and evaluate the physico-chemical properties of any newly identified crystal modifications of Efavirenz and Pyrimethamine; and

iii) Elaborate on any unexplored characteristics of known crystal modifications of Efavirenz and Pyrimethamine that may be encountered.

Figure 6.1 summarises the four phases of this study and some of the main contributions of these research outcomes to the pharmaceutical sciences.

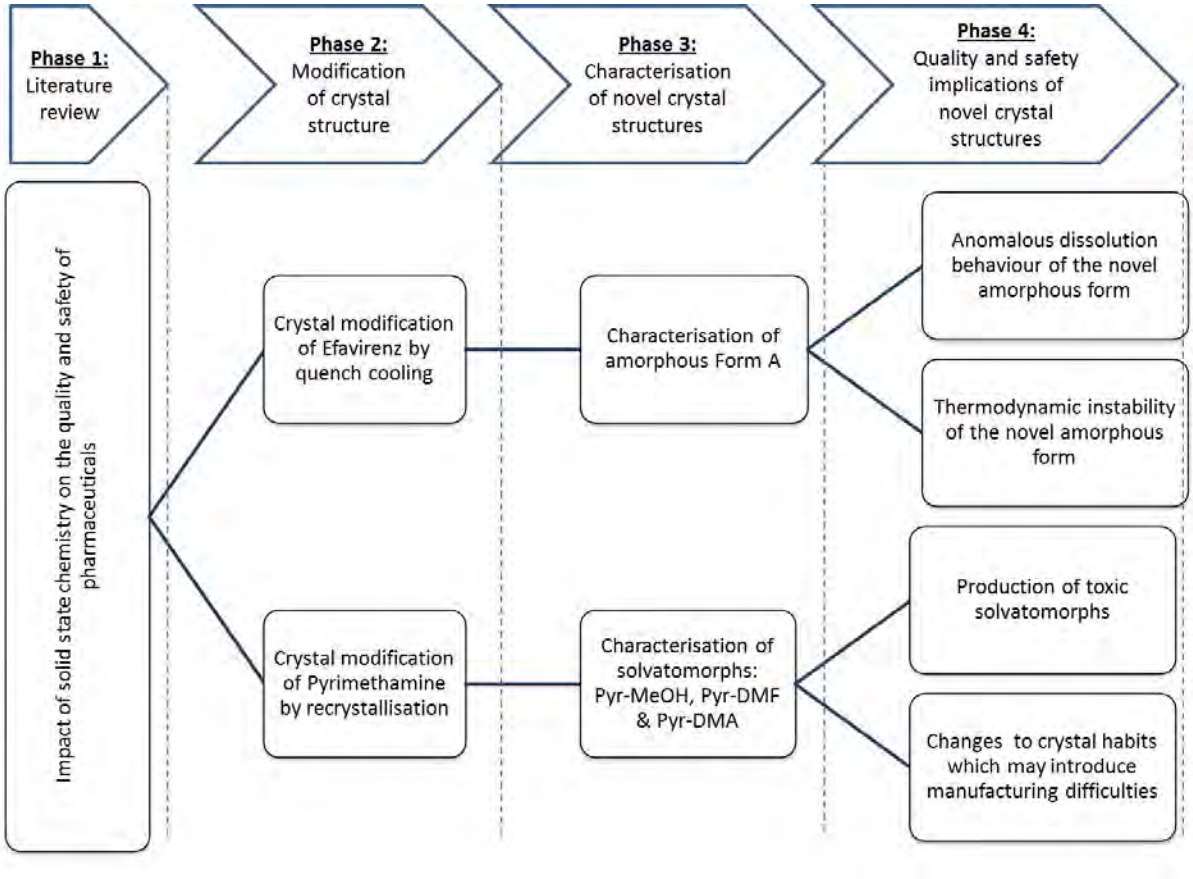

Figure 6.1 Four phases of this study and some of the main contributions of these research outcomes to the pharmaceutical sciences.

The first manuscript (Chapter 2), entitled "***Anomalous dissolution behaviour of a novel amorphous form of Efavirenz"***, was published in the *American Journal of Pharmtech Research, 2012, 2(2):272-292*. It set out to evaluate whether or not the quench cooling technique would modify the crystal structure of Efavirenz, and whether the resultant product would potentially impact on its safety and/or quality. The resultant product from quench cooling (Form A) was extensively characterised by using XRPD, DSC, CAM, DRIFT-IR, HSM and SEM techniques. The findings indicated that the resultant form was a novel amorphous form of Efavirenz.

Since the expectation is for an amorphous form to achieve a higher rate and/or extent of dissolution than its crystalline counterparts, the dissolution and solubility of Form A were compared to those of the preferred crystalline form (Form I). A two-dimensional matrix approach was used during this investigation, i.e. powder dissolution studies were performed by testing different sample sizes (50 mg, 200 mg and 600 mg) in different media (2% (w/v) and 1% (w/v) SLS) to evaluate the dissolution behaviour of Forms A and I under varying experimental conditions. f_2-similarity factor calculations showed that the rate and extent of dissolution of Form A was significantly lower than that of Form I (f_2 < 50). Form I managed to achieve complete dissolution within 30 minutes, irrespective of the sample size in the different media. Contrary, the highest percentage dissolution being achieved by Form A

was ± 60% after 45 minutes for the smallest sample size (50 mg sample), when tested in the 2% (w/v) SLS dissolution medium (most favourable conditions).

The poor dissolution behaviour of amorphous Form A had contradicted the expected outcomes. In contrast, solubility studies revealed that the solubility of Forms A and I in 1% (w/v) (9.1 mg/ml vs.11.0 mg/ml) and 2% (w/v) SLS (21.1 mg/ml vs. 22.3 mg/ml) was comparable, which suggested that a potential mechanical impediment may have caused the anomalous dissolution behaviour of Form A. Subsequent investigation for any such anomalous behaviour revealed that Form A had inherently impaired its own dissolution, due to agglomeration. The extent of agglomeration was found to be proportional to the sample size. This agglomeration behaviour was later explained by the research findings, as presented in Chapter 3, which had focused on the thermodynamic stability and crystallisation of Form A.

To minimise the effects of surface properties and of the agglomeration of particles on the dissolution behaviour of Forms A and I, intrinsic dissolution experiments (both forms having a constant surface area) were performed. Intrinsic dissolution studies revealed that the intrinsic dissolution behaviour of Forms A and I did not differ significantly. Further investigation revealed that Form A had undergone a solvent mediated transformation into the thermodynamically stable Form I, which explained the similarities in the intrinsic dissolution results obtained. The rates and extent of the phase transformations (Form A into Form I) during the powder dissolution experiments were found to be inconsistent, due to varying sizes of the agglomerates (thus varying exposure of the Form A surface for solvent mediated transformation), which had resulted in varying powder dissolution results.

The findings from Chapter 2 had encouraged the subsequent investigation of the thermodynamic stability of Efavirenz Form A. The second manuscript (Chapter 3), entitled "***Crystallisation behaviour of Efavirenz Form A: Introducing an alternative quantitation technique****",* is currently in the process of submission for publication in *AAPS PharmSciTech*. In this manuscript, crystallisation kinetic studies (non-isothermal and isothermal) had been performed on Form A, from which the crystallisation activation energy, half-life and crystallisation mechanisms of Form A were derived.

Non-isothermal DSC showed that Form A had adhered to the Lasocka's relationship and illustrated that the crystallisation of Form A had occurred through a site-saturated mechanism and that the growth rate of the crystalline phase had been limited by surface incorporation. The T_g of Form A was calculated as 28.5˚C, which offered insight into the poor physical stability of Form A and its significant susceptibility towards phase transformation (corroborating the anomalous dissolution results presented in Chapter 2).

HSM not only elucidated the thermally induced crystallisation of Form A into Form I, but also illustrated that the crystallisation process had coincided with changes in the visual appearance of the solid phase. Although the literature reports on the previous employment of HSM to quantify recrystallisation under *isothermal conditions* (for the purpose of activation energy determinations), no reports of it having been employed for *non-isothermal* determinations, were found. Similarly,

translucency measurements by means of CMP had also not yet been utilised in the investigation of amorphous to crystalline phase transitions. As a result, it was decided to quantify the non-isothermal recrystallisation of Form A, by using the well-known DSC technique and to investigate the potential of applying these two new approaches/techniques (HSM and CMP) in non-isothermal kinetic quantification. The outcomes of these studies were then compared. The results from the DSC studies were subjected to two thermal models (KAS and Matusita), and was it found that the calculated recrystallisation activation energies were similar (181.50 ± 7 kJ/mol vs. 183.63 ± 7 kJ/mol). Because the recrystallisation activation energies from the two models were comparable, it was decided to use the DSC-KAS recrystallisation activation energy as reference value, with which to compare the results obtained from the HSM and CMP non-isothermal kinetics. The results from HSM were subjected to the KAS model, and the activation energy was calculated as 210.12 ± 10.1 kJ/mol. The results from the translucency measurements (CMP) indicated that the recrystallisation activation energy of Form A was 185.5 ± 8.5 kJ/mol. Although the results from HSM did not compare favourably with those of DSC-KAS, the outcome from CMP compared well with that of DSC-KAS, which presented a new, cost-effective, alternative means for the quantification of recrystallisation activation energy during amorphous to crystalline transformations.

This study also commented on the physical stability of Form A under isothermal conditions (30˚C, 35˚C and 40˚C). The results obtained from using the JMAEK model revealed that its half-lives were approximately 70, 5.3 and 1.5 hours at 30˚C, 35˚C and 40˚C, respectively. The anomalous dissolution behaviour and the thermodynamic instability of Form A emphasised the unsuitability of this amorphous form for use in the pharmaceutical industry.

In the second part of this study, the quality and safety implications of Pyrimethamine crystal modifications (obtained through solvent recrystallisation) were investigated. The study methodology and outcomes of the Pyrimethamine work are summarised in Figure 6.2.

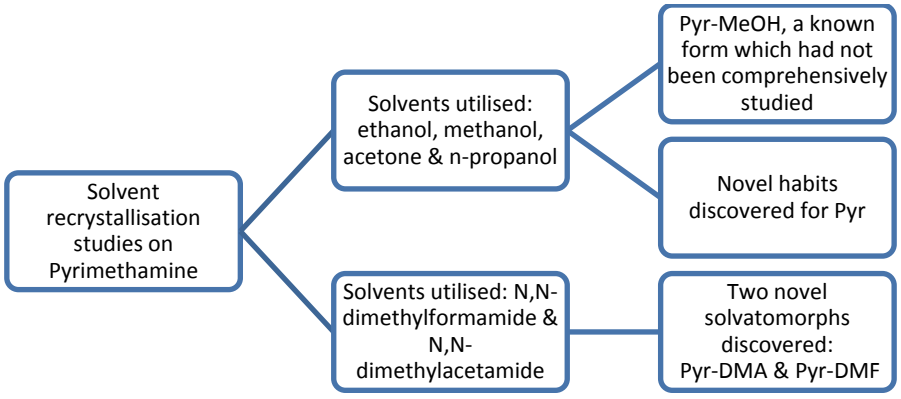

Figure 6.2 A schematic summary of the Pyrimethamine studies being performed and of the outcomes that were achieved.

The third and fourth manuscripts (Chapters 4 and 5) report on how recrystallisation may influence the safety and quality/manufacturability of the antimalarial API, Pyrimethamine. Four organic solvents (ethanol, methanol, acetone and n-propanol) were used during recrystallisations studies presented in Chapter 4, whereas N,N-dimethylformamide and N,N-dimethylacetamide were used as recrystallisation solvents for the studies presented in Chapter 5. The recrystallisation products from both studies were comprehensively characterised by means of various physico-chemical characterisation techniques (XRPD, DSC, TGA, KF, HSM, DRIFT-IR, GC, SC-XRD and SEM).

The third manuscript (Chapter 4), entitled "***The risk of recrystallization: Changes to the toxicity and morphology of Pyrimethamine***", published in the *Journal of Pharmacy and Pharmaceutical Sciences*, 2014, 17(2):190-206, evaluated how recrystallisation from ethanol, methanol, acetone and n-propanol would alter the solid state chemistry and safety of Pyrimethamine.

The final manuscript (Chapter 5), entitled "***Characterisation of two novel solid-state forms of Pyrimethamine****",* is currently in the process of submission for publication in the *European Journal of Pharmaceutical Sciences*. This study focused on how recrystallisation from N,N-dimethylformamide and N,N-dimethylacetamide had altered the solid state chemistry and safety of Pyrimethamine.

The products obtained from recrystallisation with methanol (Pyr-MeOH), N,N-dimethylformamide (Pyr-DMF) and N,N-dimethylacetamide (Pyr-DMA) were all found to be solvatomorphs, with solvent contents largely exceeding the allowable limits as set by the ICH Q3C guidelines. Ethanol, acetone and n-propanol had been unsuccessful in modifying the crystal structure of anhydrous Pyrimethamine (Pyr). These solvents had, however, altered the morphology/habit thereof, showcasing novel solid state properties of Pyr. The different morphologies (cubic and octagonal plates) were extensively characterised by means of *in-silico* computational predictions, which correlated well with the SEM observations. Powder flow studies indicated that these different morphologies had significantly different powder flow and compressibility behaviour, which may cause manufacturing difficulties.

Even though the existence of the methanol solvatomorph (Pyr-MeOH) had been reported on, the structural features, characteristics and thermodynamic stability thereof had not yet been elucidated and described in the available literature at the time of publication. For this reason, Pyr-MeOH had been subjected to an in-depth study, which revealed that the solvent molecules had occurred as inversion-related pairs in isolated sites. Such topology allows for a higher than average potential towards H-bonding between the host and the solvent molecules, as was confirmed by the desolvation activation energy determinations. Pyr-MeOH was extensively characterised, and the characteristics (DSC, XRPD, DRIFT-IR and solubility properties), unique to this form, were emphasised to serve as means for identifying and distinguishing it from the preferred anhydrous form (Pyr). This was done in an attempt to minimize the risk of this toxic form inadvertently being incorporated into a final pharmaceutical product. Furthermore, this study also presented an easy and reproducible recrystallisation method to prepare Pyr-MeOH, as an alternative to the method being described in the literature.

Characterisation of the recrystallisation products from DMF and DMA identified them as novel 1:1 stoichiometric solvatomorphs. The thermal behaviour of these two solvatomorphs was found to be comparable. DSC, TGA and VTXRPD revealed that desolvation had coincided with crystal collapse and recrystallisation into Pyr for both solvatomorphs. These findings were visually confirmed by means of HSM. Non-isothermal desolvation activation energy calculations showed that these forms had required significantly less energy than Pyr-MeOH to desolvate, which may have been attributed to the significantly different topologies of solvent molecule inclusion, as corroborated by single crystal XRD.

All the recrystallisation studies performed on Pyrimethamine (Chapters 4 and 5) indicated that recrystallisation, using the selected solvents, poses a threat to the safety, efficacy and/or manufacturability of Pyrimethamine.

From this study it had become evident that the continuous perusal by scientists to obtain new API crystal forms should be approached with awareness and caution, as the modification of crystal forms may not always result in a safe and efficacious crystal form.

The main contributions and/or deliverables of this study include:

- Two manuscripts were published in two internationally accredited pharmaceutical science journals;
- Two manuscripts are in the process of submission for publication in internationally accredited pharmaceutical science journals;
- Two detailed crystal structure elucidation studies have been published in the Cambridge Crystallographic Data Centre (CCDC) database (CCDC numbers: 868963 and 1025028); and
- Comprehensive guidance on how to detect and identify undesirable crystal modifications of Efavirenz and Pyrimethamine, as discussed in this study, is offered to the pharmaceutical industry.

In conclusion, it is believed that this study would not only contribute to the pharmaceutical sciences industry, but also to the medicines regulatory sciences, as it would help ensure that safe and effective APIs and FPPs of Efavirenz and Pyrimethamine are available to patients in need.

"*Wherever the art of medicine is loved, there is also a love of humanity*"

Hippocrates

Annexure A

American Journal of PharmTech Research (AJPTR)

Author guidelines

Author guidelines

American Journal of PharmTech Research (AJPTR) is a **Bimonthly** journal which publishes original research articles, review articles, case reports and short communications in the field of pharmaceutical and allied sciences. The manuscript would be considered under the specific branches of pharmaceutical and allied sciences. Those branches are as follows:

Research and Review manuscript is to be submitted for publication in following subjects

- Pharmaceutical sciences
- Allied sciences

Table A.1 Branches of pharmaceutical and allied sciences

Pharmaceutical Sciences	**Allied sciences**
Pharmaceutics	Biology
Formulation science (solids, topical, parenteral)	Biochemistry
Pharmacology and toxicology	Health outcomes research
Nanotechnology	Microbiology
Medicinal chemistry	Neurosciences
Biopharmaceutics	Pathology
Pharmacoeconomics	Biomaterial sciences
Pharmacognosy	Natural chemistry
Pharmacogenomics	Green chemistry
Biotech	Physiology
Pharmainformatics	Medical sciences
Pharmaceutical technology	
Drug regulatory affairs	
Analytical chemistry	

- **AJPTR** allows free unlimited access to abstract and full-text. The journal focuses on rapid publication with facilities of online research article tracking & Email/SMS alert etc. Manuscripts are accepted for review with the understanding that the work has not been published and that it is not under consideration for publication elsewhere, and that its submission for publication has been approved by all authors and institution where the actual work was carried out.

A.1 Cover letter

During submission of the article, a cover letter should be included giving the authors full address and telephone/fax number.

- The type of article (Research or Review) along with the title and the type of branch under which the article to be published should be mentioned.

- The corresponding author should mention the undertaking that animal studies carried out were in accordance with their country or institutional ethical committee and also state that the manuscript has not been published elsewhere (except in the form of an abstract or as part of a published lecture or academic thesis).
- Fill in the cover letter and send along with your manuscript. Without these forms (Cover letter) your manuscript will not be considered for publication.

A.2 Original research article

A.3 Manuscript preparation

The manuscript should be prepared in English using "MS Word" with 1 inch margin on all sides (Top, Bottom, Left and Right side) of the page. "Times New Roman" font should be used. The font size should be of 12pt but main Title should be of 16pt bold uppercase, main headings should be of 14pt uppercase, subheadings should be of 12pt bold lowercase. Manuscripts should be concisely typewritten in 1.5 spaces in A4 sized sheets. The pages shall be numbers consequently. The length of Review/Science Education article should not exceed 25 manuscript pages to include figures, tables and references. No abbreviations on acronyms shall be used in the titles or Abstract acronyms except for measurements. There shall not be decorative borders anywhere in the text including the title page. The entire MS word document with graphs and illustrations shall not exceed 2 MB.

A.4 Sequence for Manuscripts Submission

1. Article Title
2. Authors and Co-Authors details and their affiliations
3. Abstract (200 to 250 words)
4. Key words (maximum 6)
5. Introduction
6. Materials and Methods
7. Results and Discussion
8. Conclusion
9. Acknowledgement (optional)
10. References
11. Figure
12. Tables

A.5 ARTICLE TITLE:

The title must be as brief as possible, comprehensive and descriptive. It should not be more than 20 words. Title should be of 16pt bold uppercase.

A.6 AUTHORS AND CO-AUTHORS DETAILS AND THEIR AFFILIATIONS

Each author must provide their full name including their forenames and surname. The Corresponding Author of the manuscript must be marked with an asterisk, and should be listed first. The corresponding author must include a telephone and e-mail address at the bottom left corner of the title page. If any of the co-authors are from different organizations, their addresses too should be mentioned and indicated using numbers after their names. A maximum of 6 authors should be allowed.

A.7 ABSTRACT:

Should start on a new page after the title page and should present the novelty of the study, the main findings or object of present work, and principle conclusions, not more than 250 words. All the three categories, Review Articles, Original Research papers and Short Communications should have an Abstract.

A.8 KEYWORDS:

3-6 keywords are to be provided by the authors. These keywords should be typed at the end of the abstract on the same page.

A.9 INTRODUCTION:

The introduction should not be an extensive literature review although it should provide sufficient background information for the reader to understand and evaluate the results of the present study.

A.10 MATERIALS AND METHODS:

The section should include sufficient technical information to allow the experiments to be performed. Procedural detail that has been published previously should be referred to by citation.

A.11 RESULTS AND DISCUSSION:

Results should be described as concisely as possible in one of the following ways: text, table(s), or figure(s). The reproducibility and statistical significance of measurements, material or biological data, must be included where relevant. The **Discussion** should provide an interpretation of the results and their significance with regard to previously published work. There should not be any significant repetition of the experimental procedures or reiteration of the introduction.

A.12 CONCLUSION:

A short, paragraph summarizing the most important finding(s) of the research is required.

A.13 ACKNOWLEDGMENTS:

The source of any financial support, gifts, technical assistance and advice received for the work being published must be indicated in the Acknowledgments section.

A.14 REFERENCES:

Referencing is a standardized way of acknowledging the sources of information and ideas that you have used in your research work and which allows the sources to be identified. It is important to be consistent when you are referencing. The Vancouver style of referencing is predominantly used in the medical field and Para medical science. When referencing your work in the Vancouver style, it is very important that you use the right punctuation and that the order of details in the reference is also correct. References should be numbered consecutively in the order in which they are first mentioned in the text (not in alphabetic order). Download a PowerPoint presentation on reference styles (How to write reference) and using the reference checking facility of the journal.

For Journal Reference

Desai BG, Annamalai AR, Divya B, Dinesh BM. Effect of enhancers on permeation kinetics of captopril for transdermal system. Asian J Pharma 2008; 2: 35-37.

For Book Reference

Ancel HC, Allen LV, Popovich NG. Pharmaceutical dosage forms and drug delivery systems. 5th ed., New Delhi: Lippincott Williams & Wilkins; 2005: 311-12.

For Chapters in Book Reference

Porter RJ, Meldrum BS. Antiepileptic drugs. In, Katzung BG(ed). Basic and clinical pharmacology. 6th ed., Norwalk (CN): Appleton and Lange; 1995; 361-80.

Government publications

Government of India. Ministry of health and family welfare. Indian Pharmacopoeia Vol. I & II. The Controller of Publication, New Delhi; 1996: 762-10.

A.15 FIGURES

Figures should be numbered consecutively with Arabic numerals (i.e. Figure 1, 2, 3 etc.).
Provide a brief title with each figure.

- All figures should be cited in the text.
- File formats accepted are Microsoft Word (figures must be a single page), PowerPoint (figures must be a single page), PNG, JPEG, TIFF, BMP, CDX (ChemDraw) or TGF (ISIS/Draw).

Sample of Figures.

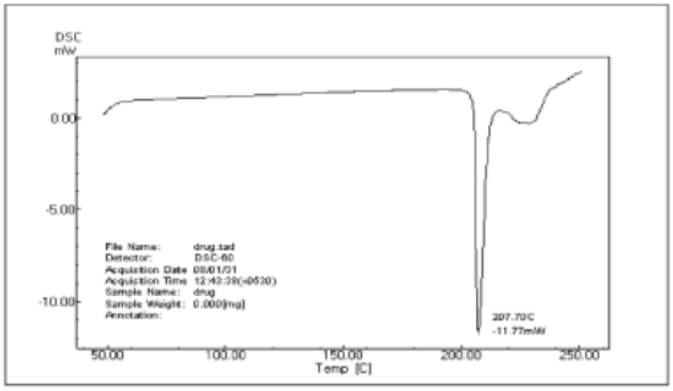

Figure 1: DSC image of Timolol maleate. Timolol maleate showed a characteristic endothermic peak at 207.70˚C, which corresponds to its melting point.

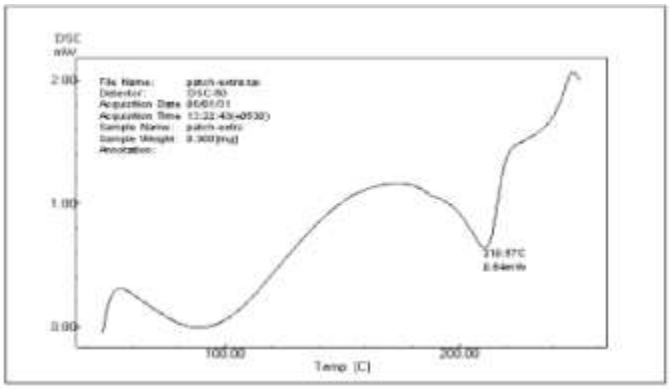

Figure 2: DSC image of optimised formulation 19 (Timolol maleate + PVA + PVP).

A.16 TABLES

- Please keep the number of tables to a minimum.
- Tables should be numbered consecutively (Table 1, Table 2 etc) and each table must start on a separate page at the end of the manuscript.
- Each table must have a title. Each table legend, in paragraph form, should briefly describe the content and define any abbreviations used. If values are cited in a table, the unit of measurement must be stated.
- Tables should not be ruled.
- Tables should be created using Microsoft Word table formatting tools (do not use the tab key to form rows and columns of data as tab information is lost when the document is processed.

Sample of tables

Table 1. Evaluation Parameters of Tablets.

Parameter	Formulations		
	F3	*F6*	*F9*
1) Thickness (mm)	6.15	6.12	6.12
2) Diameter (mm)	12.10	12.10	12.10
3) Weight variation	2.05	2.60	1.75
4) Hardness (kg/cm^2)	4.5	4.5	4.0
5) Disintegration Time (min)	12.10	10	8
6) Friability (%)	0.78	0.81	0.88
7) Content Uniformity	93.70±1.50	91.86±4.5	95.57±3.36
8) Cum.% Drug Released	73.05	61.65	81.11

Table 2 In-vitro Dissolution Parameters of all Formulations

Formulation	Method	Cum. % Drug Released	Cum. % Drug Retained	Dissolution Rate ($g^{1/3}$ /min)	Dissolution Efficiency DE^{60} %	T^{50} (min)	T^{90} (min)
F1	Common Solvent	41.08	58.92	0.79×10^{-3}	31.66	44	101
F2		77.58	22.42	1.56×10^{-3}	56.66	47	101
F3		89.12	10.88	2.15×10^{-3}	75.00	40	97
F4		38.78	61.22	0.65×10^{-3}	28.33	47	98
F5		66.17	33.83	1.28×10^{-3}	48.33	47	103
F6		86.78	13.22	1.93×10^{-3}	68.33	40	103
F7		47.9	52.10	0.83×10^{-3}	36.66	48	105
F8		82.21	17.79	1.85×10^{-3}	66.66	41	106
F9		96.01	3.93	2.61×10^{-3}	86.66	37	96
F1	Physical Mixture Basket	38.71	61.29	0.61×10^{-3}	23.33	54	104
F2		61.59	38.41	1.16×10^{-3}	43.33	47	102
F3		82.16	17.84	1.70×10^{-3}	61.66	45	101
F4		34.13	65.87	0.50×10^{-3}	20.00	62	107
F5		59.29	40.71	1.05×10^{-3}	41.66	50	105
F6		79.85	20.15	1.63×10^{-3}	56.66	47	103
F7		43.32	56.68	0.70×10^{-3}	30.00	47	104
F8		68.48	31.52	1.42×10^{-3}	51.66	45	100
F9		86.73	13.27	1.91×10^{-3}	65.00	45	102
F1	Physical Mixture Paddle	38.73	61.27	0.58×10^{-3}	25.00	54	90
F2		56.99	43.01	1.07×10^{-3}	38.33	61	100
F3		82.12	17.88	1.51×10^{-3}	56.66	42	102
F4		34.78	65.22	0.59×10^{-3}	23.33	53	106
F5		60.64	39.36	1.10×10^{-3}	38.33	51	103
F6		77.59	22.41	1.58×10^{-3}	56.66	41	101
F7		45.61	54.39	0.82×10^{-3}	31.66	48	106
F8		72.98	27.02	1.41×10^{-3}	51.66	49	104
F9		88.99	11.01	1.86×10^{-3}	65.00	47	98
Pure Drug		27.37	72.63	0.37×10^{-3}	18.33	40	90

A.17 REVIEW ARTICLES

Review articles should not be more than 25 pages and contain comprehensive coverage of relevant literature. Review articles should preferably be written by scientists who have in-depth knowledge of the topic. All format requirements are similar to those applicable to Research papers. Review articles need not to be divided into sections such as Materials and methods, and Results and discussion, but should definitely have an abstract and introduction.

A.18 SHORT COMMUNICATIONS

The research and technical communications section of this journal (maximum 3,000 words) is open to interesting results worthy of publication without requiring extensive introduction and discussion. This section should be organized as follows: Abstract, Introduction, Materials and methods, Results and discussion (combined). Not more than 10 references should be provided. Tables, figures and references are to be arranged in the same way as for research papers. Brevity of presentation is essential for this section.

A.19 COPYRIGHT

Submission of the manuscript represent that the manuscript has not been published previously and is not considered for publication elsewhere. Authors would be required to sign a CTA form (Copy Right Transfer Agreement) once the manuscript is accepted which would be sent to the corresponding author's email. The corresponding author can download the form and after getting authors and co-authors signature it can be send as an attachment file after scanning to the journal or by post/courier along with the publication charges.

A.20 ETHICAL MATTERS

Authors involved in the use of experimental animals and human subjects in their research article should seek approval from the appropriate Ethical committee in accordance with "Principles of Laboratory Animal Care". The Method section of the manuscript should include a statement to prove that the investigation was approved and that informed consent was obtained.

A.21 GALLEY PROOFS

Galley proofs would be sent unless indicated otherwise to the corresponding author. It is the responsibility of the corresponding author to ensure that the galley proof is to be returned without delay with correction (if any). The authors are responsible for the contents appearing in their published manuscripts.

A.22 PROCESSING FEES FOR PUBLICATION

Manuscripts submitted to AJPTR are assumed to be submitted under the Open Access publishing model. There is no charge for the processing of papers but author(s) of accepted paper is required to pay a publication charge of 1500 Rupees for Indian authors & $ 70 USD for international authors (Cost towards processing, maintenance of paper in secured data storage system, databases; to meet various overhead expenses like employees charges etc.). Published papers appear electronically and are freely available from our website.

Table A.2 Processing fee summary

<table>
<tr><th>Article category</th><th>Authors from overseas</th><th>Authors from India</th></tr>
<tr><td>Research article</td><td rowspan="4">$70 USD</td><td rowspan="4">Rs 1500</td></tr>
<tr><td>Review article</td></tr>
<tr><td>Case reports</td></tr>
<tr><td>Short communications</td></tr>
<tr><td>Fast track publication</td><td>$100 USD</td><td>Rs 2000</td></tr>
</table>

A.23 Conflict of Interest statement

It must be declared by authors.

Annexure B

Supplementary information for Chapter 2

B.1 HPLC method validation for solubility and dissolution studies on Efavirenz

Introduction and purpose

An HPLC method (based on the chromatographic conditions specified in the USP Salmous Efavirenz capsules monograph (as cited in Chapter 2)) was developed and validated for the quantitative analysis of Efavirenz from the solubility, powder dissolution and intrinsic dissolution experiments performed in 0.1 N HCl (pH 1.2), acetate buffer (pH 4.5), phosphate buffer (pH 6.8), 1 % (w/v) SLS and 2% (w/v) SLS. The purpose of the validation was to ensure that all quantitative measurements that were made were accurate, reliable and suitable for its intended purpose.

The method validation was based on the ICH Q2 (R1) guidelines (ICH, 2005:1-13). The validation parameters that were evaluated were based on the objective of the analytical method.

B.1.1 Equipment and materials

- An Agilent 1200 HPLC with Rev.B 02.01-SR2 [260] ChemStation LC 3D software (Agilent Technologies, Santa Clara, California) with a Phenomenex C18 HPLC column (5 µm, 4.6 mm X 25 cm) (Phenomenex, Torrance, California) were used for the method development, validation and subsequent analysis of the solubility and dissolution samples. For HPLC conditions please refer to Table B.1.
- A Crison Basic-20 pH meter (Crison, Capri, Italy) was utilised for pH determinations.
- A Sartorius R200D analytical balance (Labotec, Midrand, South Africa) was used for weighing of all samples and standards.
- Deionised water was used for the preparation of all aqueous solutions and/or media. The deionised water was generated using a Merck-Millipore Milli-Q water system (Merck, Modderfontein, South Africa).
- A-grade, class 1 glassware was used.
- A Scientech Ultrasonic bath (Labotec, Midrand, South Africa) was used to sonicate all solutions.
- Binder® ED23 laboratory oven (Labotec, South Africa)

The equipment listed above was used to perform the method validation study. The instruments used for experimental procedures (solubility, powder dissolution and intrinsic dissolution), such as dissolution tester, solubility baths, etc. are discussed in sections B.1.3 – B.1.5.

Table B.1 HPLC conditions and parameters used for solubility and dissolution experiments

Condition / Parameter:	Description
Solution 1:	0.8 mg/ml of ammonium acetate in water, adjusted to pH 7.5 with 2% (v/v) ammonium hydroxide if required
Mobile phase:	Acetonitrile and Solution 1 (3:2)
Mode:	Liquid Chromatography
Detector and wavelength:	UV, 252 nm
Injection volume:	20 µl
System suitability:	Column efficiency: not less than 5000 theoretical plates Tailing factor: not more than 1.8 %RSD of 5 replicate injections of standard solution: not more than 2.0%
Standard stock solution:	Dissolve approximately 13.89 mg Efavirenz RS in methanol (using sonication if required) and dilute to 250 ml with mobile phase [55.56 µg/ml].
Standard solution:	Transfer 25 ml of standard stock solution to a 50 ml volumetric flask and dilute to volume with the respective media [27.78 µg/ml]. *The media being 1% (w/v) SLS, 2% (w/v) SLS, 0.1 N HCl, acetate buffer pH 4.5 and phosphate buffer pH 6.8.*

The materials used for the method validation/analysis were as follows:

- **HPLC mobile phase:** Acetonitrile (Merck, South Africa) and ammonium acetate (Merck, South Africa) were used to prepare the mobile phase.
- **0.1 N HCl:** was prepared using a dilution of 1 ml 32% HCl (Merck, South Africa) in 1 liter Milli-Q water (pH = 1.2 ± 0.05).
- **Acetate buffer pH 4.5:** was prepared as follows: 11.4 ml glacial acetic acid (Merck, South Africa) was dissolved in 100 ml Milli-Q water. 14 ml of this solution was mixed with 2.99 g sodium acetate trihydrate (Merck, South Africa) and 900 ml Milli-Q water. The pH was then adjusted (if

necessary) to a pH of 4.5 ± 0.05. The solution was then diluted with Milli-Q water to the final volume of 1 liter.

- **Phosphate buffer (pH 6.8):** was prepared as follows: 6.805 g potassium dihydrogen phosphate (Merck, South Africa) and 0.896 g sodium hydroxide (Merck, South Africa) were dissolved in 800 ml Milli-Q water. The pH was then adjusted (if necessary) to a pH of 6.8 ± 0.05. The solution was then diluted with Milli-Q water to 1 liter.
- **1% SLS:** a 1% (w/v) solution of sodium lauryl sulfate (Merck, South Africa) in water.
- **2% SLS:** a 2% (w/v) solution of sodium lauryl sulfate (Merck, South Africa) in water.
- HPLC grade methanol (Merck, South Africa).
- USP Efavirenz reference standard, batch number EFE/0809011 (USP, Arlington Virginia, USA) was used for the quantitative analysis.

B.1.2 Method development

The HPLC conditions described in the USP Salmous monograph of Efavirenz capsules were used to analyse the powder dissolution, solubility and intrinsic dissolution samples. Preliminary investigations were performed in order to determine to what extent the samples should be diluted prior to analysis.

For preliminary investigations, reference standard solutions of Efavirenz (with different concentrations) were prepared in all the media and analysed using the HPLC conditions as specified in the monograph (Table B.1). Solubility and powder dissolution experiments were designed to utilise the same concentration range (~1.7 – 41.7 µg/ml), whereas intrinsic dissolution experiments required a wider range (~1.0 – 200.0 µg/ml). Solubility and powder dissolution experiments were performed in the same media (0.1 N HCl, acetate buffer pH 4.5, phosphate buffer pH 6.8, 1% (w/v) SLS and 2% (w/v) SLS), whereas intrinsic dissolution experiments were performed only in 1% (w/v) SLS. For this reason linearity and range analysis for all the media (except 1% (w/v) SLS) used the concentration range ~1.7 – 41.7 µg/ml, and 1% (w/v) SLS had to cover a range of ~1.0 - 200.0 µg/ml. The reference standard solutions prepared for the solubility and powder dissolution experiments are summarised in Table B.2, and the reference standard solutions prepared for the intrinsic dissolution and solubility study in 1% (w/v) SLS are summarised in Table B.3.

Table B.2 Preparation of different Efavirenz standard solutions in 0.1 N HCl, acetate buffer pH 4.5, phosphate buffer pH 6.8 and 2% (w/v) SLS for solubility and powder dissolution experiments (preliminary investigations)

Solution	Description of preparation
Solution A	Dissolve approximately 20.84 mg Efavirenz RS in 10 ml methanol (using sonication if required) and dilute to 250 ml with mobile phase [~83.36 µg/ml]. Transfer 25 ml of this solution to a 50 ml volumetric flask and dilute to volume with the respective media [~41.68 µg/ml]. *The media being 2% (w/v) SLS, 0.1 N HCl, acetate buffer pH 4.5 and phosphate buffer pH 6.8.*
Solution B	Dissolve approximately 13.89 mg Efavirenz RS in 10 ml methanol (using sonication if required) and dilute to 250 ml with mobile phase [~55.56 µg/ml]. Transfer 25 ml of this solution to a 50 ml volumetric flask and dilute to volume with the respective media [~27.78 µg/ml]. *The media being 2% (w/v) SLS, 0.1 N HCl, acetate buffer pH 4.5 and phosphate buffer pH 6.8.*
Solution C	Dilute 10 ml of *Solution B* to 20 ml with the respective media [~13.89 µg/ml].
Solution D	Dilute 5 ml of *Solution B* to 20 ml with the respective media [~6.95 µg/ml].
Solution E	Dilute 5 ml of *Solution D* to 10 ml with the respective media [~3.48 µg/ml].
Solution F	Dilute 5 ml of the *Solution E* to 10 ml with the respective media [~1.74 µg/ml].

Table B.3 Preparation of different Efavirenz standard solutions in 1% (w/v) SLS for intrinsic dissolution (preliminary investigations)

Solution	Description of preparation
Solution G	Dissolve approximately 100.00 mg Efavirenz RS in 50 ml methanol (using sonification if required) and dilute to 500 ml with 1% (w/v) SLS [~200.0 µg/ml].
Solution H	Transfer 20 ml of *Solution G* to a 25 ml volumetric flask and dilute to volume with 1% (w/v) SLS [~160.0 µg/ml].
Solution I	Transfer 12 ml of *Solution G* to a 20 ml volumetric flask and dilute to volume with 1% (w/v) SLS [~120.0 µg/ml].
Solution J	Transfer 5 ml of *Solution G* to a 20 ml volumetric flask and dilute to volume with 1% (w/v) SLS [~50.0 µg/ml].
Solution K	Transfer 2 ml of *Solution G* to a 20 ml volumetric flask and dilute to volume with 1% (w/v) SLS [~20.0 µg/ml].
Solution L	Transfer 1 ml of *Solution G t*o a 20 ml volumetric flask and dilute to volume with 1% (w/v) SLS [~10.0 µg/ml].
Solution M	Transfer 2 ml of *Solution L* to a 10 ml volumetric flask and dilute to volume with 1% (w/v) SLS [~2.0 µg/ml].
Solution N	Transfer 1 ml of *Solution L* to a 10 ml volumetric flask and dilute to volume with 1% (w/v) SLS [~1.0 µg/ml].

Standard calibration curves for Efavirenz in all the media were constructed and are depicted in Figure B.1. From Figure B.1 it is clear that a linear relationship exists between the mAu response (i.e. area of the Efavirenz peak in the chromatogram) and the concentration of Efavirenz in all the media in the respective ranges. The solutions exhibited mAu response values which ranged between ~78 – 2 500 mAu (for the range ~1.7 – 41.7 µg/ml) and ~40 – 10 500 mAu (for the range ~1.0 – 200.0 µg/ml), which were within the analytical range of the HPLC system.

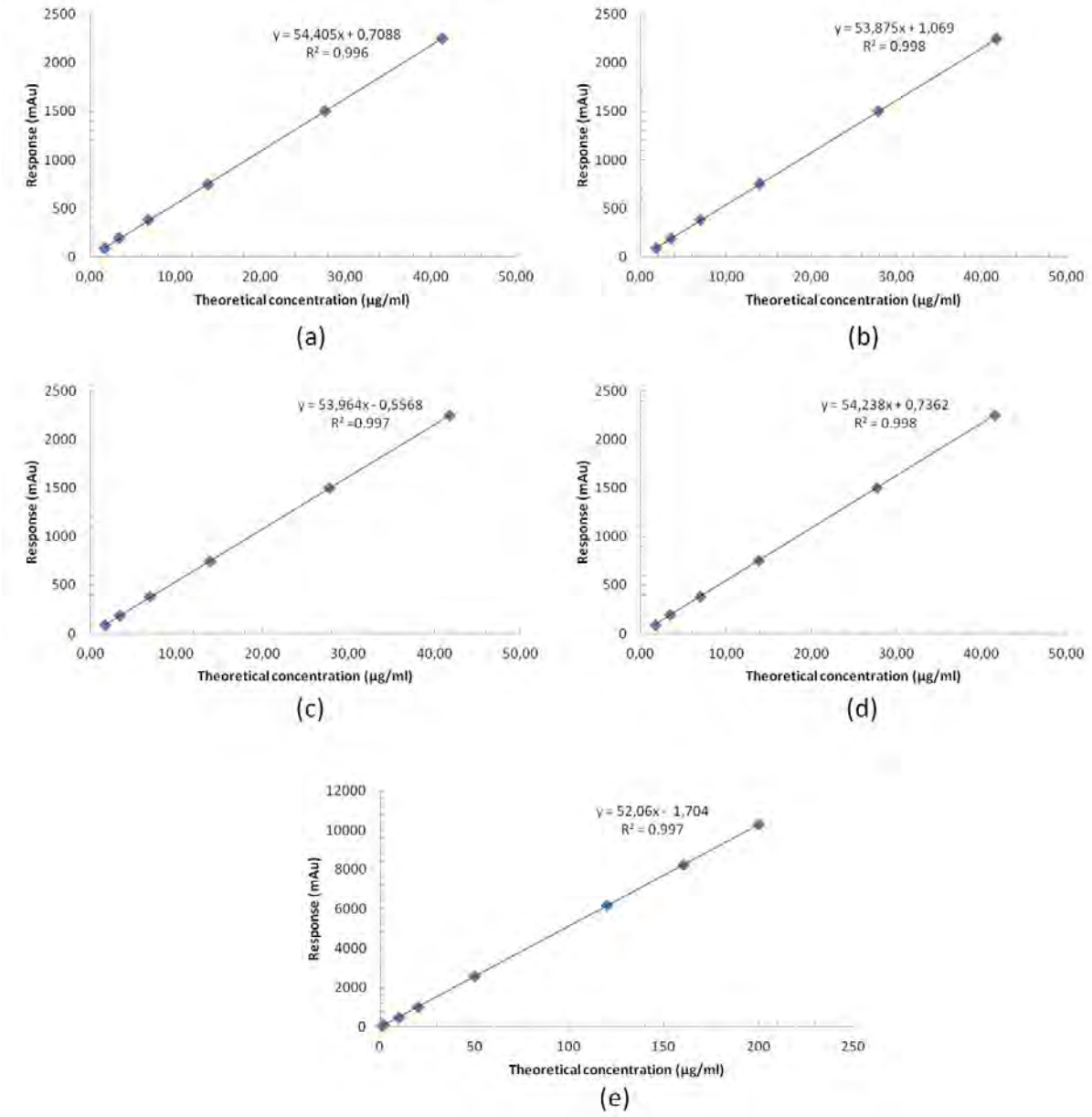

Figure B.1 Standard calibration curves for Efavirenz in (a) 0.1 N HCl, (b) acetate buffer pH 4.5, (c) phosphate buffer pH 6.8, (d) 2% (w/v) SLS and (e) 1% (w/v) SLS.

B.1.3 Description of the method used for solubility studies

The solubility of Efavirenz Form A and Form I was determined in 0.1 N HCl (pH 1.2), acetate buffer (pH 4.5), phosphate buffer (pH 6.8), 1% (w/v) and 2% (w/v) SLS.

The solubility samples were prepared in triplicate as follows: approximately 200 mg of sample (i.e. Form A and Form I respectively) and 5 ml of each medium (i.e. respective medium) were transferred into a test tube. The test tubes were sealed and affixed to a mechanical rotator, which was installed into a temperature regulated water bath. The temperature of the water bath was set at 37 ± 0.2 ºC.

The test tubes were rotated at 50 ± 2 rpm inside the water bath for a period of 24 hours, after which the solutions were filtered through a 0.45 µm Millipore® filter (Millipore, South Africa) to remove any undissolved matter.

Aliquots from the filtered solutions were then suitably diluted to ensure that the responses obtained from the analysis of the diluted solutions were within the established response range (~1.7 – 41.7 or ~1.0 – 200.0 µg/ml, depending on the medium).

The concentrations of Efavirenz in the diluted solutions were determined using the linear equations presented in Figure B.1. The concentration of Efavirenz dissolved in the original 5 ml of media was determined using equation B.1.

$$\delta = \left(\frac{Area - c}{m \times 1000}\right) \times D_f \qquad \text{(equation B.1)}$$

Where: δ = concentration of Efavirenz expressed as mg/ml; *Area* = Response value (i.e. area of the Efavirenz peak in the chromatogram); *c* = y-intercept of linear equation, *m* = slope of linear equation, D_f = dilution factor based on degree of dilution to obtain a response value in the respective ranges (see section B.1.2) and 1000 = conversion factor from µg/ml to mg/ml.

B.1.4 Description of the method used for powder dissolution studies

Efavirenz Form A and Form I were subjected to powder dissolution studies according to the method developed by Lötter *et al.* (1983:59-66).

Particle size is an important factor to consider when performing dissolution studies, thus all the powdered samples were sieved to ensure particle size uniformity. Sieved fractions of 106 – 250 nm were used in the dissolution studies.

Powder dissolution studies were performed using an Erweka D700 dissolution tester (Erweka, Heusenstramm, Germany) which was equipped with a heater-circulator. The dissolution studies were performed at a constant temperature of 37 ± 0.5 °C. The paddle assembly was used, which was rotated at a speed of 50 rpm. Dissolution was performed using 900 ml of 1% (w/v) and 2% (w/v) SLS as dissolution media. Powder dissolution studies were performed in 12 vessels for each of the two forms, in each medium.

Samples were prepared as follows: Weigh and transfer approximately 50, 200 or 600 mg of the sample (i.e. Form A or Form I) into test tubes. Thereafter weigh and transfer glass beads (with a diameter of 0.1 mm) (Sigma Aldrich, Johannesburg, South Africa) corresponding to 50% of the sample weight (thus 25 mg, 100 mg or 300 mg) into the aforementioned test tubes. Withdraw 10 ml of medium from each vessel once the medium has reached 37 ± 0.5 °C. Transfer the withdrawn

medium (10 ml) to the corresponding test tube and agitate the suspended sample for 30 seconds using a Vortex Genie shaker (Scientific Industries Inc., Bohemia, New York) before rinsing the contents into the dissolution vessel. The addition of the medium to the test tubes should be 1 minute apart to allow enough time for the agitation and transferral of the contents to the respective vessels (thus allowing 1 minute between sampling).

Withdraw 5 ml of sample (using in-line filtering system with Millipore® 0.45 µm filters (Microsep, Sandton, South Africa)) from all vessels at 7.5, 15, 30 and 45 minutes and replace the amount withdrawn with 5 ml of fresh, pre-heated medium (37 ± 0.5 °C). Dilute the withdrawn solution suitably prior to HPLC analysis. Ensure that the responses obtained from the analysis of the diluted solutions are within the established response range (~1.7 – 41.7 or ~1.0 – 200.0 µg/ml, depending on the medium).

The concentrations of Efavirenz in the diluted solutions were determined using the linear equations presented in Figure B.1. The concentration of Efavirenz dissolved in the original solution (withdrawn solution) was determined using equation B.1. The calculated concentration was then expressed as the % dissolved using equation B.2.

$$\%\ Dissolved = \left(\frac{E_c}{T_c}\right) \times 100 \qquad \text{(equation B.2)}$$

Where E_c is the experimental concentration calculated using equation B.1 and T_c is the theoretical concentration of the sample calculated by dividing the actual sample weight (expressed in mg) with the medium volume (900 ml).

B.1.5 Description of the method used for intrinsic dissolution studies

Intrinsic dissolution studies were performed on Efavirenz Form A and Form I based on the intrinsic dissolution guidelines of the British Pharmacopoeia (BP, 2014) and United States Pharmacopoeia (USP, 2014). Aluminium dies with an inner radius of approximately 13 mm (total surface area of compacted powder = 1.327 cm^2) were used during the studies.

The intrinsic dissolution studies were performed using an Erweka D700 dissolution tester (Erweka, Heusenstramm, Germany) which was equipped with a heater-circulator. The paddle assembly was used, which was rotated at a speed of 50 rpm. Dissolution was performed using 900 ml of 1% (w/v) SLS as dissolution medium. Intrinsic dissolution studies were performed in 12 vessels for each of the two forms.

Transfer 900 ml of medium (1% (w/v) SLS) into the vessels and let the temperature of the medium equilibrate to 37 ± 0.5°C.

Weigh and transfer approximately 1.00 g of sample (i.e. Form A or Form I) to the dies and subject it to a compression force of 3 ton for one minute using a Beckman 00-25 hydraulic press (Beckman, Glenrothes, Scotland). Transfer the samples to the respective vessels once the medium temperature has equilibrated to 37 ± 0.5 °C, and start the paddle agitation.

Withdraw 5 ml samples (using in-line filtering system with Millipore® 0.45 µm filters (Microsep, Sandton, South Africa) at 7.5, 15, 30, 60, 120, 180 and 240 minutes and replace the amount withdrawn with 5 ml of fresh, pre-heated medium (37 ± 0.5 °C). Suitably dilute the withdrawn solutions prior to HPLC analysis to ensure that the responses obtained are within the established response range (~1.0 – 200.0 µg/ml).

The concentrations of Efavirenz in the diluted solutions were determined using the linear equations presented in Figure B.1. The cumulative concentration per time point for the fixed area of the die (1.327 cm^2) was calculated using equations B.3 and B.4.

$$Concentration = \left(\frac{\frac{Area - c}{m}}{Die\ surface\ area} \right) \times D_f \qquad \text{(equation B.3)}$$

Where: *Concentration* is the concentration of Efavirenz expressed as µg/ml; *Die surface area* = 1.327 cm^2; *Area* = Response value (i.e. area of the Efavirenz peak in the chromatogram); *c* = y-intercept of linear equation, *m* = slope of linear equation and D_f = dilution factor based on degree of dilution to obtain a response value in the respective range.

$$Cummulative\ concentration = C_{ptp} + C_{ctp} \qquad \text{(equation B.4)}$$

Where: *Cumulative concentration* is expressed in µg/ml; C_{ptp} = concentration at previous time point(s) and C_{ctp} = Concentration at current time point.

B.1.6 Validation parameters and acceptance criteria

The parameters and their respective acceptance criteria selected for the validation are summarised in Table B.4.

Table B.4 Validation parameters and their acceptance criteria

Validation parameter	Acceptance criteria
Specificity	No interference from the solvents and mobile phase at the retention time of the principle (Efavirenz) peak.
Linearity and range	A regression line with a correlation coefficient (r^2) not less than 0.99 using at least 5 concentration points across the chosen range (~ 1.7 – 41.7 µg/ml and ~1.0 – 200.0 µg/ml).
Accuracy	Recovery must be between 98.0 - 102.0%. At least 9 determinations should be made over a minimum of 3 concentrations (3 determinations per concentration) covering the analytical range.
Precision (Repeatability):	% RSD of recovery values is not more than 2.0%. At least 9 determinations should be made over a minimum of 3 concentrations (3 determinations per concentration) covering the analytical range.
Limit of quantification (LOQ)	LOQ established to determine the lowest amount of Efavirenz that can be quantitatively determined with suitable precision and accuracy.
Robustness	The sample solution (Sample solution O and U) should not show degradation of more than 2.0% over a period of 24 hours at 45°C.

The ICH guideline for validation of analytical methods states that: "*the extent to which intermediate precision should be established depends on the circumstances under which the procedure is intended to be used"* (ICH Q2 (R1):10). Intermediate precision was not included in this study as it was not deemed necessary since all experiments were performed using the same laboratory equipment and executed by one analyst for comparative purposes (i.e. comparative solubility and dissolution studies). The solubility, intrinsic dissolution and powder dissolution methods developed for this study

are not intended for standardisation (for instance inclusion in a pharmacopoeia), thus does not necessitate evaluation of intermediate precision.

B.1.7 Procedures and results

B.1.7.1 Specificity

Inject the mobile phase and all the different media (solubility and or dissolution media) and reference standard solution (~ 27 μg/ml) separately using the chromatographic conditions as specified in Section B.1.1. The chromatograms of the solvents / media should not exhibit any interference at the retention time of the principle Efavirenz peak (as observed in the Efavirenz reference standard chromatogram).

All the different media used in the solubility studies and dissolution experiments were injected separately (Fig. B.2 (a)-(e)). None of the media revealed any interference at the retention time of the Efavirenz peak (Fig B.2 (f)- retention time ~13.5 minutes) and therefore the method could be deemed specific to analyse Efavirenz.

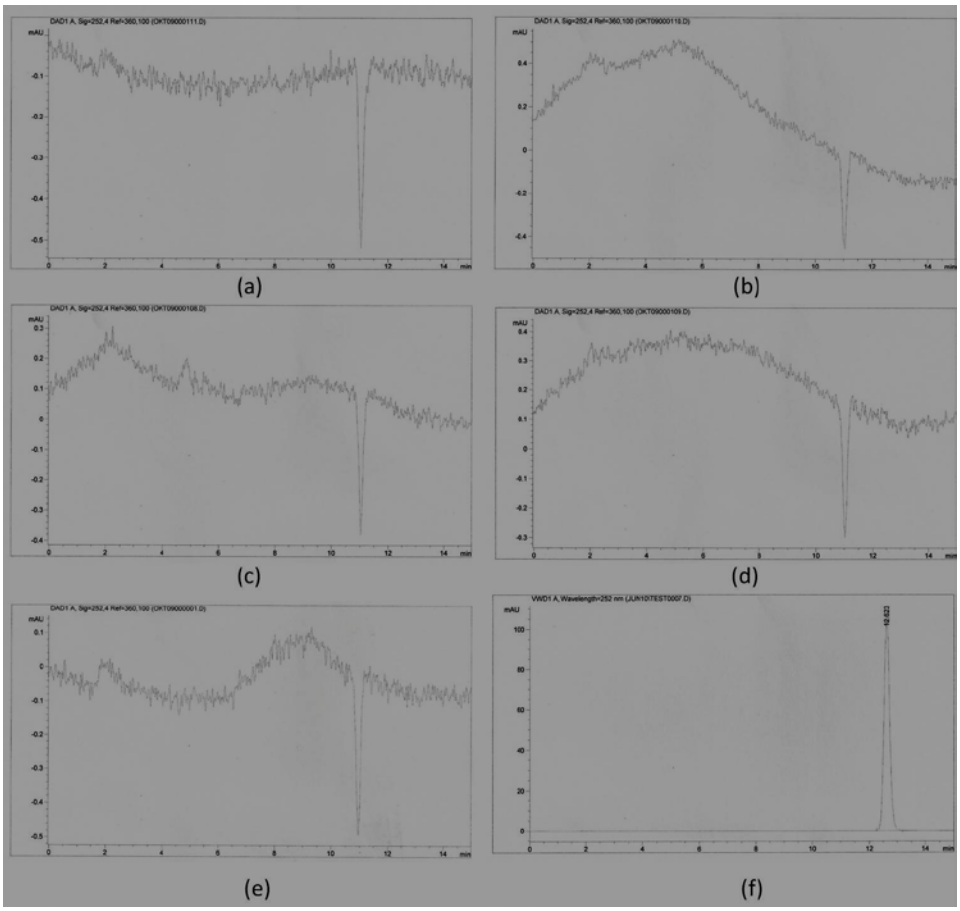

Figure B.2 HPLC chromatograms of (a) mobile phase, (b) 0.1 N HCl, (c) acetate buffer pH 4.5, (d) phosphate buffer pH 6.8, (e) SLS (the same for 1% (w/v) and 2% (w/v) SLS), and (f) Efavirenz reference standard solution (~27 µg/ml) ***Note the scale of the solutions (a) – (e) are very small, subsequently showing the baseline at a very high level of zoom in comparison with the standard chromatogram, showing a stable baseline. The baseline is in fact stable considering the scale.***

B.1.7.2 Linearity and range

Solubility and powder dissolution experiments were designed to utilise the same concentration range (~1.7 – 41.7 µg/ml), whereas intrinsic dissolution experiments required a wider range (~1.0 – 200.0 µg/ml). Solubility and powder dissolution experiments were performed in the same media (0.1 N HCl, acetate buffer pH 4.5, phosphate buffer pH 6.8, 1% (w/v) SLS and 2% (w/v) SLS) whereas intrinsic dissolution experiments were performed only in 1% (w/v) SLS. For this reason linearity and range analysis for all the media (except 1% (w/v) SLS) used the concentration range ~1.7 – 41.7 µg/ml, and 1% (w/v) SLS had to cover a range of ~1.0 - 200.0 µg/ml – Figure B.3.

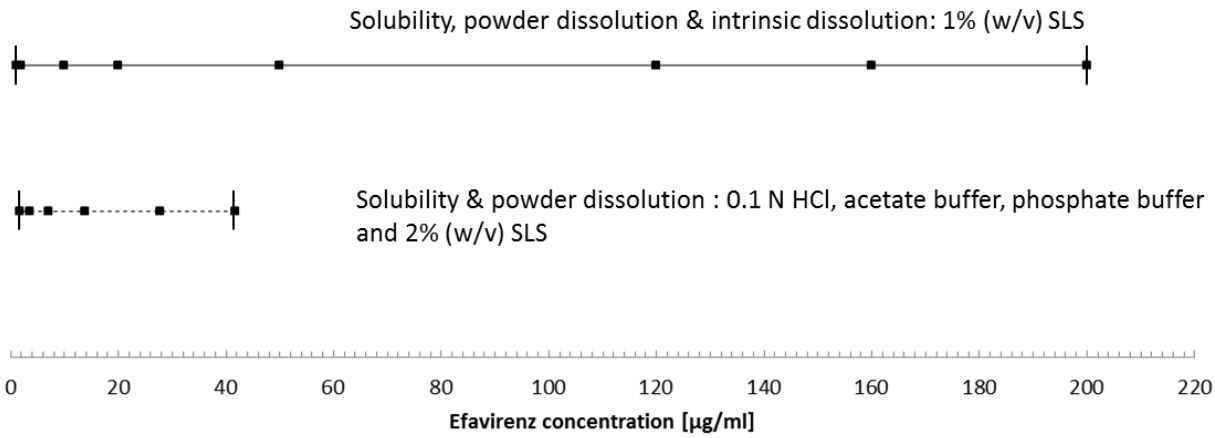

Fig. B.3 The concentration ranges employed for solubility and powder dissolution experiments ranging from ~1.7 – 41.7 µg/ml (0.1 N HCl, acetate buffer pH 4.5, phosphate buffer pH 6.8 and 2% (w/v) SLS) and the concentration range employed for solubility, intrinsic dissolution and powder dissolution (~1.0 – 200.0 µg/ml) in 1% (w/v) SLS.

Prepare volumetric solutions (in five-fold) of the Efavirenz reference standard in 0.1 N HCl, acetate buffer pH 4.5, phosphate buffer pH 6.8 and 2% (w/v) SLS with concentrations ranging from ~1.7 – 41.7 µg/ml – Table B.5 (solutions O-T). For 1% (w/v) SLS, prepare volumetric solutions of the Efavirenz reference standard with concentrations ranging from ~1.0 – 200.0 µg/ml (Table B.6, solutions U - AB). Inject the different solutions using the HPLC chromatographic system as described in Table B.1, and record the areas of the Efavirenz peaks. Plot the average peak area values as a function of their respective concentrations and perform least squares linear regression analysis to calculate the correlation coefficient.

Table B.5 Preparation of different Efavirenz standard solutions for linearity and range applicable to 0.1 N HCl, acetate buffer pH 4.5, phosphate buffer pH 6.8 and 2% (w/v) SLS for solubility and powder dissolution experiments

Solution	Description of preparation
Solution O	Dissolve approximately 20.84 mg Efavirenz RS in 10 ml methanol (using sonication if required) and dilute to 250 ml with mobile phase [~83.36 µg/ml]. Transfer 25 ml of this solution to a 50 ml volumetric flask and dilute to volume with the respective media [~41.68 µg/ml]. *The media being 2% (w/v) SLS, 0.1 N HCl, acetate buffer pH 4.5 and phosphate buffer pH 6.8.*
Solution P	Dissolve approximately 13.89 mg Efavirenz RS in 10 ml methanol (using sonication if required) and dilute to 250 ml with mobile phase [~55.56 µg/ml]. Transfer 25 ml of this solution to a 50 ml volumetric flask and dilute to volume with the respective media [~27.78 µg/ml]. *The media being 2% (w/v) SLS, 0.1 N HCl, acetate buffer pH 4.5 and phosphate buffer pH 6.8.*
Solution Q	Dilute 10 ml of Solution P to 20 ml with the respective media [~13.89 µg/ml].
Solution R	Dilute 5 ml of Solution P to 20 ml with the respective media [~6.95 µg/ml].
Solution S	Dilute 5 ml of Solution R to 10 ml with the respective media [~3.48 µg/ml].
Solution T	Dilute 5 ml of the Solution S to 10 ml with the respective media [~1.74 µg/ml].

Table B.6 Preparation of different Efavirenz standard solutions for linearity and range applicable to 1% (w/v) SLS (solubility, powder dissolution and intrinsic dissolution experiments)

Solution	Description of preparation
Solution U	Dissolve approximately 100.00 mg Efavirenz RS in 50 ml methanol (using sonification if required) and dilute to 500 ml with 1% (w/v) SLS [~200.0 µg/ml].
Solution V	Transfer 20 ml of Solution U to a 25 ml volumetric flask and dilute to volume with 1% (w/v) SLS [~160.0 µg/ml].
Solution W	Transfer 12 ml of *Solution U* to a 20 ml volumetric flask and dilute to volume with 1% (w/v) SLS [~120.0 µg/ml].
Solution X	Transfer 5 ml of *Solution U* to a 20 ml volumetric flask and dilute to volume with 1% (w/v) SLS [~50.0 µg/ml].
Solution Y	Transfer 2 ml of *Solution U* to a 20 ml volumetric flask and dilute to volume with 1% (w/v) SLS [~20.0 µg/ml].
Solution Z	Transfer 1 ml of *Solution U t*o a 20 ml volumetric flask and dilute to volume with 1% (w/v) SLS [~10.0 µg/ml].
Solution AA	Transfer 2 ml of Solution Z to a 10 ml volumetric flask and dilute to volume with 1% (w/v) SLS [~2.0 µg/ml].
Solution AB	Transfer 1 ml of Solution Z to a 10 ml volumetric flask and dilute to volume with 1% (w/v) SLS [~1.0 µg/ml].

Plots of the average responses for the volumetric solutions (Tables B.5 and B.6) in the different media as a function of their concentrations are presented in Figure B.4 together with the linear equations and correlation coefficients.

Each data point (in Figure B.4) represents the average of five determinations, and the error bars the standard deviation from the average at that point. The regression lines in all the media had a correlation coefficient greater than 0.99 over the respective ranges. The regression lines in all the media had y-intercepts which did not differ significantly (p-value > 0.05) from zero.

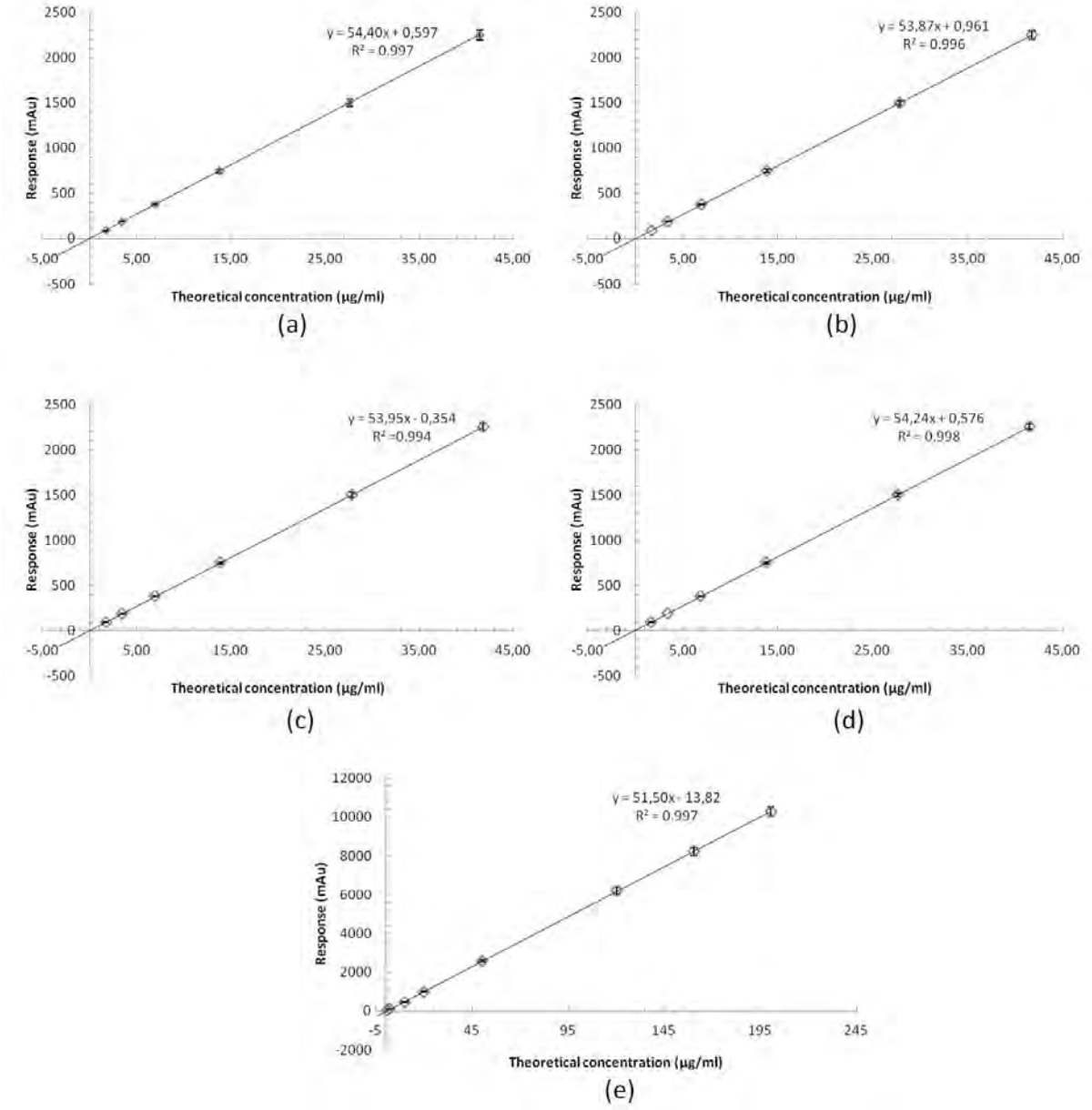

Figure B.4 Standard calibration curves for Efavirenz in (a) 0.1 N HCl, (b) acetate buffer pH 4.5, (c) phosphate buffer pH 6.8, (d) 2% (w/v) SLS and (e) 1% (w/v) SLS - error bars indicate standard deviation.

B.1.7.3 Accuracy and repeatability

For accuracy and repeatability determinations, the minimum and maximum concentrations of the respective ranges (1.7 – 41.7 µg/ml and 1.0 – 200.0 µg/ml) were chosen together with one mid-range concentration: Solutions O, P and T for the 1.7 - 41.7 µg/ml range (Table B.5) and Solutions U, V and AB for the 1.0 – 200.0 µg/ml range (Table B.6).

Prepare fresh volumetric solutions of Solution O, P, T as well as U, V and AB (**in triplicate**) as specified in Tables B.5 and B.6. Label these solutions in the various media as minimum, mid-range and maximum.

Inject the different solutions using the HPLC chromatographic system and conditions as described in Table B.1, and record the areas of the Efavirenz peaks. Use the linear regression lines (from Figure B.4) to calculate the % recovery for accuracy.

The accuracy and repeatability results obtained are tabulated in Table B.7.

The % recovery results reported in Table B.7 ranged between 99.6 -101.9% (acceptance criterion 98.0 – 102.0%). The repeatability for the recovery results was found to be satisfactory with %RSD values ranging between 0.03 – 1.13% (acceptance criterion ≤ 2.0%).

Table B.7 Accuracy and repeatability results for the HPLC analysis of Efavirenz solutions in 1% (w/v) SLS, 2% (w/v) SLS, 0.1 N HCl, acetate buffer pH 4.5 and phosphate buffer pH 6.8

	Theoretical concentration														
	Minimum					**Mid-range**					**Maximum**				
	1	**2**	**3**	**4**	**5**	**1**	**2**	**3**	**4**	**5**	**1**	**2**	**3**	**4**	**5**
	Accuracy: % Recovery														
R_1:	101.2%	101.7%	101.9%	101.1%	101.2%	99.7%	100.8%	100.0%	100.1%	100.0%	99.8%	99.8%	99.9%	99.9%	99.9%
R_2:	100.0%	100.7%	100.6%	100.0%	101.8%	99.7%	101.5%	99.9%	99.7%	100.3%	99.9%	99.9%	100.0%	100.2%	100.4%
R_3:	101.5%	100.3%	99.6%	99.7%	101.2%	99.7%	101.7%	99.8%	100.2%	99.7%	100.5%	99.9%	99.8%	100.0%	99.9%
Average:	100.9%	100.9%	100.7%	100.3%	101.4%	99.7%	101.3%	99.9%	100.0%	100.0%	100.1%	99.9%	99.9%	100.0%	100.0%
Repeat-ability (%RSD)	0.79%	0.68%	1.13%	0.70%	0.32%	0.03%	0.48%	0.11%	0.26%	0.30%	0.36%	0.07%	0.11%	0.15%	0.27%

Where **1** = 1% (w/v) SLS, **2** = 2% (w/v) SLS, **3** = 0.1 N HCl, **4** = Acetate buffer pH 4.5, **5** = Phosphate buffer pH 6.8, **R_1** = replicate no. 1, **R_2** = replicate no. 2 and **R_3** = replicate no. 3.

B.1.7.4 Limit of quantification (LOQ)

The LOQ values in all the media were calculated based on the standard deviation of the response and slope approach as described in the ICH Q2(R1) guidelines (2005:11) – Table B.8.

Calculate the LOQ values in all the media using equation B.5 and the linear regression data obtained in Section B.1.7.2.

$$LOQ = \frac{10\sigma}{S} \qquad \text{(equation B.5)}$$

Where: σ is the standard deviation of the y-intercept of the regression line and S the slope of the calibration curve.

Table B.8 LOQ values for the HPLC analysis of Efavirenz in the various media

Medium	LOQ (µg/ml)
0.1 N HCl	0.77
Acetate buffer pH 4.5	0.79
Phosphate buffer pH 6.8	0.84
1% (w/v) SLS	0.75
2% (w/v) SLS	0.89

The lowest concentration used to establish linearity and range (± 1.0 µg/ml for 1% (w/v) SLS and 1.7 µg/ml for all other media) exceeded the LOQ values calculated for all the media. As mentioned earlier, the withdrawn solutions were suitably diluted prior to analysis (within the established range) to ensure that all the results obtained were determined with suitable precision and accuracy.

B.1.7.5 Robustness

The solubility studies were performed at 37 °C over period of 24 hours. It was therefore necessary to investigate the stability of Efavirenz in the respective solubility media. It was decided to subject Solution O (all media other than 1% (w/v) SLS) and Solution U (1% (w/v) SLS) to robustness testing at 45 °C.

Calculate the Efavirenz concentration of Solutions O and U (immediately after preparation) using the HPLC method and applicable linear regression equation in Figure B.1. Thereafter store these solutions in a temperature controlled laboratory oven (Binder, Labotec, South Africa) at 45°C for 24

hours. Calculate the Efavirenz concentration in the solutions and calculate the % recovery using equation B.6.

$$\%Recovery = \frac{C_{24\,hrs}}{C_{0\,hrs}} \times 100\% \qquad \text{(equation B.6)}$$

Where: % Recovery = percentage recovery of Solution O or U after 24 hours storage at 45°C, C_{0hrs} = calculated concentration of Solution O or U (µg/ml) immediately after preparation, C_{24hrs} = calculated concentration of Solution O or U (µg/ml) 24 hours post storage at 45 °C.

The results obtained are tabulated in Table B.9.

Table B.9 Recovery values obtained for the robustness study

	0.1 N HCl (pH 1.2)	**Acetate buffer (pH 4.5)**	**Phosphate buffer (pH 6.8)**	**1% (w/v) SLS**	**2% (w.v) SLS**
Initial concentration – C_{0hrs} (µg/ml)	41.68	41.75	41.41	201.47	41.19
Concentration after 24 hours at 45°C – C_{24hrs} (µg/ml)	41.22	41.21	40.99	200.45	40.65
% Recovery	98. 9%	98.7%	99.0%	99.5%	98.7%

The % Recovery for Efavirenz in all solubility media when stored at 45 °C for 24 hours ranged between 98.7 – 99.5%, thus the concentrations of the samples did not deviate by more than 2.0% from the initial concentrations, conforming to the robustness criterion.

B.1.7.6 System suitability requirements

The HPLC system suitability was evaluated prior to starting with the analysis. Solutions of Efavirenz RS in all the media were prepared having concentrations of ~ 25 µg/ml (as specified in the Efavirenz Capsule monograph) and injected in five-fold. A standard stock solution was prepared: 0.5 mg/ml Efavirenz RS was dissolved initially at 10% (v/v) of the final volume with HPLC grade methanol, and then diluted with the respective media to final volume. A portion of the standard stock solution was then diluted with the mobile phase to obtain a final concentration of 25 µg/ml. The column efficiency, tailing factor and %RSD of the five replicate injections were evaluated. The results obtained are tabulated in Table B.10.

Table B.10 Summary of HPLC system suitability results obtained

	Media				
	0.1 N HCl	**Acetate buffer pH 4.5**	**Phosphate buffer pH 6.8**	**1% (w/v) SLS**	**2% (w/v) SLS**
Column efficiency (NLT 5000 theoretical plates)	9458	9667	9841	10104	9957
Tailing factor (NMT 1.8)	1.1	1.2	1.2	1.2	1.1
%RSD of 5 replicate injections (NMT 2.0%)	0.9%	0.7%	0.7%	1.1%	0.9%

The HPLC system complied with the system suitability requirements in all media.

Conclusion

An HPLC method (based on the chromatographic conditions specified in the USP Salmous monograph of Efavirenz capsules) was developed and validated for the quantitative analysis of Efavirenz from the solubility, powder dissolution and intrinsic dissolution experiments performed in 0.1N HCl (pH 1.2), acetate buffer (pH 4.5), phosphate buffer (pH 6.8), 1 % (w/v) SLS and 2% (w/v) SLS. The purpose of the validation was to ensure that all quantitative measurements that were made were accurate and reliable and that the method was suitable for its intended purpose. This method was proven to be specific and had linear responses within the range of ~1.7 – 41.7 µg/ml (all media except 1% (w/v) SLS) and ~1.0 – 200.0 µg/ml (for 1% (w/v) SLS). Accuracy and repeatability were demonstrated. Robustness with respect to the samples revealed that Efavirenz remained stable (within acceptable limits) for 24 hours when stored at 45 °C in the respective media.

A summary of the results and acceptance criteria are presented in Table B.11.

As can be seen from Table B.11, all the method validation parameters were within their specified acceptance limits, thus the method can be deemed suitable for its intended purpose.

Table B.11 Summary of the results and acceptance criteria for the validation study

Parameter	Acceptance limits	Result	Compliance statement
Specificity	No interference of the mobile phase or media at the retention time of Efavirenz.	None of the solvents/media interfered with the principle peak (Efavirenz, retention time ~13.5 min).	Complies
Linearity and range	A regression line with a correlation coefficient (r^2) not less than 0.99 using at least 5 concentration points across the selected ranges.	Regression lines correlation coefficients (r^2) in the media ranged between 0.994 – 0.998 across their respective concentration ranges.	Complies
Accuracy	Recovery must be between 98.0 - 102.0%. At least 9 determinations should be made over a minimum of 3 concentrations (3 determinations per concentration) covering the analytical range.	Recovery values from all media ranged between 99.6 – 101.9% (n=9 per medium).	Complies
Precision (Repeatability):	% RSD of recovery values is not more than 2.0%. At least 9 determinations should be made over a minimum of 3 concentrations (3 determinations per concentration) covering the analytical range.	% RSD of the recovery values (n=9 per solubility medium) ranged between 0.03 – 1.13% across the respective ranges.	Complies
Limit of quantification (LOQ)	LOQ established to determine the lowest amount of Efavirenz that can be quantitatively determined with suitable precision and accuracy.	LOQ values calculated in all media ranged between 0.75-0.89 µg/ml. The lowest concentration used to establish linearity and range (±1 µg/ml) exceeded the LOQ values calculated for all of the solubility media.	Complies
Robustness	The sample solution (Sample solution O and U) should not show degradation of more than 2.0% over a period of 24 hours at 45°C.	The % Recovery for Efavirenz in all media when stored at 45°C for 24 hours ranged between 98.7 – 99.5% (0.5 – 1.3% degradation)	Complies

Remarks

The solubility of Efavirenz in the different media was determined to enable the choice of the most discriminatory medium for dissolution studies that would follow. The solubility of Efavirenz in physiological media (0.1 N HCl, acetate buffer pH 4.5 and phosphate buffer pH 6.8), ranged from 7.5 – 11.4 µg/ml, which rendered these media unsuitable for dissolution studies (solubility too low). For this reason dissolution studies continued in 1% and 2% (w/v) SLS only, where solubility values of Efavirenz were much higher (11 - 21 mg/ml) and therefore would have a better chance to discriminate between the forms.

Bibliography

BP - Refer to British Pharmacopoeia.

BRITISH PHARMACOPOEIA. 2014. [Web:]: http:pharmacopoeia.co.uk. Date of access: 28 October 2014.

ICH see INTERNATIONAL CONFERENCE ON HARMONISATION OF TECHNICAL REQUIREMENTS FOR REGISTRATION OF PHARMACEUTICALS FOR HUMAN USE.

INTERNATIONAL CONFERENCE ON HARMONISATION OF TECHNICAL REQUIREMENTS FOR REGISTRATION OF PHARMACEUTICALS FOR HUMAN USE. 2005. ICH Harmonised Tripartite Guideline. Validation of analytical procedures: text and methodology Q2(R1). http://www.emea.europe.eu. Date of access: 24 September 2014.

LÖTTER, A.P., FLANAGAN, D.R., PALEPU, N.R. & GUILLORY, J.K. 1983. A simple reproducible method for determining dissolution rates of hydrophobic powders. Pharmaceutical Technology, April: 59-66.

USP – Refer to United States Pharmacopoeia.

UNITED STATES PHARMACOPOEIA. 2014. [Web:]: http:uspnf.com. Date of access: 28 October 2014.

Annexure C

AAPS Pharm SciTech Author guidelines

The following instructions pertain to submissions to the American Association of Pharmaceutical Scientists' (AAPS) electronic journals: *The AAPS Journal* and *AAPS PharmSciTech*.

C.1 Introduction

The AAPS Journal (ISSN 1550-7416) is a peer-reviewed online-only journal owned by the American Association of Pharmaceutical Scientists. The journal covers all areas of pharmaceutical research, except pharmaceutical technology and engineering, which are covered by its sister journal, *AAPS PharmSciTech*. The Journal is indexed by PubMed/Medline, Index Medicus, Institute of Scientific Information's Science Citation Index Expanded®, and Chem Abstracts.

Editor-in-Chief, Ho-Leung Fung, Ph.D., oversees an international editorial board of leading researchers in the pharmaceutical sciences. Fung is a professor of pharmaceutical sciences at the University at Buffalo, The State University of New York.

AAPS PharmSciTech (ISSN 1530-9932) is a peer-reviewed online-only journal owned by the American Association of Pharmaceutical Scientists. The journal's mission is to disseminate scientific and technical information on drug product design, development, evaluation, and processing to the global pharmaceutical research community. The Journal is indexed by PubMed/Medline, Index Medicus, Institute of Scientific Information's Science Citation Index Expanded®, and Chem Abstracts.

Editor-in-Chief, Lee E. Kirsch, Ph.D., oversees an international editorial board of leading researchers in the pharmaceutical sciences. Kirsch is professor of pharmacy at the University of Iowa, College of Pharmacy.

C.2 Types of manuscripts

The AAPS Journal AAPS Pharm SciTech publish the following article types. For examples of published articles, please visit www.PharmaGateway.net.

C.2.1 Reviews

Reviews, usually by invitation and organized into themed issues, report on recent advances in pharmaceutical research. Unsolicited reviews are considered only if they are authored by investigators who have demonstrated expertise in the relevant areas.

C.2.2 Mini-Reviews

Mini-Reviews discuss a more narrowly focused topic of recent research. Unsolicited reviews are considered only if they are authored by investigators who have demonstrated expertise in the relevant areas.

C.2.3 Original Research Papers

Original Research Papers contain innovative, hypothesis-driven research that is supported by sound experimental design, methodology, and data interpretation.

C.2.4 Brief Technical Notes

Brief Technical Notes, normally more limited in scope than Original Research Papers, must be of high quality, general interest, and sufficient importance to warrant publication.

C.2.5 Rapid Communications

Rapid Communications provide a venue for fast-breaking research updates or other news items. The justification for rapid communication should be stated in the cover letter during submission.

C.2.6 Regulatory Notes

Regulatory Notes provide a summary of regulatory decisions made and rationale for the regulatory decision made on a product. These notes are typically submitted by invitation only, but Authors may propose notes to the Editors.

C.2.7 Editorials, Commentaries, or Summaries

Editorials, Commentaries, or Summaries are usually published by invitation only. These articles contain topical issues of public and scientific interest.

C.2.8 Meeting Reports

Meeting Reports on AAPS or AAPS-affiliated meetings provide readers with summaries of such meetings, including consensus views. When a meeting report purports to be a Consensus Report, authors should review and adhere to the Consensus Report Review and Publishing Guidelines available at http://www.aapspharmaceutica.com/inside/refguide/ConsensusReport-2007.pdf. The corresponding author must complete and submit the Corresponding Author's Consent to Publish Consensus Report (http://www.aapspharmaceutica.com/inside/refguide/Consensus_Rpt_-3) and all contributing authors must complete and submit the Contributing Author's Consent to Publish Consensus Report , available at http://www.aapspharmaceutica.com/inside/refguide/consensus Rpt - contributing author consent form.pdf.

C.2.9 *Meeting Notices*

A Meeting Notice provides readers with information on an upcoming AAPS or AAPS-affiliated meeting, including title of the meeting, date, time, location, an outline and description of meeting topics, and a list of invited speakers. If possible, Meeting Notices should include contact information for the organizers and a URL to the meeting's webpage. Meeting Notices should be submitted to the AAPS Editorial Office two to three months prior to the meeting.

C.2.10 Letters to the Editor

Letters to the Editor may be submitted by readers commenting on articles already published by the journal.

All articles published in the journal will follow the Springer Online First production workflow, enabling publication on the SpringerLink website after receipt of author corrections to page proofs.

C.3 Manuscript submission

AAPS uses Editorial Manager™ as its peer review tracking system. Manuscripts must be submitted online by the Corresponding Author to the appropriate journal (see below).

The AAPS Journal: http://www.editorialmanager.com/aapsj/

AAPS PharmSciTech: http://www.editorialmanager.com/aapspt/

You may be required to register as a new user with Editorial Manager upon your first visit. Straightforward login and registration procedures can be found on the Web site. Editorial Manager allows authors to track the progress of manuscript review in real time. Detailed, step-by-step instructions for submitting manuscripts can be found on the Web site. Manuscripts must be created and saved in Microsoft® Office Word for Windows. All correspondence regarding your manuscript must go through Editorial Manager.

C.3.1 Special Features, Appendices, and Supplementary Material

Special features, appendices, and supplementary material can be accommodated and may contain highly interactive features or large databases. All authors are encouraged to take full advantage of the Web-only capabilities of online publishing, including 3-D, video, and interactive graphics. If a desired technical feature is not covered in the Author's Instructions, please contact the AAPS Editorial Office (see below).

The AAPS Journal: AAPSJsubmit@aaps.org

AAPS PharmSciTech: AAPSPTsubmit@aaps.org

All special features must be created by the Author.

Authors who wish to publish electronic supplementary material to their article (Excel files, images, audio/video files) must submit the supplementary files/materials with their manuscript submission via our online peer review tracking system, Editorial Manager. These files may be submitted as one file or multiple files as desired by the authors. Accepted formats for these files include .doc, .docx, .xls, .xlsx, .jpg, .pdf, and for videos, .mpeg-3 format. Note that supplementary files are not automatically included in the reviewer’s PDF. Therefore, please note in a cover letter if these materials should be evaluated by reviewers only and not be published should the manuscript be accepted, or if the supplemental

files should be included for review and be published with the article should the manuscript be accepted for publication. If the supplemental files are intended for publication, callouts using, “supplemental 1,” “supplemental 2,” etc., should be placed in the appropriate location within the text of the manuscript body.

C.3.2 Hypertext Links

Authors may identify uniform resource locators (URLs) for websites that provide the reader with additional information on the topic addressed in the manuscript. Although URLs are an important feature of electronic publishing, authors are encouraged to be selective in their choice of sites to include. Do not include URLs for web pages with newspaper or journal articles that will be removed or archived to another Web page. Links to pharmaceutical manufacturers or other sources of product information are acceptable; however, providing a URL to the reader should not be substituted for adequate discussion within the manuscript itself. Do not include links to sites that are not accessible without a password.

C.4 Terms of manuscript consideration

C.4.1 AAPS Journals Ethics Policy

The Editors-in-Chief of the three Journals of AAPS, *Pharmaceutical Research*, *The AAPS Journal*, and *AAPS PharmSciTech*, along with the AAPS Publications Committee developed an integrated ethics policy to guide decision-making across the three journals. The document is based on the recommendations on publication ethics policies for medical journals published by the World Association of Medical Editors (WAME), posted at http://wame.org/resources/ethics-resources, and subscribed to by almost 1,000 journals.

Authors are required to review and adhere to the AAPS Journals Ethics Policy (http://www.aaps.org/journalsethics) in full prior to submitting manuscripts to *The AAPS Journal*, *AAPS PharmSciTech*, or *Pharmaceutical Research*. Excerpts from the Policy are outlined below.

C.4.2 Full Disclosure

During the manuscript submission process, all authors will be required to confirm that the manuscript has not been previously published in any language anywhere and that it is not under simultaneous consideration by another journal. Moreover, *The AAPS Journal* and *AAPS PharmSciTech* policy regarding compound disclosure centers on the data. If specific data relating to the study compound are reported, then the Journal requires identification so that reviewers and readers can judge, based on general principles, whether the data are plausible and internally consistent, and to potentially allow future examination and/or validation of the results and conclusions reported. If, however, a library of compounds is used to generate correlations, such as in QSAR when the scope and diversity of the compounds are described, then it is possible that the specific chemical compositions of the compounds need not be identified, subject to the discretion of the reviewers and the Editor.

C.4.3 Conflicts of Interest

Authors will be required to declare all conflicts of interest (or their absence) during the submission of a manuscript. This conflict declaration includes conflicts or potential conflicts of all listed authors. If any conflicts are declared, AAPS will publish them with the paper. In cases of doubt, the circumstance should be disclosed so that the editors may assess its significance.

Conflicts may be financial, academic, commercial, political or personal. Financial interests may include employment, research funding (received or pending), stock or share ownership, patents, payment for lectures or travel, consultancies, nonfinancial support, or any fiduciary interest in a company.

C.5 Copyright transfer

The Copyright Revision Act of 1976 (Public Law 94-533) requires that Authors transfer their copyrights to the Publisher, American Association of Pharmaceutical Scientists, in order to provide for the widest possible dissemination of professional and scientific literature. A signed Transfer of Copyright form must be submitted online with the manuscript. The Transfer of Copyright form for an accepted manuscript must be on file with the AAPS Editorial Office prior to production for publication. Corresponding Authors may print and sign the form on behalf of all authors.

C.6 Ethics in Animal and Clinical Investigations

C.6.1 Human Subjects and Clinical Trials

AAPS Journals require author(s) at the time of manuscript submission to make a statement in the cover letter, indicating documented review and approval from a formally constituted review board (Institutional Review Board or Ethics committee) for all studies involving people, medical records, and human tissues, per the uniform guidelines from the World Medical Association (http://www.wma.net/en/30publications/10policies/HB-E-2011.pdf). Studies and research using human subjects, medical records, and human tissues (including educational research) must also state this compliance within the Methods Section.

The AAPS Journals also require that controlled clinical trials must be registered in a publicly available database or the Journals will not publish the results of these trials. Manuscripts submitted to the Journals must include trial registration information in the cover letter. To register a clinical trial, authors should go to the NIH registry www.clinicaltrials.gov or the International Standard Randomized Controlled Trials database (http://isrctn.org). Further information can be obtained from the International Committee of Medical Journal Editors (ICMJE) at http://www.icmje.org/publishing_10register.html.

C.6.2 Animal Use and Assurances

AAPS Journals require author(s) at the time of manuscript submission to make a statement in the cover letter, indicating that animal experiments are conducted in full compliance with local, national,

ethical,). Investigations using experimental animals (including educational research) must also state this compliance within the Methods Section.

C.7 Originality of manuscripts

Authors of manuscripts submitted to the American Association of Pharmaceutical Scientists are obliged to present accurate representation of the research performed along with an objective discussion of the significance of their findings. The author's submission should be original work that reflects research undertaken with integrity and honesty, and that conforms to ethical practices outlined in the AAPS Journals Ethics Policy. Authors should be willing to reply to any reasonable request from editors, referees, and scientist for materials, methods, or data necessary for verification of the conclusions reported in the paper.

C.7.1 Use of Copyrighted Tables and Figures

A copy of the granted permission to use copyrighted figures and tables must be included with the submitted manuscript.

C.7.2 Peer Review

All submissions will be reviewed anonymously by at least two independent Reviewers. Authors are encouraged to submit names and email addresses of expert reviewers, but selection remains a prerogative of the Editor(s). Authors may include supplementary notes to facilitate the review process. If an accepted paper is cited that has not yet appeared in print and is required for evaluation of the submitted manuscript, authors should provide an electronic version for use by the Reviewers. Authors are responsible for all statements in their work, including changes made by the copyeditor after a manuscript is accepted.

C.8 Manuscript organization

Several components of the manuscript must be submitted as individual files within Editorial Manager: cover letter, title page, manuscript body (including references list), individual figure files, and the Transfer of Copyright.

(*indicates item is required for all manuscript types, unless otherwise specified)

C.8.1 Cover Letter

A cover letter is recommended, but not required. Please note: a cover letter is required for a Rapid Communication submission.

Authors who wish to submit names and email addresses of recommended reviewers for the peer review process may also indicate those in the cover letter.

*C.8.2 Title Page**

The title page must be submitted as a separate file, and should include the title of the article, author names with full first name (no degrees), each author's affiliation, and a suggested running head (of less than 50 characters, including spaces). The affiliation should comprise the department, institution (usually university or company), city, and state (or nation) and should be typed as a footnote to the author's name. For the corresponding author designated to correspond with the Editorial Office and review proofs, indicate his/her complete mailing address, office/cellular telephone number, fax number, and e-mail address.

*C.8.3 Transfer of Copyright Form**

A signed copy of the Transfer of Copyright must be submitted online as part of the manuscript submission process. The Transfer of Copyright is available at http://www.aaps.org/journalsethics.

C.8.4 Abstract

Only Reviews, Mini Reviews, Original Research Articles, Rapid Communications and Meeting Reports require an abstract. The abstract is limited to 250 words or less. For Research Articles, the abstract should include a brief (2 to 3 sentences) statement for each of the following sections: Introduction, Methods and Materials, Results and Discussion, and Conclusion written in paragraph form. All abstracts must be written in one paragraph, with no subheadings, equations, tables, reference citations or graphics.

*C.8.5 Keyword**

Provide a list of no more than 5 key words.

C.8.6 Introduction

Required for Reviews, Mini Reviews, Original Research Articles, and Meeting Reports only.

*C.8.7 Main Text Body**

Please include continuous line numbers in the manuscript body file.

For Original Research Articles, Brief Technical Notes, Rapid Communications, organize the main text as follows: Introduction, Materials and Methods, Results, Discussion, and Conclusion. Combining Results and Discussion is discouraged. The use of subheadings to divide the text is encouraged. Primary, secondary, and third level headings should be clearly defined, but do not use numbers or letters.

Table C.1 Recommended word counts are as follows

Reviews, original research articles and meeting reports	5000
Mini reviews	2500
Brief technical notes, meeting reports and rapid communications	1200

Use abbreviations sparingly, and define them at the first insertion in the text. Define all abbreviations used in tables within the table footnotes Use the metric system for all measurements. Express metric abbreviations in lowercase letters without periods (cm, mL, sec). Define all symbols used in equations and formulas. When symbols are used extensively, the authors may include a list of all symbols in a table.

Numbers should be reported to reflect the precision of the instrumentation utilized. Calculated numbers, such as means and standard deviations, should be expressed to no more than 1 significant digit beyond the precision of the instrument. Normally, data reported to more than 3 significant figures should be justified. The precision of the variability (e.g., standard deviation) should not exceed that of the reported mean value.

C.8.8 Conclusion

The conclusion should be a brief paragraph, containing 3 to 4 sentences, that summarizes the findings presented.

C.8.9 Acknowledgments

Include funding source(s) and other contributions. If the work has been funded by NIH, please provide name(s) of funding institute(s) and grant number(s). This information is required for automatic deposit into PUBMED Central by the Publisher.

C.9 References

References should conform to Vancouver style and be numbered consecutively in the order in which they are cited in the text. Cite in the text by the appropriate Arabic numeral enclosed in parentheses, e.g., (1), (2-5), etc.

Table C.2 Maximum reference limits are as follows:

Reviews, original research articles and meeting reports	100
Mini reviews	40
Brief technical notes, meeting reports and rapid communications	20

References to unpublished peer-reviewed, personal communications, including conference abstracts, and papers in preparation or in review, cannot be listed, but they can be notated parenthetically in the text.

Abbreviations for journal names should conform to those of Vancouver style. The style and punctuation of the references should conform to the following examples:

Type Example

1. Journal article Smith JJ. The world of science. Am J Sci. 1999;36:234–5.
2. Journal article with DOI (and with page numbers) O'Mahony S, Rose SL, Chilvers AJ, Ballinger JR, Solanki CK, Barber RW, et al. Finding an optimal method for imaging lymphatic vessels of the upper limb. Eur J Nucl Med Mol Imaging. 2004;31:555–63. doi:10.1007/s00259-003-1399-3.
3. Journal article by DOI (before issue publication with page numbers) O'Mahony S, Rose SL, Chilvers AJ, Ballinger JR, Solanki CK, Barber RW, et al. Finding an optimal method for imaging lymphatic vessels of the upper limb. Eur J Nucl Med Mol Imaging. 2004. doi:10.1007/s00259-003-1399-3.
4. Article in electronic journal by DOI (no paginated version) Slifka MK, Whitton JL. Clinical implications of dysregulated cytokine production. Dig J Mol Med. 2000. doi:10.1007/s801090000086.
5. Journal article in a supplement Frumin AM, Nussbaum J, Esposito M. Functional asplenia: demonstration of splenic activity by bone marrow scan. Blood 1979;59 Suppl 1:26–32.
6. Book chapter Wyllie AH, Kerr JFR, Currie AR. Cell death: the significance of apoptosis. In: Bourne GH, Danielli JF, Jeon KW, editors. International review of cytology. London: Academic; 1980. p. 251–306.
7. OnlineFirst chapter in a series (without a volume designation but with a DOI) Saito Y, Hyuga H. Rate equation approaches to amplification of enantiomeric excess and chiral symmetry breaking. Top Curr Chem. 2007. doi:10.1007/128_2006_108.
8. Book, authored Blenkinsopp A, Paxton P. Symptoms in the pharmacy: a guide to the management of common illness. 3rd ed. Oxford: Blackwell Science; 1998.
9. Online document Doe J. Title of subordinate document. In: The dictionary of substances and their effects. Royal Society of Chemistry. 1999. http://www.rsc.org/dose/title of subordinate document. Accessed 15 Jan 1999.
10. Online database Healthwise Knowledgebase. US Pharmacopeia, Rockville. 1998. http://www.healthwise.org. Accessed 21 Sept 1998.
11. Supplementary material/private homepage Doe J. Title of supplementary material. 2000. http://www.privatehomepage.com. Accessed 22 Feb 2000.
12. University site Doe, J.: Title of preprint. http://www.uni-heidelberg.de/mydata.html (1999). Accessed 25 Dec 1999.
13. FTP site Doe, J.: Trivial HTTP, RFC2169. ftp://ftp.isi.edu/in-notes/rfc2169.txt (1999). Accessed 12 Nov 1999.
14. Organization site ISSN International Centre: The ISSN register. http://www.issn.org (2006). Accessed 20 Feb 2007.

For a full description of the Vancouver reference style, including numerous examples, please access http://www.nlm.nih.gov/bsd/uniform_requirements.html.

C.10 Tables

Tables must be created in Microsoft Word table format. Tables should be numbered (with Roman numerals) and referred to by number in the text. Center the title above the table, and type explanatory footnotes (indicated by superscript lowercase letters) below the table. Data must be placed in separate cells of the table to prevent text and numbers from shifting when the table is converted for publication on the Internet. Empty cells may be inserted to create spacing. Tables should not duplicate information provided in the text. Instead, tables should be used to provide additional information that illustrates or expands on a specific point the author wishes to make. Each table should be self-explanatory.

C.11 Figures

The AAPS Journal and *AAPS PharmSciTech* offer authors the use of color figures in online published manuscripts, free of charge. Figures (as well as photographs, drawings, diagrams, and charts) are to be numbered in one consecutive series of Arabic numerals in the order in which they are cited in the text. The captions for illustrations and figures should be separated from the text and collated in a separate section called, ''Legend to Figures." All electronic artwork must be submitted online via our online peer review tracking system, Editorial Manager. Figure files should be submitted in .tiff or .eps format (1200 dpi for line and 300 dpi for half-tones and gray-scale art); however, .jpeg, .gif, and .bmp files may also be submitted as long as the dpi specifications above are met. Use of a professional graphics program such as Adobe® Photoshop to edit and/or save photographs and graphics is highly recommended. Because of difficulties with exporting graphics from Microsoft PowerPoint, original graphics (those imported into PowerPoint) must be saved in an acceptable file format (above). Microsoft PowerPoint and Microsoft Word figure files will not be accepted.

Table C.3 The maximum combined count for tables and figures are as follows:

Reviews, original research articles and meeting reports	15 (suggested)
Mini reviews	6
Brief technical notes, meeting reports and rapid communications	6

C.12 Footnotes

Footnotes should be avoided. When their use is absolutely necessary, footnotes should be numbered consecutively using Arabic numerals and should be typed at the bottom of the page to which they refer. Place a line above the footnote, so that it is set off from the text. Use the appropriate superscript numeral for citation in the text.

Annexure D

Journal of Pharmacy & Pharmaceutical Sciences

(J Pharm Pharm Sci) Author guidelines

D.1 Instructions to authors

Manuscripts (in English and single spaced), together with a cover letter from the author responsible for all correspondence, should be submitted via the online submission process, as a file saved in Microsoft Word (.doc). DO NOT UPLOAD DOCX FILES. Spelling, punctuation, sentence structure, spacing, length, and consistency of usage in form and descriptions should be checked before submission. Please also check References for accuracy. Ensure that all figures and tables are mentioned in the text, and that all references are cited in the text.

D.2 Types of manuscripts

The Journal of Pharmacy and Pharmaceutical Sciences (JPPS) publishes research articles, research reports, technical notes, scientific commentaries, news, views and review articles in the physical, chemical, biological, biotechnical, clinical, and socioeconomic-pharmacoeconomic, regulatory aspects of the pharmaceutical sciences.

D.2.1 Formulation development studies are only acceptable if they provide a clear advancement in the field. Applying known formulation techniques to another drug does not suffice. A study of **natural products** will not be accepted if it only reports the pharmacological data of a certain plant or plant extracts. Identification and separation of potential active ingredients coupled with carefully planned pharmacological studies may be acceptable.

D.2.2 Medicinal chemistry papers will be considered if new classes of drugs are studied or if there is a reasonable rationale for developing a new derivative of an old drug. Clear identification and separation of the compounds are needed. Mere synthesis of another derivative will not suffice.
Routine **bioequivalence** studies, i.e., a comparison of the bioavailability of two or more products, will not be accepted for publication.

D.2.3 Analytical method development for formulations will not be acceptable unless it contains experiments with sufficient scientific rigor and breakthrough data.

D.3 English proof reading and writing

Manuscript will be accepted only when the writing style and the use English language are deemed appropriate. Authors may choose to contact editing services such as those listed below with full realization that the Journal accept no responsibility or liability regarding the service rendered and its associated business transaction.

•Psi-On Technical and Consulting
•Scientific Proofreading Services
•American Journal Experts, Scientific Editing

•BluePencil Science
•San Francisco Edit
•Proof-Reading-Service
•ScienceDocs
•Alpha Science Editors
•Language Edit
•SciTechedit International
•Asiascienceediting
•English Journal Experts
•Manuscript Editor Online
•Cambridge Proofreading LTD

Please submit a single Word.doc version of your manuscript that includes all tables and figures at appropriate locations. The file name should include your last (family) name and a keyword from the title of your manuscript. The file name cannot be longer than 30 characters, and should contain only letters or numbers. Do not use punctuation or symbols in the file name.

D.4 Format:

For each section, the sub-title appears as BOLD CAPITAL, and subsequent titles as Bold Sentence and then, if required, Bold Italic Sentence. Text should be set in Times New Roman font, 11 point. Leave only one (1) space after periods. Start new paragraphs with an indent except for the first paragraph after a title. Do not use spaces to create indents. Use line returns only at the end of paragraphs and do put blank lines between paragraphs. Use the Symbol font for symbols and special characters. Do not use equation editors or footnoting utilities in your files. Equations should be numbered consecutively with Arabic numerals in parentheses on the right hand side of the page. Number pages (bottom, centre). Use proper Superscripts and Subscripts, not raised or lowered text.

D.5 Title Page:

The title page should include the title of the article, author's name with full first name (no degrees), and author’s affiliation. The affiliation should comprise the department, institution (usually university or company), city, and state (or nation) and should be typed as a footnote to the author's name. For office purposes, the title page should include the name and complete mailing address including country, and email address of the one author designated to review proofs. The title page should start below the top margin, be single-spaced, and no space left before the Abstract.

D.6 Abstract:

A structured abstract of fewer than 300 words is required of research articles and reports and should be arranged, in one paragraph, under the following headings: PURPOSE, METHODS, RESULTS, CONCLUSIONS. Review articles also require an abstract, which need not be organized under these

headings. The purpose of a structured abstract is to assist authors in organizing their thoughts - not only to highlight their work, but also to aid readers to grasp quickly the essence of the paper.

D.7 Novelty of the Work: Provide a brief description of not more than four short sentences regarding the novelty of the paper in the cover letter.

D.8 The Main Body of the Manuscript:

This section must contain Introduction, Methods, Results and Discussion. **Do not combine Results and Discussion**.

Under INTRODUCTION clearly state the novelty of the work.

Ethics in Animal and Clinical Investigations:

Investigations using experimental animals must adhere to the "Guide to the Care and Use of Experimental Animal Care" (Canadian Council on Animal Care guidelines, 1984). All papers containing animal data must Include a statement from your university's Animal Ethics Committee approving your protocol. Investigations with human subjects must follow the Declaration of Helsinki guidelines (1964) and be approved by the institutional human experimentation committee, or equivalent, and have signed in-formed consent.

Ethics Approval for Animal and Human Studies:

Statement that approval has been received must be included under the METHODS Section.

D.9 Statistical Approach:

The number of repeat measurements and the variance of the means must be clearly depicted in the texts and in the illustrations.

Reasonable significant figures (usually three) must be used as elaborated in Levy G. Significant figures or significant nonsense? Clin Pharmacol Ther, 59:363, 1996 or Wikipedia.

The significant figures (SF) of a number are all certain digits plus the first uncertain digit. For example, if an assay has a sensitivity of 1 mg/L, a concentration of 32.32 mg/L has one extra uncertain and unnecessary figure. Hence, it should be reported as 32.3 which contains three SFs. See below for calculation of SFs:

- 31 has 2 SF
- 301 has 3 SFs
- 0.022 has 2 SFs (leading zeros don’t count
- 4.300 has 4 SFs (trailing zeros after decimal point count)
- 310 has 3 SFs (rounded off since a trailing zero with no decimal point is ambiguous)

D.10 Figures:

Figures should be numbered in one consecutive series of Arabic numerals in the order in which they are cited in the text, and designed to fit the column or page size of the Journal. All parts of a figure must be “grouped” with no segmented text box. Left justify the title below the figure (bold font). Keys to symbols should be a part of the figure, and not a part of the caption. Use the same typeface for all figures. Labels should be in title case. Figure legends should be informative and self-explanatory.

D.11 Tables:

Tables should be numbered consecutively (with Arabic numerals), referred to by number in the text and designed to fit the column or page size of the Journal. Prepare numerical illustrations (e.g., tables) using the "table" function (rows and columns). Do not make table using text functions such as tabs, spaces or lines. Hide lines except under the column headings. Left justify the title above the table (bold font). Captions should be typed separately. Table legends should be informative and self-explanatory.

D.12 Footnotes:

Footnotes should be avoided. When their use is necessary, footnotes should be numbered consecutively using Arabic numerals and should be typed at the bottom of the page to which they refer. Place a line above the footnote, so that it is set off from the text.

D.13 Abbreviations:

Try to use abbreviations sparingly. When used extensively, provide a list of all non-standard abbreviations on a separate page before the reference section. Use the metric system for all measurements without periods (cm, ml, s). Define all symbols used in equations and formulas. When symbols are used extensively, include a list of all symbols in the notation section. Do not abbreviate the word "Figure" or "Table" in titles or text.

D.14 References:

References should be numbered consecutively in the order in which they are cited in the text. Cite in the text by the appropriate Arabic numeral enclosed in parentheses, e.g., (1) or (2-5), not super or sub scripted. References to unpublished personal communications should be avoided. Use ( ) for reference citation in the text. Place punctuation AFTER the reference. For each reference, use a single continuous paragraph with no extra space or line break. Do not use "add-ins" such as EndNotes. Abbreviations for journal names should conform to those in the Bibliographic Guide for Editors and Authors (American Chemical Society, Washington, D.C.). Although CSPS accepts various reference formats, the Vancouver style is preferred. Alternatively, the references should conform to the following style and punctuation:

Journal Article:

Davies NM, Jamali F. COX-2 selective inhibitors cardiac toxicity: Getting to the heart of the matter. J Pharm Pharm Sci, 2004; 7:332-336.

Book:

Mutschler, D.; Derendorf, H., Drug Actions, Basic Principles and Therapeutic Aspects. CRC, Ann Arbor, MI, USA, 1995.

Contribution to a Book:

Jamali, F., Stereochemically Pure Drugs: An Overview, in Wainer IW: Drayer D (eds), Drug Stereochemistry: Analytical Methods and Pharmacology. 2nd ed., Marcel Dekker, INC, New York, NY, pp 375-384, 1993.

D.15 Acknowledgments:

All acknowledgments (including those for grant and financial support) should be typed in one paragraph directly preceding the reference section. Authors of manuscripts submitted to JPPS are requested to state the source of all funding that enabled the research described to be undertaken.

D.16 Manuscript Submission:

Manuscripts will be received by Online Submission. Manuscripts are reviewed anonymously by independent referees. To facilitate the review process, the authors should submit supplementary material such as a cited accepted (but not published) paper, which may be required for assessment of the submitted manuscript. Careful preparation of manuscripts and subsequent review of page proofs are essential, as the authors are responsible for all statements and content.

D.17 Copyright and Reference Citation:

Submitted manuscripts must not be published previously or be currently under consideration for publication elsewhere. Acceptance of a manuscript for publication in the Journal will automatically place the manuscript under the terms and conditions of Creative Commons license (Attribution-ShareAlike). Authors must cite the source of any quotation or statement inserted in the manuscript. Authors must obtain permission from publisher for any illustration and table copied or adapted from a published material. Such permissions must arrive in the Journal office via direct e-mail or fax from the publisher or original letter before the manuscript can be published.

D.18 Submission Preparation Checklist

As part of the submission process, authors are required to check off their submission's compliance with all of the following items, and submissions may be returned to authors that do not adhere to these guidelines.

1. Have included a novelty statement as instructed under Authors Instruction.

2. Have read the new Author Instructions including the requirement for a novelty statement and the type of manuscript.
3. The text adheres to the stylistic and bibliographic requirements outlined in the Author Guidelines, which is found in About the Journal.
4. The submission file is in Microsoft Word document file format.
5. The submission has not been previously published, nor is it before another journal for consideration.
6. The Authors have read and approved the copyright policy of the Journal which is according to the terms and conditions of Creative Common license (Attribution-ShareAlike) License.
7. Authors have cited the source of any quotation or statement inserted in the manuscript. Authors have obtained permission from publisher for any illustration and table copied or adapted from a published material. Such permissions must arrive in the Journal office via direct e-mail or fax from the publisher or original letter before the manuscript can be published.
8. Authors will realize that the manuscript will be accepted only when the writing style and the use English language are deemed appropriate. Authors may choose to contact editing services such as those listed above under "English Proof Reading and Writing" with full realization that the Journal accept no responsibility or liability regarding the service rendered and its associated business transaction.

D.19 Copyright Notice

Submitted manuscripts must not be published previously or be currently under consideration for publication elsewhere. Acceptance of a manuscript for publication in the Journal is with the authors' approval of the terms and conditions of the Creative Commons copyright license Creative Common license (Attribution-ShareAlike) License. Authors must cite the source of any quotation or statement inserted in the manuscript. Authors must obtain permission from publisher for any illustration and table copied or adapted from a published material. Such permissions must arrive in the Journal office via direct e-mail or fax from the publisher or original letter before the manuscript can be published.

D.20 Privacy Statement

The names and email addresses entered in this journal site will be used exclusively for the stated purposes of this journal and will not be made available for any other purpose or to any other party.

Annexure E

Supplementary information for Chapters 4 & 5

E.1 Method development and validation of a UV spectrophotometric method for the determination of Pyrimethamine

Introduction and purpose

An UV spectrophotometric method was developed and validated for the quantitative analysis of Pyrimethamine (from Pyr-MeOH, Pyr-DMF and Pyr-DMA) from the solubility experiments performed in 0.1M HCl (pH 1.2), acetate buffer (pH 4.5) and phosphate buffer (pH 6.8). The purpose of the validation was to ensure that all quantitative measurements that were made were accurate and reliable and that the method developed was suitable for its intended purpose.

The method validation was based on the ICH Q2 (R1) guidelines (ICH, 2005:1-13). The validation parameters evaluated were determined based on the objective of the analytical method.

E.1.1 Equipment and materials

- A Cary-50 UV spectrophotometer (Varian, Palo Alto, California) was used for method development, validation and subsequent analysis of solubility samples.
- A Crison Basic-20 pH meter (Crison, Capri, Italy) was utilised for pH determinations.
- A Sartorius R200D analytical balance (Labotec, Midrand, South Africa) was used for weighing of all samples and reference material.
- Deionised water was used for the preparation of all aqueous solutions and/or media. The deionised water was generated using a Merck-Millipore Milli-Q water system (Merck, Modderfontein, South Africa).
- A Binder FD 23 incubator (Binder, Bohemia, New York) was utilised for the robustness study.
- A-grade, class 1 glassware was used.

The materials used in the method validation/analysis were as follows:

- **0.1M HCl:** was prepared using a dilution of 1 ml 32% HCl (Merck, South Africa) in 1 liter Milli-Q water (pH = 1.2 ± 0.05).
- **Acetate buffer (pH 4.5):** was prepared by dissolving 11.4 ml glacial acetic acid (Merck, South Africa) in 100 ml Milli-Q water. 14 ml of this acetic acid solution was mixed with 2.99 g sodium acetate trihydrate (Merck, South Africa) and 900 ml Milli-Q water. The pH was thereafter adjusted

(if necessary) to a pH of 4.5 ± 0.05. The solution was then diluted with water to the final volume of 1 liter.

- **Phosphate buffer (pH 6.8):** was prepared as follows: 6.805 g potassium dihydrogen phosphate (Merck, South Africa) and 0.896 g sodium hydroxide (Merck, South Africa) were dissolved in 800 ml Milli-Q water. The pH was then adjusted (if necessary) to a pH of 6.8 ± 0.05. The solution was then diluted with water to 1 liter.
- USP Pyrimethamine reference standard, batch number PYR0409007 (USP, Arlington Virginia, USA), was used for quantitative analysis.

E.1.2 Method development

The UV absorbance spectra of Pyrimethamine in 0.1M HCl (pH 1.2), acetate buffer (pH 4.5) and phosphate buffer (pH 6.8) at a concentration of ~ 27 µg/ml were recorded (Figure E.1)

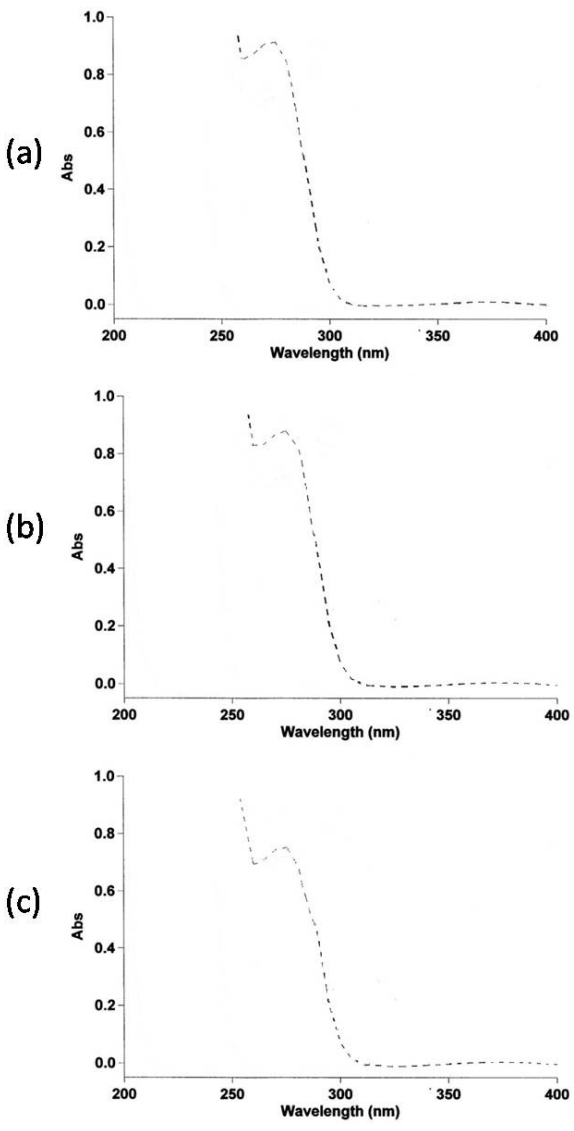

Figure E.1 The UV spectra of Pyrimethamine in (a) 0.1M HCl (pH 1.2), (b) acetate buffer (pH 4.5) and (c) phosphate buffer (pH 6.8).

Pyrimethamine exhibited an UV absorbance maximum (UV_{max}) at 275 nm (Fig. E.1), which corresponded with that reported by the USP Pyrimethamine tablets monograph dissolution method (USP, 2014).

Five volumetric solutions of Pyrimethamine with different concentrations were prepared in the three different solubility media - Table E.1. The UV absorbance values of these solutions were determined at the UV_{max} (275 nm).

Table E.1 Preparation of Pyrimethamine solutions in concentrations ranging from 3.6 – 36 µg/ml

Solution	Preparation	Concentration
A	Accurately weigh approximately 18.0 mg Pyrimethamine reference standard and dissolve it in 500 ml of the specific medium*	36.0 µg/ml
B	Dilute 15 ml of Solution A to a final volume of 20 ml using the specific medium*	27.0 µg/ml
C	Dilute 5 ml of Solution A to a final volume of 10 ml using the specific medium*	18.0 µg/ml
D	Dilute 5 ml of Solution A to a final volume of 20 ml using the specific medium*	9.0 µg/ml
E	Dilute 10 ml of Solution A to a final volume of 100 ml using the specific medium*	3.6 µg/ml

*medium can be either 0.1M HCl, acetate buffer (pH 4.5) or phosphate buffer (pH 6.8)

Standard calibration curves for Pyrimethamine in the three solubility media were constructed and are depicted in Figure E.2. From Figure E.2 it is clear that a linear relationship exists between the UV absorbance values and the concentrations of the Pyrimethamine in the three media in the concentration range of 3.6 – 36.0 µg/ml. The samples exhibited absorbance values which ranged between 0.10 and 1.17 which were within the analytical range of the UV spectrophotometer.

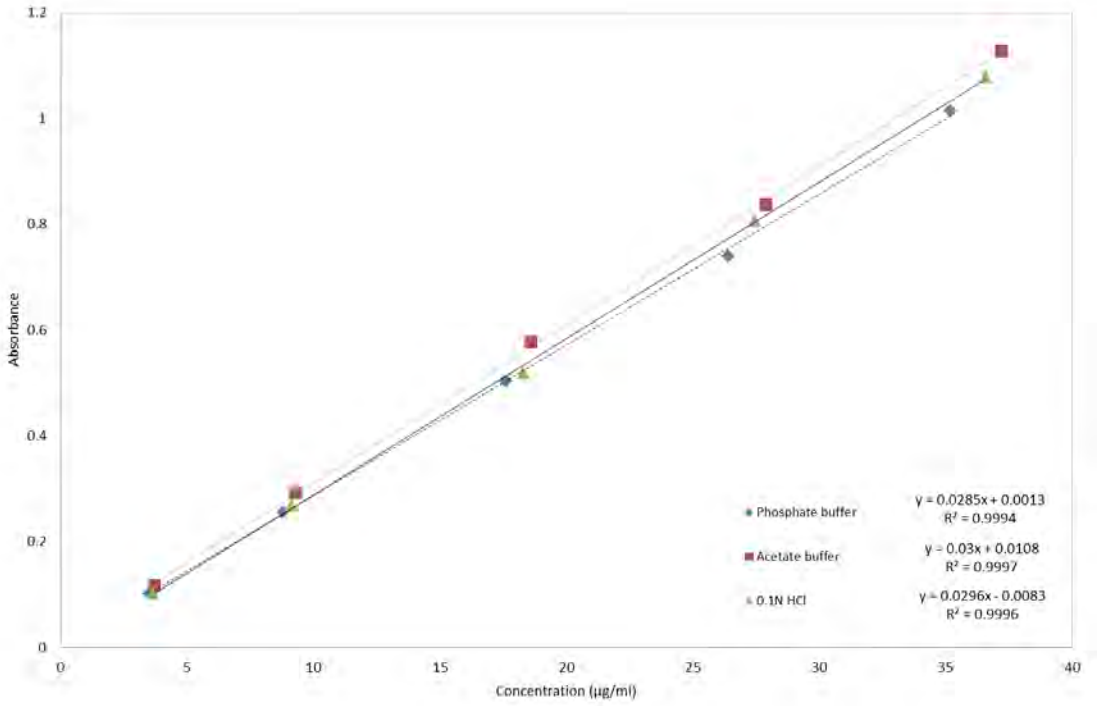

Figure E.2 Standard calibration curves for Pyrimethamine in 0.1M HCl (pH 1.2), acetate buffer (pH 4.5) and phosphate buffer (pH 6.8).

E.1.3 Description of the method used for the solubility studies

The solubility of the three solvatomorphs (i.e. Pyr-MeOH, Pyr-DMF and Pyr-DMA) was determined in 0.1M HCl (pH 1.2), acetate buffer (pH 4.5) and phosphate buffer (pH 6.8).

The solubility samples were prepared in triplicate by transferring approximately 50 mg of sample (i.e. respective solvatomorphs) and 5 ml of the medium (i.e. respective medium) into a test tube. The test tubes were sealed and affixed to a mechanical rotator, which was installed into a temperature regulated water bath. The temperature of the water bath was set to three different temperatures per experiment (30 ± 0.5 ºC, 35 ± 0.5 ºC and 40 ± 0.5 ºC). The test tubes were rotated at 50 ± 2 rpm inside the water bath for a period of 24 hours, after which the solutions were filtered through a 0.45 µm Millipore® filter (Millipore, South Africa) to remove any undissolved matter. Aliquots from the filtered solutions were then suitably diluted (with the specific medium) to ensure that the UV absorbance of the diluted solutions (at 275 nm in a 10 mm cell) was within the established absorbance response range (0.10 - 1.17).

The concentrations of Pyrimethamine in the diluted solutions were determined using the linear equations presented in Figure E.2. The quantities of Pyrimethamine dissolved in the original 5 ml media were determined using equation E.1:

$$\delta = \left[\frac{Abs - c}{m \times 1000}\right] \times D_f$$ (equation E.1)

Where: δ = solubility - concentration of Pyrimethamine expressed as mg/ml; *Abs* = UV absorbance value at 275 nm; *c* = y-intercept of linear equation, *m* = slope of linear equation, D_f = dilution factor based on degree of dilution to obtain an UV absorbance value in the range: 0.10 and 1.17 and 1000 = conversion factor from µg/ml to mg/ml.

E.1.4 Method validation

E.1.4.1 Validation parameters and acceptance criteria

The parameters and their respective acceptance criteria that were selected for the validation are summarised in Table E.2.

Table E.2 Validation parameters and their acceptance criteria

Validation parameter	Acceptance criteria
Specificity	No interference from the solvents incorporated in the solvatomorphs (i.e. methanol, N,N-dimethylformamide and N,N-dimethylacetamide) at the absorbance maximum of Pyrimethamine.
Linearity and range	A regression line with a correlation coefficient (r^2) not less than 0.99 using at least 5 concentration points across the chosen range (3.6 – 36.0 µg/ml).
Accuracy	Recovery must be between 98.0 - 102.0%. At least 9 determinations should be made over a minimum of 3 concentrations (3 determinations per concentration) covering the analytical range.
Precision (Repeatability):	% RSD of recovery values is not more than 2.0%. At least 9 determinations should be made over a minimum of 3 concentrations (3 determinations per concentration) covering the analytical range.
Limit of quantification (LOQ)	LOQ established to determine the lowest amount of Pyrimethamine that can be quantitatively determined with suitable precision and accuracy.
Robustness	The sample solution (Sample solution U) should not show a deviation of more than 2% from the initial value when stored over a period of 24 hours at 45°C.

The ICH guideline for validation of analytical methods states that: "*the extent to which intermediate precision should be established depends on the circumstances under which the procedure is intended to be used"* (ICH Q2(R1):10). Intermediate precision was not included in this study as it was not deemed necessary to do so, since all experiments were performed using the same laboratory equipment and executed by one analyst for comparative purposes (i.e. comparative solubility studies). The solubility method developed for this study is not intended for standardisation (for instance inclusion in a pharmacopoeia), thus does not necessitate evaluation of intermediate precision (ICH 2005:10).

E.1.5 Procedure and results

E.1.5.1 Specificity

The potential interference from methanol, N,N-dimethylformamide and N,N-dimethylacetamide (that may be released from the solvated crystal lattices of Pyr-MeOH, Pyr-DMF and Pyr-DMA respectively) on the detection of Pyrimethamine, needs to be evaluated.

Prepare the solutions specified in Table E.3. Record the UV absorption spectra of these solutions within the range 200 – 400 nm in a 10 mm cell, using the applicable solubility medium as blank.

The absorbance maximum of Pyrimethamine was found to be at 275 nm in all the media (Figure E.1). The UV absorbance spectra of Solutions F – N (Figures E.3 – E.5) did not reveal any peaks at 275 nm. It can thus be concluded that the solvents incorporated in the solvatomorphs (i.e. methanol, N,N-dimethylformamide and N,N-dimethylacetamide) do not interfere at the absorbance maximum of Pyrimethamine.

Table E.3 Preparation of solutions for specificity study

Solution	Composition
F	20 ml methanol & 80 ml 0.1M HCl
G	20 ml methanol & 80 ml acetate buffer (pH 4.5)
H	20 ml methanol & 80 ml phosphate buffer (pH 6.8)
I	20 ml DMF & 80 ml 0.1M HCl
J	20 ml DMF & 80 ml acetate buffer (pH 4.5)
K	20 ml DMF & 80 ml phosphate buffer (pH 6.8)
L	20 ml DMA & 80 ml 0.1M HCl
M	20 ml DMA & 80 ml acetate buffer (pH 4.5)
N	20 ml DMA & 80 ml phosphate buffer (pH 6.8)

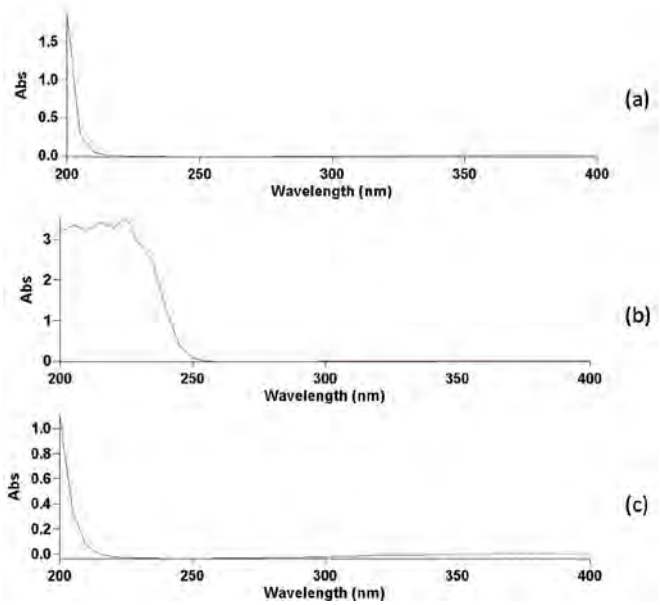

Figure E.3 The UV spectra of (a) Solution F (methanol & 0.1M HCl), (b) Solution G (methanol & acetate buffer (pH 4.5)) and (c) Solution H (methanol & phosphate buffer (pH 6.8)).

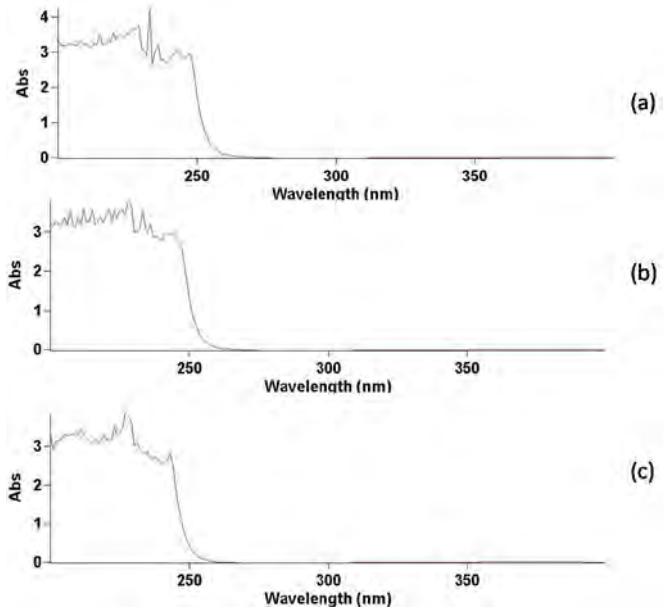

Figure E.4 The UV spectra of (A) Solution I (DMF & 0.1M HCl, (B) Solution J (DMF & acetate buffer (pH 4.5)) and (C) Solution K (DMF & phosphate buffer (pH 6.8)).

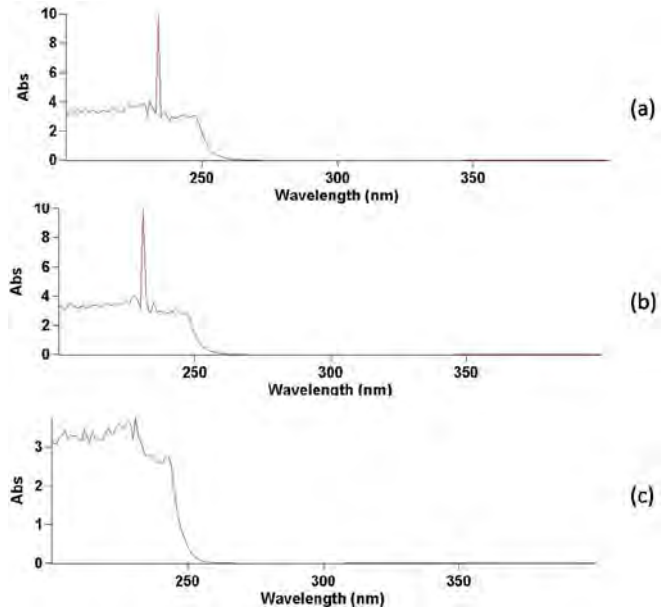

Figure E.5 The UV spectra of (A) Solution L (DMA & 0.1M HCl, (B) Solution M (DMA & acetate buffer (pH 4.5)) and (C) Solution N (DMA & phosphate buffer (pH 6.8)).

E.1.5.2 Linearity and range

Prepare volumetric solutions (in five-fold) of the Pyrimethamine reference standard in the various solubility media with concentrations ranging from 3.6 – 36.0 µg/ml – Table E.4. Determine the UV absorbance values of the solutions described in Table E.4 at the UV_{max} (275 nm), using the respective solubility medium to blank the UV spectrophotometer in a 10 mm cell. Plot the average UV absorbance values obtained as a function of their concentrations, perform least squares linear regression analysis and calculate the correlation coefficient.

Table E.4 Preparation of Pyrimethamine solutions in concentrations ranging from 3.6 – 36.0 µg/ml for linearity and range analysis

Solution	Preparation	Concentration
O	Accurately weigh approximately 18.0 mg Pyrimethamine reference standard and dissolve it in 500 ml of the specific medium*	~36.0 µg/ml
P	Dilute 15 ml of Solution O to a final volume of 20 ml using the specific medium*	~27.0 µg/ml
Q	Dilute 5 ml of Solution O to a final volume of 10 ml using the specific medium*	~18.0 µg/ml
R	Dilute 5 ml of Solution O to a final volume of 20 ml using the specific medium*	~9.0 µg/ml
S	Dilute 10 ml of Solution O to a final volume of 100 ml using the specific medium*	~3.6 µg/ml

*medium can be either 0.1M HCl, acetate buffer (pH 4.5) or phosphate buffer (pH 6.8)

Plots of the average UV absorbance values for the volumetric solutions in the three solubility media as a function of their concentrations with their respective linear regression equations and correlation coefficients are presented in Figure E.6.

Each data point (in Figure E.6) represents the average of five determinations, and the error bars the standard deviation from the average at that point. The regression lines in all three solubility media had a correlation coefficient greater than 0.99 over the concentration range of 3.6 – 36.0 µg/ml. The regression lines in all three solubility media had y-intercepts which did not differ significantly (p-value > 0.05) from zero.

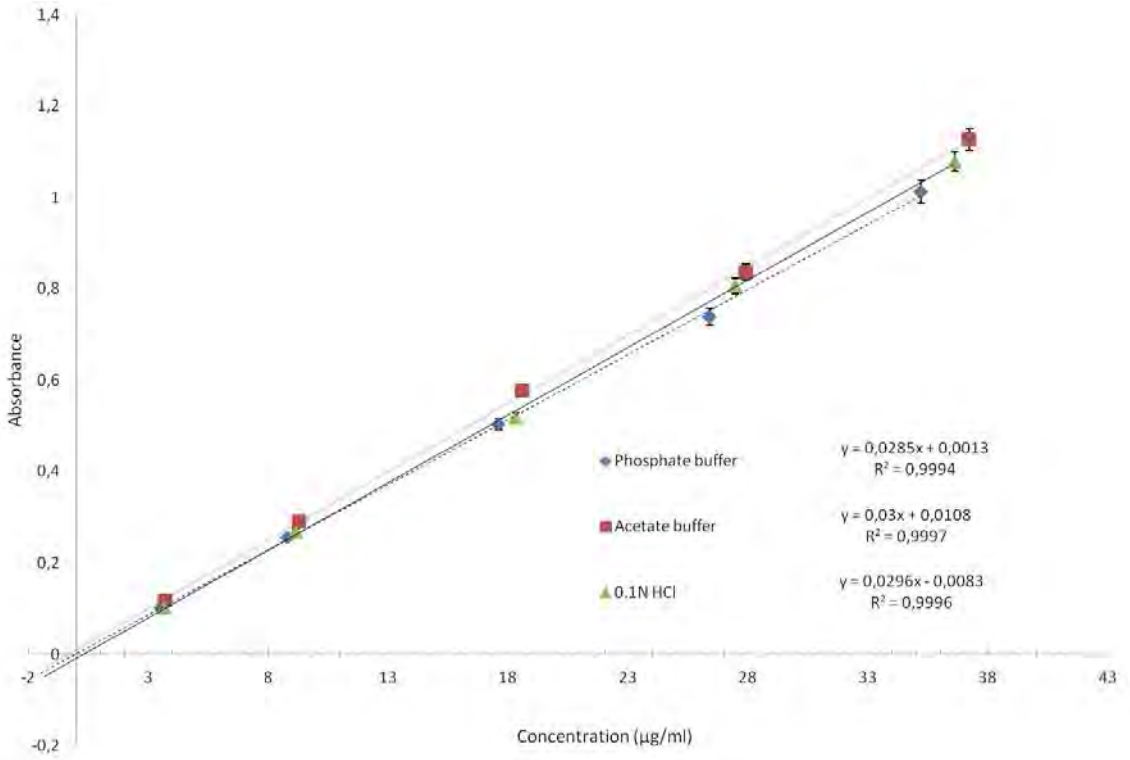

Figure E.6 Standard calibration curves for Pyrimethamine in 0.1M HCl (pH 1.2), acetate buffer (pH 4.5) and phosphate buffer (pH 6.8) with error bars indicated.

E.1.5.3 Accuracy and repeatability

Prepare three volumetric solutions (in triplicate) of the Pyrimethamine reference standard in the various solubility media with the concentrations specified in Table E.5. Determine the UV absorbance values of the solutions described in Table E.5 in a 10 mm cell at the UV_{max} (275 nm), using the respective solubility medium to blank the UV spectrophotometer. Use the equation for the linear regression graph obtained for linearity and range testing (section E.1.5.2) to calculate the % recovery for accuracy.

Table E.5 Preparation of Pyrimethamine solutions in concentrations ranging from 3.6 – 36.0 µg/ml for accuracy and repeatability analysis

Solution	Preparation	Concentration
T	Accurately weigh approximately 18.0 mg Pyrimethamine reference standard and dissolve it in 500 ml of the specific medium*	~36.0 µg/ml
U	Accurately weigh approximately 13.5 mg Pyrimethamine reference standard and dissolve it in 500 ml of the specific medium*	~27.0 µg/ml
V	Accurately weigh approximately 18.0 mg Pyrimethamine reference standard and dissolve it in 500 ml of the specific medium* Dilute 10 ml of this solution to a final volume of 100 ml using the specific medium*	~3.6 µg/ml

*medium can be either 0.1M HCl, acetate buffer (pH 4.5) or phosphate buffer (pH 6.8)

The accuracy and repeatability results obtained are tabulated in Table E.6.

Table E.6 Accuracy and repeatability results for the UV spectrophotometric analysis of pyrimethamine solutions in 0.1M HCl (pH 1.2), acetate buffer (pH 4.5) and phosphate buffer (pH 6.8)

	Solution V ≈ 3.6 µg/ml			**Solution U ≈ 27 µg/ml**			**Solution T ≈ 36.0 µg/ml**		
	0.1M HCl	Acetate buffer	Phosphate buffer	0.1M HCl	Acetate buffer	Phosphate buffer	0.1M HCl	Acetate buffer	Phosphate buffer
	Accuracy: % Recovery								
Sample 1:	98.0%	98.1%	100.7%	100.3%	98.8%	98.1%	100.8%	100.0%	100.9%
Sample 2:	99.4%	98.2%	100.3%	100.3%	98.8%	98.1%	101.0%	100.0%	101.0%
Sample 3:	98.0%	98.3%	99.9%	100.3%	98.7%	98.1%	100.9%	99.9%	100.9%
Average:	98.5%	98.2%	100.3%	100.3%	98.7%	98.1%	100.9%	99.9%	100.9%
Repeatability % RSD	0.82%	0.14%	0.40%	0.03%	0.04%	0.01%	0.10%	0.04%	0.07%

The % recovery results reported in Table E.6 were between 98.0 -101.0% (acceptance criterion 98.0 – 102.0%). The repeatability for the recovery results was found to be satisfactory with %RSD values ranging between 0.01 – 0.82% (acceptance criterion ≤ 2.0%).

E.1.5.4 Limit of quantification (LOQ)

The LOQ values in all three solubility media were calculated based on the standard deviation of the response and slope, an approach described in ICH Q2(R1) (2005:11) – Table E.7.

Calculate the LOQ values in all three solubility media using equation E.2 and the linear regression data obtained in Section E.1.5.2.

$$LOQ = \frac{10\sigma}{S} \qquad \text{(equation E.2)}$$

Where: σ is the standard deviation of the y-intercept of the regression line and S the slope of the calibration curve.

Table E.7 LOQ values for the UV spectrophotometric analysis of Pyrimethamine in the various solubility media

Medium	LOQ (µg/ml)
0.1M HCl	2.7
Acetate buffer pH 4.5	2.4
Phosphate buffer pH 6.8	2.3

The lowest concentration used to establish linearity and range (± 3.6 µg/ml) exceeded the LOQ values calculated for all of the solubility media.

As mentioned in the solubility study method (Section E.1.3) the final diluted solutions (used for quantification) had UV absorbance values which ranged between 0.10 and 1.17, which correlated with a concentration of 3.6 – 36.0 µg/ml to ensure the results obtained are determined with suitable precision and accuracy.

E.1.5.5 Robustness

The solubility studies were performed at 30, 35 & 40 °C over period of 24 hours. It was therefore necessary to investigate the stability of Pyrimethamine in the respective solubility media. It was decided to subject Solution U (in all respective media – Table E.5) to robustness testing at 45°C.

Calculate the Pyrimethamine concentration of Solution U (immediately after preparation) using the applicable linear regression equation in Figure E.6. Thereafter store this solution in a temperature

controlled incubator at 45°C for 24 hours. Determine the UV absorbance values of the solutions in a 10 mm cell at the UV_{max} (275 nm), using the respective solubility medium to blank the UV spectrophotometer. Calculate the Pyrimethamine concentration in the solutions and calculate the % recovery using equation E3.

$$\%Recovery = \frac{C_{24\,hrs}}{C_{0\,hrs}} \times 100\% \qquad \text{(equation E.3)}$$

Where: % Recovery = percentage recovery of Solution U after 24 hours storage at 45°C, C_{0hrs} = calculated concentration of Solution U (µg/ml) immediately after preparation, C_{24hrs} = calculated concentration of Solution U (µg/ml) 24 hours post storage at 45 °C.

The results obtained are tabulated in Table E.8.

Table E.8 Recovery values obtained for robustness study

	0.1M HCl (pH 1.2)	**Acetate buffer (pH 4.5)**	**Phosphate buffer (pH 6.8)**
Initial concentration – C_{0hrs} (µg/ml)	27.22	28.60	25.76
Concentration after 24 hours at 45°C – C_{24hrs} (µg/ml)	27.13	28.30	25.87
% Recovery	99.7%	99.0%	100.4%

The % recovery for Pyrimethamine in all three solubility media when stored at 45°C for 24 hours did not deviate from the initial value by more than 2.0%, conforming to the robustness criterion.

E.1.6 Conclusion

An UV spectrophotometric method was developed and validated for the quantitative analysis of Pyrimethamine (from Pyr-MeOH, Pyr-DMF and Pyr-DMA) from the solubility experiments performed in 0.1M HCl (pH 1.2), acetate buffer (pH 4.5) and phosphate buffer (pH 6.8).

This method was proven to be specific and had linear responses within the range of 3.6 – 36.0 µg/ml. Accuracy and repeatability were demonstrated. Robustness with respect to the samples revealed that Pyrimethamine remained stable (within acceptable limits) for 24 hours when stored at 45 °C.

A summary of the results and acceptance criteria are presented in Table E.9.

Table E.9 Summary of the results and acceptance criteria for the validation study

Parameter	Acceptance limits	Result	Compliance statement
Specificity	No interference from the solvents incorporated in the solvatomorphs (i.e. methanol, N,N-dimethylformamide and N,N-dimethylacetamide) at the absorbance maximum of Pyrimethamine.	No interference of the incorporated solvents were detected in all three solubility media.	Complies
Linearity and range	A regression line with a correlation coefficient (r^2) not less than 0.99 using at least 5 concentration points across the chosen range (3.6 – 36.0 µg/ml).	Regression lines with correlation coefficients (r^2) greater than 0.99 at concentrations ~ 3.6, 9.0, 18.0, 27.0 & 36.0 µg/ml in all three solubility media were obtained.	Complies
Accuracy	Recovery must be between 98.0 - 102.0%. At least 9 determinations should be made over a minimum of 3 concentrations (3 determinations per concentration) covering the analytical range.	Recovery values from all solubility media ranged between 98.0 – 101.0% (n=9 per solubility medium).	Complies
Precision (Repeatability):	% RSD of recovery values is not more than 2.0%. At least 9 determinations should be made over a minimum of 3 concentrations (3 determinations per concentration) covering the analytical range.	% RSD of the recovery values (n=9 per solubility medium) ranged between 0.01 – 0.82% covering the analytical range of 3.6 - 36.0 µg/ml.	Complies

Table E.9 Summary of the results and acceptance criteria for the validation study (continued)

Parameter	Acceptance limits	Result	Compliance statement
Limit of quantification (LOQ)	LOQ established to determine the lowest amount of Pyrimethamine that can be quantitatively determined with suitable precision and accuracy.	LOQ values calculated in all three solubility media ranged between 2.3 – 2.7 µg/ml. The lowest concentration used to establish linearity and range (±3.6 µg/ml) exceeded the LOQ values calculated for all of the solubility media.	Complies
Robustness	The sample solution (Sample solution U) should not show degradation of more than 2.0% over a period of 24 hours when stored at 45°C.	The % Recovery for Pyrimethamine in all three solubility media when stored at 45°C for 24 hours did not deviate from the initial value by more than 2.0% (-1.0% to +0.4%).	Complies

As can be seen from Table E.9, all the method validation parameters were within their specified acceptance limits, thus the method can be deemed suitable for its intended purpose.

E.1.6 Bibliography

ICH see INTERNATIONAL CONFERENCE ON HARMONISATION OF TECHNICAL REQUIREMENTS FOR REGISTRATION OF PHARMACEUTICALS FOR HUMAN USE.

INTERNATIONAL CONFERENCE ON HARMONISATION OF TECHNICAL REQUIREMENTS FOR REGISTRATION OF PHARMACEUTICALS FOR HUMAN USE. 2005. ICH Harmonised Tripartite Guideline. Validation of analytical procedures: text and methodology Q2(R1). http://www.emea.europe.eu. Date of access: 24 September 2014.

USP see UNITED STATES PHARMACOPOEIA.

UNITED STATES PHARMACOPOEIA. Pyrimethamine tablets monograph. [Web:] www.uspnf.com. Date of access: 1 November 2014.

E.2 Structural data

Please refer to the CD included herewith for electronic cif files or visit http://www.ccdc.cam.ac.uk/pages/Home.aspx.

Annexure F

European Journal of Pharmaceutical Sciences

(Eur J Pharm Sci) Author guidelines

F.1 Introduction

Manuscripts submitted to the journal are accepted on the understanding that: (1) they are subject to editorial review, (2) they have not been and will not be published in whole or in part in any other journal and (3) the recommendations of the Declarations of Helsinki and Tokyo, for humans, and the European Community guidelines as accepted principles for the use of experimental animals, have been adhered to. The European Journal of Pharmaceutical Sciences will, therefore, only consider manuscripts that describe experiments which have been carried out under approval of an institutional or local ethics committee.

F.2 Types of Papers

F.2.1 Research articles

F.2.2 Review articles

The manuscript of a review article should be arranged as described for research articles but according to the following sections: title page, abstract and keywords (indexing terms, normally 3-6 items), Introduction, Specific sections determined by the author, Conclusions, Acknowledgements, References, Figure legends and Figures, Tables. Sections ranging from the Introduction to the Conclusions should be numbered. Subdivisions within a section should also be numbered within that section: 2.1., 2.2., 2.3. etc. All pages should be numbered consecutively, the title page being p.1.

F.2.3 Commentaries and Mini-reviews

One page suggestions for comprehensive reviews, commentaries or mini-reviews should be sent to the Editor-in-Chief at ejps@sdu.dk for consideration. Please see detailed information on commentaries and mini-reviews below.

F.2.4 Commentaries (Guidance)

The definition of a Commentary for EJPS is three-fold. Firstly, it can be an argued piece of provocative scientific writing purporting to take a balanced position on a controversial pharmaceutical science topic. A second option is for the author to approach the topic from a particular viewpoint on one side of an argument. A third option is to provide a topical update on a hot topic in Pharmaceutical Sciences and this can be more informative than controversial.

Commentaries will be commissioned by the editors in advance or invited from non-commissioned authors if they wish to initially submit a one page summary of the intended Commentary to the editors in advance. All manuscripts will be assessed by 2-3 independent referees.

The journal is looking for stimulating and provoking essays, with referenced material, but without an extensive reference list. Commentaries can contain one summary figure and/or table and should have no more than 30 references to preferably recent peer-reviewed material. The word count should be approximately 2,000 words maximum. The commentary should have a short abstract summary of 150 to 200 words and 4-5 key words should be included, The text should be broken down into 4-5 numbered sections beginning with an Introduction and ending with a Conclusions section. A model of the structures is to be found in Eur. J. Pharm. Sci. 19, 1-11 by R.D. Combes

F.2.5 Mini-review (Guidance)

Mini-reviews are thought provoking reviews of contemporary pharmaceutical research. Themes are as described in the Scope of the Journal section.

Mini-reviews will usually be commissioned by the editors in advance, but contributions are invited from non-commissioned authors if they wish to initially submit a one page summary of the intended review to the editors in advance. All manuscripts will be assessed by 2-3 independent referees.

The structure of the mini-review is as follows: a title page followed by a 200-300 word abstract with 4-5 key words. The text is then divided into numbered sections finishing with a Summary section. References should be kept to a maximum of 60 and should be mostly to recent peer-reviewed material. There is a combined maximum of 5 figures / tables. Authors are encouraged to submit their original unpublished work as part of the review if appropriate. The total length of the review should be a maximum of 4,000 words.

F.3 Ethics in publishing

For information on Ethics in publishing and Ethical guidelines for journal publication see http://www.elsevier.com/publishingethics and http://www.elsevier.com/journal authors/ethics.

F.4 Conflict of interest

All authors are requested to disclose any actual or potential conflict of interest including any financial, personal or other relationships with other people or organizations within three years of beginning the submitted work that could inappropriately influence, or be perceived to influence, their work. See also http://www.elsevier.com/conflictsofinterest. Further information and an example of a Conflict of Interest form can be found at: http://help.elsevier.com/app/answers/detail/a_id/286/p/7923.

F.5 Submission declaration

Submission of an article implies that the work described has not been published previously (except in the form of an abstract or as part of a published lecture or academic thesis or as an electronic preprint, see http://www.elsevier.com/postingpolicy), that it is not under consideration for publication

elsewhere, that its publication is approved by all authors and tacitly or explicitly by the responsible authorities where the work was carried out, and that, if accepted, it will not be published elsewhere including electronically in the same form, in English or in any other language, without the written consent of the copyright-holder.

F.6 Changes to authorship

This policy concerns the addition, deletion, or rearrangement of author names in the authorship of accepted manuscripts:

Before the accepted manuscript is published in an online issue: Requests to add or remove an author, or to rearrange the author names, must be sent to the Journal Manager from the corresponding author of the accepted manuscript and must include: (a) the reason the name should be added or removed, or the author names rearranged and (b) written confirmation (e-mail, fax, letter) from all authors that they agree with the addition, removal or rearrangement. In the case of addition or removal of authors, this includes confirmation from the author being added or removed. Requests that are not sent by the corresponding author will be forwarded by the Journal Manager to the corresponding author, who must follow the procedure as described above. Note that: (1) Journal Managers will inform the Journal Editors of any such requests and (2) publication of the accepted manuscript in an online issue is suspended until authorship has been agreed.

After the accepted manuscript is published in an online issue: Any requests to add, delete, or rearrange author names in an article published in an online issue will follow the same policies as noted above and result in a corrigendum.

F.7 Article transfer service

This journal is part of our Article Transfer Service. This means that if the Editor feels your article is more suitable in one of our other participating journals, then you may be asked to consider transferring the article to one of those. If you agree, your article will be transferred automatically on your behalf with no need to reformat. More information about this can be found here: http://www.elsevier.com/authors/article-transfer-service.

F.8 Copyright

This journal offers authors a choice in publishing their research: Open access and Subscription.

F.8.1 For subscription articles

Upon acceptance of an article, authors will be asked to complete a 'Journal Publishing Agreement' (for more information on this and copyright, see http://www.elsevier.com/copyright). An e-mail will be sent to the corresponding author confirming receipt of the manuscript together with a 'Journal Publishing Agreement' form or a link to the online version of this agreement.

Subscribers may reproduce tables of contents or prepare lists of articles including abstracts for internal circulation within their institutions. Permission of the Publisher is required for resale or

distribution outside the institution and for all other derivative works, including compilations and translations (please consult http://www.elsevier.com/permissions). If excerpts from other copyrighted works are included, the author(s) must obtain written permission from the copyright owners and credit the source(s) in the article. Elsevier has preprinted forms for use by authors in these cases: please consult http://www.elsevier.com/permissions.

F.8.2 For open access articles

Upon acceptance of an article, authors will be asked to complete an 'Exclusive License Agreement' (for more information see http://www.elsevier.com/OAauthoragreement). Permitted reuse of open access articles is determined by the author's choice of user license (see http://www.elsevier.com/openaccesslicenses).

F.9 Retained author rights

As an author you (or your employer or institution) retain certain rights. For more information on author rights for:
Subscription articles please see
http://www.elsevier.com/journal-authors/author-rights-and-responsibilities.
Open access articles please see http://www.elsevier.com/OAauthoragreement.

F.10 Role of the funding source

You are requested to identify who provided financial support for the conduct of the research and/or preparation of the article and to briefly describe the role of the sponsor(s), if any, in study design; in the collection, analysis and interpretation of data; in the writing of the report; and in the decision to submit the article for publication. If the funding source(s) had no such involvement then this should be stated.

F.11 Funding body agreements and policies

Elsevier has established agreements and developed policies to allow authors whose articles appear in journals published by Elsevier, to comply with potential manuscript archiving requirements as specified as conditions of their grant awards. To learn more about existing agreements and policies please visit http://www.elsevier.com/fundingbodies.

F.12 Open access

This journal offers authors a choice in publishing their research:

Open access

- Articles are freely available to both subscribers and the wider public with permitted reuse
- An open access publication fee is payable by authors or their research funder

Subscription

- Articles are made available to subscribers as well as developing countries and patient groups through our access programs (http://www.elsevier.com/access)
- No open access publication fee

All articles published open access will be immediately and permanently free for everyone to read and download. Permitted reuse is defined by your choice of one of the following Creative Commons user licenses:

F.12.1 Creative Commons Attribution (CC BY): lets others distribute and copy the article, to create extracts, abstracts, and other revised versions, adaptations or derivative works of or from an article (such as a translation), to include in a collective work (such as an anthology), to text or data mine the article, even for commercial purposes, as long as they credit the author(s), do not represent the author as endorsing their adaptation of the article, and do not modify the article in such a way as to damage the author's honor or reputation.

F.12.2 Creative Commons Attribution-NonCommercial-ShareAlike (CC BY-NC-SA): for non-commercial purposes, lets others distribute and copy the article, to create extracts, abstracts and other revised versions, adaptations or derivative works of or from an article (such as a translation), to include in a collective work (such as an anthology), to text and data mine the article, as long as they credit the author(s), do not represent the author as endorsing their adaptation of the article, do not modify the article in such a way as to damage the author's honor or reputation, and license their new adaptations or creations under identical terms (CC BY-NC-SA).

F.12.3 Creative Commons Attribution-NonCommercial-NoDerivs (CC BY-NC-ND): for noncommercialpurposes, lets others distribute and copy the article, and to include in a collective work (such as an anthology), as long as they credit the author(s) and provided they do not alter or modify the article.

To provide open access, this journal has a publication fee which needs to be met by the authors or their research funders for each article published open access.

Your publication choice will have no effect on the peer review process or acceptance of submitted articles.

The open access publication fee for this journal is **$3000**, excluding taxes. Learn more about Elsevier's pricing policy: http://www.elsevier.com/openaccesspricinF.

F.13 Language (usage and editing services)

Please write your text in good English (American or British usage is accepted, but not a mixture of these). Authors who feel their English language manuscript may require editing to eliminate possible grammatical or spelling errors and to conform to correct scientific English may wish to use the English Language Editing service available from Elsevier's WebShop (http://webshop.elsevier.com/languageediting/) or visit our customer support site (http://support.elsevier.com) for more information.

F.14 Informed consent and patient details

Studies on patients or volunteers require ethics committee approval and informed consent, which should be documented in the paper. Appropriate consents, permissions and releases must be obtained where an author wishes to include case details or other personal information or images of patients and any other individuals in an Elsevier publication. Written consents must be retained by the author and copies of the consents or evidence that such consents have been obtained must be provided to Elsevier on request. For more information, please review the Elsevier Policy on the Use of Images or Personal Information of Patients or other Individuals, http://www.elsevier.com/patient-consent-policy. Unless you have written permission from the patient (or, where applicable, the next of kin), the personal details of any patient included in any part of the article and in any supplementary materials (including all illustrations and videos) must be removed before submission.

F.15 Submission

Submission to this journal proceeds totally online and you will be guided stepwise through the creation and uploading of your files. The system automatically converts source files to a single PDF file of the article, which is used in the peer-review process. Please note that even though manuscript source files are converted to PDF files at submission for the review process, these source files are needed for further processing after acceptance. All correspondence, including notification of the Editor's decision and requests for revision, takes place by e-mail removing the need for a paper trail.

F.16 Referees

Please submit the names and institutional e-mail addresses of several potential referees. For more details, visit our Support site. Note that the editor retains the sole right to decide whether or not the suggested reviewers are used.

F.17 Additional Information

Editorial review: All manuscripts are generally submitted to 2-3 referees who are chosen for their ability to evaluate the work. Supplementary material may be included to facilitate the review process.

Authors may request that certain referees should not be chosen. Members of the editorial board will usually be called upon for advice when there is disagreement among the referees or between

referees and authors, or when the editors believe that the manuscript has not received adequate consideration by the referees.

All referees' comments must be responded to, and suggested changes be made. The author should detail the changes made in response to the referees' comments and suggestions in an accompanying letter. If the author disagrees with some changes, the reason, supported by data, should be given. The editors may refuse to publish manuscripts from authors who persistently ignore referees' comments. Handwritten additions or corrections will not be accepted. Only complete retyping of the pages affected by revision is acceptable. A revised manuscript should be received by the editorial office no later than 2 months after the editorial decision was sent to the author(s); otherwise it will be processed as a new manuscript.

F.19 Preparation

F.19.1 Use of word processing software

It is important that the file be saved in the native format of the word processor used. The text should be in single-column format. Keep the layout of the text as simple as possible. Most formatting codes will be removed and replaced on processing the article. In particular, do not use the word processor's options to justify text or to hyphenate words. However, do use bold face, italics, subscripts, superscripts etc. When preparing tables, if you are using a table grid, use only one grid for each individual table and not a grid for each row. If no grid is used, use tabs, not spaces, to align columns.

The electronic text should be prepared in a way very similar to that of conventional manuscripts (see also the Guide to Publishing with Elsevier: http://www.elsevier.com/guidepublication). Note that source files of figures, tables and text graphics will be required whether or not you embed your figures in the text. See also the section on Electronic artwork.

To avoid unnecessary errors you are strongly advised to use the 'spell-check' and 'grammar-check' functions of your word processor.

F.19.2 LaTeX

You are recommended to use the Elsevier article class elsarticle.cls (http://www.ctan.org/tex-archive/macros/latex/contrib/elsarticle) to prepare your manuscript and BibTeX (http://www.bibtex.org) to generate your bibliography.

For detailed submission instructions, templates and other information on LaTeX, see http://www.elsevier.com/latex.

F.20 Article structure

Subdivision - numbered sections

Divide your article into clearly defined and numbered sections. Subsections should be numbered 1.1 (then 1.1.1, 1.1.2, ...), 1.2, etc. (the abstract is not included in section numbering). Use this numbering

also for internal cross-referencing: do not just refer to 'the text'. Any subsection may be given a brief headinF. Each heading should appear on its own separate line.

F.20.1 Introduction

State the objectives of the work and provide an adequate background, avoiding a detailed literature survey or a summary of the results.

F.20.2 Material and methods

Provide sufficient detail to allow the work to be reproduced. Methods already published should be indicated by a reference: only relevant modifications should be described.

F.20.3 Results

Results should be clear and concise.

Text, tables and figures must show minimal overlap, and must be internally consistent.

F.20.4 Discussion

This should explore the significance of the results of the work, not repeat them. **A combined Results and Discussion section is often appropriate**. Avoid extensive citations and discussion of published literature.

F.20.5 Conclusions

The main conclusions of the study may be presented in a short Conclusions section, which may stand alone or form a subsection of a Discussion or Results and Discussion section.

F.20.6 Appendices

If there is more than one appendix, they should be identified as A, B, etc. Formulae and equations in appendices should be given separate numbering: Eq. (A.1), Eq. (A.2), etc.; in a subsequent appendix, Eq. (B.1) and so on. Similarly for tables and figures: Table A.1; FiF. A.1, etc.

F.21 Essential title page information

F.21.1 Title

Concise and informative. Titles are often used in information-retrieval systems. Avoid abbreviations and formulae where possible.

F.21.2 Author names and affiliations

Where the family name may be ambiguous (e.F., a double name), please indicate this clearly. Present the authors' affiliation addresses (where the actual work was done) below the names. Indicate all affiliations with a lower-case superscript letter immediately after the author's name and in front of the appropriate address. Provide the full postal address of each affiliation, including the country name and, if available, the e-mail address of each author.

F.21.3 Corresponding author

Clearly indicate who will handle correspondence at all stages of refereeing and publication, also post-publication. **Ensure that phone numbers (with country and area code) are provided in addition to the e-mail address and the complete postal address.**

Contact details must be kept up to date by the corresponding author

F.21.4 Present/permanent address

If an author has moved since the work described in the article was done, or was visiting at the time, a 'Present address' (or 'Permanent address') may be indicated as a footnote to that author's name. The address at which the author actually did the work must be retained as the main, affiliation address. Superscript Arabic numerals are used for such footnotes.

F.22 Abstract

A concise and factual abstract is required. The abstract should state briefly the purpose of the research, the principal results and major conclusions. An abstract is often presented separately from the article, so it must be able to stand alone. For this reason, References should be avoided, but if essential, then cite the author(s) and year(s). Also, non-standard or uncommon abbreviations should be avoided, but if essential they must be defined at their first mention in the abstract itself.

F.23 Graphical abstract

A Graphical abstract is mandatory for this journal. It should summarize the contents of the article in a concise, pictorial form designed to capture the attention of a wide readership online. Authors must provide images that clearly represent the work described in the article. Graphical abstracts should be submitted as a separate file in the online submission system. Image size: please provide an image with a minimum of 531 × 1328 pixels (h × w) or proportionally more, but should be readable on screen at a size of 200 × 500 pixels (at 96 dpi this corresponds to 5 × 13 cm). Bear in mind readability after reduction, especially if using one of the figures from the article itself. Preferred file types: TIFF, EPS, PDF or MS Office files. See http://www.elsevier.com/graphicalabstracts for examples.

F.24 Keywords

Immediately after the abstract, provide a maximum of 6 keywords, using American spelling and avoiding general and plural terms and multiple concepts (avoid, for example, 'and', 'of'). Be sparing with abbreviations: only abbreviations firmly established in the field may be eligible. These keywords will be used for indexing purposes.

F.25 Chemical compounds

You can enrich your article by providing a list of chemical compounds studied in the article. The list of compounds will be used to extract relevant information from the NCBI PubChem Compound database and display it next to the online version of the article on ScienceDirect. You can include up to 10

names of chemical compounds in the article. For each compound, please provide the PubChem CID of the most relevant record as in the following example: Glutamic acid (PubChem CID:611). The PubChem CIDs can be found via http://www.ncbi.nlm.nih.gov/pccompound. Please position the list of compounds immediately below the 'Keywords' section. It is strongly recommended to follow the exact text formatting as in the example below:

Chemical compounds studied in this article Ethylene glycol (PubChem CID: 174); Plitidepsin (PubChem CID: 44152164); Benzalkonium chloride (PubChem CID: 15865)

More information is available at: http://www.elsevier.com/PubChem.

F.26 Abbreviations

Abbreviations are a hindrance for the reader. Use as few abbreviations as possible and write out names of compounds, receptors, etc., in full throughout the text of the manuscript, with the exceptions given below. Unnecessary and nonsense abbreviations are not allowed. Generic names should not be abbreviated. As an example, AMP, HAL, HIST, RAMH, TAM, SST, for amphetamine, haloperidol, histamine, (R)-α -methylhistamine, tamoxifen, somatostatin, are not accepted. Abbreviations which have come to replace the full term (e.F., GABA, DOPA, PDGF, 5-HT, for Y -aminobutyric acid, 3,4-dihydroxyphenylalanine, PDGF, 5-hydroxytryptamine) may be used, provided the term is spelled out in the abstract and in the body of the manuscript the first time the abbreviation is used. Unwieldy chemical names may be abbreviated. As an example, 8-OH-DPAT, DOI, DTG, BAPTA, for 8-hydroxy-2-(di-n-propylamino)tetralin, 1-(2,5-dimethoxy-4-iodophenyl)-2-aminopropane, 1,3- di(2-tolyl)-guanidine, 1,2-bis(o-aminophenoxy)ethane-N,N,N',N'-tetraacetic acid, are acceptable; however, the full chemical name should be given once in the body of the manuscript and in the abstract, followed in both cases by the abbreviation. Code names may be used, but the full chemical name should be given in the text and in the abstract. Authors not conforming to these demands may have their manuscripts returned for correction with delayed publication as a result.

F.26.1 Some abbreviations may be used without definition

ADP
CDP
GDP
IDP5' - pyrophosphates of adenosine,
UDP cytidine, guanosine inosine, uridine AMP etc.
adenosine 5'-monophosphate etc. ADP etc.
adenosine 5'-diphosphate etc. ATP etc.
adenosine 5'- triphosphate etc.
CM-cellulose, carboxymethylcellulose
CoA and acetyl-CoA coenzyme A and its acyl derivatives DEAE-cellulose O-(diethylaminoethyl)-cellulose

DNA deoxyribonucleic acid
EGTA ethylene glycol-bis(β-aminoethyl ether)
N,N,N',N'-tetraacetic acid
FAD flavin-adenine dinucleotide
FMN flavin mononucleotide
GSH,
GSSG glutathione,
reduced and oxidized Hepes4-(2-hydroxyethyl)-1-piperazine-ethanesulphonic acid
NAD nicotinamide-adenine dinucleotide
NAD Pnicotinamide-adenine dinucleotide phosphate
NMN nicotinamide mononucleotide
Pi, P Piorthophosphate, pyrophosphate
RNA - ribonucleic acid
Tris2-amino-2-hydroxymethylpropane-1,3-diol

Two alternative conventions are currently in use in some cases. For example, for the phosphoinositides there are both the abbreviations recommended by the IUPAC-IUB and those of the Chilton Convention (e.F., PtdIns(4,5)P2 vs. PIP 2for phosphatidylinositol 4,5-biphosphate). The journal will accept either of these forms but not their combination.

F.26.2 Abbreviations of units of measurements and other terms are as follows:

F.26.2.1 Units of mass
kilogram - kg
gram - g
milligram – mg
microgram - µg
nanogram - ng
mole (gram-molecule) - mol
millimole - mmol
micromole – µmol
nanomole - nmol
picomole - pmol
femtomole - fmol
equivalent eq

F.26.2.2 Units of time
hour - h
minute - min

second - s
millisecond - ms
microsecond - µs

F.26.2.3 Units of volume

litre - l
millilitre - ml
microlitre - µl

F.26.2.4 Units of length

metre - m
centimetre - cm
millimetre - mm
micrometre - µm
nanometre - nm

F.26.2.5 Units of concentration

molar - mol/l - M
millimolar - mM
micromolar - µM
nanomolar - nM
picomolar - pM

F.26.2.6 Units of heat, energy, electricity

Joule - J
degree Celsius (centigrade) - °C
Coulomb - C
ampere - A
volt - V
ohm - Ω
Siemens - S

F.26.2.7 Units of radiation

Curie - Ci
counts per minute - cpm
disintegrations per minute - dpm
Becquerel - Bq

F.26.2.8 Miscellaneous

gravity - g
dissociation constant - Kd
median doses - LD50, ED50
probability - P
routes of drug administration - i.v., i.p., s.c., i.m.
square centimetre - cm^2
standard deviation - S.D.
standard error of the mean - S.E.M.
Svedberg unit of sedimentation coefficient - S Hill coefficient nH

The isotope mass number should appear before the atomic symbol, e.F., [3H]noradrenaline, [14C]choline. Ions should be written: Fe3+, Ca2+, Mg2+. The term absorbance (A) is preferred to extinction or optical density. For abbreviations not included in this list consult: Units, Symbols and Abbreviations, A Guide for Biological and Medical Authors and Editors, 1994 (The Royal Society of Medicine, London), ISBN 0-905958-78-0, or Scientific Style and Format. The CBE Manual for Authors, Editors, and Publishers, 6th edn. (Cambridge University Press, Cambridge), ISBN 0-521-47154-0.

F.27 Acknowledgements

Collate acknowledgements in a separate section at the end of the article before the references and do not, therefore, include them on the title page, as a footnote to the title or otherwise. List here those individuals who provided help during the research (e.F. lab technicians, statisticians, colleagues providing help preparing the manuscript).

F.28 Nomenclature and Units

Only generic and chemical names of drugs should be used, although a proprietary equivalent may be indicated once, in parentheses. Pharmacological and Chemical Synonyms, E.E.J. Marler, 9th edn. (Elsevier, Amsterdam, 1990) may be consulted.

The nomenclature of chemical substances should be consistent, clear and unambiguous, and should conform to the usage of the American Chemical Society and the convention recommended by the International Union of Pure and Applied Chemistry (IUPAC). When in doubt, writers should consult the indexes of Chemical Abstracts; the various reports and pamphlets of the American Chemical Society Committee on Nomenclature, Spelling and Pronunciation; and from the International Union of Biochemistry and Molecular Biology (IUBMB): Biochemical Nomenclature and Related Documents (Portland Press, London).

When drugs, which are mixtures of stereoisomers are used, the fact that they have a composite nature and the implication of this for interpretation of the data and drawing of conclusions should be

made clear. The use of the appropriate prefix is essential. Use of the generic name alone without prefix would be taken to refer to agents with no stereoisomers. The nomenclature of the various isomers and isomeric mixtures can be found in: (i) IUPAC, Nomenclature of Organic Chemistry, eds. J. Rigaudy and S.P. Klesney (Pergamon Press, London), 1979, p. 481; (ii) Signs of the times: the need for a stereochemically informative generic name system, Simonyi, M., J. Gal and B. Testa, 1989, Trends Pharmacol. Sci. 10, 349. For nomenclature of peptides, see Neuropeptides, Vol. 1, 1981, p. 231.

The nomenclature of receptors and their subtypes should conform to the TIPS 1995 Receptor & Ion Channel Nomenclature Supplement (Trends Pharmacol. Sci. Receptor Nomenclature Supplement 1995). Copies of this supplement are available from the publisher (Elsevier Trends Journals, Oxford Fulfilment Centre, P.O. Box 800, Kidlington, Oxford OX5 1DX, UK. Tel.: (44-1865) 843-699; Fax: (44-1865) 843-911).

The trivial name of the enzyme may be used in the text, but the systematic name and classification number according to Enzyme Nomenclature, rev. edn. (Academic Press, New York, NY, 1984) should be quoted the first time the enzyme is mentioned.

F.29 Database linking

Elsevier encourages authors to connect articles with external databases, giving their readers oneclick access to relevant databases that help to build a better understanding of the described research.

Please refer to relevant database identifiers using the following format in your article: Database: xxxx (e.F., TAIR: AT1G01020; CCDC: 734053; PDB: 1XFN). See http://www.elsevier.com/databaselinking for more information and a full list of supported databases.

F.30 GenBank accession numbers

Gene accession numbers refer to genes or DNA sequences about which further information can be found in the databases at the National Center for Biotechnical Information (NCBI) at the National Library of Medicine. Authors wishing to enable other scientists to use the accession numbers cited in their papers via links to these sources, should reference this information in the following manner:

For each and every accession number cited in an article, authors should type the accession number in **bold, underlined text**. Letters in the accession number should always be capitalised. (See Example1 below.) This combination of letters and format will enable Elsevier's typesetters to recognize the relevant texts as accession numbers and add the required link to GenBank's sequences.

Example 1: "GenBank accession nos. **AI631510** , **AI631511** , **AI632198** , and **BF223228**), a B-cell tumor from a chronic lymphatic leukemia (GenBank accession no. **BE675048**), and a T-cell lymphoma (GenBank accession no. **AA361117**)".

Authors are encouraged to check accession numbers used very carefully. **An error in a letter or number can result in a dead link**.

In the final version of the **printed article**, the accession number text will not appear bold or underlined (see Example 2 below).

Example 2: "GenBank accession nos. AI631510, AI631511, AI632198, and BF223228), a B-cell tumor from a chronic lymphatic leukemia (GenBank accession no. BE675048), and a T-cell lymphoma (GenBank accession no. AA361117)".

In the final version of the **electronic copy**, the accession number text will be linked to the appropriate source in the NCBI databases enabling readers to go directly to that source from the article (see Example 3 below).

Example 3: "GenBank accession nos. AI631510, AI631511, AI632198, and BF223228), a B-cell tumor from a chronic lymphatic leukemia (GenBank accession no. BE675048), and a T-cell lymphoma (GenBank accession no. AA361117)".

F.31 Formulas and equations

Structural chemical formulas, process flow diagrams and complicated mathematical expressions should be very clearly presented. All subscripts, superscripts, Greek letters and unusual characters must be identified. Structural chemical formulas and process flow diagrams should be prepared in the same way as graphs.

Present simple formulae in the line of normal text where possible and use the solidus (/) instead of a horizontal line for small fractional terms, e.F., X/Y. In principle, variables are to be presented in italics. Powers of e are often more conveniently denoted by exp. Number consecutively any equations that have to be displayed separately from the text (if referred to explicitly in the text).

F.32 Footnotes

Footnotes should be used sparingly. Number them consecutively throughout the article, using superscript Arabic numbers. Many wordprocessors build footnotes into the text, and this feature may be used. Should this not be the case, indicate the position of footnotes in the text and present the footnotes themselves separately at the end of the article. Do not include footnotes in the Reference list.

F.33.1 Table footnotes

Indicate each footnote in a table with a superscript lowercase letter.

F.34 Artwork

Image manipulation

Whilst it is accepted that authors sometimes need to manipulate images for clarity, manipulation for purposes of deception or fraud will be seen as scientific ethical abuse and will be dealt with accordingly.

For graphical images, this journal is applying the following policy: no specific feature within an image may be enhanced, obscured, moved, removed, or introduced. Adjustments of brightness, contrast, or color balance are acceptable if and as long as they do not obscure or eliminate any information present in the original. Nonlinear adjustments (e.F. changes to gamma settings) must be disclosed in the figure legend.

F.34.1 Electronic artwork

- General points
- Make sure you use uniform lettering and sizing of your original artwork.
- Embed the used fonts if the application provides that option.
- Aim to use the following fonts in your illustrations: Arial, Courier, Times New Roman, Symbol, or use fonts that look similar.
- Number the illustrations according to their sequence in the text.
- Use a logical naming convention for your artwork files.
- Provide captions to illustrations separately.
- Size the illustrations close to the desired dimensions of the printed version.
- Submit each illustration as a separate file.

A detailed guide on electronic artwork is available on our website: http://www.elsevier.com/artworkinstructions

You are urged to visit this site; some excerpts from the detailed information are given here.

F.34.2 Formats

If your electronic artwork is created in a Microsoft Office application (Word, PowerPoint, Excel) then please supply 'as is' in the native document format.Regardless of the application used other than Microsoft Office, when your electronic artwork is finalized, please 'Save as' or convert the images to one of the following formats (note the resolution requirements for line drawings, halftones, and line/halftone combinations given below):

EPS (or PDF): Vector drawings, embed all used fonts.

TIFF (or JPEG): Color or grayscale photographs (halftones), keep to a minimum of 300 dpi.

TIFF (or JPEG): Bitmapped (pure black & white pixels) line drawings, keep to a minimum of 1000 dpi.
TIFF (or JPEG): Combinations bitmapped line/half-tone (color or grayscale), keep to a minimum of 500 dpi.

Please do not:

- Supply files that are optimized for screen use (e.F., GIF, BMP, PICT, WPG); these typically have a low number of pixels and limited set of colors;
- Supply files that are too low in resolution;
- Submit graphics that are disproportionately large for the content.

F.34.3 Color artwork

Please make sure that artwork files are in an acceptable format (TIFF (or JPEG), EPS (or PDF), or MS Office files) and with the correct resolution. If, together with your accepted article, you submit usable color figures then Elsevier will ensure, at no additional charge, that these figures will appear in color on the Web (e.F., ScienceDirect and other sites) regardless of whether or not these illustrations are reproduced in color in the printed version. **For color reproduction in print, you will receive information regarding the costs from Elsevier after receipt of your accepted article**. Please indicate your preference for color: in print or on the Web only. For further information on the preparation of electronic artwork, please see http://www.elsevier.com/artworkinstructions.

Please note: Because of technical complications which can arise by converting color figures to 'gray scale' (for the printed version should you not opt for color in print) please submit in addition usable black and white versions of all the color illustrations.

F.34.4 Figure captions

Ensure that each illustration has a caption. Supply captions separately, not attached to the figure. A caption should comprise a brief title (**not** on the figure itself) and a description of the illustration. Keep text in the illustrations themselves to a minimum but explain all symbols and abbreviations used.

F.35 Tables

Number tables consecutively in accordance with their appearance in the text. Place footnotes to tables below the table body and indicate them with superscript lowercase letters. Avoid vertical rules. Be sparing in the use of tables and ensure that the data presented in tables do not duplicate results described elsewhere in the article.

F.36 References

F.36.1 Citation in text

Please ensure that every reference cited in the text is also present in the reference list (and vice versa). Any references cited in the abstract must be given in full. Unpublished results and personal communications are not recommended in the reference list, but may be mentioned in the text. If these references are included in the reference list they should follow the standard reference style of the journal and should include a substitution of the publication date with either 'Unpublished results' or 'Personal communication'. Citation of a reference as 'in press' implies that the item has been accepted for publication and a copy of the title page of the relevant article must be submitted.

F.36.2 Reference links

Increased discoverability of research and high quality peer review are ensured by online links to the sources cited. In order to allow us to create links to abstracting and indexing services, such as Scopus, CrossRef and PubMed, please ensure that data provided in the references are correct.

Please note that incorrect surnames, journal/book titles, publication year and pagination may prevent link creation. When copying references, please be careful as they may already contain errors. Use of the DOI is encouraged.

F.36.3 Web references

As a minimum, the full URL should be given and the date when the reference was last accessed. Any further information, if known (DOI, author names, dates, reference to a source publication, etc.), should also be given. Web references can be listed separately (e.F., after the reference list) under a different heading if desired, or can be included in the reference list.

F.36.4 References in a special issue

Please ensure that the words 'this issue' are added to any references in the list (and any citations in the text) to other articles in the same Special Issue.

F.36.5 Reference management software

This journal has standard templates available in key reference management packages EndNote (http://www.endnote.com/support/enstyles.asp) and Reference Manager (http://refman.com/support/rmstyles.asp). Using plug-ins to wordprocessing packages, authors only need to select the appropriate journal template when preparing their article and the list of references and citations to these will be formatted according to the journal style which is described below.

F.36.6 Reference formatting

There are no strict requirements on reference formatting at submission. References can be in any style or format as long as the style is consistent. Where applicable, author(s) name(s), journal

title/book title, chapter title/article title, year of publication, volume number/book chapter and the pagination must be present. Use of DOI is highly encouraged. The reference style used by the journal will be applied to the accepted article by Elsevier at the proof stage. Note that missing data will be highlighted at proof stage for the author to correct. If you do wish to format the references yourself they should be arranged according to the following examples:

F.36.7 Reference style

Text: All citations in the text should refer to:

1. Single author: the author's name (without initials, unless there is ambiguity) and the year of publication;
2. Two authors: both authors' names and the year of publication;
3. Three or more authors: first author's name followed by 'et al.' and the year of publication.

Citations may be made directly (or parenthetically). Groups of references should be listed first alphabetically, then chronologically.

Examples: 'as demonstrated (Allan, 2000a, 2000b, 1999; Allan and Jones, 1999). Kramer et al. (2010) have recently shown ....'

List: References should be arranged first alphabetically and then further sorted chronologically if necessary. More than one reference from the same author(s) in the same year must be identified by the letters 'a', 'b', 'c', etc., placed after the year of publication.

F.36.7.1 Examples

Reference to a journal publication:

Van der Geer, J., Hanraads, J.A.J., Lupton, R.A., 2010. The art of writing a scientific article. J. Sci. Commun. 163, 51–59.

Reference to a book:

Strunk Jr., W., White, E.B., 2000. The Elements of Style, fourth ed. Longman, New York.

Reference to a chapter in an edited book:

Mettam, F.R., Adams, L.B., 2009. How to prepare an electronic version of your article, in: Jones, B.S., Smith , R.Z. (Eds.), Introduction to the Electronic Age. E-Publishing Inc., New York, pp. 281–304.

F.36.8 Journal abbreviations source

Journal names should be abbreviated according to the List of Title Word Abbreviations: http://www.issn.org/services/online-services/access-to-the-ltwa/.

F.37 Video data

Elsevier accepts video material and animation sequences to support and enhance your scientific research. Authors who have video or animation files that they wish to submit with their article are strongly encouraged to include links to these within the body of the article. This can be done in the same way as a figure or table by referring to the video or animation content and noting in the body text where it should be placed. All submitted files should be properly labeled so that they directly relate to the video file's content. In order to ensure that your video or animation material is directly usable, please provide the files in one of our recommended file formats with a preferred maximum size of 50 MB. Video and animation files supplied will be published online in the electronic version of your article in Elsevier Web products, including ScienceDirect: http://www.sciencedirect.com.

Please supply 'stills' with your files: you can choose any frame from the video or animation or make a separate image. These will be used instead of standard icons and will personalize the link to your video data. For more detailed instructions please visit our video instruction pages at http://www.elsevier.com/artworkinstructions. Note: since video and animation cannot be embedded in the print version of the journal, please provide text for both the electronic and the print version for the portions of the article that refer to this content.

F.38 Audio Slides

The journal encourages authors to create an AudioSlides presentation with their published article. AudioSlides are brief, webinar-style presentations that are shown next to the online article on ScienceDirect. This gives authors the opportunity to summarize their research in their own words and to help readers understand what the paper is about. More information and examples are available at http://www.elsevier.com/audioslides. Authors of this journal will automatically receive an invitation e-mail to create an AudioSlides presentation after acceptance of their paper.

F.39 Supplementary data

Elsevier accepts electronic supplementary material to support and enhance your scientific research. Supplementary files offer the author additional possibilities to publish supporting applications, high resolution images, background datasets, sound clips and more. Supplementary files supplied will be published online alongside the electronic version of your article in Elsevier Web products, including ScienceDirect: http://www.sciencedirect.com. In order to ensure that your submitted material is directly usable, please provide the data in one of our recommended file formats. Authors should submit the material in electronic format together with the article and supply a concise and descriptive caption for each file. For more detailed instructions please visit our artwork instruction pages at http://www.elsevier.com/artworkinstructions.

F.40 Submission checklist

The following list will be useful during the final checking of an article prior to sending it to the journal for review. Please consult this Guide for Authors for further details of any item.

Ensure that the following items are present:

One author has been designated as the corresponding author with contact details:

- E-mail address
- Full postal address
- Phone numbers

All necessary files have been uploaded, and contain:

- Keywords
- All figure captions
- All tables (including title, description, footnotes)

Further considerations

- Manuscript has been 'spell-checked' and 'grammar-checked'
- References are in the correct format for this journal
- All references mentioned in the Reference list are cited in the text, and vice versa
- Permission has been obtained for use of copyrighted material from other sources (including the Web)
- Color figures are clearly marked as being intended for color reproduction on the Web (free of charge)
- and in print, or to be reproduced in color on the Web (free of charge) and in black-and-white in print
- If only color on the Web is required, black-and-white versions of the figures are also supplied for printing purposes

For any further information please visit our customer support site at http://support.elsevier.com.

F.41 After acceptance

F.41.1 Use of the Digital Object Identifier

The Digital Object Identifier (DOI) may be used to cite and link to electronic documents. The DOI consists of a unique alpha-numeric character string which is assigned to a document by the publisher upon the initial electronic publication. The assigned DOI never changes. Therefore, it is an ideal medium for citing a document, particularly 'Articles in press' because they have not yet received their full bibliographic information. Example of a correctly given DOI (in URL format; here an article in the journal Physics Letters B):
http://dx.doi.org/10.1016/j.physletb.2010.09.059

When you use a DOI to create links to documents on the web, the DOIs are guaranteed never to change.

F.41.2 Online proof correction

Corresponding authors will receive an e-mail with a link to our online proofing system, allowing annotation and correction of proofs online. The environment is similar to MS Word: in addition to editing text, you can also comment on figures/tables and answer questions from the Copy Editor. Web-based proofing provides a faster and less error-prone process by allowing you to directly type your corrections, eliminating the potential introduction of errors.

If preferred, you can still choose to annotate and upload your edits on the PDF version. All instructions for proofing will be given in the e-mail we send to authors, including alternative methods to the online version and PDF.

We will do everything possible to get your article published quickly and accurately - please upload all of your corrections within 48 hours. It is important to ensure that all corrections are sent back to us in one communication. Please check carefully before replying, as inclusion of any subsequent corrections cannot be guaranteed. Proofreading is solely your responsibility. Note that Elsevier may proceed with the publication of your article if no response is received.

F.41.3 Offprints

The corresponding author, at no cost, will be provided with a personalized link providing 50 days free access to the final published version of the article on ScienceDirect. This link can also be used for sharing via email and social networks. For an extra charge, paper offprints can be ordered via the offprint order form which is sent once the article is accepted for publication. Both corresponding and co-authors may order offprints at any time via Elsevier's WebShop (http://webshop.elsevier.com/myarticleservices/offprints). Authors requiring printed copies of multiple articles may use Elsevier WebShop's 'Create Your Own Book' service to collate multiplearticles within a single cover (http://webshop.elsevier.com/myarticleservices/booklets).

F.42 Additional information

No responsibility is assumed by the Publisher for any injury and/or damage to persons or property as a matter of products liability, negligence or otherwise, or from any use or operation of any methods, products, instructions or ideas contained in the material herein. Because of the rapid advances made in the medical sciences, independent verification of diagnoses and drug doses should be made.

F.43 Author inquiries

You can track your submitted article at http://help.elsevier.com/app/answers/detail/a_id/89/p/8045/.
You can track your accepted article at http://www.elsevier.com/trackarticle. You are also welcome to contact Customer Support via http://support.elsevier.com.

Acknowledgements

To God all the glory

A special thanks to all listed below:

- Dr. Marius Brits, my promoter and friend, who inspired, supported and guided me throughout this study.
- Dr. Erna Swanepoel for all her expertise, guidance and input as assistant promotor.
- Prof. Mino Caira (University of Cape Town), for his help with single crystal XRD work.
- The Laboratory for Applied Molecular Modelling (NWU) for access to - and use of Material Studio and high performance computers.
- My family: Emtia, Brahm, Anne, Jaco, Marlize and Nelia for their love, support and understanding.
- The RIIP® incorporating CENQAM® for the use of their equipment.
- All the personnel/friends at the RIIP® incorporating CENQAM® for their support and friendship, in particular Dr. (tannie) Elsa van Tonder (now retired), Prof. Theo Dekker (now retired), Mia Staats (nee de Jager), Ilene Brits and Andre Joubert.
- The NWU library and its personnel, especially Anriette Pretorius.
- Dr. Louwrens Tiedt for his time and experience on SEM microscopy.
- Prof. Jan Steenekamp for particle size analysis.
- The NWU, RIIP® incorporating CENQAM® and PharmaCen unit for financial support.
- My friends at DI Consultants.
- Prof. Douglas Oliver and Isabel Oliver for moral support.